Characterization of genome partitioning system of *Deinococcus radiodurans*

By

Vijaya Kumar Charaka

LIFE01200704005

Bhabha Atomic Research Centre

A thesis submitted to the
Board of Studies in Life Sciences
In partial fulfillment of requirements
For the Degree of

DOCTOR OF PHILOSOPHY
of
HOMI BHABHA NATIONAL INSTITUTE

December 2012

HOMI BHABHA NATIONAL INSTITUTE

RECOMMENDATIONS OF THE VIVA VOCE BOARD

As members of the Viva Voce Board, we certify that we have read the dissertation prepared by **Vijaya Kumar Charaka** entitled '**Characterization of genome partitioning system of *Deinococcus radiodurans*'** and recommend that it may be accepted as fulfilling the dissertation requirement for the Degree of Doctor of Philosophy.

Chairman – Prof. A. K. Sharma

_____ **Date:**

External examiner: Dr. J. Gowrishankar

_____ **Date:**

Member - Prof. J. R. Bandekar

_____ **Date:**

Member - Prof. (Mrs) J. K. Sainis

_____ **Date:**

Member - Prof. Dulal Panda

_____ **Date:**

Guide – Prof. H. S. Misra

_____ **Date:**

Final approval and acceptance of this dissertation is contingent upon the candidate's submissionof the final copies of the dissertation to HBNI.

I hereby certify that I have read this dissertation prepared under my direction and recommend that it may be accepted as fulfilling the dissertation requirement.

Date:

Place: **(H. S. Misra)**

(Guide)

STATEMENT BY AUTHOR

This dissertation has been submitted in partial fulfillment of requirements for an advanced degree at Homi Bhabha National Institute (HBNI) and is deposited in the library to be made available to borrowers under rules of the HBNI.

Brief quotations from this dissertation are allowable without special permission, provided that accurate acknowledgement of source is made. Requests for permission for extended quotation from or reproduction of this manuscript in whole or in part may be granted by the Competent Authority of HBNI when in his or her judgment the proposed use of the material is in the interests of scholarship. In all other instances, however, permission must be obtained from the author.

Vijaya Kumar Charaka

DECLARATION

I, hereby declare that the investigation presented in the thesis has been carried out by me. The work is original and has not been submitted earlier as a whole or in part for a degree / diploma at this or any other Institution / University.

Vijaya Kumar Charaka

ACKNOWLEDGEMENTS

I express my deep and heartfelt sincere gratitude to my guide, **Prof. H. S. Misra**, Head, Molecular Genetics Section, Molecular Biology Division, for suggesting this research problem and for sustained guidance and encouragement throughout the period of research. I also express my utmost gratitude to him for his constructive criticism, valuable suggestions and good wishes.

I express my sincere thanks to Prof. A. K. Sharma, Head, and FTD for his encouragement, moral support and valuable guidance, which inspired me to do my best. I am also grateful to Prof. (Mrs) J. K. Sainis, Raja Ramanna Fellow, Prof. J. R. Bandekar, Head, RBHSD and Prof. Dulal Panda, School of Bioscience and Bioengineering, IIT Bombay, members of my doctoral committee for providing valuable suggestions during the completion of this work.

It is my great privilege to acknowledge Dr. S. K. Apte, Associate Director (B), BMG and Head, MBD for his encouragement, moral support and valuable guidance, inspired me to do my best. I thank Prof. Marc Bramkamp, Ludwig - Maximilians University for his invaluable support both on academic and personal fronts, I am extremely grateful to him. I am always very influenced by his vast knowledge, perfect scientific concepts, hard working nature, and sincerity in this area of science.

I take this opportunity to thank all my lab mates and friends Dr. Swati Kota, A. D. Das, Dr. Y.S.Rajpurohit, Dr. Nivedita P. Khairnar, Dr. Shruti Desai, Dr. Vidya Kamble, Ms. Kruti Mehta, Ms. Alka Gupta, Dr. Rajinikanth, Maralihalli, Catriona Donovan, Boris. S, Juri. B and Sunil D. Dhotre and all other friends for their constant support.

I acknowledge Department of Atomic Energy, Bhabha Atomic Research Centre financial assistance for my Ph.D. At the end, my heartfelt gratitude to all my family members who have always encouraged and supported me.

December, 2012

MBD, BARC **Vijaya Kumar Charaka**

TABLE OF CONTENTS

Synopsis	**1-16**
List of figures	**17-18**
List of Tables	**19**
List of abbreviations	**20-52**
Chapter 1 General introduction and review of literature	**20-51**
1.1 Mechanisms of bacterial genome segregation	**22-24**
1.2 Mechanisms of Plasmid segregation	**24-37**
1.2.1 Type I partition system	**25-33**
1.2.2 Type II partition system	**33-34**
1.2.3 Type III partition system	**35**
1.2.4 Type IV partition system	**35-36**
1.2.5 Transcriptional regulation of *parAB* genes	**36-37**
1.3 Mechanisms of chromosome segregation in bacteria	**37-44**
1.4 *Deinococcus radiodurans* as a model organism	**44-51**
Chapter 2 Materials and methods	**52- 83**
2.1. Materials	**53-54**
2.2 Composition of commonly used analytical reagents	**54-63**
2.3 Methods	**63- 83**
2.3.1 Microbiological methods	
2.3.2 Methods used in molecular studies	
2.3.2.1 Isolation of plasmid DNA (mini prep)	
2.3.2.2 Large scale preparation of plasmid DNA	
2.3.2.3 Genomic DNA isolation	
2.3.2.4 Agarose gel electrophoresis	
2.3.2.5 PCR amplification	
2.3.2.6 DNA manipulation.	
2.3.2.7 Bacterial transformation	
2.3.2.8 Methods used in proteins purification	
2.3.2.9 Microscopy	
2.3.2.10 Statistical Analyses	
Chapter 3 Results	**84 -186**
Chapter 3.1 Identification of genome partitioning elements	**86-102**
3.1.1 Methods	**86-87**
3.1.2 Results	**87 -102**
3.1.2.1 Identification of centromere like sequences in *D. radiodurans*	**87 – 90**
3.1.2.2 Bioinformatic analysis of trans factors in *D. radiodurans*	**90 -102**
3.1.2.2.1 Genetic organization of '*par*' operon	**90**
3.1.3.2.2 Comparison of ParB family proteins with ParB's of this bacterium	**91 – 94**
3.1.3.2.3 Comparative analysis of ParA family proteins with ParA's of this bacterium	**95- 98**

3.1.3.2.4 Phylogenetic analysis of 'Par' proteins **98 -102**

Chapter 3.2 Functional characterization of chromosome I partition system **103-144**

3.2.1 . Materials and methods **105-111**

3.2.1.1. Expression of recombinant ParB1 and ParA1

3.2.1.2 Purification of recombinant ParA1 /ParB1proteins

3.2.1.3 DNA protein interaction studies

3.2.1.4 Measurements of ATPase activity

3.2.1.5 Cloning of *seg*S elements on mini-F plasmid and plasmid stability studies

3.2.1.6 Determination of plasmid to chromosome ratio

3.2.1.7 Construction of *parB1* deletion mutant in *D. radiodurans*

3.2.1.8 Generation of GFP - ParB1 / GFP- ParA1 translation fusion protein

3.2.1.9 Microscopic studies

3.2.1.10 Oligomerization studies using sedimentation assay and light scattering

3.2.2.0 Results **111 - 144**

3.2.2.1 ParA1 and ParB1 were expressed in *E. coli* and purified to homogeneity

3.2.2.2 ParB1 showed specific interaction with predicted centromere

3.2.2.3 ParA1 is a DNA binding ATPase *in vitro*

3.2.2.4 Interaction of ParA1 with DNA

3.2.2.5 ParA1 interaction with ParB1 bound with DNA

3.2.2.6 *In vivo* characterization of chromosome I of partition proteins

Chapter 3.3 Molecular studies on chromosome II partitioning proteins **145 -174**

3.3. 1 Materials and Methods **147-152**

3.3. 1.1 Cloning of recombinant ParA2 protein

3.3.1.2 Expression and purification of recombinant proteins

3.3.1.3 DNA protein interaction studies

3.3.1.4 Measurements of ATPase and GTPase activities

3.3.1.5 Sedimentation Analysis

3.3.1.6 Construction of *parB2* deletion mutant in *D. radiodurans*

3.3.1.7 Microscopic studies

3.3.1.8 Co-localization of ParA2-CFP and FtsZ-YFP and Fluorescence microscopic Studies

3.3.2.0 Results **153-174**

3.3.2.1 The *parB2* mutant of *D. radiodurans* showed pleiotropic phenotypes

3.3.2.2 Mechanism(s) of ParA2 inhibition of cell division

3.3.2.3 ParA2 effect on characteristics features of recombinant $FtsZ_{Ec}$

3.3.2.4 Cell division inhibition through Nucleoid occlusion mechanism in ParA2 expressing cells

Chapter 4 Discussion **175-182**

Chapter 5 Summary and future perspectives **183- 188**

Reference **189 -198**

SYNOPSIS

Introduction:

An accurate duplication and transmission of genetic information is a fundamental attribute of the life and that determines the successful inheritance of different phenotypes in daughter cells. Chromosome segregation in eukaryotic system are relatively better understood, whereas the understanding of segregation mechanism in prokaryotes remains obscure (Leonard *et al.*, 2005). In 1963 a passive model was first proposed, which suggested that the separation of duplicated chromosomes occurs by formation of the septa at the mid of the cell. Information obtained by employing the recent advances in microscopy and electrophoresis etc. suggested that DNA segregation in bacteria is an active process (Draper and Gober, 2002;Ebersbach and Gerdes, 2005;Fogel and Waldor, 2005;Gerdes *et al.*, 2010;Gordon and Wright, 2000;Moller-Jensen and Gerdes, 2007). In bacteria, the genome partitioning occurs mainly by pushing or pulling of duplicated genome toward the cell poles. This involves three core components (i) centromere like sequence or *cis*-element (Lin and Grossman, 1998;Martin *et al.*, 1991) (ii) a centromere binding protein (Schumacher *et al.*, 2010;Vecchiarelli *et al.*, 2010) and (iii) an actin homologue of bacterial ATPase, which through the dynamics created during polymerization/depolymerization of this protein provide force leading to the separation of daughter chromosomes in opposite direction (Ebersbach and Gerdes, 2001;Fogel and Waldor, 2006;Salje *et al.*, 2010;Shebelut *et al.*, 2010). There are different types of *cis* elements like *parS* in P1 plasmid, *parC* in R1 plasmid (Gerdes *et al.*, 2010) and chromosomal centromeres (similar to *Bacillus subtilis*) have been reported from the

bacteria harboring single circular chromosome and or a low copy plasmid. After genome sequencing, several bacteria having multiple chromosomes have been reported from diverse phylogenetic groups. Some of these are the *Agrobacterium tumefaciens, Sinorhizobium meliloti* (Choudhary et al., 1994), *Deinococcus radiodurans* (White *et al.*, 1999) and human pathogen *Vibrio cholerae* (Egan *et al.*, 2005) and *Burkholderia cenocepacia* (Dubarry *et al.*, 2006) which harbor multipartite genome. The molecular basis of multipartite genome segregation and the nature of chromosome partitioning systems in these organisms are not well understood. However, in case of *Vibrio cholerae*, it has been shown that both the chromosomes have distinct replication machinery and the localization and segregation systems are different as well as chromosome specific.

Deinococcus radiodurans R1 (DEIRA), a member of *Deinococcaceae* family, is a non-pathogenic, pink pigmented non-sporulating, Gram positive bacterium. It shows extraordinary tolerance to ionizing radiation, far UV radiation, hydrogen peroxide and other DNA damaging agents including desiccation (Slade and Radman, 2011). Apart from these features, DEIRA shows ploidy with four genome, chromosome I, chromosome II, a megaplasmid and a small plasmid (White *et al.*, 1999). The mechanisms underlying the maintenance of ploidy and faithful inheritance of multipartite genome during normal as well as radiation stressed growth are not known and would be worth investigating. Genome of this bacterium was annotated with putative operons made up of *parA-parB* genes. Except small plasmid, other genome replication units have their own sets of putative ParA and ParB proteins. Centromeric sequences are not known in any of these genomes. The presence of multiple sets of 'Par' proteins has been reported in bacteria harboring multipartite genome system. This raises a question on the possible

functional redundancy amongst these proteins. Understanding the functionality of 'Par' proteins encoded on different replication units in

D. radiodurans would be a step forward in understanding the mechanism(s) of chromosome segregation in bacteria harboring complex genome system. Therefore, we have planned to study the mechanisms of genome segregation in *Deinococcus radiodurans*.

Here we propose to undertake the above study in following objectives

Objective1. Cloning and purification of recombinant ParA and ParB proteins of *Deinococcus radiodurans*.

Objective2. Generation of ParA and ParB translational fusion with different fluorescent proteins.

Objective3. Monitoring the *in vivo* interaction of fluorescent tagged recombinant proteins, among each other, and with bacterial genomes by fluorescence microscopy.

Objective4. Generation of *parB* deletion mutant (s) and studying the redundancy of different *parB*(s) in genome segregation and individual genomes in cell survival.

The work carried out to address the above objectives will be presented in this thesis in following chapters

Chapter 1: General Introduction and Review of Literature

Chapter 2: Materials and Experimental Procedures

Chapter 3: Results

3.1 Identification of genome partitioning elements using bioinformatic approaches.

3.2 Functional characterization of chromosome I partitioning system

3.3 Molecular studies on chromosome II partitioning proteins

Chapter 4: General Discussion

Chapter 5: Summary, Conclusion and Future prospective

Chapter 1. General introduction and review of literature:

This chapter describes general information on both plasmid and chromosome partitioning systems, various hypotheses proposed to explain the mechanism of genome segregation and important features about model organism *Deinococcus radiodurans*.

Chapter 2. Materials and Methods:

This chapter describes the details of materials used along with their sources, and general methods used in this study. Different techniques and approaches used in this study will be described under the categerory of (1) Bioinformatic analysis – use of readily available online tools like Blast (2) Biochemical techniques including protein purification, EMSA, ATPase assay and Light scattering etc. (3) Recombinant DNA technology and molecular biology techniques including cloning, generation of deletion mutants and their conformation and (4) microscopic studies.

Chapter 3: Results:

This chapter starts with a preamble describing the hypotheses and the logical anticipation from this study. The results obtained to test the hypotheses along with other new findings

during the course of this investigation are presented. The results obtained from this study have been presented in three sub-chapters. Each starts with a brief introduction, experimental procedures and results obtained from that specific study, followed by a brief discussion on the findings specific to the results are included in this section.

Chapter 3.1: Identification of genome partition elements using bioinformatic approaches:

The consensus centromeric sequences of both P1 plasmid type (*parS*) and chromosomal type (BS) elements as reported initially from *Bacillus subtilis* were searched in the genome of this bacterium. The results showed the presence of heptameric and hexameric boxes similar to plasmid type *parS* element on chromosome I, chromosome II and the megaplasmid. However, the organization of these boxes in all the three genetic elements was different from typical *parS* element characterized from P1 plasmid. In addition, the IHF (**I**ntegrative **H**ost **F**actor) binding site present at the central region of P1 *parS* was absent in the hypothetical *parS* element of *D. radiodurans*. Further, the Blast-N analysis showed that chromosome I also had three more putative centromeric sequences nearly identical to *parS* of *B. subtilis*, which has been reported in nearly 69% of bacterial chromosome sequences so far. These differ marginally from each other and are located in different regions of chromosome I and therefore, named as *segS*1, *segS*2, *and segS*3 elements. Chromosome II and megaplasmid do not contain typical *segS* type centromeric sequences. Thus, the possibility of the aberrant P1 type *parS* elements found in this study may have a role in segregation of these secondary genome elements cannot be ruled out. In spite of the facts that single nucleotide change in boxes and absence of IHF binding

site abolish the productive interaction of ParB with *parS* element, the possibility of these aberrant *parS* sequences working in this organism may be worth investigating.

The Genome of this bacterium has been annotated with putative 'Par' proteins like ParA and ParB, mainly on the basis of the amino acid sequence similarities with known 'Par' proteins and the position of *parAB* operon on respective chromosome. Amino acid sequences of these proteins were searched for functional motifs through Clustal-X analysis. ParB proteins showed higher similarities with the known chromosomal type ParB proteins. Multiple sequence alignment of ParB proteins with similar proteins in database showed the presence of all functional motifs of typical ParB's characterized in other systems with some minor variations in HTH region. ParA proteins however, are much diverged than the ParB proteins from other bacteria. Multiple sequence alignment of ParA type proteins shows some variation in the N- terminal region as compared to the other well characterized ParA proteins. Based on phylogenetic analysis we sub-categorized ParA1, ParB1 (DR0013, DR0012) (ParA and ParB of chromosome I) into chromosomal type 'Par' proteins where as the ParA's and ParB's of accessory chromosome i.e. of chromosomal II (DRA0001, DRA0002) and megaplasmid (DRB0001, DRB0002 and DRB0031, DRB0030) were found along with another sub-family, which are distinct from the chromosomal ParA and assumed to behave differently than the normal ParA and ParB known in bacterial genome segregation.

Chapter 3.2: Functional characterization of chromosome I partition system.

This chapter contains the results obtained from both *in vivo* and *in vitro* functional characterization of ParA and ParB proteins and three putative centromeric sequences (*segS*1, *segS*2 and *segS*3) of chromosome I. Coding sequences of both the proteins ParA

and ParB of chromosome I (hereafter referred as ParA1 and ParB1) were cloned, recombinant proteins purified and identities ascertained using a mass spectrometer. ParA1 was found to be a dsDNA binding ATPase while ParB1 showed sequence specific centromere binding protein having nearly similar affinity with all the three chromosomal centromeric sequences (*segS*1/*segS*2/*segS*3). ParA type proteins undergo polymerization on dsDNA in the presence of ATP, which upon interaction with ParB bound with centromeres results into depolymerization. The polymerization/depolymerization dynamics of ParA type proteins provided a motor function for the segregation of duplicated genome. Polymerization characteristics of ParA1 was therefore, studied in the presence of ParB1 and s*egS* elements in different combinations. By using sedimentation analysis and light scattering experiments, it was demonstrated that along with the activation of ATPase activity there is a change in the amount of oligomeric structure formation, which was in agreement with the *in vivo* result. It was shown that ParA1 undergoes polymerization in presence of ParB1 bound to centromeric sequences in presence of ATP. After certain period of incubation, the depolymerization is triggered resulting in decrease of light scattering as well as amount of ParA1 in pellet.

In vivo functional characterization was carried out by (i) deleting the *parB1* gene from genome of *D. radiodurans* and monitoring the effect of deletion on growth and anucleation, and (ii) cloning the *segS* elements on an unstable mini-F plasmid pDAG203, and monitoring its stable inheritance in *E. coli*. The N-terminal translation fusion was generated with GFP and the ParB localization on the genome of *D. radiodurans* was demonstrated. Wild type *E. coli* expressed with GFP-ParB showed GFP fluorescence throughout the cell. While *E. coli* harboring pDAGS3 an unstable mini-F plasmid bearing

*segS*3 centromere, and expressing GFP-ParB showed discrete foci formation on nucleoid. This suggested that ParB1 could interact with nucleoid only when found *segS* type centromere sequences. Further, *E. coli* cells harboring mini-F plasmid (pDAG203) and its *segS* bearing derivatives like pDAGS1, pDAGS2 and pDAGS3, were checked for stable inheritance of respective plasmids. Stable inheritance of recombinant plasmid and not pDAG203 vector, was observed in *E. coli*, which supported the role of *segS* elements as bacterial centromeres. Requirement of cognate ParA1/ParB1 proteins for 100% inheritance of pDAGS3 phenotype in daughter cells of *E. coli* harboring this plasmid along with other findings suggested that *segS*3 and ParA1 / ParB1 constitute the functional partitioning system for the segregation of chromosome I of *D. radiodurans*.

The *parB1* deletion mutant (Δ *parB1*) affected the growth of the bacterium under normal conditions and produced a higher frequency of anucleation as compared to the wild type further suggesting that ParB1 has a role in chromosome segregation. N-terminal translation fusion were generated with GFP and the ParA localization on the genome of *D. radiodurans* was demonstrated in different combination of centromere sequences and ParB1 protein, ParA1 alone or in presence of ParB1 has shown co-localization along with the DNA, by using time lapse experiments we were able to demonstrate differential dynamics of GFP-ParA1 protein in the presence of ParB1 and different centromere sequences. These results together suggested that chromosome I partitioning system function by pulling mechanism during genome segregation.

Chapter 3.3: Molecular studies on chromosome II partitioning proteins

This chapter describes the findings on the characterization of (i) ParA2 and its role in genome segregation and cell division and (ii) ParB2 role in genome maintenance. Recombinant proteins were made in *E. coli*, purified and confirmed by mass spectrometry. The *parB*2 deletion mutant of *D. radiodurans* showed anucleation and unusually increased the cell size compared to the wild type. Membrane staining of *parB*2 mutant showed nearly 60% of the cells had disruption of septal growth. Similar phenotype was seen when ParA2 was over expressed in wild type background. Since, both deletion mutant of *parB*2 and over expression of ParA2 in *D. radiodurans* would have higher amount of ParA2 with respect to ParB2 than wild type, the possibility of this ratio change or absence of ParB2 in cell expressing ParA2, could have affected cell division has been hypothesized. ParA2 was over expressed in *E. coli* and observed under microscope. ParA2 over expression in *E. coli* in the absence of ParB2 caused cell elongation and lethality due to arrest in the cell division. Here in this chapter, we also investigated the mechanism underlying the inhibition of cell division by ParA2. The co-expression of FtsZ-YFP (pLAU85 plasmid) and ParA2 in *E. coli* showed the inhibition of FtsZ ring formation. We also generated C-terminal CFP fusion of ParA2 and these cells were examined under fluorescence microscope. The results showed ParA2 binding throughout the genome and FtsZ-YFP foci growth was interrupted at the vicinity of nucleoid. The functional complementation of ParA2 to *slm*A mutant (nucleoid binding protein) of *E. coli* confirmed that ParA2 inhibits cell division by bringing about nucleoid occlusion at the vicinity of FtsZ ring progression. These results suggested that ParA2B2 proteins in their native stoichiometry possibly regulate genome maintenance

while any change in the ratio of these proteins in a cell, resulted in cell division arrest, until possibly duplicated genome is not fully segregated.

Chapter 4: General discussion

Mechanisms underlying bacterial genome segregation have been studied in bacteria either harboring a single circular chromosome and or a low copy number plasmid. *D. radiodurans* is amongst the several bacteria which harbor multipartite genome system. Some of these also confer ploidy. Coincidently, most of the multipartite genome harboring bacteria are stress tolerant to biotic and abiotic stress. Genome ploidy was considered as the probable factors that were implicated to efficient DSB repair and eventually the gamma radiation tolerance in *D. radiodurans*. Furthermore, the prokaryotes are mostly found with a single circular chromosome and therefore, the maintenance of multipartite genome and ploidy in bacterial system has been of great curiosity. These features make this bacterium an attractive model system to study the mechanisms of genome segregation and maintenance. In this chapter we will discuss on the identification of P1 type as well as chromosomal type centromeric sequences, the experimental validation of the predicted functions for both centromeric sequences and ParA and ParB proteins in chromosome I segregation. Using BLAST short sequence homology search analysis the consensus sequences of P1*parS* and *B. subtilis* type chromosomal centromeres were found. Further analysis revealed that although chromosome I had all the boxes as found in *parS* of P1 plasmid, the spacing between these boxes were different from the typical *parS* structure and the IHF binding site was absent. Since, the consensus structure of inverted boxes, spacing between these boxes and IHF binding have been shown to be important features in *parS* required for productive

interaction with ParB therefore, the possibility of P1 type centromere functioning in chromosome I segregation was nearly ruled out. Experimental evidence was obtained corroborating these facts that ParB interaction with *parS* element was non-specific. BS type element (named as *segS*) found in chromosome I was eventually characterized as the true centromere for chromosome I partitioning and demonstrated its functionality both *in vivo* and *in vitro*. The presence of multiple centromere's on both the primary and secondary chromosomes of bacteria containing multipartite genome system has been reported earlier (Dubarry *et al.*, 2006;Fogel and Waldor, 2005;White *et al.*, 1999).

Characterization of ParA1 and ParB1 showed a few interesting observations. ParB1 interacted almost with equal affinity with all three *cis* elements (*segS*1/*S*2/*S*3). Incubation of ParB1 and *segS* elements with ParA1 showed different levels of stimulation in ATPase activity of ParA1. Similarly, ParA1 incubated with ParB1 and *segS* elements showed an increase in the size of macromolecules as measured by change in light scattering. Interestingly, the effect of ATP on these characteristics increase was different with different *segS* elements. These observations are intriguing, given the facts that ParA polymerization on dsDNA and depolymerization after interacting with ParB1-centromere complex. Various possibilities explaining this result are discussed. Another observation was that the recombinant plasmid pDAGS1/ pDAGS2 and pDAGS3 having *segS*1 *segS*2 and *segS*3 cloned on unstable mini-F plasmid pDAG203 respectively, showed the differential requirement of ParA1 and ParB1 for their stable inheritance in *E. coli*. The differential stabilization of pDAGS1, pDAGS2 and pDAGS3 is also discussed.

Deletion of *parB*1 increased the frequency of the chromosome loss in *D. radiodurans*, however, that doesn't show any change in the cell morphology while *parB2* deletion

showed both anucleation and cell morphology change. These results on this one hand nearly ruled out the functional redundancy amongst various ParB's that exist in this bacterium. On the other hand it brought more specific questions on how *parB2* deletion affected cell morphology. Similar results were obtained when ParA2 was over expressed in both in *D. radiodurans* and in *E. coli*. In these cells the anucleation was not observed. Here we will be discussing about the information on coordination of cell division with genome segregation as existed in different bacterial systems with respect to the 'Par' proteins. Likewise, all the results obtained under this study are discussed within the existing information on the subject, hypothesized, speculated and interpreted to a logical conclusion.

Chapter 5: Summary, conclusion and future prospective

This chapter briefly summarizes the work presented in this thesis by highlighting the potential observations and results obtained that supported the hypotheses and also the unanswered questions / new hypotheses generated during this course of the study. Along with several interesting findings reported in this thesis, we have been characterized both the centromeres and partitioning proteins encoded on chromosome I of *D. radiodurans*. It has also been demonstrated that chromosome I has multiple chromosomal type centromeric sequences and 'Par' proteins that are functionally similar to the 'Par' proteins known in single chromosome harboring bacteria. Molecular interaction studies of ParA1, ParB1 and centromeric sequences as a function of ATP, indicated that chromosome I partitioning seems to follow Type I genome segregation mechanism i.e. pulling mechanism. Interestingly, we observed that in spite of having common motifs 'Par' proteins of accessory chromosomes are grouped with different class of proteins in

phylogenetic tree and apparently they express different functions. However, ParB1 and ParB2 both are involved in genome maintenance but ParB2 also regulates cell division perhaps by titrating ParA2 from inhibiting FtsZ ring formation and cytokinesis. Molecular studies on ParA2 inhibition of cell division suggest that ParA2 brings about nucleoid occlusion and blocks the growth of FtsZ ring in *E. coli* and septal growth in *D. radiodurans*. Also the conclusion drawn from this study will be deciphered.

This study has answered some of the questions and tested the hypotheses proposed by both experimentally and through bioinformatic analysis, it has left several unanswered questions. The immediate ones may that require attention include (i) The real-time monitoring of ParB1 protein interaction with centromere's and demonstration of ParA1 dynamic movement on genome leading to duplicated genome segregation, (ii) how do three *segS* function in chromosome I partitioning *in vivo*, (iii) functional redundancy of various ParA and ParB proteins during genome segregation, (iv) ParA2 characterization has provided strong clues that this protein is linked between cell division and genome segregation, the factors determining for ParA2 performing one of the two functions at molecular levels would be worth studying, and (v) there are putative centromeric sequences marginally different from typical *parS*, it would be interesting to see if aberrant *parS* present on chromosome II and megaplasmid may function as centromeric region on these replication units and that would be a novel finding indicating a logical shift in paradigm.

Publications:

Published :

- **Charaka, V. K. and Misra, H. S. (2012) Functional characterization of chromosome I partitioning system in *Deinococcus radiodurans* for its role in genome segregation. J. Bacteriol. 194:5739-5748.**

- **Charaka, V.K.umar and Misra, H.S. (2013) ParA2, A hypothetical walker type DNA binding ATPase of *Deinococcus radiodurans*, arrests septal growth by Nucleoid occlusion mechanism. J. Bioscience. 38:487-497.**

- **Kota, S., Charaka, V.K.,and Misra, H.S. (2010) Characterization of an ATP-regulated DNA-processing enzyme and thermo tolerant phosphoesterase in the radioresistant bacterium *Deinococcus radiodurans*. Biochem J. 431:149-157.**

Communicated:

- **Kota,S., Charaka,V.K.,Ringgaard,S., Waldor,M.K. and Misra,H.S (2013)PprA has a role in maintenance of damaged genome in *Deinococcus radiodurans*, pLOS one (*Under revision*)**

Signature of Student:

Date:

Doctoral Committee:

S. No.	Name	Designation	Signature	Date
1.	Prof. A. K. Sharma	**Chairman**		
2.	Prof. H. S. Misra	**Guide**		
3.	Prof. J. R. Bandekar	**Member**		
4.	Prof. (Mrs) J. K. Sainis	**Member**		
5.	Prof. Dulal Panda	**Member**		

Reference List

Choudhary,M., Mackenzie,C., Nereng,K.S., Sodergren,E., Weinstock,G.M., and Kaplan,S. (1994) Multiple chromosomes in bacteria: structure and function of chromosome II of *Rhodobacter sphaeroides* 2.4.1T. *J Bacteriol* 176: 7694-7702.

Draper,G.C., and Gober,J.W. (2002) Bacterial chromosome segregation. *Annu Rev Microbiol* 56: 567-597.

Dubarry,N., Pasta,F., and Lane,D. (2006) ParABS systems of the four replicons of *Burkholderia cenocepacia*: new chromosome centromeres confer partition specificity. *J Bacteriol* 188: 1489-1496.

Ebersbach,G., and Gerdes,K. (2001) The double par locus of virulence factor pB171: DNA segregation is correlated with oscillation of ParA. *Proc Natl Acad Sci U S A* 98: 15078-15083.

Ebersbach,G., and Gerdes,K. (2005) Plasmid segregation mechanisms. *Annu Rev Genet* 39: 453-479.

Egan,E.S., Fogel,M.A., and Waldor,M.K. (2005) Divided genomes: negotiating the cell cycle in prokaryotes with multiple chromosomes. *Mol Microbiol* 56: 1129-1138.

Fogel,M.A., and Waldor,M.K. (2005) Distinct segregation dynamics of the two Vibrio cholerae chromosomes. *Mol Microbiol* 55: 125-136.

Fogel,M.A., and Waldor,M.K. (2006) A dynamic, mitotic-like mechanism for bacterial chromosome segregation. *Genes Dev* 20: 3269-3282.

Gerdes,K., Howard,M., and Szardenings,F. (2010) Pushing and pulling in prokaryotic DNA segregation. *Cell* 141: 927-942.

Gordon,G.S., and Wright,A. (2000) DNA segregation in bacteria. *Annu Rev Microbiol* 54: 681-708.

Leonard,T.A., Moller-Jensen,J., and Lowe,J. (2005) Towards understanding the molecular basis of bacterial DNA segregation. *Philos Trans R Soc Lond B Biol Sci* 360: 523-535.

Lin,D.C., and Grossman,A.D. (1998) Identification and characterization of a bacterial chromosome partitioning site. *Cell* 92: 675-685.

Martin,K.A., Davis,M.A., and Austin,S. (1991) Fine-structure analysis of the P1 plasmid partition site. *J Bacteriol* 173: 3630-3634.

Moller-Jensen,J., and Gerdes,K. (2007) Plasmid segregation: spatial awareness at the molecular level. *J Cell Biol* 179: 813-815.

Salje,J., Gayathri,P., and Lowe,J. (2010) The ParMRC system: molecular mechanisms of plasmid segregation by actin-like filaments. *Nat Rev Microbiol* 8: 683-692.

Schumacher,M.A., Piro,K.M., and Xu,W. (2010) Insight into F plasmid DNA segregation revealed by structures of SopB and SopB-DNA complexes. *Nucleic Acids Res* 38: 4514-4526.

Shebelut,C.W., Guberman,J.M., van,T.S., Yakhnina,A.A., and Gitai,Z. (2010) *Caulobacter* chromosome segregation is an ordered multistep process. *Proc Natl Acad Sci U S A* 107: 14194-14198.

Slade,D., and Radman,M. (2011) Oxidative stress resistance in *Deinococcus radiodurans*. *Microbiol Mol Biol Rev* 75: 133-191.

Vecchiarelli,A.G., Han,Y.W., Tan,X., Mizuuchi,M., Ghirlando,R., Biertumpfel,C. et al. (2010) ATP control of dynamic P1 ParA-DNA interactions: a key role for the nucleoid in plasmid partition. *Mol Microbiol* 78: 78-91.

White,O., Eisen,J.A., Heidelberg,J.F., Hickey,E.K., Peterson,J.D., Dodson,R.J. et al. (1999) Genome sequence of the radioresistant bacterium *Deinococcus radiodurans* R1. *Science* 286: 1571-1577.

LIST OF FIGURES

Fig 1.1: P1 *parS* structure

Fig 1.2: Diffusion ratchet Model

Fig1.3: F plasmid segregation models

Fig 1.4: Pulling model

Fig 1.5: Pushing mechanism

Fig1.6: Role of 'Par' proteins in *B. subtilis*

Fig 1.7: Segregation mechanism in *C. crescentus*

Fig 1.8: ESDSA mechanism in *D. radiodurans*

Fig 3.1.1: Centromere sequences on chromosome I of *D. radiodurans*

Fig 3.1.2: Analysis of P1 type of centromere like sequence in *D. radiodurans*

Fig 3.1.3: Multiple alignment of ParB protein with chromosomal ParB

Fig3.1.4: 3-D model of ParB1of *D. radiodurans*

Fig 3.1.5: Graphic representation of deviant walker type motifs in *Deinococcal* ParA proteins

Fig 3.1.6: Multiple Alignment of ParA proteins

Fig 3.1.7: 3-D model of ParA1 of *D. radiodurans*

Fig 3.1.8 a: Phylogenetic tree of ParB proteins

Fig 3.1.8b: Phylogenetic tree of 'ParA' proteins

Fig 3.2.1a: Cloning, expression and purification of 'ParB1' protein

Fig 3.2.1b: Cloning, expression and purification of 'ParA1' protein

Fig. 3.2.2: ParB1 interaction with *segS* type centromere's of chromosome I

Fig 3.2.3: DNA binding activity of ParA1

Fig 3.2.4: ATPase activity of ParA1

Fig 3.2.5: Interaction of ParA1 with DNA by using sedimentation analysis

Fig 3.2.6: Light scattering analysis

Fig 3.2.7: Stimulation of ParA1 ATPase activity

Fig 3.2.8: Interaction of ParA1 with ParB1 nucleoprotein complex

Fig 3.2.9: Interaction of ParA1 with ParB1 nucleoprotein complex studied using Light scattering analysis

Fig 3.2.10: Centromere activity assay of *segS* elements using plasmid stability test in *E. coli*

Fig 3.2.11: Construction and expression of pDSW parA1parB1 plasmid:

Fig 3.2.12: Generation of Δ*parB1* mutant

Fig 3.2.13: Effect of ParB1 deletion on genome maintenance in *Deinococcus radiodurans*

Fig 3.2.14: Effect of ParB1 deletion on *D. radiodurans* cell morphology

Fig 3.2.15: Generation of GFP-ParB1 translational fusion protein

Fig 3.2.16: Interaction of ParB1 with nucleoid.

Fig 3.2.17: Localization of GFP-ParA1 in *E. coli* cells

Fig 3.2.18: Dynamics of GFP – ParA1 in *E. coli* cells

Fig 3.2.19: GFP –ParA1 florescence distribution in *E .coli* cells

Fig3.3.1: Generation of pNOK A0002 plasmid

Fig 3.3.2: Growth curve analysis
Fig 3.3.3: Effect on chromosome segregation
Fig3.3.4: Effect of ParB2 on cell morphology
Fig3.3.5: ParB2 effect on cell division process
Fig 3.3.6: Effect of ParA2 expression on growth characteristics of *E. coli*
Fig 3.3.7: Effect of ParA2 expression on increase in cell size of *E. coli*
Fig3.3.8: Analysis of ParA2 expression on increase in cell size of *E. coli*
Fig3.3.9: Effect of ParA2 expression on FtsZ ring formation in *E. coli*
Fig 3.3.10: Expression and purification of ParA2 protein
Fig 3.3.11: Interaction of ParA2 with FtsZ by using GTPase assay
Fig3.3.12: Interaction of ParA2 with FtsZ by using sedimentation analysis
Fig3.3.13: *In vitro* activity characterization of recombinant ParA2
Fig 3.3.14: Localization of ParA2 in *E. coli* cells
Fig 3.3.15: Functional complementation studies

LIST OF TABLES

Table 2.1	**Composition of stock solutions**
Table 2.2	**Antibiotic stock solutions**
Table 2.3	**List of bacterial strains used in this study**
Table 2.4	**List of primers used in this study**
Table 2.5	**List of plasmids used in this study**
Table 2.6	**Composition of 10 % separating polyacrylamide gel**
Table 2.7	**Gradient gel composition**
Table 3.1:	**Organization of 'par' genes in *D .radiodurans***
Table3.2:	**Effect of ParB1 Deletion on anucleation of *D. radiodurans***

LIST OF ABERIVATIONS:

D. radiodurans	*Deinococcus radiodurans*	LB	Luria Broth
E. coli	*Escherichia coli*	TYG	Tryptone yeast extract Glucose media
B. subtilis	*Bacillus subtilis*	FISH	Florescence in-situ hybridization
C. crescentus	*Caulobacter cresentus*	PCR	Polymerase chain reaction
S. enterica	*Salmonella enteric*	PFGE	Pulsed field gel electrophoresis
V. cholerae	*Vibrio cholera*	RT	Room Temperature
T. thermophilus	*Thermus thermophilus*	W/V	weight/volume
P. aeruginosa	*Pseudomonas aeruginosa*	Ni-NTA	nickel-nitrilo acetic acid
B. coencephacia	*Burkholderia coencephacia*	EDTA	Ethylene diamine tetra acetic acid
S. colicolor	*Streptomyces coelicolor*	dsDNA	Double stranded DNA
		HTH	Helix Turn Helix
		RMSD	Root-mean-square deviation
		MSA	Multiple sequence alignment

CHAPTER 1

General Introduction and Review of Literature

Segregation is defined as a process that assures stable genome transmission from one generation to another. Precise duplication and transmission of genetic information is a fundamental attribute of the life and determines the successful inheritance of different phenotypes in daughter cells. The failure of chromosome segregation causes genetic defects leading to either the suppression or activation of gene functions and thereby changes in phenotype. The basic mechanism of chromosome segregation is relatively better understood in eukaryotes (Yanagida, 2005). In these systems, the chromosome replication, segregation and cell division are temporally separated. Chromosomes are duplicated in S-phase and remain together during G2 phase. Partitioning occurs in M-phase and then the cell divides after the chromosomes have segregated to opposite halves of the cell. The chromosomal duplication and segregation are mainly driven by the cyclin dependent kinases. During the early metaphase stage the sister chromatid pairs are captured by the microtubules that move the two sister chromatids to the opposite poles by an GTP dependent process (Tessema *et al.*, 2004). A large number of proteins involved in replication and segregation were characterized and their roles in eukaryotic genome segregation have been documented.

In prokaryotes, genome segregation mechanisms have been studied mostly in bacteria harboring single circular chromosome and low copy number plasmids like F plasmid, P1 plasmid and R1 plasmid of *E. coli* (Ebersbach *et al.*, 2005;Ghosh *et al.*, 2006;Gitai, 2006;Gordon and Wright, 2000;Leonard *et al.*, 2005). Any missegregation results in decrease in copy number or generation of plasmid free cells. These cells are subsequently cleared off due to post segregation killing mechanisms (Gerdes and Molin, 1986). Unlike the well-characterized biology of the eukaryotic mitotic apparatus, much is still unknown

about the genome partitioning mechanisms and proteome in prokaryotes. The major factors that limit the studies on genome segregation in bacteria include (i) the size of the organism, (ii) inseparable cell division phases and duplication phase (iii) most mutations of partitioning genes show pleiotropic effects (Leonard *et al.*, 2005). In addition, the cytogenetic features in bacteria like organization of chromosome within the cell (Bloom and Joglekar, 2010), chromosome number variation within bacterial genera and lack of high resolution microscopic techniques that can image less than 2 micron size bacterial cell are some of the other features that makes study on genome segregation in bacteria much more challenging than eukaryotes.

1.1 Mechanisms of bacterial genome segregation

For maintenance of plasmids or chromosomes various mechanisms are involved few of them are described in this chapter. Several hypotheses or models have been proposed for explaining the mechanism of genome segregation in bacteria. First model was proposed by Jacob and co workers in 1963, which state that chromosome segregation is a passive mechanism i.e. duplicated chromosomes are separated due to insertion of the septa in the mid of the cell. Passive model of genome segregation could not accommodate the findings showing that duplicated DNA is separated due to insertion of the membrane at a single point that was the basis of passive model, further studies had shown insertion of the new membrane material occurs throughout the cell (Hiemstra *et al.*, 1987;Wientjes and Nanninga, 1989). Distribution of newly synthesized membrane into cell membrane, visualization of DNA movements in *B. subtilis* and *C. crescentus* (movement of DNA is much faster than the cell elongation rate) has weakened Jacob and co-workers hypothesis. This indicated the involvement of other factors in separation of two sister chromosomes.

The driving force or tension responsible for bringing bacterial chromosomes steadily apart was questioned and initially conditional mutants were isolated which were associated with DNA topological problems e.g. change in resolution, which perturbed the chromosome segregation (Lemon and Grossman, 2001;Sawitzke and Austin, 2000). Studies on these observations indicated many factors or proteins are involved in active partition mechanism.

In 1996, Grossman proposed *extrusion capture* model for active chromosome segregation, according to this model the force for separation is provided by some powerful threading machines like DNA polymerase or RNA polymerase (Lemon and Grossman, 2001). Replisosme is localized at mid position of the cell where DNA polymerase initiates replication and duplicated DNA is pushed outwards to replisosme. Separated sister chromosomes are captured by the membrane anchoring regions and DNA is spooled outward from mid of the cell towards opposite side of the cell. Subsequently, Dworkin and Losick also suggested that the force required for chromosome segregation is provided by the RNA polymerase. They showed that inhibition of RNA polymerase activity by streptolydigin restricted DNA movement as compared to untreated cells. It was hypothesized that transcription of the oppositely oriented genes near the origin of replication generates force, which could result in bulk movement of DNA. However it's unlikely that these polymerases are molecules that are involved in separation of duplicated DNA due to following reasons: DNA is long flexible polymer, DNA polymerase or RNA polymerases are unable to push the low rigid and high flexible polymer to opposite side of the cell (Dworkin and Losick, 2002)**.** The variation in spatiotemporal organization of replisosme from organism to organism, which

is at mid cell position in *B. subtilis* while it is at the ¾ position of the cell in *C. crescentus* (Jensen *et al.*, 2001) and lack of defined start site of partition ruled out the involvement of either RNA or DNA polymerase in the chromosome segregation. Recent well accepted model involves existence of mitotic like machinery (Actin or Tubulin like proteins), which actively segregate DNA (plasmid or chromosome) into daughter cells.

1.2 Mechanisms of plasmid segregation

In general, plasmids or chromosome encode two trans acting factors (ParA and ParB) and one cis factor (centromere like sequence). One of the trans acting factors is an NTPase protein (Motor protein) named as ParA (P1, pB171plasmid, etc), ParM (R1 plasmid), SopA (F plasmid), Soj (*B. subtilis*) and another is a site specific DNA binding protein (adapter protein) named as ParB (P1 plasmid, pB171 plasmid, etc), ParR (R1 plasmid), SopB (F plasmid) and Spo0J (*B. subtilis*) which binds to specific centromere sequence these were named as *parS*, *parC*, *sopC* etc. These centromere like sequence are diverged from one partition system to another either in organization or localization of centromere like sequence differs in different segregation systems. In brief the organization of centromere sequence in plasmids comprises either direct repeats (*sopC*, P1 *parS*) or indirect repeats (*parS* of *B. subtilis*) (Table 1.1).

General mechanism of segregation is described as an adapter protein (ParB) specifically interacts to the centromere like sequence (*parS*) to form a high nucleoprotein complex, when NTPase protein (ParA) interacts with this nucleoprotein complex (adaptor-centromere complex) which specifically stimulate the NTPase activity, ultimately separating duplicated genome to opposite poles (Ebersbach and Gerdes, 2005;Gitai, 2006;Gordon and Wright, 2000;Leonard *et al.*, 2005). In spite of having nearly similar

functions of partitioning proteins and centromere's reported from different bacteria the molecular mechanisms of segregation are found to be different for chromosome and plasmid.

Based on type of NTPase proteins in plasmids, the '*par*' systems are classified into four types. (1) Type I '*par*' system encode Walker box containing P- loop ATPase proteins and reported in P1, F, pB171, pTAR, pTP228 plasmid. (2) Type II '*par'* system comprised of NTPase protein having structurally actin like fold of mammalian system and reported from R1 plasmid of *E. coli.* (3) Type III '*par'* system involves NTPase protein showing structural homology with tubulin like GTPase domain and reported from pBtoxsis plasmid and (4) Type IV '*par*' system is best studied in case of pSK+ plasmid.

1.2.1Type I partition system:

Type I NTPase class proteins are most widely distributed from plasmid to chromosome e.g. P1 ParA (P1 plasmid), SopA (F plasmid), Soj (*B. subtilis*), MinD (cell division inhibitor protein). Typically type I '*par*' family proteins encode Walker type motif or deviant Walker type motif. Based on size of NTPase protein Type I partition system is divided into two sub-classes Type Ia and Type Ib (Gerdes *et al.*, 2010). Type Ia NTPase family includes *parABS* of P1 plasmid and *sopABC* of F plasmid. NTPase size ranges from 200 to 400 amino acids, whose N- terminal region contain extra helix turn helix region which aids in auto regulation process (Austin and Abeles, 1983;Ogura and Hiraga, 1983). Type Ib NTPase family includes *parFGH* from pTP228 plasmid of *S. enterica*, *parABC* from pB171 plasmid and δ/ω from pSM19035. NTPase protein in this family are smaller in size lacking N-terminal region, doesn't auto regulate gene expression, however in presence of ParB, ParA autoregulate its gene expression.

P1 plasmid

P1 '*par*' family consists of six members which are broadly distributed throughout bacterial genera for e.g. P1 prophage and P7 prophage in *E. coli*, pMT1 in *Yersinia pestis*, pWR100 in *Shigella flexneri* etc (Dabrazhynetskaya *et al.*, 2009). Active segregation mechanism was first seen in P1 prophage plasmid. Localization studies of P1 plasmid indicated that plasmid is either positioned at mid or at ¼ position within the cell (Erdmann *et al.*, 1999;Mascarenhas *et al.*, 2005;Ringgaard *et al.*, 2009). Faithful inheritance of plasmid depend upon the function of partitioning genes (*parABS*) (Erdmann *et al.*, 1999). Motor protein in P1 Plasmid named as ParA. P1 ParA is a 44 kDa P-loop type ATPase encoded in '*par*' operon and plays important role in partition of plasmid as well as in auto regulation of partition genes. ParA has an intrinsic weak ATPase activity, which gets specifically stimulated by its cognate ParB-*parS* nucleoprotein complex. ParA protein can be broken down into N-terminal region, HTH region, and C-terminal region (Dunham *et al.*, 2009). N-terminal region is an extended α helix region (1-43 residues) which is known to play important role in dimerization, winged helix turn helix region (44-104) contain DNA binding region that will help in regulation of protein (Bouet and Funnell, 1999), C-terminal region contains walker type motif region as well as ParB interacting domain. Nucleotide (ATP) binds to C-terminal region and hydrolyzes the ATP into ADP in presence of DNA or cognate ParB protein.

ParB encoded on P1 plasmid is a 38 kDa adaptor protein which binds to centromere like sequence to form nucleoprotein complex. ParB protein consists of N-terminal domain and C-terminal domain. N-terminal region (1-144 residues) contain ParA interacting domain (Surtees and Funnell, 1999). Where as, C- terminal region (144 – 233) contains the

necessary information for binding to centromere sequences. Crystal structure of P1 ParB shown that amino acid residues form seven α helical region (Helix turn helix region) connected by 4 flexible amino acids to an independent domain consisting of three anti parallel β strands. Packing of these β strands dimerizes Par B. Dimeric ParB protein interacts with P1 *parS* in two fold (Surtees and Funnell, 1999). Initially HTH domains of ParB monomer bind to the heptameric sequence of P1 *parS.* Beta dimer domains independently bind to hexameric repeats of P1 *parS*. Two arms of ParB assists in DNA binding where as IHF (Integrative Host Factor) bind to specific DNA sequence (IHF binding site) that makes DNA to bend (Funnell, 1988). Due to bending of *parS* ParB spans both arms of P1 *parS* simultaneously (Schumacher and Funnell, 2005) and aid in formation of nucleoprotein complex. Its intrinsic weak ATPase activity is specifically stimulated by ParB-*parS* specific nucleoprotein complex. It is hypothesized that force required for partition is provided by ATPase protein.

Plasmid type '*parS*' is a 34 bp DNA fragment which is located downstream to the *parAB* gene. ParB protein known to interact specifically to P1 *parS* centromere sequence. The P1 *parS* is a complex structure having four copies of heptameric sequences (A box with consensus G/$_{T}$TGAAAT) and two copies of hexameric sequence (B box with consensus TCGCCA)**.** Broadly P1 *parS* can be divided into three regions left and right and central region, central region contains consensus WATCAANNNNTTR (W is dA or dT, R is dA or dG, and N is any nucleotide) sequence (Hales *et al.*, 1994) to which **I**ntegration **H**ost **F**actor (IHF) binds and causes DNA looping, bending of DNA helps in bringing left and right boxes in close proximity through which ParB interacts with right and left hand side of *parS.*

ParB initially binds to *parS* sequence with high affinity and is followed by the loading of the additional ParB molecules onto the looped site through specific and nonspecific interaction with the DNA (Schumacher, 2007). Mutational analysis defined boundaries of the *parS* sequence, deletion of left handed sequence i.e. box A1B1 doesn't changed stability of plasmid but deletion or substitution of base pair in right hand region i.e. A2, A3, B2 and A4 boxes had completely depleted partition activity (Martin *et al.*, 1991).

Fig 1.1: P1 *parS* structure: The P1 *parS* is 32 bp DNA sequence consisting of heptameric sequences (Box A)and hexameric sequence (Box B).

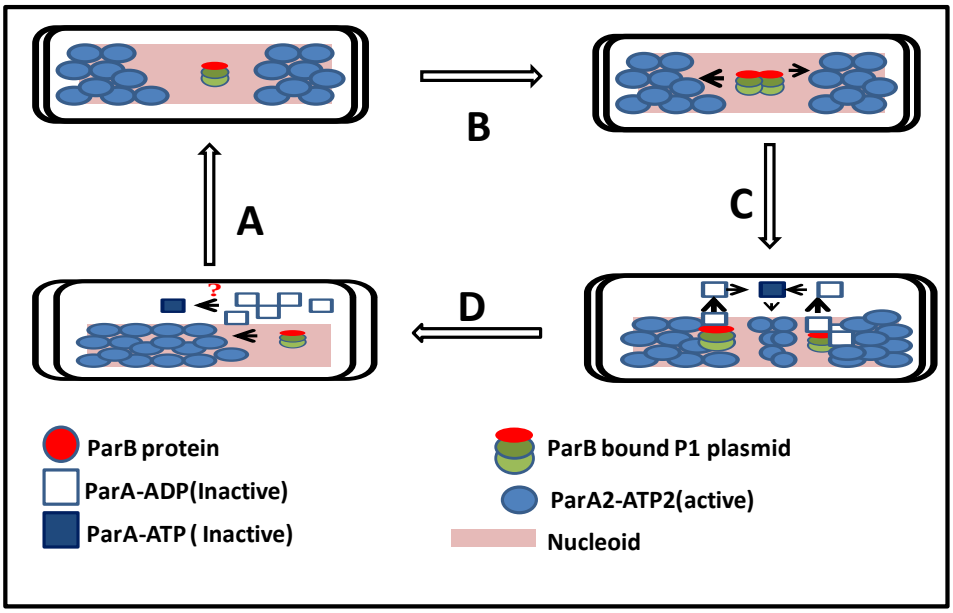

Fig 1.2: Diffusion ratchet Model: A) ParA interacts with ATP and undergo conformation change $ParA_2$-ATP_2 B) $ParA_2$ dimer interacts with nucleoid and extend towards the ParB bound plasmid C) $ParA_2$-ATP_2 interacts with ParB: *parS* nucleoprotein complex $ParA_2$-ATP_2 is converted into ParA-ADP at the junction of the ParB-*parS* complex, ParA-ADP form diffuses from junction of ParB nucleoprotein complex and by

unknown mechanism Par-ADP form is converted back to ParA-ATP form and cycle repeated.

Localization studies of P1 plasmid with in cell by FISH or by using translation fusion of ParA or ParB indicated that plasmids are localized at mid cell position or ¼ positions. Further deletion of *parA* or *parB* locus disrupted localization of the plasmid within the cell (Erdmann *et al.*, 1999;Gordon *et al.*, 2004;Hatano and Niki, 2010;Li and Austin, 2002;Sengupta *et al.*, 2010). Vecchiarelli in 2010 proposed diffusion ratchet model for explaining the localization of P1 plasmid with in cell. Using different biochemical techniques they showed that ParA binds to the ATP and undergo conformational change to $ParA_2$-ATP_2 dimer form, this form nonspecifically binds to nucleoid (Roberts *et al.*, 2012;Vecchiarelli *et al.*, 2010). When $ParA_2$-ATP_2 interacts with ParB bound with *parS* its ATPase activity is stimulated. During this process, the ParA ATP gets converted into ParA-ADP and dissociates from nucleoid. Hydrolysis of ATP allows ParA to move ParB-*parS* in the direction of high concentration of $ParA_2$-ATP_2 form and dragging P1 plasmid in the same direction. According to this model nucleotide bound state is important for ParA function, ParA-ADP bound form acts as a repressor where ParA-ATP form functions in the plasmid stability. ParA-ATP form associates with DNA nonspecifically (Vecchiarelli *et al.*, 2010).

F plasmid segregation

Another best studied example of Type Ia partition system is F plasmid. It is a 100 kb prototypical conjugative plasmid which can integrate itself into chromosome (*E. coli*). This F plasmid also had shown similar partitioning apparatus as P1 prophage plasmid. Partition apparatus in F plasmid are known as Sop (system of partition) i.e. *sopABC*. ParB protein in F Plasmid is known as SopB, motor protein called as SopA and

centromere sequence as *sopC*. Centromere sequence of F plasmid consists of 12 direct repeats of 43 base pair (Helsberg and Eichenlaub, 1986) which is different from the hexameric and heptameric sequence of P1 plasmid. SopB protein consists of N-terminal, C-terminal and middle regions, the C-terminal region of protein binds to the centromeric region (*sopC*) region (Ravin *et al.*, 2003). Similar to the P1 ParA, SopA binds to nucleoid in ATP dependent manner, intrinsic ATPase activity is stimulated by DNA or (SopB-*sopC*) nucleoprotein complex. FISH and different microscopic analysis indicated, segregation of F plasmid is asymmetric i.e. one plasmid remain at ¼ position, duplicated DNA is segregated to new ¼ (quarter) position in a time dependent manner (Onogi *et al.*, 2002). Directionality of the movement is dependent upon the concentration of nucleoid bound SopA protein. Still exact mechanism of F plasmid is not obscure. However, different models have been proposed for accommodating both *in vitro* and *in vivo* results on segregation of F plasmid.

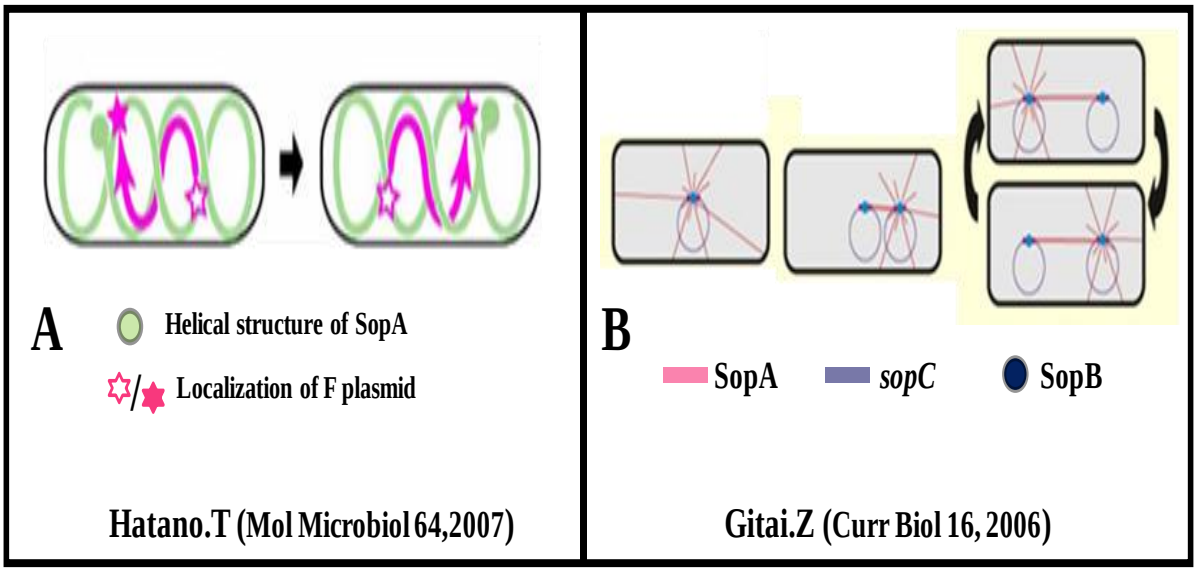

Fig1.3: F plasmid segregation models: **A)** Duplicated plasmid are separated at one end of the pole and traversed towards opposite pole (magnate star) this complete process is associated with SopA helical movement (Green structure). **B)** SopA polymers (indicated in pink) are assembled on SopB- *sopC* nucleoprotein complex (indicated in purple) to form a radial arrays structures. After replication, daughter plasmids are separated by the polymerization SopA proteins.

First model was proposed depending on microscopic results. According to this model SopA forms an oscillating polymer, interaction of SopB-*sopC* with SopA move the plasmid towards higher concentration of SopA (Hatano *et al.*, 2007). This model also hypothesized the involvement of some unknown host factors in positioning of F plasmid. Drawback of this model is that it couldn't explain why SopA nucleates at ¼ positions or why F plasmid is positioned at ¼ positions (Hatano *et al.*, 2007). The other model is based on *in vitro* results of SopA. SopA forms long axial filament in presence of SopB nucleoprotein, so it is hypothesized that formation of asters around the SopB nucleoprotein complex, resulted in placement of plasmid to ¼ or ¾ positions within the cell (Gitai, 2006). Aster model for F plasmid is homologous to the pushing model of R1 plasmid. Present model (astral model) failed to explain the oscillatory phenomenon of SopA within the cell (Gitai, 2006;Hatano *et al.*, 2007). Summary of steps explaining the most acceptable mechanism of F plasmid segregation is given in Figure 1.3.

pB171 plasmid partition system:

Type Ib partitioning system is encoded in few plasmids like pB171 virulence plasmid of *E. coli.* Unlike other low copy number plasmids, the pB171 plasmid encodes two partition systems namely Par1 & Par2. Both of these '*par*' systems are functional and synergistically aid in the stabilization of plasmid. Two centromere like sequences (*parC1* and *parC2*) are identified in the upstream region of the respective '*par*' operons. Par1

type system encodes ParR, ParM homologous protein where as Par2 encodes ParB and ParA type homologous proteins (Ebersbach and Gerdes, 2001;Ebersbach and Gerdes, 2005). However these proteins lack N-terminal region which is normally observed in Type Ia system. Hence walker type ParA of pB171 plasmid doesn't show any repressor activity and ParB protein acts as co-repressor for regulating (Ebersbach and Gerdes, 2005) gene expression.

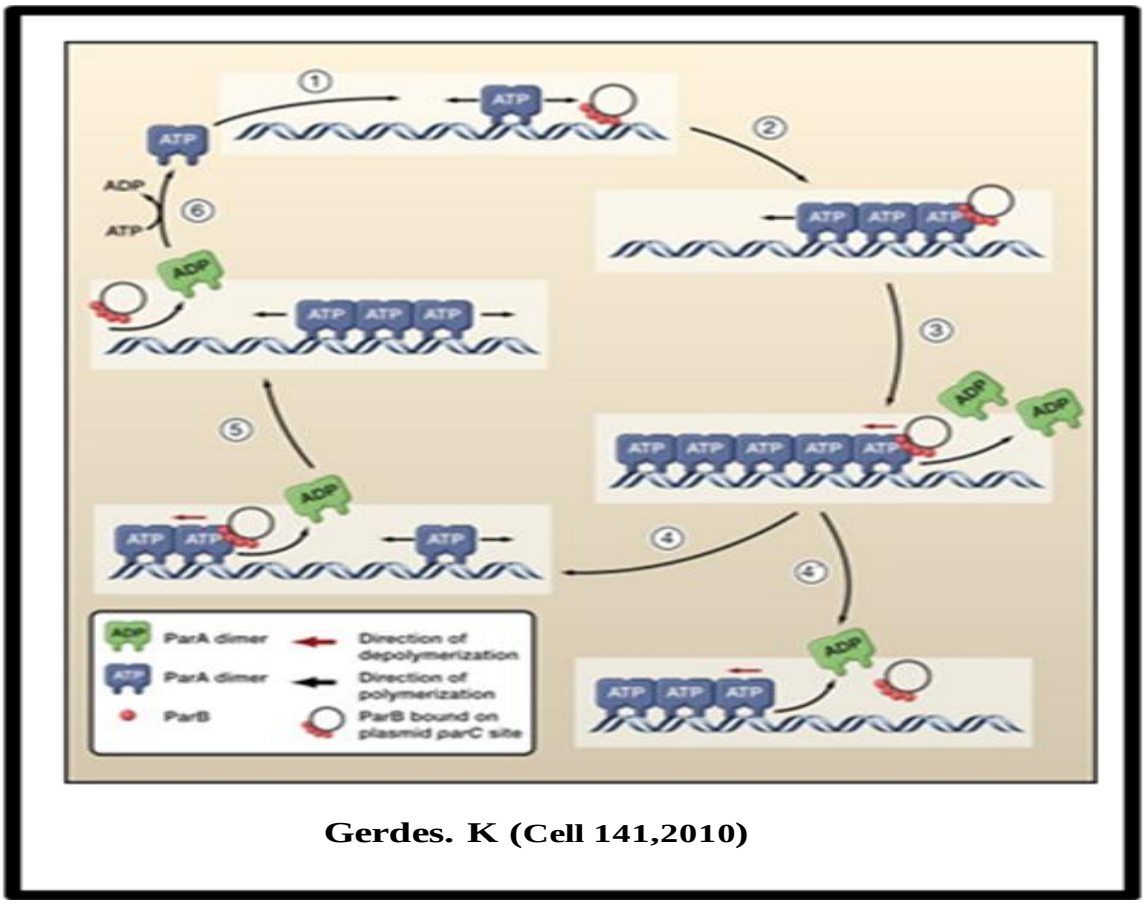

Fig 1.4: Pulling model: **1)** ParA interacts with ATP and undergoes confirmation change. **2)** ParA2–ATP2 binds to nucleoid and extends bidirectionally and extended polymer interacts with the ParB bound plasmid. **3)** ParA-ATP is converted to ParA-ADP form due to interaction of ParB nucleoprotein complex. **4)** Continued interaction of ParB nucleoprotein complex with the next ParA-ATP results in pulling of plasmid towards higher concentration of ParA. **5&6)** Plasmid is released at the pole, ParA-ADP form is converted back to the ParA-ATP form and cycle repeats.

The model for Type Ib plasmid pB171 partitioning has emerged from a microscopy studies by Ringgaard and colleagues. The studies indicated that Type Ib plasmids are localized at mid of the cell or ¼ position i.e. localization of plasmid is similar to the Type Ia plasmid. Co-visualization of ParA and ParB of pB171 deduced pulling type segregation mechanism (Ringgaard *et al.*, 2009). According to this model, ParA interacts with the nucleoid and starts oligomerization in bidirectional fashion. ParA polymers when encounters ParB bound to centromere, results in ATP hydrolysis at the junction of ParB-*parC* causing depolymerization of ParA filament. Continued interaction of ParB nucleoprotein complex with the next ParA-ATP complex in the filament ultimately results in the retraction of ParA and eventually the pulling of plasmid DNA towards higher ParA-ATP concentration.

1.2.2 Type II partition system:

Type II segregation system contains actin like fold NTPase family proteins, best studied example is R1 plasmid (*par RMC* system)**.** The *par RMC* locus contains actin like homologue ParM, centromere binding protein ParR and centromere region (*parC*). Homologues of *parRMC* are identified in plasmid of both Gram positive and Gram negative bacteria (Ebersbach and Gerdes, 2001;Schumacher, 2007) but not reported in any bacterial chromosomes till now. The *parC* centromere region consists of five 11 bp tandem repeats and each repeat is separated by 39 bp. The electron microscopy studies revealed, ParR protein forms ring shaped complexes of 15 -20 nm diameter, due to arrangement of six ParR molecules with N-terminal region facing the outward ring and C-terminal region facing towards centre of the ring. N-terminal basic structures are spaced regularly 3.5nm apart which is almost equal to the one turn of the B-DNA

structure. The studies on pSK41 plasmid of *Staphylococcus aureus* supported the above explained structure of type II partitioning system. Here the dimeric ParR of pSK41 contribute to the formation of ring like structure (Gerdes *et al.*, 2010). ParM has characteristic actin like fold, and nucleotide binding pocket formed in the inter domain region. By several methods it is demonstrated that ParM forms double right handed helical filament with crossover distance of 300A^{o} and distance between monomers is 49A^{o} whereas actin filament show 360A^{o} (cross over distance) and 55A^{o} (inter monomer distance) (Galkin *et al.*, 2009).

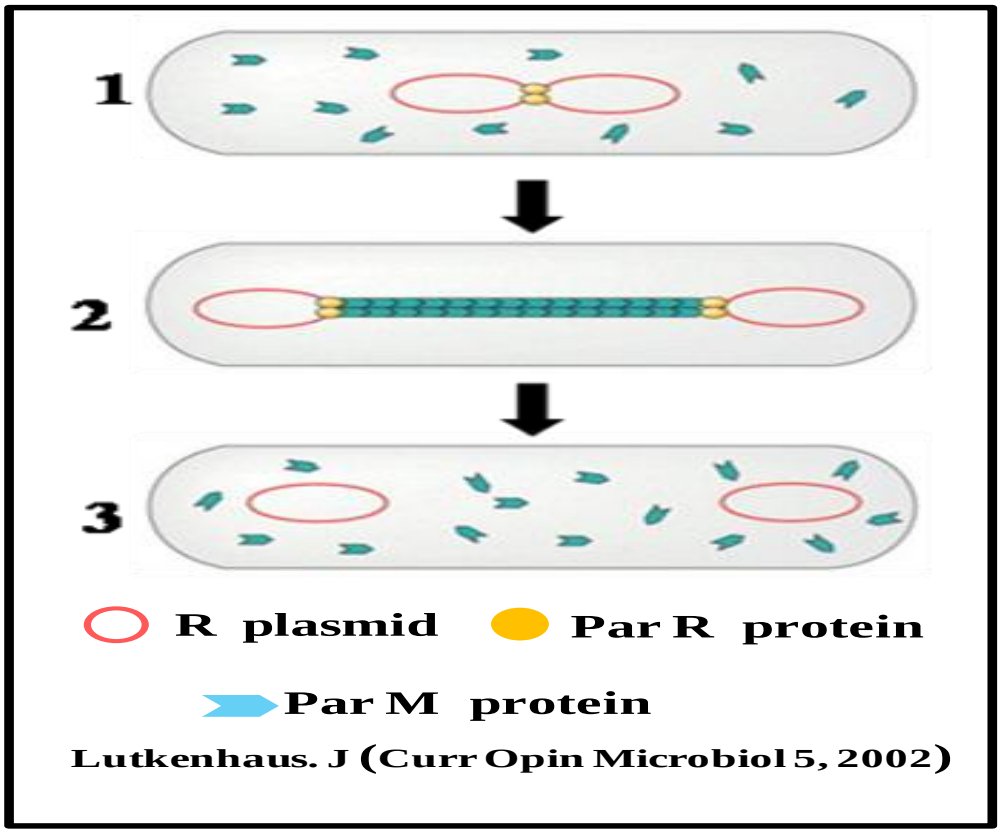

Fig 1.5: Pushing mechanism:1) Monomeric ParM interacts with each other to form unstable filaments.2) ParM filament get stabilised when it interacts with the ParR bound plasmid, plasmid are pushed towards opposite ends due to insertion of monomeric ParM molecules at the junction of ParR and ParM. 3) As division proceeds ParM filament is destabilised which results in separation of plasmids.

Segregation follows pushing mechanism, the ParM monomeric form interacts with each other to form transient unstable polymers, these polymer get disassembles unidirectionally much faster than the polymerization. Transiently formed ParM filament gets stabilized by attaching to ParR- *parC* complex (Galkin *et al.*, 2009). Monomeric ParM is inserted at the junction of ParR-*parC* complex, due to insertion of ParM monomers bidirectionally these plasmids are separated towards opposite direction of the cell. ParM within filament exists in two forms, closed form (ParM-ATP or ParM-GTP) and open form (ParM-ADP or ParM-GDP). Hydrolysis of ATP to ADP +Pi makes inter domain region very rigid hence closed form is converted into open form.

1.2.3 Type III partition system:

Type III partition system is recently characterized in *B. subtilis* plasmids. The best studied examples of type III system are pX101 plasmid, pBtoxis plasmid from *Bacillus anthracis* and *Bacillus thurgensis*. Type III partition system consists of TubZ (GTPase) protein which contain characteristic T4 loop motif, TubR (adaptor protein) and *tubC* (centromere) (Larsen *et al.*, 2007;Ni *et al.*, 2010). Initially the essentiality of these proteins was identified in replication process (Tinsley and Khan, 2006). However, recently the role of these proteins is shown in plasmid stabilization. *In vitro* studies showed that TubZ proto filaments (2-10) are tangled together to form unidirectional filament which is extending from one end to another end of the cell (Larsen *et al.*, 2007). In these type of plasmids TubR binds to the centromere like sequences (*tubC*) and serves as a high local concentration for binding sites for tread milling TubZ protein. Once plasmids are bound these plasmid are transported to opposite side of the pole. Upon reaching the membrane due to impact of plasmid to membrane layers plasmids are

released from TubZ filament. Critical element in Type III segregation system is TubZ filament. The TubZ dynamics depends on two factors, concentration of TubZ protein and GTP hydrolysis which are interlinked with each other i.e. once concentration exceeds the critical concentration, it activates GTPase activity like FtsZ protein and starts polymerizing. Over all, the model in pX101 plasmid look like Tram (train) hence mechanism in this plasmid is named as Tram model for Type III partition system (Schumacher, 2012).

1.2.4 Type IV partition system:

Partition mechanism used by majority of well studied plasmid involves '*par*' as mentioned above. However few plasmids like pSK1 of *Staphylococcus* don't encode typical classical partition proteins, the way by which it ensures stable inheritance is not understood properly (Guynet and de la, 2011). Plasmid R388 of *E. coli* are known example of Type IV partition system. R388 plasmid is an representative of a minimal conjugative plasmid genome which is maintained as four copies per *E. coli* and R388 plasmid encodes similar homologues of partition and they are named as StbA , StbB , *stbC* (Guynet et al., 2011). Deletion of the *stbA* gene increase frequency of plasmid missegregation and indicating StbA is important for partition. Overall conclusion of these studies indicates R388 plasmid segregates by passive mechanism or by taking advantage of the host chromosome segregation.

1.2.5 Transcriptional regulation of *parAB* expression:

Regulation of partitioning genes expression is essential and any change in the levels of expression of these genes causes change in phenotype. Transcriptional regulation of '*par'*

genes has been studied mostly in plasmid type partitioning system, the regulation of '*par'* gene in chromosomal type partitioning systems still remains obscure. In plasmid type Ia partitioning system, the ParA functions both in DNA partitioning as well as in the regulation of *parAB* operon expression. The role of ParA as a transcriptional regulator is essential for maintaining relative levels of ParA and ParB within the cell. Change in the ratio of ParA to ParB causes the defect in the partitioning as well as regulation of *parAB* genes expression. ParA can exist in two forms like ParA-ATP and ParA-ADP. The ParA-ADP form act as transcription repressor by binding to the promoter region of the *parA* and down regulate *parAB* operon (Bouet and Funnell, 1999;Dunham *et al.*, 2009). *In vivo* and *in vitro* studies have indicated that ParB can stimulate the repressor activity of ParA, acting as a co-repressor by altering ATP recycling process. This occurs mainly by increase in net levels of ParA-ADP. In pB171 plasmid or pTAR plasmid , which mainly confer type Ib partitioning system and also in case of type II plasmid partition system, the ParB or its homologue is shown to regulate '*par*' genes (Jensen et.al 1994). In pB171 plasmid the ParR (ParB homologue) regulates *parMR* operon by binding to *parC* a 10bp repetitive sequence located upstream to *parMR* operon. It is hypothesized that the regulation of both operons' (*parMR, parAB*) in type Ib partitioning system occurs by binding of ParB protein to the *parS* site located upstream of these genes. Binding of ParB or ParR to *parS* or *parC* sites, respectively form high order nucleoprotein complex, which prevent access to RNA polymerase and there by regulate dual operons.

1.3 Mechanisms of chromosome segregation in bacteria:

In chromosomes, '*par*' homologues i.e. (ParA and ParB) are identified from different Gram -positive, Gram - negative and archea bacteria (Dubarry *et al.*, 2006; Yamaichi

and Niki, 2000). Most of these bacteria contain single circular chromosome with single independent partition system like *B.subtilis*, *Mycobacterium*, and *Streptomyces*. Some interesting exceptions are like *Vibrio cholerae* (2 Chromosomes), *Deinococcus radiodurans* (2 chromosomes and 2 plasmids), *Brukholderia* (4 chromosomes) (Dubarry *et al.*, 2006), which have multipartite genome system. Homologues '*par*' systems are identified in bacteria harboring single circular chromosome or multiple chromosomes differs from plasmid '*par*' system in few aspects. (1) plasmids encode single centromere sequence where as chromosomes has shown multiple *parS* sites and location of these centromere sequence in few bacteria is near to the origin of replication or some time scattered throughout the genome, 2) Deletion or point mutation of *parAB* genes doesn't always cause chromosome loss where as in plasmid it perturbed the segregation process. Some of the well studied bacterial chromosome segregation systems are *Bacillus subtilis*, *Caulobacter crescentus* and *Vibrio cholerae*.

Bacillus Subtilis

B. subtilis has ability to form spores which under favorable conditions germinate and grow vegetativley. Vegetative growth cycle involves symmetrical cell division and genome partitioning. Under unfavorable conditions the growth cycle involves asymmetrical division (Errington, 2003). Genome partitioning has been extensively studied in both the conditions i.e. vegetative as well as in sporulation condition. Partitioning proteins in *B. subtilis* are named as Soj (ParA) and Spo0J (ParB). Inactivation or deletion of *spo0J in* vegetative cells showed increased frequency of chromosome loss by nearly 100 fold comes about 1-2% of anucleation (Lee *et al.*, 2006). The *spo0J* deletion also perturbed cell size, distorted nucleoid and showed guillotined

cell as compared to wild type. The Spo0J specifically interacts with 16bp region (tGTTtCAcGTGAAAAa/g) (Lin and Grossman, 1998) sites located within 20% of origin proximal region known as *parS* sequence to form higher oligomeric structures (Draper and Gober, 2002;Lee *et al.*, 2003;Lin and Grossman, 1998) and it is observed that *parS* sequence is highly conserved across the bacterial species (Livny *et al.*, 2007). Even though *parS* are distributed over nearly 20% from origin proximal region, the Spo0J-GFP formed single bright foci indicating formation of the highly organized structure (Lee *et al.*, 2003;Lin and Grossman, 1998). In the absence of Soj protein, Spo0J formed multiple small foci indicating binding of Spo0J to the *parS* sequence is independent of Soj, but formation of complex structure depends on the Soj protein. Soj belongs to Type Ia Walker ATPase family proteins containing deviant Walker motif. Initially Soj was identified as genetic suppressor of the Spo0J mutant i.e. deletion of Soj restored normal expression of sporulating specific genes as well as anucleation effect. Unlike of Spo0J mutant Soj mutant doesn't shown any anucleation phenotype or change in cell length. However, functional role of Soj in stabilization of the unstable plasmid has been demonstrated, indicating its role in genome segregation.

Further the role of Soj in genome segregation has been studied by isolating *smc/soj* deletion mutant different point mutations like Soj K16A, Soj K16Q, Soj D125A, and Soj G12V in walker motifs. It is shown that all these mutants exhibit the loss of sporulation activity or intensity of foci formation or association with DNA. However, it still remains to be seen does Soj-Spo0J mediates partitioning in the classical cytomotive filament manner or not (Pulling mechanism).

Overall results despite of some conflicting reports indicate that there is a minor role of the Spo0J and Soj proteins in chromosome segregation during sporulation, but it is relatively consistent during normal growth. In addition, it seems likely that Spo0J/Soj act

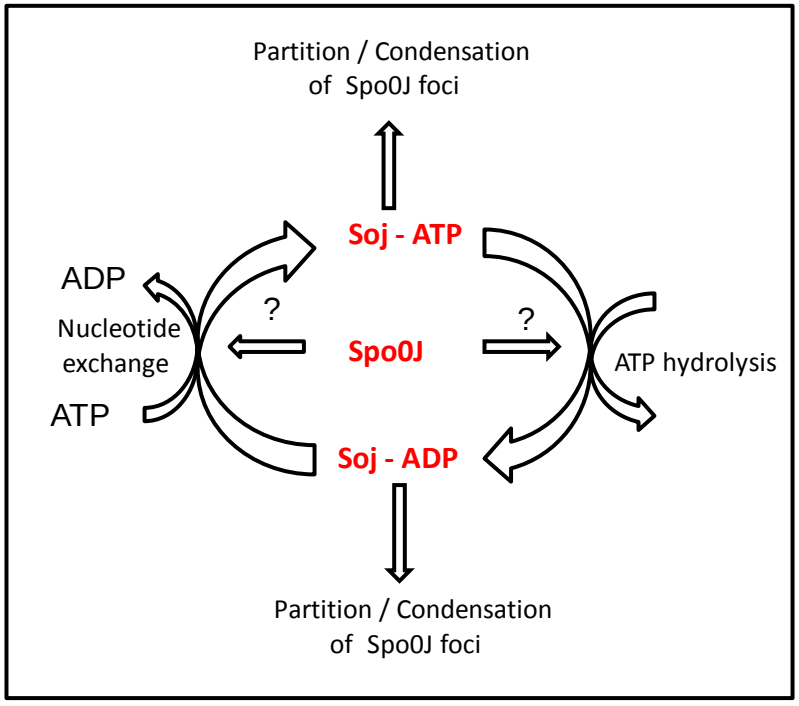

Fig1.6: Role of 'Par' proteins in *B. subtilis:* Role of the Soj is dependent on the nucleotide binding state. Soj exists in ADP and ATP bound form. Soj- ATP interacts with the Spo0J. This interaction mediates in chromosome segregation. In the cytomotive filament Soj-ATP is converted to Soj- ADP. ADP bound Soj filament bind in the upstream region of the sporulating genes and regulate gene expression**.**

as a check point to regulate entry of cells into sporulation, but the exact stimulus for such a checkpoint still undefined.

Escherichia coli

E. coli posses 4.6.Mb single circular chromosome. From studies on sub cellular localization of the *E. coli* replisome proteins, revealed chromosome duplication occurs at the mid cell position. Unlike other bacteria *E. coli* genome is devoid of well characterized 'Par' proteins. Recent studies on chromosome segregation showed apart from 'Par'

proteins other factors like Topoisomerase, FtsK, MukBEF proteins are also involved in chromosome segregation. Among these factors, the mutation in *muk BEF* genes of *E. coli* had shown formation of anucleated cells, change in the DNA content of the cells as well as abnormal chromosome positioning. MukB in *E. coli* and SMC in *B. subtils* and *Streptococcus pneumonia* localize on the chromosome near to the origin of replication (Sullivan et al 2009; Minnen et al 2011), binding of SMC proteins is enhanced through the ParB – *parS* complex, suggesting that both the systems seem to be taking during chromosome segregation. However role of the MukBEF in chromosome segregation is unknown. Recently interaction between MukB and Topoisomerase IV domain has been demonstrated in *E. coli* (Li et al 2010) indicating that the MukB could support chromosome partitioning by promoting resolution of intertwined circular duplicated chromosomes.

Caulobacter crescentus:

Caulobacter crescentus is a Gram negative oligotrophic bacteria containing single chromosome which encodes single *'par'* operon. Partitioning genes in this organism are named as *parA* and *parB* which are essential for growth and division (Mohl *et al.*, 2001;Mohl and Gober, 1997). Unlike other organisms *Caulobacter crescentus* divides asymmetrically to produce swammer and stalked cells. The swammer cells have single cell with polar flagellum and doesn't initiate DNA replication. In the developmental process swammer cells will be converted into stalked cell by shading flagellum and chemotaxis receptors. Deletion or over expression of 'Par' proteins resulted in chromosome loss as well as cell filamentation, this suggesting 'Par' mediated segregation is linked to cell cycle process (Thanbichler and Shapiro, 2006). Chromosome in *C.*

crescentus is localized at polar region i.e. *oriC* is anchored at one of pole and terminus to opposite pole. Upon duplication of *oriC* one of the copy traversed to opposite pole before septum formation, indicating *C. crescentus* follows polar asymmetric segregation.

Time lapse microscopy studies revealed chromosome segregation is a multistep process.

1) First step is slow process where one copy is retracted towards old pole and second copy is translocated to opposite pole (new pole).
2) Final step is rapid, where *ori* is translocated to opposite pole, rapid movement occurred due to retraction of Par A filament.

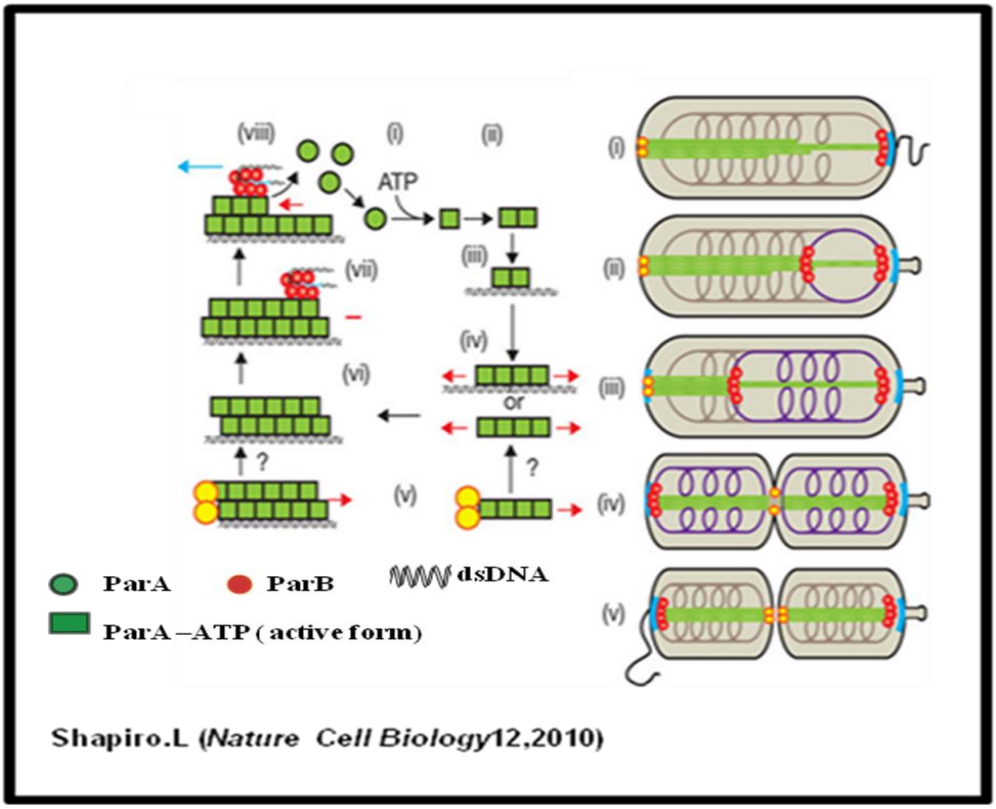

Fig 1.7 Segregation mechanism in *C. crescentus* : 1) ParA nucleates on the opposite side of the cell and extends bi directionally. 2-3) The interaction of ParB nucleoprotein complex stimulates depolymerization of ParA oligomers on the DNA.4) After DNA

segregation, cell septum formation occurs on the mid of the cell.5) Results in formation of new daughter cells.

Using super resolution microscopy it was shown that nucleation of ParA occurs at opposite side of *ori* and is determined by TipN protein. ParA form filamentous structures due to interaction of ParA-ATP with the DNA. Filament grows towards origin of replication from the ParA nucleation point. Before DNA replication is completed, the length of the ParA nucleoprotein structure is maintained due to its weak intrinsic ATPase activity (Easter, Jr. and Gober, 2002). Once DNA is duplicated, the sister chromosomes are separated due to force generated by replication process or due to entropy in DNA resulting the pulling of duplicated ParB-*parS* nucleoprotein complex apart (Dworkin and Losick, 2002;Lemon and Grossman, 2001). Interaction of ParA with ParB nucleoprotein complex results in pulling of newly duplicated DNA towards opposite pole along with the retracted ParA filament (Shebelut *et al*., 2010)**.** Above proposed mechanism shares maximum similarities with the segregation of *V. cholerae* chromosome I (Fogel and Waldor, 2006) as well as with pB171 plasmid (Ringgaard *et al.*, 2009).

Vibrio cholerae

V. cholerae is canonical model of bacteria containing multiple chromosomes (Egan *et al.*, 2005). Genomic DNA is divided into chromosome I (2,961,149 bp) and chromosome II (1,072,315 bp). Individual chromosome encodes independent partition system. Mechanism of chromosome I and chromosome II '*par*' system is non redundant as the segregation of chromosomes is independent (Fogel and Waldor, 2005). By using plasmid stability assay it was demonstrated that '*par*' system of individual chromosome stabilizes unstable plasmid. Hence it is considered to be actively involved in chromosome

segregation. Genetic and microscopic studies also showed chromosome I and chromosome II distinctly localized within cell i.e. chromosome I origin localized at the ¾ position (cell poles), similar to other known asymmetric chromosome segregating bacteria. Whereas chromosome II localized at the mid of the cell and follow bidirectional pattern of chromosome segregation. The *ori C* region of chromosome I duplicates at ¾ position of the cell and segregate towards opposite pole. Movement of origin is correlated to the ParB-GFP movement in actively growing cells with respect to time. During initial phases of cell cycle, the ParB1 binds at *parS* site and ParA1 is required for the polar localization of the ParB1-*parS* complex. Pulling type mechanism is proposed for chromosome I segregation. Before cell division, the replicated chromosome anchored to the pole by interaction of ParA1 to unknown protein, then ParA1 nucleates at the septum forming location and polymerizes or bands or networks in the direction of opposite pole. In segregation process, firstly the ParB interacts with *parS* to form ParB-*parS* complex and then this complex is captured by ParA retracting it to the new pole and as a result the ParB bound *parS* gets segregated to new pole. It is like other '*par*' directed pulling mechanism which is already described in other organisms (Fogel and Waldor, 2006).

Unlike chromosome I which has one *parS* site, chromosome II has nine *parS*2 sites (Yamaichi *et al.*, 2007). Native ParA2 hydrolyse ATP similar to Type I ParA. It forms ordered filamentous structure on non specific DNA in presence of ATP. It is hypothesized that there may be some cross talk between chromosome I and chromosome II '*par*' systems as they share nearly 45% similarities at the amino acid level (Jha *et al.*, 2012;Yamaichi *et al.*, 2007). By genetic analysis, the deletion of chromosome I 'Par' proteins resulted to mislocalization of origin of replication of chromosome I, where as

segregation of chromosome II is not affected. The *parAB2* deletion resulted in gross change in localization of origin and segregation, which lead to the loss of chromosome II but no effect on chromosome I segregation or localization (Fogel and Waldor, 2005). This solo study as the example of genome segregation in multipartite genome containing bacteria provided the strong evidence that both the chromosomes are being maintained independently using their cognate partitioning system. The other good model system for such study is *Deinococcus radiodurans*, has been investigated under this study.

1.4 *Deinococcus radiodurans* as a model organism:

Deinococcus radiodurans belongs to the *Deinococcaceae* family, is well known for exceptional ability to withstand the lethal effects of different DNA damaging agents, such as ionizing radiation, ultraviolet (UV) light, and desiccation etc. (Cox *et al.*, 2010;Rainey *et al.*, 2005;Slade and Radman, 2011). Till now, more than 45 species were isolated from diverse environments among these *D. radiodurans* is best characterized. It was first isolated in canned meat that had been irradiated at 4,000 Gray (Gy) in order to achieve sterility (Duggan *et al*., 1963). Phylogenetic analysis suggested *Deinococcus* is closely related to the genus *Thermus* (heat-resistant bacteria). *D. radiodurans* is a Gram positive, non pathogenic, non motile, non spore forming and pinkish orange pigmented bacterium. In spite of staining as Gram-positive, the cell wall composition differs from other Gram-positive bacteria in respect to its lipid composition. Anderson in 1985 characterized in detail the lipid composition of *D. radiodurans*. Their study showed that of the total membrane lipid, 43% is composed of phosphor glycolipids containing a series of alkyl amines as structural components, and some unknown lipid constituents which appear to be derived from a novel precursor phosphatidylglycerolalkylamine. *D. radiodurans*

grows optimally at 32^{o}C in rich medium and is an obligate aerobe. Cells are naturally competent and genetic tools are available for conditional expression or complete inactivation of genes as shown by different groups (Funayama *et al.*, 1999;Lecointe *et al.*, 2004;Meima and Lidstrom, 2000).

Deinococcus radiodurans R1 has the ability to survive high doses of gamma radiation as well as UV radiation without any mutation (Moseley and Evans, 1983). In the exponential growing *D. radiodurans* showed 10% survival at 8kGy, where as exponentially growing *E. coli*, showed 10% survival at 150 Gy only i.e. *D. radiodurans* showed over 100 fold greater resistance than *E. coli* (Minton, 1994). Compared to other organisms, the *D. radiodurans* can sustains 150 to 200 double stranded DNA breaks (DSBs) under aerobic irradiation conditions, all of which are mended within four hours following irradiation (Daly and Minton, 1995;Slade *et al.*, 2009). It has been demonstrated that DSB repair in this bacterium is contributed by RecF pathway (Misra *et al.*, 2006) and incidentally, over expression of RecBC from *E. coli* made this bacterium sensitive top gamma radiation (Khairnar *et al.*, 2008). In exponential phase, *D. radiodurans* is 33 fold more resistant to UV than *E. coli*. In addition to gamma and UV, *D. radiodurans* can survive the lethal effects of alkylating agents which add bulky groups without showing any mutagenesis (Sweet and Moseley, 1976). *D. radiodurans* is mutable by N-methyl-N9-nitro-N-nitrosoguanidine and other agents that can cause mispairing of bases during DNA replication. Unusual tolerance of *D. radiodurans* to different DNA damaging agents is due to different mechanism involved in prevention or tolerance against DNA damaging agents or presence of extra ordinary repair mechanism and few other factors like polyploidy, organization of nucleoid.

Ionization radiation passes through matter and generating different free radicals like HO•, H+ and e^{-aq} due to radiolysis of water molecules (Daly *et al.*, 2010). This free radical indiscriminately oxidizes or damage DNA, RNA, proteins and lipids. Compared to most of the organism, proteins in *D. radiodurans* are highly protected from ROS with in cells, but as such proteins do not have an inherent property of protection. Daly in 2010 reported chemical mechanisms are involved in protection against radiation i.e. multiple factors are observed in the *D. radiodurans* filtrate like orthophosphate (13 mM), Mn^{+2} (200µM) and peptides (3mM) which are known to protect proteins against the radiation. Other than preventing protein oxidation Mn^{+2} mimics the SOD and can scavenge different ROS (Reactive Oxygen Species). Daly and colleagues hypothesized that this phenomena is contributing to the large shoulders in ionizing radiation dose response curves. Alternatively Minsky and coworkers proposed that the increased concentration of Mn^{+2} with in cell could contribute to the condensation of *D. radiodurans* genome by neutralizing the repulsion of phosphate groups in DNA backbone. Some more antioxidants were also present in *D. radiodurans* other than Mn^{+2} complexes like deinoxanthin (Deinococcal carotenoid) which is more effective in scavenging ROS than other known carotenoids, pyrroloquinoline quinone (PQQ) coenzyme (Khairnar *et al.*, 2003;Misra *et al.*, 2004), which detoxifies ROS more efficiently than other natural antioxidants. Interestingly, it is found that *D. radiodurans* devoid of PQQ becomes hypersensitive to gamma radiation and mechanistically this antioxidant molecules is shown to be inducer of protein kinase and has a role in DSB repair per se (Rajpurohit *et al.*, 2008). Oxidative damage of DNA is repaired by excision repair pathways mainly by base excision repair. DNA glycosylases (Moe *et al.*, 2012;Sandigursky *et al.*, 2004) and

DNA repair polymerase Pol X (Bentchikou *et al.*, 2007) have been shown for their roles in DNA metabolism associated with base excision repair. DNA polymerase X a homologue of polymerase beta in eukaryotes is characterized as a short patch base excision repair polymerase (Khairnar and Misra, 2009).

In 1995, Minton and Daly showed the DNA double strand break repair kinetics of *Deinococcus radiodurans*, in wild type and *recA* mutant by pulse field gel electrophoresis. Even though *recA* mutant is very sensitive to gamma radiation, initial joining of the fragments was observed on the gel. Based on these results they proposed that initial period of DNA repair may proceed either through Single Strand Annealing (SSA) or by non-homologous end joining method which is RecA independent. Phase II may progress through RecA dependent homologous recombination. Thus a biphasic DNA repair model was proposed (Minton, 1995).

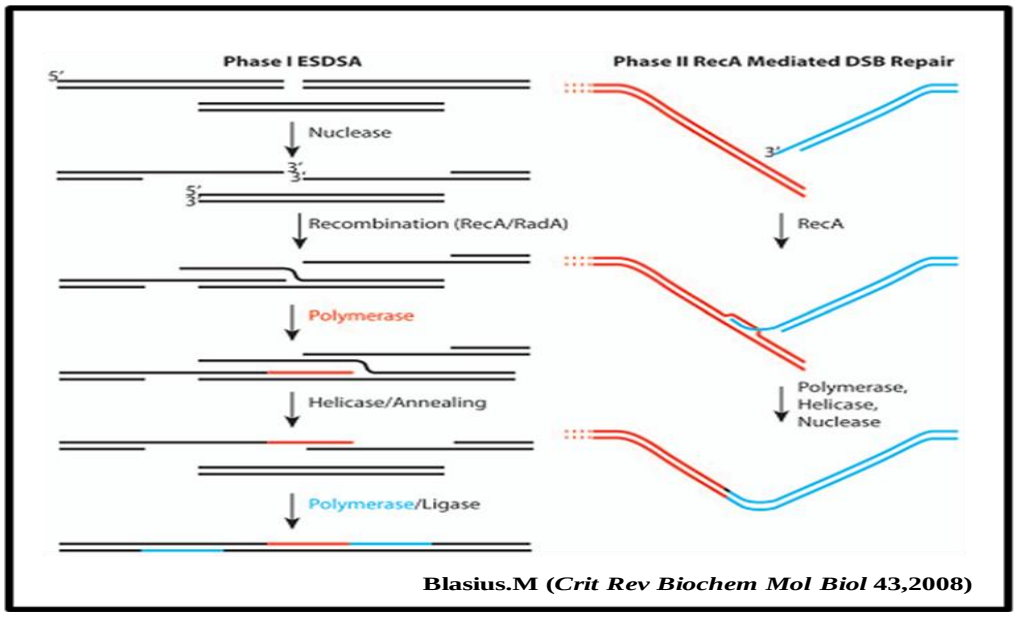

Fig 1.8: ESDSA mechanism in *D. radiodurans*: Two stages of genome reconstitution in *D. radiodurans.* The first stage, extended synthesis dependent single strand annealing (ESDSA) is dominated by nuclease and DNA polymerase functions. The second stage is

a more conventional RecA mediated double strand break repair process focused on the final splicing of large chromosomal segments.

Recently, Zahradka and his group in 2006 analyzed the repair of the *D. radiodurans* DNA shattered by ionizing radiation by an adaptation of the classical Meselson-Stahl experiment. They found that in *D. radiodurans* DNA fragment assembly coincides with a massive DNA synthesis that occurs at a much higher rate in irradiated cells than in unirradiated growing cultures and the reassembled genome appears to be composed of a patchwork of contiguous blocks of old and newly synthesized DNA (Zahradka *et al.*, 2006). Based on these findings they proposed a mechanism called **E**xtended **S**ynthesis **D**ependent **S**trand **A**nnealing (ESDSA).

According to the ESDSA model, the single-stranded tail of a recessed fragment invades a partially overlapping fragment and primes DNA synthesis through a moving D-loop producing long stretches of single strand DNA that anneal to complementary sequences. Dissociation of the newly synthesized DNA from the template produces thereby facilitating the precise reconstruction of long double strand DNA intermediates. These intermediates subsequently recombine to reform a circular chromosome. Two enzymes play a key role in the ESDSA model, PolA, which participates in the initial DNA synthesis step, and RecA, that ensures the maturation of the linear intermediates into full size circular chromosomes through a classical recombination process. Thus *polA* and *recA* mutants are highly radiation sensitive (Zahradka *et al.*, 2006). A number of hypothetical ORF's have been characterized for their roles in radiation resistance. The most notable ones include the DRA0282 as human Ku like proteins (Das and Misra, 2011), DR2417 as a novel beta CASP family nuclease (Das and Misra, 2012), DR2518 as

a DNA damage inducible Serine / threonine protein kinase (Rajpurohit and Misra, 2010), DRB01000 as ATP type DNA ligase (Kota *et al.*, 2010), DR0505 as a thermo stable Mre11 type novel esterase (Kota *et al.*, 2010) etc.

Genome structure of *Deinococcus radiodurans*

White & coworkers published the sequence of 3,284,156 base pairs genome of *D. radiodurans* in 1999, which revealed that this bacterium harbors multipartite genome structure consisting of two chromosomes (2,648,638 and 412,348 base pairs), a mega plasmid (177,466 base pairs), and a small plasmid (45,704 base pairs) (White *et al.*, 1999). Out of 3187 total ORF's annotated 2185 ORF's matched with the known homologues public database and 1002 ORF's showed no matches. Total 95 gene families are identified after PSI-blast analysis, among these P-loop nucleotidase is the largest family consisting of 120 genes, second largest in HTH family proteins (DNA binding proteins) consisting of 72 genes. Majority of chromosome I components including partitioning proteins shares similarities with the chromosome of *T. thermophilus* indicating that chromosome I shares common ancestry with *T. thermophilus* where as remaining genetic elements acquired separately due to horizontal gene transfer mechanism. Chromosome I contain most of the essential genes required for replication, division, growth. Whereas chromosome II and mega plasmid contain genes that play important role in cell response to extreme conditions i.e. chromosome II and mega plasmid encode nearly 30% regulatory response genes, two of three hemolysins, four of the nine extracellular protease and ABC transporters which can import amino acids, peptide fragments. Few genes are also present on chromosome II which are involved on production of amino acids, urea. Mega plasmid contains genes that are required for

synthesis of dNTP's or dNTP precursor molecules like periplasmic alkaline phosphate which are essential for restoration of damage site. Origin of replication is annotated based on oligomer skew and presence of certain genes like (*dnaA, dnaN*) for chromosome I and presence of *parA* for chromosome II, origin of replication is annotated for megaplasmid based on the oligomer skew analysis or sequence similarities with predicted origin of replication.

Genome of this bacterium is usually condensed to form toroidal structures (Levin-Zaidman *et al.*, 2003;Levin-Zaidman *et al.*, 2003;Minsky *et al.*, 2006). Minsky and colleagues for the first time showed that in *D. radiodurans* genome exist as donut-like DNA structures, as detected by transmission electron microscopy. They further showed that this compact form of nucleoid remains unaltered after high doses of γ-irradiation. Compact nucleoid organization gives close proximity to repair the damaged DNA. Mechanisms underlying the maintenance of ploidy and faithful inheritance of multipartite genome of *D. radiodurans* during normal growth are not known. As the understanding of the mechanisms underlying bacterial genome segregation has come from bacteria harboring single circular chromosome and low copy plasmids, the bacteria harboring multipartite genome structure would be an interesting model system to understand the maintenance and faithful inheritance of complex bacterial genome. Next to *V. cholera*e, *D. radiodurans* also harbors multipartite genome structure. Genome of this bacterium is also annotated with putative *parA-parB* genes. Except small plasmid, other genome replicating units have their own sets of putative ParA and ParB proteins which are encoded in an operon. Centromeric sequences however, are not known in any of these genome replicating units. The presence of multiple sets of 'Par' proteins has been

reported in bacteria including *D. radiodurans* that harbor multipartite genome system. This raises the possibility of functional redundancy amongst these proteins in *D. radiodurans*. Functional characterization of 'Par' proteins encoded on different replication units in *D. radiodurans* would be a first step forward in understanding the mechanism(s) of chromosome segregation. Under this study, therefore, we proposed to characterize the 'Par' proteins of chromosome I and chromosome II and to understand the mechanism underlying for the segregation of chromosome I in *Deinococcus radiodurans.*

CHAPTER 2

Materials and Methods

2.1. Materials

Plastic ware and glassware

Disposable polypropylene microcentrifuge tubes (1.5ml and 2ml), micropipette tips, Polypropylene SS34 tubes and GSA bottles were obtained from Tarsons, India or Axygen, USA. PCR tubes were also obtained from Axygen, USA. All these plasticwares and glasswares were sterilized by autoclaving. Glasswares were also sterilized by baking at higher temperature for 3h. Cryovials (2 ml) and low temperature storage boxes were procured from Laxbro, India and Axygen, USA.

Chemicals and media ingredients

Dehydrated components of culture media (Bacto-tryptone and Bacto-yeast extract) and agar-agar (Bacto-agar) powder were obtained from Difco Laboratories, USA. Fine chemicals were from Sigma Chemical Company, USA or Roche Biochemicals GmbH, Germany or S.R.L. Ltd., India or Bangalore Genei (P) Ltd., India. Inorganic salts, urea for sequencing, organic solvents and acids of Excel-R or Anal-R quality were from Qualigens (Glaxo) India Ltd. or Sigma Chemical Company, USA. Molecular Biology Grade phenol was purchased from SRL, India.

Enzymes and other molecular biology reagents

T4 DNA polymerase, restriction endonucleases, T4 Polynucleotide Kinase, T4 DNA ligase, and DNA polymerase (Klenow fragment) were obtained from New England Biolabs, USA or Bangalore Genei (P) Ltd., India or Roche Biochemicals GmbH, Germany. Shrimp Alkaline Phosphatase was from USB-Amersham, UK. Lysozyme

(from chicken egg-white), DNAase I (from bovine pancreas) and RNAase (from bovine pancreas) were procured from Sigma Chemical Company, USA. *Pwo*-DNA polymerase and deoxynucleotidetriphosphates (dNTP's) were from Roche Biochemical Germany. Taq DNA polymerase and DNA molecular weight standards were from Bangalore Genei (P) Ltd., India. PCR extraction kit, Gel extraction kit and RNA extraction kit were from QIAGEN, Germany. All the primers used in this study were from Metabion, India.

Radionucleotides and Photographic materials

[32p] ɣ-ATP was from Board of Radiation and Isotope Technology (BRIT), India. X-ray films of medical type were from Garware Polyester Ltd., India.

Preparation of dialysis tubing

Dialysis tubing was cut in as per requirement and soaked in sterile 50mM Tris HCl, 100mM NaCl buffer, pH 7.5 for overnight at 4^{o}C. The buffer was replaced with similar buffer containing 2 % Glycerol and 10 mM EDTA and autoclaved and stored at 4^{o}C.

Composition of stock solutions

Stock solutions mentioned in Table 2.1 were prepared in GDDW and sterilized without adjusting the pH wherever necessary. Preparation of all the antibiotic stock solutions is given in Table 2.2. were prepared with sterile diluents and stored as aliquots at -20°C. Different antibiotic containing LB or TYG plates were made by addition of required amount of antibiotic's to agar media just prior to pouring the plates (~50°C). Plates containing antibiotics were usually used within 1 day of pouring or else stored at 4°C.

Table 2.1 Composition of stock solutions

Chemical	Concentration		Storage
	Stock	Final	
Adenosine triphosphate (ATP)	10mM	1mM	-20°C
Ammonium persulfate (APS)	100mg/ml	1 mg/ml	-20°C
BSA	10.00%	As required	-20°C
$CaCl_2$	1.0 M	100mM	4°C
dNTPs	100 mM	As required	-20°C
DTT	1.0 M	1mM	-20°C
Ethidium bromide	5 mg/ml	0.5 mg/ml	RT.
EDTA (Na salt)	0.5 M	As required	RT.
D-glucose	20.00%	As required	4°C
Glycerol	98%	As required	RT.
KCl	2.0M	As required	RT.
IPTG	1.0M	As required	-20°C
$MgCl_2$	1.0 M	As required	4°C
$MgSO_4$	1.0 M	10 mM	4°C
PMSF	100mM	1mM	-20°C
SDS (Sodium salt)	10%	As required	RT.
Sodium acetate	3.0 M	As required	RT.

Sodium chloride	**5.0 M**	**As required**	**RT.**
Sodium citrate	**1.0M**	**10 mM**	**RT.**
Sucrose	**25%**	**As required**	**4°C**
Tris.HCl	**1.0 M**	**As required**	**RT.**

Table 2.2 Antibiotic stock solutions

Antibiotic	**Stock Solution (mg/ml)**	**Working Concentration (μg/ml)**
Ampicillin	**100 in sterile DW**	**(100) a**
Chloramphenicol	**34 in Ethanol**	**(15-100) b**
Kanamycin	**25 in sterile DW**	**(5-30) c**
Spectinomycin	**100 in sterile DW**	**(50-75) d**

Notes :

A: 100 μg/ml used for high copy number plasmids such as pDSW209 and pNOKOUT.

B: Chloramphenicol 15μg ml^{-1} was used for maintenance of mini-F plasmid (pDAG203) in *E. coli* and chloramphenicol 100μg ml^{-1} was used to condense the nucleoid.

C: For maintaining knockout derivatives of *D. radiodurans*.

D: For maintance of expression vector in *D. radiodurans*.

2.2 Composition of commonly used analytical reagents

1 M Tris.HCl

121.1 gm. of Tris base was dissolved in 800 ml GDDW and adjusted its pH and concentration as required and autoclaved, stored at RT.

1M DTT

3.08 gm of dithiothreitol powder was dissolved in 20 ml of sterile MilliQ grade water. Solution was filter sterilized using 0.22μm Whatman filter disc and stored at -20^{o}C.

0.5 M EDTA (pH = 8.0)

186.1 gm. of disodium EDTA salt was dissolved in 800 ml GDDW and pH was adjusted to 8.0 using 10 N NaOH. The final volume was made up to 1 litre and sterilized by autoclaving, finally stored at RT.

Phenol

The molecular biology grade phenol was obtained from Sigma chemical company, USA and frozen in –20^{o}C. The frozen phenol thawed at 68°C and a pinch of stabilizer i.e. 8'-hydroxyquinoline was added to it. The phenol was then equilibrated by adding an equal volume of 1 M Tris HCl (pH = 8.0) and finally stored in 100mM Tris HCl in dark at 4°C.

Phosphate Buffered Saline

Dissolve 8 gm NaCl, 0.2 gm KCl, 1.44 gm Na_2HPO_4 and 0.24 gm KH_2PO_4 in 800 ml distilled water and adjusted pH to 7.4 using dilute HCl, volume was made up to 1000 ml and sterilized by autoclaving. The buffer finally stored at RT.

GTE (for Alkaline miniprep)

GTE solution was prepared by diluting the respective stock solutions as mentioned in Table 2.1 to 50 mM Glucose, 25 mM Tris.HCl (pH= 8.0); 10 mM EDTA (pH= 8.0). Solution was autoclaved and stored at 4°C.

5 M Potassium acetate (for Alkaline miniprep)

59 gm. of potassium acetate dissolved in 100 ml Milli Q grade water to it 23 ml of glacial acetic acid was added to obtain the final pH of 4.8. Then volume was made up to 300 ml using sterile water stored at 4°C after autoclaving.

PMSF (100mM)

348 mg of the phenyl methyl sulfonyl fluoride (PMSF) powder was dissolved in 20 ml isopropanol and vortexed vigorously until it get dissolved, small aliquots were stored by wrapping vials with aluminum foil and stored at -20^{o}C.

$T_{10}E_1$

10 mM Tris.HCl (pH= 8.0), 1 mM EDTA (pH = 8.0) were prepared by diluting respective stock solution.

10 x TBE

108 gm. of Tris base, 55 gm. of boric acid (borate) and 40 ml of 0.5 M EDTA (pH = 8.0) were resuspended in distilled water and the volume was made up to 1 litre.

50 x TAE

242 gm Tris base was dissolved in 800 ml of distilled water to it 57.1 ml of glacial acetic acid and 100 ml of 0.5 M EDTA pH 8.0 was added. Solution was autoclaved and stored at RT.

Metal affinity purification matrices

Immobilized metal affinity chromatography matrix was obtained from GE healthcare (Sweden) as fast flow metal chelating materials and Ni-NTA agarose from QIAgen (Germany).

Composition of media

All the media described here were sterilized by autoclaving at 15 P.S.I. for 20 min and stored at RT., unless otherwise mentioned. To prepare solidified media 1.5% of Agar-agar was added.

Luria Bertani Broth (LB)

NaCl, 10 gm.; Bacto-yeast extract, 5 gm.; Bacto-tryptone, 10 gm.; was resuspended in distill water, final volume made up to 1 litre and the pH adjusted to 7.4 with NaOH.

TGY medium

Tryptone, 5g; Yeast Extract, 3g, Glucose, 1g were dissolved in 1000 ml of distilled water and pH=7.4 was adjusted with NaOH.

2x TGY medium

Tryptone, 10g; Yeast Extract, 6g, Glucose, 1.0g were dissolved in 1000 ml of distilled water and pH=7.4 was adjusted with NaOH.

Composition of other reagents used in molecular biology studies

6x DNA loading dye

DNA loading dye was made by adding 0.25 % bromophenol blue, 0.25 % xylene cyanol and 50 % glycerol and this solution was autoclaved and stored at 4^{o}C.

DNAase I

5 mg DNAase I, 2.6 ml sterile (98 %) glycerol and 150 µl 5 M NaCl. were mixed to dissolve in 2.25 ml sterile Milli Q grade water by repeatedly tapping or vortexing, dispensed as 500 µl aliquots and stored at -20°C.

RNAase A (10 mg/ml)

50 mg RNAase A was dissolved in 5 ml of 10mM sodium acetate (pH 5.2). The solution was heated at 115^{o}C for 15 min and allowed to decrease slowly to RT. To this, 500µl of 1MTris.HCl (pH = 7.5) was added and stored at –20^{o}C.

Lysozyme

Lysozyme was freshly prepared at a concentration of 50 mg/ml in 10 mM Tris.HCl (pH = 8.0).

10 mM dNTPs (for PCR and blunting reactions)

40 µl each of the four deoxynucleotide triphosphate solutions (25 mM stock) were mixed and adjusted volume to 100 µl with sterile distilled water and stored at -20°C.

Acrylamide Stock (30%)

29.2gm acrylamide and 0.8 gm of N, N-Methylene (bis) acrylamide was dissolved in 70 ml distilled water. The mixture was stirred for 30 min to assure complete dissolution and then the volume was made up to 100 ml. Then solution was filtered through Whatman 540 filter disc and stored at 4^{o}C.

Acrylamide Stock (40%)

38gm acrylamide and 2 gm of N, N-Methylene (bis) acrylamide was dissolved in 70 ml double distilled water at 37^{o}C. The mixture was stirred for 30 min to assure complete dissolution and then the volume was made up to 100 ml. The solution was filtered through Whatman 540 filter disc and stored at 4^{o}C.

2x Laemmelli Cracking buffer

460 mg of SDS, 7.6 mg of EGTA, 20 mg of sodium azide, 2 ml of Glycerol, 150 μl of 100mM PMSF, 1.0 ml β-mercaptoethanol in 2.5 ml of 0.5M Tris-HCl, pH 6.8 and 40μl of 0.5 % bromophenol blue was added and volume was made up to 10 ml with distilled water.

10 x SDS PAGE electrophoresis buffer

30 gm Tris base, 144 gm Glycine and 10 gm SDS was dissolved in 800 ml distilled water. The volume was made up to 1000ml with distilled water.

Destain solution I

500 ml of methanol was mixed with 100 ml of glacial acetic acid, volume made to 1 litre with distilled water. The solution was kept in dark bottle and in air-tight container. This can be used for two to three times.

Destain solution II

Destain II was prepared with 100 ml methanol, 100ml glacial acetic acid and 20 ml of glycerol in 1000 ml solution. The contents were mixed thoroughly and stored in dark bottle and air tight container.

Coomassie Brilliant Blue staining dye

0.5 gms of Coomassie Brilliant Blue R250 was dissolved in 42.5 ml GDDW. To this, 50 ml of methanol and 7.5 ml of glacial acetic acid was added. Solution was stirred and filtered through Whatman 540 filter paper.

Malachite Green Reagent

Solution A: 0.4% Malachite green (w/v) in dH_20 (30ml). Prepare by vigorously stirring on magnetic stirrer for 30 min.

Solution B: 4.2% Ammonium molybdate (w/v) in 5M HCl. Prepare by vigorously stirring with magnetic stirrer for 30 min.

Solution C: 1.5% Tween 20(w/v) in dH_2O. Prepare by vigorously stirring with magnetic stirrer for 30 min.

Solution D: Mix 1 volume of solution B+3 volumes of solution A. Prepare by vigorously stirring with a magnetic stirrer for 30 min. Then filter through Whatmann filter paper to obtain a yellow colored solution. This stock is stable for 2-3 weeks in dark.

Working solution:

Before use, mix 1ml of solution C with 32 ml of solution D. Prepare by vigorously stirring with a magnetic stirrer for 30 min.

TBS (Tris- Buffered Saline)

20 ml of 1M Tris-HCl, pH 7.6 was mixed with 200 ml of 5M NaCl and volume was made up to 1000 ml with sterile distilled water. The solution was stored at RT.

TTBS

0.05% Tween 20 in TBS.

Blocking solution

3 gm of skimmed milk powder was mixed with 100ml TBS was dissolved and stored at 4^{o}C.

Antibody Buffer

3 gm of skimmed milk powder was mixed with 100ml TTBS solution and used fresh.

Transfer Buffer:

48 mM Tris base; 39mM Glycine; 20% methanol.(5.82 gm Tris base+2.92 gm Glycine+200ml methanol and make up to 1 lit with DW).

2.3 Methods

2.3.1 Microbiological methods

Maintenance of the bacterial stocks

Bacterial stocks were maintained at RT and under frozen conditions. Room temperature stocks were made in soft agar LB medium containing 0.2 % glycerol. The medium was dissolved by heating at 100^{o}C and cooled down to 48^{o}C before it was dispensed to airtight screw capped tubes to 80% of the total capacity. The vials were loosely capped and sterilized by autoclaving. They were allowed to cool down to RT before the caps

were tightened and incubated at 37^{o}C overnight. The bacterial cells were stabbed with needle wire and preserved at RT.

Alternatively, bacterial culture stocks were preserved at freezing temperature in presence of cryoprotectants. The logarithmically growing culture was spun and resuspended in minimal medium and /or LB medium to cells density of 10^{9} cells per ml. The cell suspension was mixed with 20% glycerol in polypropylene screw capped tubes and stored in freezing temperature tolerant boxes, at –70^{o}C. The stocks were numbered and entered in the bacterial culture book with full details.

Growth of the bacterial strains

Different bacterial strains used in this study are summarized in Table 2.3. Bacterial culture was taken from long-term storage stocks directly on LB / TGY agar plates and or plates containing appropriate antibiotics if required. The plates were incubated at appropriate temperature for overnight. Single isolated colonies were inoculated in liquid broth with or without antibiotics and allowed to grow at 37^{o}C for *E. coli* and 32^{o}C for *D. radiodurans* at shaking speed of 150 rpm overnight. The overnight grown liquid culture was diluted to 1:100 in fresh broth with selection pressure if required. The culture was allowed to grow with shaking at 200 rpm at appropriate temperature. The aliquots were drawn at different time intervals and optical density was measured at 600 nm. In parallel an appropriate dilutions were plated on suitable agar plates and the numbers of colonies were counted. The growth curve drawn under defined set of conditions was used in determining the different growth phases of the culture for different experiments. Total number of colonies appeared on agar plates after different treatments of *D. radiodurans* cells were taken for calculating the survival efficiency.

Table 2.3 List of bacterial strains used in this study

Strain	Genotype	Source
D. radiodurans	**wild type**	**lab stock**
***E. coli* MG1655**	**rph1 ilvG rfb-50**	**lab stock**
***E. coli* DH5alpha**	***F- / endA1 hsdR17 glnV44 thi-1 recA1 gyrA relA* Δ *(lacIZYA-argF) U169 deoR (Φ80dlac*Δ *(lacZ)M15)***	**lab stock**
***E. coli* BL21 (DE3) *pLys*S**	***F-ompT gal [dcm] [lon] hsdSB DE3::T7RNA***	**lab stock**
***E. coli* JM109**	***end*A1, *rec*A1, *gyr*A96, *thi*, *hsd*R17 (r_k^-, m_k^+), *rel*A1, *sup*E44, Δ(lac-proAB),**	**lab stock**
Δ ParB1 *D. radiodurans*	**DR_0012(mutant)**	**this study**
ΔParB2 *D. radiodurans*	**DR_0012(mutant)**	**this study**
TB86	**ΔlacIZYA::frt ΔminCDE::frt ΔslmA::aph**	**Bernhardt ,2005**
TB89	**ΔlacIZYA::frt ΔslmA::frt**	**Bernhardt,2005**

2.3.2 Methods used in molecular studies

2.3.2.1 Isolation of plasmid DNA (mini prep)

Plasmid DNA was prepared using alkaline lysis method as described in (Sambrook J and Russell DW, 2001) brief, the bacterial cells were grown overnight in 3ml 1x LB broth with appropriate antibiotics. The cells were spun at 10,000 rpm for 30 sec and washed with TBS. The pellet was suspended thoroughly in 100 µl ice chilled GTE and 200 µl of freshly prepared alkaline SDS (0.2N NaOH, 1% SDS) was added. The mixture was incubated at RT for 5 min and 150µl pre-chilled potassium acetate (5M) was added and mixed thoroughly and quickly. The mixture was incubated on ice for 5 min and then spun at 10,000 rpm for 10 min. The supernatant was extracted with equal volume of chloroform: isoamylalcohol (24:1) and 0.6 volume of isopropyl alcohol was added. The contents were mixed and incubated at RT for 20 min before plasmid DNA was collected by centrifugation, washed and air-dried.

2.3.2.2 Large scale preparation of plasmid DNA.

Large scale preparation of plasmid DNA was carried out as described in Sambrook 2001. In brief, cells harboring high copy plasmid DNA were grown overnight with vigorous aeration in 50 ml 1x LB broth medium. The low copy number plasmid harboring bacterial culture was grown overnight in presence of antibiotics and then diluted 1:100 in 500 ml LB with antibiotic and allow to grow till OD 600 was 0.4. Appropriate antibiotic was added in the mid exponential phase culture and allowed to grow for 12-16h at 37^{o}C with vigorous shaking. Cells were harvested and washed with TBS. The plasmid DNA was prepared using alkaline lysis method. The cell pellet was completely suspended in 4 ml GTE buffer and to this 8 ml alkaline SDS solution was added. Contents were gently mixed and incubated at RT for 5mins. The nucleoprotein-SDS complex was precipitated with 6 ml of pre chilled 5M potassium acetate (pH 5.6) solution on ice for 5 min. The supernatant was collected by centrifugation at 12K for 10 min at 4^{o}C and RNase A (50μg/ml) was added and extracted with equal volume of $CHCl_3$: IAA (24:1). The upper layer was taken and DNA was precipitated with 0.6 volume of isopropanol at RT for 20 min. The DNA was collected by centrifugation at 12 K for 10 min and washed with 70% ethanol followed by absolute alcohol. The pellet was dried and DNA was dissolved in sterile water. The plasmid DNA concentration and purity were determined by measuring the OD260 and OD280, spectrophotometrically. The purity of DNA preparation was assured by finding the ratio of A260/A280. (A260 of 1.0 corresponds to 50μg/ml DNA, A260/A280 ratio indicates the purity of the DNA preparation, the ratio more than 1.65 showed the DNA free from proteins).

2.3.2.3 Genomic DNA isolation

Escherichia coli:

Bacterial chromosomal DNA was isolated using protocol as described earlier (Clark, 1971). In brief, the cell pellet was washed with TBS and preserved at –70^{o}C if not processed immediately. The pellet was thawed at 4^{o}C and homogenized in 1/10th volume of 25 % sucrose and lysozyme (200 μg/ ml) was added and mixed properly. The mixture was incubated for 10 min on ice and 10mM EDTA (pH 8.0) was added and incubated for 5 min on ice. The cells were lysed with 0.5% SDS and mixed gently to get clear lysate. The RNAase A (50μg/ml) was added and incubated at RT for 20 min. The lysate was extracted with equal volume of phenol (pH 8.0) till white precipitate stops coming. The aqueous phase was extracted once with phenol: $CHCl_3$: IAA (25:24:1) and once with $CHCl_3$: IAA. The aqueous phase was mixed with 0.3M Na acetate and 2.5 volume of chilled ethanol was added from the side of the tube to layer on the top of the DNA solution. The high molecular weight DNA was recovered by spooling on sterilized glass rod. The spooled DNA was washed with 70% ethanol and air-dried. The total DNA was recovered by centrifugation and washed with 70 % ethanol. The DNA pellet was dissolved in sterile 10 mM Tris-HCl, pH 8.0.

D. radiodurans:

The 100 ml culture was overnight grown at 150 rpm at 30^{o}C. The cells were collected, pellet was washed with 70% ethanol and resuspended in 1ml TE Buffer, add 2mg/ml lysozyme (stock 10mg/ml) and incubated at 37^{o}C for 30 min. The 600μg /ml proteinase K and 2% SDS was added and incubated at 37^{o}C for 3 hours. Supernatant was extracted

and treated with equal volumes of phenol-chloroform, incubated on ice for 10 min. Mixture was centrifuged at 10,000 rpm for 10 min. The aqueous layer was extracted with equal volumes of 24:1 mixture of chloroform-isoamyl alcohol. The supernatant was mixed with 1/10th volume of 3M sodium acetate pH 4.5 & 2 volumes of ethanol and incubated at -20^{o}C for ½ hr. DNA was collected at 12,000 rpm for 15 min and dissolved in sterile water. DNA concentration was ascertained with OD260 and on agarose gel (Das and Misra, 2012;Earl *et al.*, 2002;Kota and Misra, 2008).

2.3.2.4 Agarose gel electrophoresis

Agarose gel electrophoresis was used for the qualitative and quantitative analysis of DNA. The agarose was dissolved in required buffer by heating in microwave oven and the solution was cooled to around 50^{o}C before ethidium bromide (EtBr) (0.5μg/ml) was added and poured. It was allowed to solidify at RT for 30 min. The samples mixed with gel loading dye solution were loaded and electrophoresed. The gel was run till tracking dye has reached to 3/4th of the gel length or depending on the experimental requirement. Similar procedure was followed for preparation of the low melting point (LMP) agarose gel but the ethidium bromide (0.5μg/ml) was added at 50^{o}C and gel was polymerized at low temperature.

After the electrophoresis has completed, the DNA bands were visualized on UV trans illuminator (UVP Model 3UVTM Trans illuminator) at different wavelengths or with hand UV lamp (Model UVGL-58) depending on the necessity of the experiment.

2.3.2.5 PCR amplification.

Primer design and synthesis

Primers were designed manually using the corresponding nucleotide sequences from *D. radiodurans* genomes database and different primers used in this study are summarized in Table 2.4. The sequence of the DNA to be amplified was taken and restriction enzyme analysis was carried out using BIOEDIT software. The unique restriction sites were noted and suitable restriction endonuclease sites were incorporated into the forward and reverse primers sequence. Further some more sequences that are required for efficient cutting by the corresponding restriction endonuclease were added at the upstream to the 5'end of both the primers. The composition of the primers was adjusted to have at least 50 % G+C content (wherever possible). In any case the minimum G+C content in the primer was not less than 40 %. The approximate Tm values were determined as Tm= 2x (A+T) +4 x (G+C). Care was taken to avoid repetitive sequences at the 3' end which might results in primer dimer formation and 3' base was necessarily kept A or T while C or G was preferred as penultimate base. The complete primer sequence was subjected for its match on the other sites of the chromosome. The mismatch was adjusted in such a manner that 6-9 nucleotide of the 3' end should not have perfect match on any other site on the chromosome. The primers were commercially synthesized and purified to best purity by manufacturers.

Table 2.4: List of primers used in this study

dr0012F	**5' GGAATTCCATATGGTGTCGAAAAAATCTAGCCT 3'**
dr0012R	**5' CCGCTCGAGTTATTCCTCGGCCTCGTA 3'**
dr0013F	**5' GGAATTCCATATGATGACGGACCACGCGGGC 3'**
dr0013R	**5' CCGCTCGAGCTAGATTTTTTCGACACGTTGCA 3'**
drA0001F	**5' GGAATTCCATATG ATGGTGAGCGCTGTGA 3'**
drA0001R	**5' CCGCTCGAGTCATGCGTTTTCCCCCGGA 3'**
***segS*1F**	**5' CCACATGTCAACCGCTGTTCGCCGCT 3'**
***segS*1R**	**5' CGTACGACCTGGTTCCAACGAAGCGCGCGAA 3'**
***segS*2F**	**5' CCACATGTCTTATGCTCGCCCGCTGA 3'**
***segS*2R**	**5' CGTACGACCTGGTCCCCGTTTTCATTTGTCA 3'**
***segS*3F**	**5' CCACATGTAGAACCAGCCCGACTGGA 3'**
***segS*3R**	**5' CGTACGACCTGGTACAGGATGCACTCGTAACT 3'**
***parB1 G*F**	**5' CG GGATCCGTGTCGAAAAAATCTAGCCT 3'**

***parB1G*R**	**5' CCCAAGCTTTTATTCCTCGGCCTCGTA 3'**
***parA1 G*F**	**5' CG GGATCCATGACGGACCACGCGGGC 3'**
***parA1G*R**	**5' CCCAAGCTTCTAGATTTTTTCGACACGT 3'**
***parA2C*F**	**5'CCCAAGCTTGATGGGCAGCAGCAGCCATCAT 3'**
***parA2C*R**	**5'CGGGATCCATTGCGTTTTCCCCCGGA 3'**
GfpF	**5'CGAGCTCATGAGTAAAGGAGAAG 3'**
DP2F	**5'AGCAAGGCGGCCAGCCCGCT 3'**
DP2R	**5'CTGGCTGTGGCGTCGGT 3'**
dr0012UF	**5'GGGGTACCCAGCCGTTCCGCAGGAGGA 3'**
d0012UR	**5'CGGAATTCCGTCAGACGACTTCAAAGCT 3'**
dr0012DF	**5'GCGGATCCGGGCTCGCCTTTCTTGGTCA 3'**
dr0012DR	**5'CCCCCGAGCTCCCCGCACCCTCATCGCGATGCT 3'**
drA0002UF	**5'CCGGGCCCATTCCACAAAGTGCCACAGGCA 3'**
drA0002UR	**5'CGGAATTCAAGCAGGTCGCGCCGACGCACT 3'**
drA0002DF	**5'GCGGATCCCGGGTCCGTCAGGCGATAGA 3'**
drA0002DR	**5'CCCCCGAGCTCGGCTGCCGGCTGCGTCATGA 3'**
nptII F	**5'AGGCCACGTTGTGTCTCA 3'**
nptIIR	**5'TGCTCTGCCAGTGTTACA 3'**
***parB1*iF**	**5'TGTTCGAGCCCGAATCGC3'**
***parB1*iR**	**5'AGGTCGAGTTCGAGCTGC 3'**
***parB2*iF**	**5'GATCTCAGTCAAGCCAACGATA 3'**
***parB2*iR**	**5' ACGCACCATTCTGGGCAA 3'**

PCR reactions

Polymerase chain reaction is a very sensitive method for the amplification of desired DNA fragment of a few kilo bases from giant size genomes of single cell. PCR amplification was mostly carried out in 50µl volume. A typical PCR reaction contains template (50ng), primers 400µM, dNTP's 200µM, Taq DNA polymerase buffer 1x, 1.5 mM $MgCl_2$ and Taq DNA polymerase 2.5U.

PCR product purification using band-stab PCR technique.

In the cases where PCR amplification is carried out using primers with low Tm values and primers having differences in their Tm values, the PCR reactions are normally carried out at sub-optimum conditions. Under this condition the PCR product contains non-specific PCR products along with desired products. So, the specific products were purified by selectively taking desired product for subsequent round of the PCR amplification, which can be achieved by directly stabbing the DNA band with sterile hypodermic needles and suspending it in the PCR reaction mixture containing all the components except enzyme. The PCR reactions were carried out and products were

analyzed on agarose gel. This technique gives reasonably pure product for sequencing purpose. However, the presence of the PCR components makes this product non-suitable for ligation and cloning purpose unless they are removed by purification techniques.

PCR product purification using agarose gel electrophoresis.

PCR products were separated on molecular biology grade high melting point (HMP) agarose and also low melting point (LMP) agarose. After electrophoresis is complete, the DNA was visualized with handset UV lamp in long wavelength and desired DNA band was cut with sterile blade. DNA extraction from HMP agarose gel pieces was carried out either by commercially available gel extraction kits using manufacturer's protocols. The frozen gel pieces were spun at 12K for 10min and supernatant was transferred in a separate 1.5 ml tubes. The DNA was extracted with equal volume of phenol: $CHCl_3$: IAA (25:24:1) till white precipitate stops coming and finally precipitated with salt and ethanol. Gel extraction kits were also used from QIAGEN, Roche Biochemicals, Sigma Chemicals Company and the respective kits protocols were used in this study.

2.3.2.6 DNA manipulation.

Restriction digestion.

The protocols followed for restriction digestion with a particular enzyme were largely as described by manufacturers. The restriction digestion of DNA was carried out in presence of the specific buffers and minimum amount of enzymes required for the digestion of that DNA preparation. The ratio of enzyme to DNA was kept less than 10 and the concentration of glycerol in reaction mixture was maintained less than 10% in overall reaction. Restriction digestion of mini prep plasmid DNA has been normally carried out

by diluting plasmid DNA volume to ten fold in final reaction mixture. Restriction digestion has been mostly carried in 50-100μl. After every digestion reaction, the samples were analyzed on agarose gel to make sure of enzyme activity.

Preparation of plasmid vector for ligation

In cloning experiment, the phosphodiester bond formation could be either intermolecular or intra molecular. Intra molecular ligation between plasmid vector molecules results in increasing the background of the ligation reaction. The intermolecular ligation between vector and inserts would lead to the cloning of the insert in the vector. The later could be achieved if intra molecular ligation can be avoided and that can be done if vector is dephosphorylated specifically for blunt end cloning.

Different vectors used in this study

Different plasmids used in this study are summarized in Table 2.5.The partial maps of plasmid vectors used in this study are given in Table 2.5. The plasmids were prepared by using plasmid minikit (Roche Biochemicals) and digested with respective enzymes. The linearized plasmid DNA was gel purified and used for subsequent studies.

Dephosphorylation of DNA.

The vector plasmid DNA is digested with appropriate restriction enzyme and linearized vector DNA was gel purified and used for dephosphorylation using standard protocols for alkaline phosphatase activity. In brief 1 μg vector DNA was incubated with 10U of Calf Intestinal Phosphatase (CIP) in 20 μl reaction volume in presence of CIP Buffer (Roche Biochemicals) and incubated at 37^{o}C for 30 min. The reaction was stopped by heating the

mixture at 65^{o}C for 15min. The dephosphorylated vector was further purified with phenol: $CHCl_3$: IAA and followed by DNA precipitation by using ethanol, washed, air dried and dissolved in 10 µl sterile water. 1.0 µl 0f DNA sample was analyzed on agarose gel and 100 ng of it was used for one cohesive end ligation reaction.

Table 2.5 List of plasmids used in this study

Sr No.	Name of the plasmid	Characteristics	Source
1	pET28+a		Novagen
2	pET0012	pET28 with *parB1* at *Nde*I and *Xho*I	This study
3	pET0013	pET28 with *parA1* at *Nde*I and *Xho*I	This study
4	pETA2	pET28 with *parA2* at *Nde*I and *Xho*I	This study
5	pAMCYAN	Ap^r; *amCyan* expression vector, ColE1	Clontech
6	pA2CFP	pAM CYAN with *parA2* at *Hind* III and *BamH* I	This study
7	pLAU85	pBAD24 encoding LacI-ECFP and FtsZ-EYFP; Amp^r	Lau,2003
8	pDSW209	PDSW209-*gfp*-MCS (fusion vector)	Weiss, 1999
9	pDSWparA1B1	pDSW209 with *parA1parB1* at *BamH* I and *Hind* III	This study
10	pHJ 0012	pDSW209 with *parB1* at *BamH* I and *Hind* III	This study
11	pHJ 0013	pDSW209 with *parA1* at *BamH* I and *Hind* III	This study
12	p11559	Expression vector; Pspac PtufA::lacI Spcr in *E. coli* and in *D. radiodurans*	Lecointe,et.al 2004
13	pVH11559	p11559 with 42 bp fragement at *Nde*I and *Xho*I	This study
14	pD12GFP	pVH11559 with *gfp parB1* at *sac*I and *Xho*I	This study
15	p11559A2	p11559 with *parA2* at *Nde*I and *Xho*I	This study
16	Mini-F plasmid (pDAG203)	Mini-F Δ(sopOPABC) cat+ (6.67 kb)	Dubbary,et.al 2005
17	pDAGS1	pDAG203 with *segS*1 at *SexA*I	This study
18	pDAGS2	pDAG203 with *segS*2 at *SexA*I	This study
19	pDAGS3	pDAG203 with *segS*3 at *SexA*I	This study
20	pNOKOUT	pBluescript SK+ with 900 bp *npt*II cassate at *sma*I	Khainair, et.al 2008
21	pNOK0012	pNOKOUT with 1Kb *parB1* upstream and down stream at *Apa*I/*EcoR*I and *BamH*I /*Sac*I	This study
22	pNOKA0002	pNOKOUT with 1Kb *parB2* upstream and *parB2* down stream at *Apa*I/*EcoR*I and *BamH*I /*Sac*I	This study

End flushing of PCR amplified products

The PCR products used for blunt end ligation were end filled using T4 DNA polymerase. To suppress exonuclease activity the relatively higher concentration of dNTP's were used as suggested in supplier protocols. A typical reaction mixture contains DNA, 1 μg; T4 DNA polymerase buffer, 1x (New England Biolabs, USA), T4 DNA polymerase enzyme 10U in a total reaction volume 20 μl. The mixture was incubated at 37^0C for 30 min and reaction was stopped by heating at 65^0C for 15 min. Products were purified by using PCR purification kit (Roche).

Ligation

For sticky end ligation, normally the insert to vector molar ratios were set to 2:1 to 3:1. The amount of the insert is fixed to around 100ng and then vector amount was adjusted to a particular ratio, according to the size of the vector. For the blunt end ligation reaction, the amount of the insert was increased to 500 ng and then amount of vector was adjusted to meet the molar ratio of inserts to vector of 3:1 or 4:1. The required amount of the vector and inserts were mixed in one tube and precipitated with salt and ethanol. The precipitated DNA pellet was washed twice with 70% ethanol and once with 100 % ethanol. The air dried DNA pellet was dissolved in minimum volume of sterile water. The mixture was heated at 55^oC for 5 min and chilled quickly on ice. The ligation conditions for sticky end ligation and blunt end ligation are different. The blunt end ligation is carried out at 20^oC for overnight. On contrary, cohesive ends ligation requires 1mM ATP at 16^oC for overnight. However, excess ATP inhibits ligation reaction. The amount of ligase enzyme required for blunt end ligation is also 5-6 times more as compared to cohesive end ligation.

2.3.2.7 Bacterial transformation

Escherichia coli

Competent cells were prepared using the standard protocol. In brief, the overnight grown culture of desired *E. coli* strain was diluted to 100 fold in fresh LB medium. The culture was allowed to grow at 37^{o}C till O.D$_{600}$ reaches to 0.3 to 0.4 and thereafter the cells were chilled on ice for 30 min. The culture was transferred to pre-chilled SS34 tubes and centrifuged at 6,000 rpm for 5 min at 4^{o}C. The pellet was gently suspended and ½ culture volume of 100mM $CaCl_2$ was added and this cell suspension was incubated on ice for 45 min. Thereafter it was centrifuged at 4,000 rpm for 10 min and competent cells were gently resuspended in 0.1 culture volume of 100mM $CaCl_2$, they were used for transformation. These competent cells can be stored on ice till 16 hr and at –70^{o}C in 20 % glycerol for one month without much loss of competence.

The 200µl of the competent cells were aliquoted in 1.5 ml pre-chilled tubes and to it approximately 100ng of the plasmid DNA was added and gently mixed by tapping. The mixture was incubated on ice for 30 to 45 min and heat shocked at 42^{o}C for 2 min followed by 2 min on ice incubation. The transformation mixture was diluted with 800µl of 1x LB broth. For the expression of antibiotic resistance genes, the mixture was incubated at 37^{o}C for 30 min to 45 min. The transformation mixture was plated on LB agar plates containing appropriate antibiotics. The plates were incubated at 37^{o}C for overnight and transformants were scored and characterized.

D. radiodurans

The competent of *D. radiodurans* cells were made by freshly inoculating overnight grown culture into plain TYG media (1/50 dilutions) and allowed to grow at 32^{o}C till O.D reaches to 0.3 O.D, 1M $CaCl_2$ was added (final concentration should be 30mM). Culture was grown until O.D reaches 0.6 (i.e. approximately 90 minutes), then culture was transferred on to ice and incubated for 30 minutes. To 200 µl of culture nearly 1µg of DNA was added and allowed to incubate on ice for 10 minutes. Fresh media was added and culture was incubated at 32°C for 1 h. From the incubated culture 500 µl of culture was diluted to 5 ml fresh TYG media and remaining 500µl of culture was spinned down and plated on respective antibiotic plates (Smith *et al.*, 1989).

2.3.2.8 Methods used in proteins purification

Inducible expression of genes in *E. coli*

E. coli strain BL21 DE(3) *pLysS* harboring different pET 28a+ containing '*par*' genes was grown overnight in the presence of kanamycin (25µg/ml). The cells were diluted in fresh LB medium containing antibiotics and allowed to grow for 3-4 h to get density 0.3 O.D 600nm and then 2% ethanol was added to the culture allowed to it grow till O.D reaches 0.6, to this culture 0.2 mM of IPTG was added and growth was continued for a period of 5h. A small aliquot (200µl) was drawn for checking for the inducible synthesis of 'Par' proteins and remaining cells were harvested, washed and preserved at –70^{o}C for downstream processing. For protein analysis the cells were collected and suspended in 50µl TE buffer. To it 50µl of 2x laemmellie SDS gel buffer was added and mixture was heated at 95^{o}C for 10min and spun at 10,000 rpm for 10min. The supernatant was loaded on SDS-PAGE and electrophoresis was carried out. Gel was stained for checking if

protein was induced. Having made sure that 'Par' proteins was produced in good quantity, the remaining cell pellet was processed for large scale purification (Desai *et al.*, 2011;Kamble and Misra, 2010).

SDS-PAGE analysis of proteins

On PAGE proteins migrate according to mass / charge ratio and structural topology of that species. However, if charge is unified then these proteins will migrate on the basis of their masses and that would help in determining their molecular weights. Sodium dodecyl sulfate (SDS) is an ionic detergent which denatures proteins by 'wrapping around' the polypeptide backbone. SDS binds fairly specifically in a mass ratio of 1.4:1 and confers a negative charge to the polypeptide. Individual polypeptide chains form a complex with negatively charged molecules of sodium dodecyl sulfate and therefore migrate as a negatively charged SDS-protein complex through the pores of polyacrylamide gel. In denaturing SDS-PAGE therefore, migration is determined not by intrinsic electrical charge of the polypeptide, but by molecular weight.

Preparation of SDS-PAGE gel

SDS-PAGE gel was prepared in two different ways. (i) Ordinary SDS-PAGE having the single concentration of the gel (Table 2.5)and (ii) gradient SDS-PAGE from 14-18 % acrylamide concentrations (Table 2.6). The ordinary gel with uniform 10 % Acrylamide concentration was made as below.

Table 2.6 Composition of 10 % separating polyacrylamide gel

Acrylamide (30%)	**5.3 ml**
1.5M Tris-HCl, pH-8.8	**5.0 ml**

10 %SDS	**200 μl**
10 % ammonium per sulfate	**200 μl**
TEMED	**20 μl**
Water	**3.4 ml**
Total volume	**20 ml**

Composition of 5% stacking gel

Acrylamide (30%)	**0.83ml**
1.0 M Tris-HCl, pH 6.8	**0.63ml**
10 % SDS	**50 μl**
10 % ammonium per sulfate	**50 μl**
TEMED	**15 μl**
Water	**3.4 ml**
Total volume	**5.0 ml**

For making gradient PAGE gel, the components for 7 % and 18 % solution were mixed separately as per following compositions.

Table 2.7 Gradient gel compositions

	14%	**18%**
Distilled water	**7.7 ml**	**5.4 ml**
Acrylamide (40%)	**7.0 ml**	**9.0 ml**
Tris-HCl, pH 8.8 (1.5M)	**5.6 ml**	**5.4 ml**
SDS (10%)	**0.2ml**	**0.2 ml**
Ammonium per sulfate (10%)	**0.08 ml**	**0.06 ml**
TEMED (100%)	**0.01 ml**	**0.01ml**
Total volume	**20ml**	**20 ml**

Procedure of gel pouring

Glass plates were cleaned with liquid soap, rinsed with water and wiped with 70% ethanol. The plate sandwich made with 1.0 or 1.5 mm spacers and assembled with gel

casting stand. Plates were tightened with clamps and make sure that the screws are properly fitted. Gaps were sealed with agar and SDS-PAGE mixture for separating gel was poured. It was over layered with water-saturated n-butanol. After 20-30 min when gel is polymerized, the butanol was removed and washed with water. Stacking mixture was poured and comb was fitted in the gel. Once the stacking gel is polymerized, the comb is removed and wells were cleaned with water 3-4 times and then samples were loaded. The samples were prepared by heating equal volume of sample and 2x SDS gel loading dye at 95^0C. The denatured samples were spun at 12 k for 10 min and clear supernatant was loaded in the gel. The electrophoresis tank was filled with electrophoresis buffer (10% SDS-Tris-Glycine, pH 8.8) and gel was run for 1 h at 100 volts and then at 200 volts for 3h. Gel assembly was dismantled. The gel was taken out in plastic container and stained with different dye depending upon requirement.

Coomassie Brilliant blue staining

Coomassie blue dye binds with the basic amino acids of the polypeptide. This is an irreversible method for protein staining. The common procedure used for staining gel by this method is as below. In brief, the gel was fixed for 10 min in destain solution I (DSI) (50% methanol + 12.5 % Glacial acetic acid). DS I was discarded and Coomassie strain solution was added. Staining was continued for 10 min or till bromophenol blue dye changes color to yellow. The stain was poured back for repeated use and gel was submerged in destain solution II (DSII) and changed couple of times until the background become colorless.

Silver staining methods of protein gel

Silver staining is a highly sensitive method for the staining of the proteins and nucleic acids. The staining relies of the affinity of the silver ions for nucleophilic and aromatic groups. Silver ions are reduced to metallic silver, which under alkaline condition gives brilliant brown precipitate. This procedure can be used for staining of biomolecules in PAGE gels and agarose gels. This staining method is extremely sensitive and a protein band of 1ng can be detected. For staining, wash the gel twice for 30 min each in 10% acetic acid, 50% methanol and 0.05% formaldehyde solution or once over night with gentle shaking. Replace the solution with the 50 % ethanol and wash it twice for 20 min each. After discarding of ethanol, the gel was rinsed with deionized water for 10 sec. Then add (0.2 gm/L) sodium thiosulphate solution and keep it on shaker for exactly 1 min. Further rinse the gel with deionized water for three times for 20 sec each. The gel was incubated with silver nitrate (2gms/L) and 0.04 % HCHO for 45 min in dark. Further, rinse the gel with deionized water three times for 5sec.-10sec each under dark conditions to wash the extra stain from the gel. Add developer solution [(10 mg/L) sodium thiosulphate, (0.25 ml/L) 30% HCHO in (60gms/L) of $NaCO_3$] to the gel and keep it on shaker until the spots develops. Further add [Tris (50 gms / L in acetic acid (25 ml / L)] for 5 min. gel was documented.

Preparation of cell free extract of *E. coli*

The cell pellet was thawed on ice and 1 gm pellet was suspended in 2 ml lysis buffer A (20mM Tris-HCl, pH 7.5; 0.1mM EDTA and 1mM DTT). Lysozyme was added to a final concentration 200μg/ml and incubated on ice for 20 min. To it, Triton X-100 was added to make a final concentration of 0.1% and sonicated at 4μl and 50% duty cycle, for 3 min with the 1 min intermittent cooling on ice. Suspension was diluted to two folds and

centrifuged at 12,000 rpm (SS34, Sorvall) for 15 min. The clear supernatant was used native purification and pellet was used for denaturation purification.

Protein estimation

Using different spectrophotometric methods, the presence of proteins in a particular solution was quantitatively estimated. One method is measuring the absorbance maxima of proteins at 280 nm could be exploited for detecting the presence of proteins in eluted fractions. Other method used for the estimation of proteins was dye binding method (Bradford, 1976) using Bradford dye (BioRad) kit protocols. In brief, 200µl of the 5x dye solution was mixed with 800µl of total solution containing proteins and buffer. The content was mixed by vortexing and incubated at RT for 15 min before color development was monitored spectrophotometrically at 595nm. The OD595 was compared with a calibrated curve that was made using standard concentration of BSA. Amount of protein present in the solution was estimated.

Metal affinity purification of recombinant proteins

Immobilized Metal ion affinity Chromatography exploits molecules affinity for chelated metal ions. The amino acid histidine present in the protein forms complex with transition metal ions such as Cu^{+2}, Zn^{+2} and Fe^{+3}. Chelating sepharose fast flow with a suitable immobilized metal ion e.g.; Ni^{+2} selectively retained the protein with exposed histidine. Exposed Cysteine and Tryptophan residues may also be involved in the binding to immobilized metal ion but their contribution to the binding is much lower than the contribution of exposed histidine residues. The strength of binding is affected by buffer

pH and the metal ion selected. The most important factor affecting proteins binding is the pH; at more alkaline pH binding will most likely via deprotonated amino groups.

Native proteins purification

For affinity purification the proteins were extracted by different methods, such as sonication of cells pretreated with non-ionic detergent, by using cell lytic express (Sigma Chemicals Co). The clear supernatant was loaded onto the manually pre packed columns, in brief Chelating sepharose fast flow charged with $NiCl_2$, and washed, equilibrated with buffer in which the proteins were suspended. Clear supernatant solution was loaded on the column and proteins are allowed to bind to it at flow rate of 1 ml/ min. Columns were washed with Ni-NTA wash buffer for native proteins and eluted as described in Ni-NTA agarose native protein purification protocols of quaigen.

Denaturing condition purification

High levels of expression of recombinant protein led to the formation of insoluble aggregates in form of inclusion bodies. The recombinant protein was purified using a standard kit protocol. In brief, the inclusion pellet was solubilized in buffer containing 100mM NaH_2PO_4, 10mM Tris-Cl and 8M urea, pH8.0. The lysate was centrifuged at 10,000 rpm for 30 min at room temperature to pellet the cellular debris. To the clear supernatant, Ni-NTA was added and mixed gently by shaking at slow speed on a magnetic stirrer for 60 min at room temperature. The lysate-resin mixture was carefully loaded into an empty column. Flow through was collected and stored for SDS PAGE analysis. Column was washed with 10 column volumes of Buffer C (100mM NaH_2PO_4, 10mM Tris-Cl, 8M urea, pH 6.3). The protein fractions each of 500µl were eluted with buffer D (100 mM NaH_2PO_4, 10 mM Tris-Cl, 8 M Urea, pH-5.9) followed by buffer E

(100mM NaH_2PO_4, 10 mM Tris-Cl, 8 M urea, pH 4.5). The collected fractions as well as flow through were analyzed by SDS PAGE. Nearly pure fractions were collected. Refolding of the protein was carried out by serially dialyzing the protein in buffers with decreasing concentration of urea. protein was resuspended in 20mM Tris , 50mM NaCl , 0.5 mM EDTA and 1mM DTT, completely refolded protein is repurified using native purification method as mentioned above, purified fractions were collected, dialysis was done and stored in storage buffer containing 20mM Tris –HCl, 50mM NaCl, 1mMEDTA , 30% glycerol.

2.3.2.9 Microscopy

To understand the properties of the bacterial sample which are generated by deletion or over expression of the protein microscopy was done. In principle the specimen is illuminated with light of specific wavelength which is absorbed by the flurophores or proteins and emits higher wavelength light. Exponential growing culture was taken and live cells were mounted onto a bed of 1 % agarose in water (w/v) for viewing under the microscope. Images were acquired using a Carl Zeiss Axiovision M_{RC} fluorescence microscope, the data was analyzed using Axiovision rel 4.8 software, Acquired images were overlapped using Image J software (Donovan *et al.*, 2010).

2.3.2.10 Statistical Analyses

Statistical analyses were performed using the software Graph pad prism 5.0 software.

CHAPTER 3

RESULTS

CHAPTER 3.1

Identification of genome partitioning elements using bioinformatic approaches.

Recent methodological advances have resulted to a rapid progress in understanding the mechanisms of the DNA segregation process in prokaryotes. It was suggested that prokaryotic cells contain a mitotic-like apparatus that is responsible for the active segregation of plasmids and chromosomes prior to cell division. The bacterial plasmids encode partitioning gene cassettes (termed *par*) that are required for important events in the replicon segregation process. After genomic DNA sequencing, homologues of 'Par' proteins were identified in all 'Gram-positive' as well as 'Gram-negative' bacteria. To certain extent the role of these partitioning genes were understood in organism like *B. subtilis* (Hester and Lutkenhaus, 2007;Ireton *et al.*, 1994), *S. colicolor* (Dedrick *et al.*, 2009;Jakimowicz *et al.*, 2007), *C. crescentus* (Shebelut et al., 2010), which contain single circular chromosome. The bacteria containing multiple genome replicating units were also identified. The 'Par' homologues have been found in bacteria like *V. cholera* (Fogel and Waldor, 2005), *D. radiodurans* (White *et al.*, 1999), *Burkholderia* (Dubarry *et al.*, 2006) etc. harboring multiple genome replicating units. Genome of *D. radiodurans* (Dubarry *et al.*, 2006) is also annotated with 'Par' like proteins but centromeric sequences were not identified. Since multiple ParA's and ParB's are annotated in the genome, it would be interesting to analyze if these could have different functional motifs leading to altered specificity and interaction. Therefore, these proteins were checked for similarities and dissimilarities with their several know homologues in database and the identification of centromeric sequences in genome of this bacterium through homology search was carried out.

3.1.1 Methods:

Characterization of 'Par' proteins in *D. radiodurans* was done by retrieving sequence from database at NCBI. The sequences obtained were aligned in CLUSTAL-X, an multiple sequence alignment graphical interface computer programme (Higgins and Sharp, 1988). Also to improve the alignment, the alignments were superimposed with theoretically calculated secondary structure data. This was done to ensure that gaps would be forced in the alignment building process where only loops were present. A phylogenetic distance tree was built from this alignment using NJ algorithm, a bottom clustering method for generating phylogenetic trees. For statistical accuracy this phylogenetic tree was bootstrap for 1000 times i.e. bootstrapping is a method to measure variance of sample from desired population. Additionally, the FASTA formatted sequence (protein sequence alignment programme) for each individual 'Par' protein sequence under study was submitted to an internet protein structure function prediction server (I-TASSER) website for obtaining the homology three dimensional model of the individual protein (Roy *et al.*, 2010). Since our aim was limited to studying conservation at fold level, we did not energy minimize the structures. Similarly centromere like sequence of plasmid and chromosome of *D. radiodurans* were annotated using a DNA sequence alignment programme i.e. Blast- N (Basic Local Alignment Search Tool) analysis by adjusting search parameter to small oligonucleotide for chromosomal type of centromere sequences.

3.1.2 Results:

3.1.2.1 Identification of centromere like sequences in *D. radiodurans*:

Earlier reports indicated that the segregation process requires *cis* element and trans acting proteins. Therefore, the existence of both of these complements is expected in the genome of any bacteria. These can be either the homologues of the well characterized proteins and consensus centromeric regions and/or uncharacterized proteins and centromere's. The genome of this bacterium encodes putative partitioning proteins but no known centromeric regions.

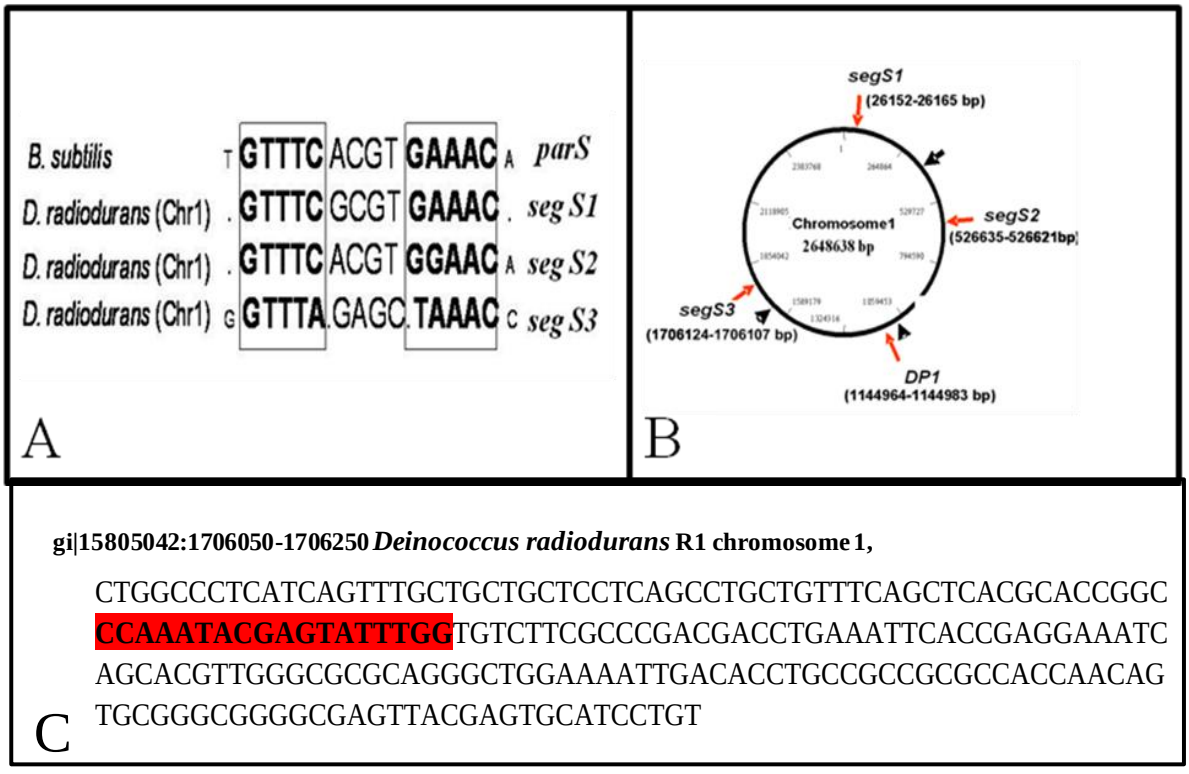

Fig 3.1.1: Centromere sequences on chromosome I of *D. radiodurans:* A) Sequence homology of *parS* like of *B. subtilis* is shown. **B)** Graphic representation of the distribution of centromere like sequence on chromosome I are represented. C) *SegS*3 sequence was retrieved from NCBI – Genome and represented over here.

B. subtilis genome was identified with the 16bp long nucleotide sequence as *parS* of this organism (Lin and Grossman, 1998). This motif was used for homology search in the genome of *D. radiodurans*. Blast-N analysis by setting parameters to small nucleotides,

showed few identical centromere like sequences present on the chromosome I (Fig 3.1.1A) which are distributed at different locations in chromosome I of *D. radiodurans* (Fig 3.1.1B). These sequences were termed as putative centromeres involved in **seg**regation and accordingly named as segS elements. Due the minor differences at nucleotide levels, these were separately named as *segS*1, *segS*2 and *segS*3. Chromosome II and megaplasmid doesn't show *Bacillus* type *parS* sequences.

Subsequently, the genome of *D. radiodurans* was searched for P1 plasmid type centromeric sequence (P1 *parS*) (Martin *et al.*, 1991). Our analysis identified few aberrant homologues of P1 *parS* on chromosome(S) and megaplasmid in *D. radiodurans* and these sequences were named as DP1 (P1 *parS* of chromosome I of *D. radiodurans*), DP2 (P1 *parS* of chromosome II of *D. radiodurans*) and MP1 (P1 *parS* of mega plasmid of *D. radiodurans*) (Fig 3.1.2). Typically, the hexameric and heptameric repeat boxes were named as box A and box B (A1 B1 A2 A3 A4 B2) and are arranged in a specific orientation in P1 *parS*. The IHF binding site is located between box A1 and boxA2. Indispensability of the arrangements of boxes and IHF binding site in segregation of P1 type plasmid has been demonstrated. The sequences identified on chromosome I, chromosome II and mega plasmid were lacking IHF binding site and these boxes were not organized in order that is reported in P1 type *parS* element. DP1 showed A1 and B1 boxes with single point mutation in right hand side of P1 *parS* and left hand side only box A2 is present and A3 and A4 boxes were absent, more over box B2 has also shown a partial match. In DP2 showed high sequence homology in left hand side i.e. A2 and B2 boxes where as few mismatches in the right hand B1 and A1 boxes. MP1 showing presence of few A1 and B2 boxes but the orientation is different as compared to P1 *parS*.

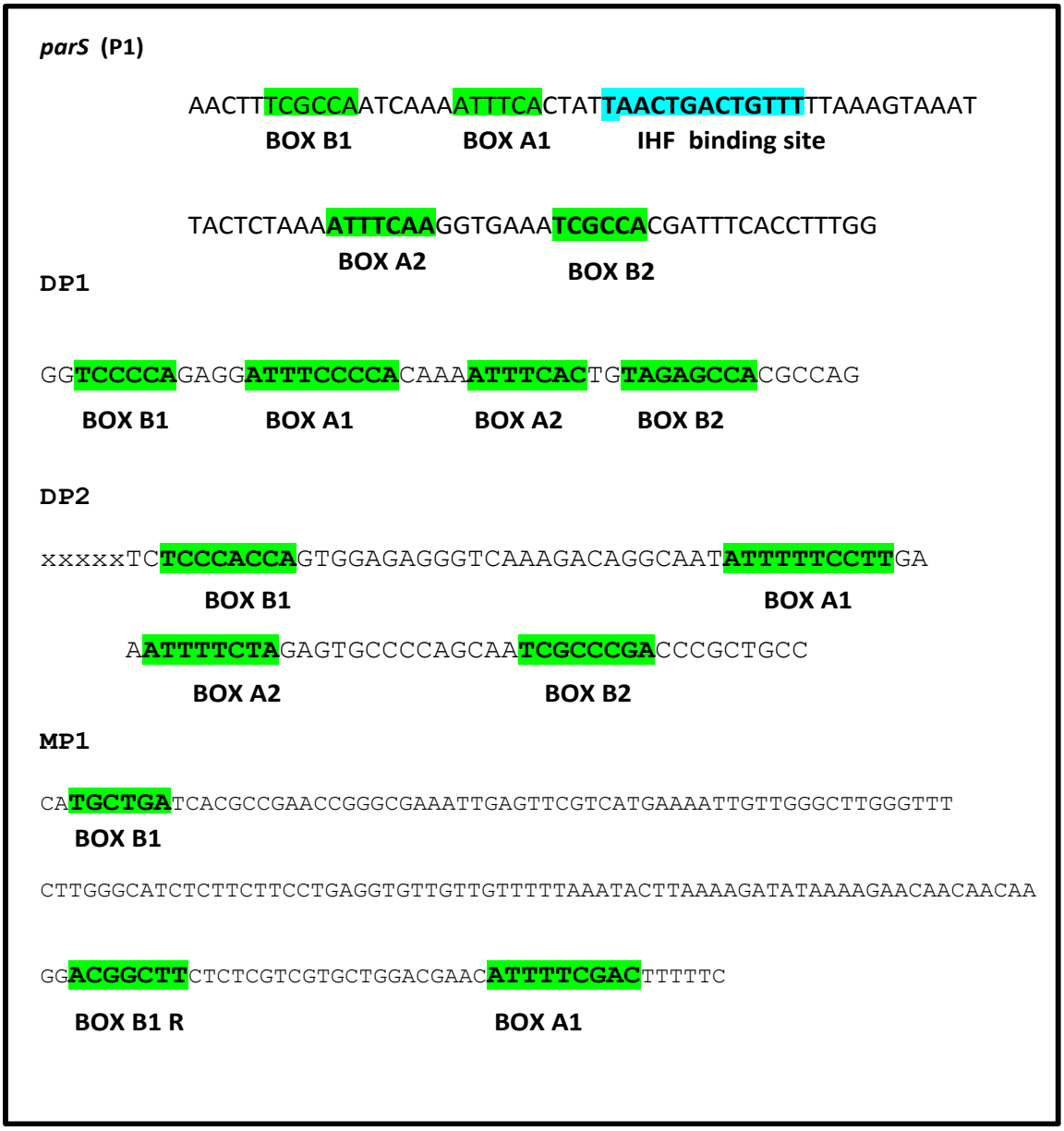

Fig 3.1.2: Analysis of P1 type of centromere like sequence in *D. radiodurans*: Representation of hexameric (BoxB1, BoxB2) and heptameric sequence (BoxA1, BoxA2) and both left, right hand side of P1 *parS* element.

Overall our analyses indicated that DP1, DP2 and MP1 are showing partial similarity but lacking typical IHF binding sites within the sequence. Earlier fine structural analysis of P1 *parS* had shown that deletion or modification of hexameric or heptameric sequence hampered the segregation of the plasmid or changed the species specificity in different bacteria (Martin *et al.*, 1991). Hence the functionality of these aberrant P1 type

centromere's identified in the genome of *D. radiodurans* become doubtful and could not be ascertained.

3.1.2.2 Bioinformatic analysis of trans factors in *D. radiodurans:*

3.1.2.2.1 Genetic organization of '*par*' operon:

The presence of homologues partitioning proteins was tested using Blast-P analysis. Several ParA like proteins and four ParB like proteins were found in entire genome of this bacterium (White et al., 1999).

The chromosomes I and chromosome II are annotated with one '*par*' operon each while megaplasmid encodes two '*par*' operon's and small plasmid doesn't encode any '*par*' operon (Table 3.1). The ORF's annotated as 'Par' proteins are given in Table 3.1.

Table 3.1: Organization of '*par*' genes in *D. radiodurans*

Genome	'Par' Protein
Chromosome I	DR0012 (ParB1) DR0013 (ParA1)
Chromosome II	DRA0002 (ParB2) DRA0001 (ParA2)
Mega plasmid	DRB0002 (ParB3) DRB0001 (ParA3) DRB0030 (ParB4) DRB0031 (ParA4)

3.1.3.2.2 Comparison of ParB family proteins with ParB's of this bacterium: Hypothetical proteins of *D. radiodurans* are annotated after genome sequencing. ParB is one of the components of the '*par*' system, which aids in accurate distribution of the plasmid/chromosome or involved in the proper positioning of chromosome/ plasmid. ParB protein recognizes centromere sequence. *D. radiodurans* consists of four ParB proteins and the multiple sequence alignment (MSA) was done to check the similarities of deinococcal ParB with other known ParB proteins. MSA results showed that ParB1 had an overall homology with the Spo0J of *T. thermophilus* and 40-60% identity with the chromosomal ParB proteins (Fig 3.1.3), whereas remaining ParB2, ParB3, and ParB4 had only ~30% identity which are different from the chromosomal type ParB's. Secondary structure prediction of ParB1 was done using structure of Spo0J (ParB) of *T. thermophilus* (Fig 3.1.3) (Leonard *et al.*, 2004). Since binding and recognition of specific DNA would depend on the structure of the protein, so we generated model structure using $Spo0J_{Tth}$ (PDB ID: 1VZ0). A model with 2^{o}A RMSD was built (Fig3.1.4), which showed closer homology with the Spo0J (ParB) of *T. thermophilus.* It consists of H2 helix and three β sheet with strands S2 and S3 separated by a H3 helix. A characteristic HTH motif formed by helices H6 and H7 and remaining helices help in compaction of the domain (Fig3.1.4a&b), except ParB1 the remaining ParB had shown extra patch of sequence in the Helix Turn Helix (HTH) region. The change in HTH region of ParB1 might allow recognizing different types of centromere like sequence within this bacterium. This protein also showed a change in the C-terminal region with the *T. thermophilus* indicating that the C-terminal variation might allow this protein to recognize cognate ParA protein during segregation process (Fig 3.1.3&4). Expect ParB1,

the remaining ParB's have shown an extra patch of sequence in the HTH region. This might allow us to hypothesize that these structural changes provide flexibility to these ParB's for their interaction with their uncharacterized cognate centromeric sequences.

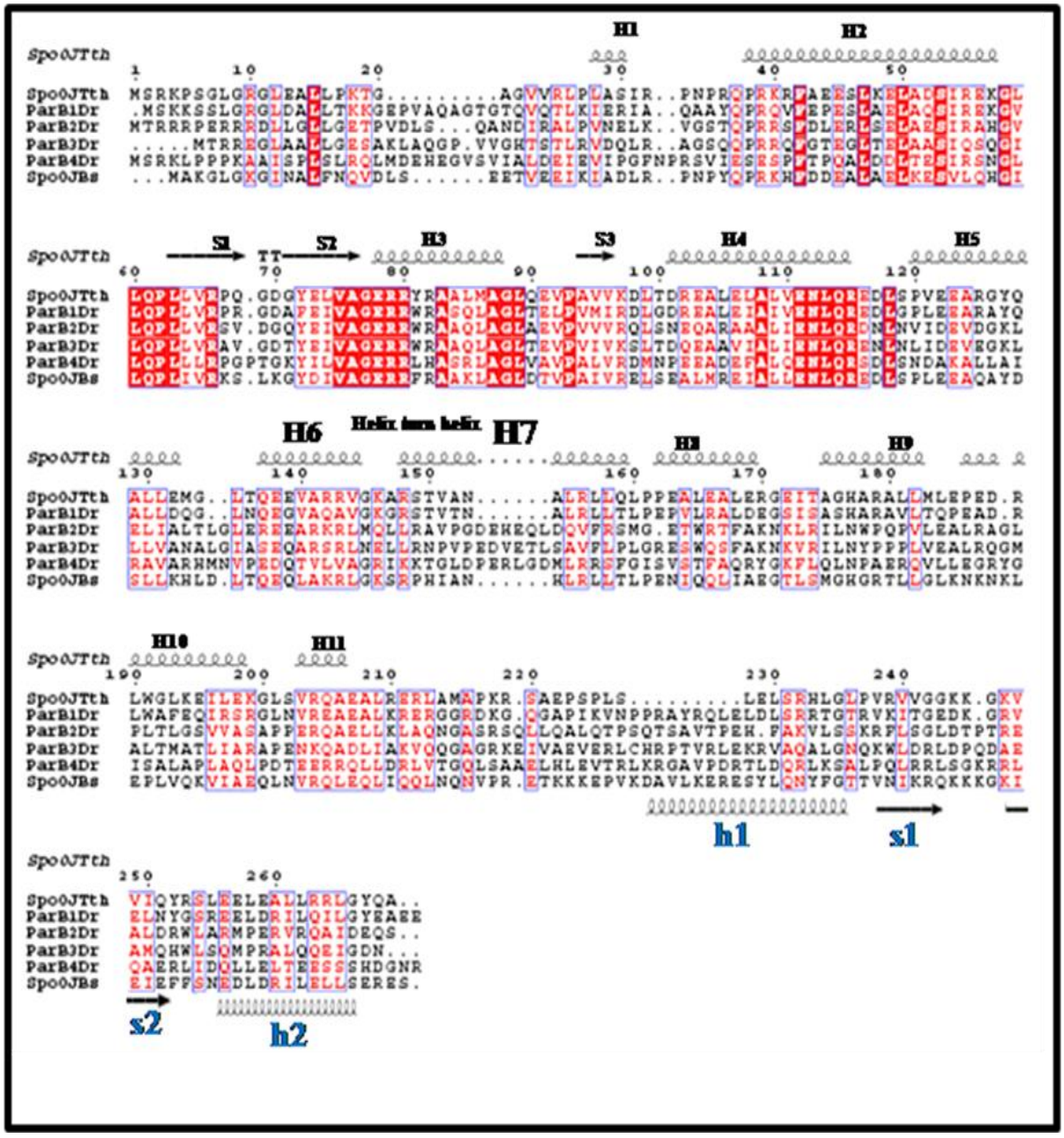

Fig 3.1.3 Multiple alignment of ParB protein with chromosomal ParB: Sequence of different ParB protein is retrieved from NCBI, homology between sequences is checked by Clustal-X analysis. Boundaries of the secondary structure were defined by using online Espript program. The secondary structure shown in this figure corresponds to those of domain of Spo0J of *T. thermophilus* (PDB.ID: 1VZ0). Secondary structure of C-terminal region was analyzed by using Psipred (Protein structure predication) online software and represented in ESPript (Easy Sequencing in post script) online software which renders sequence similarity and secondary structure information.

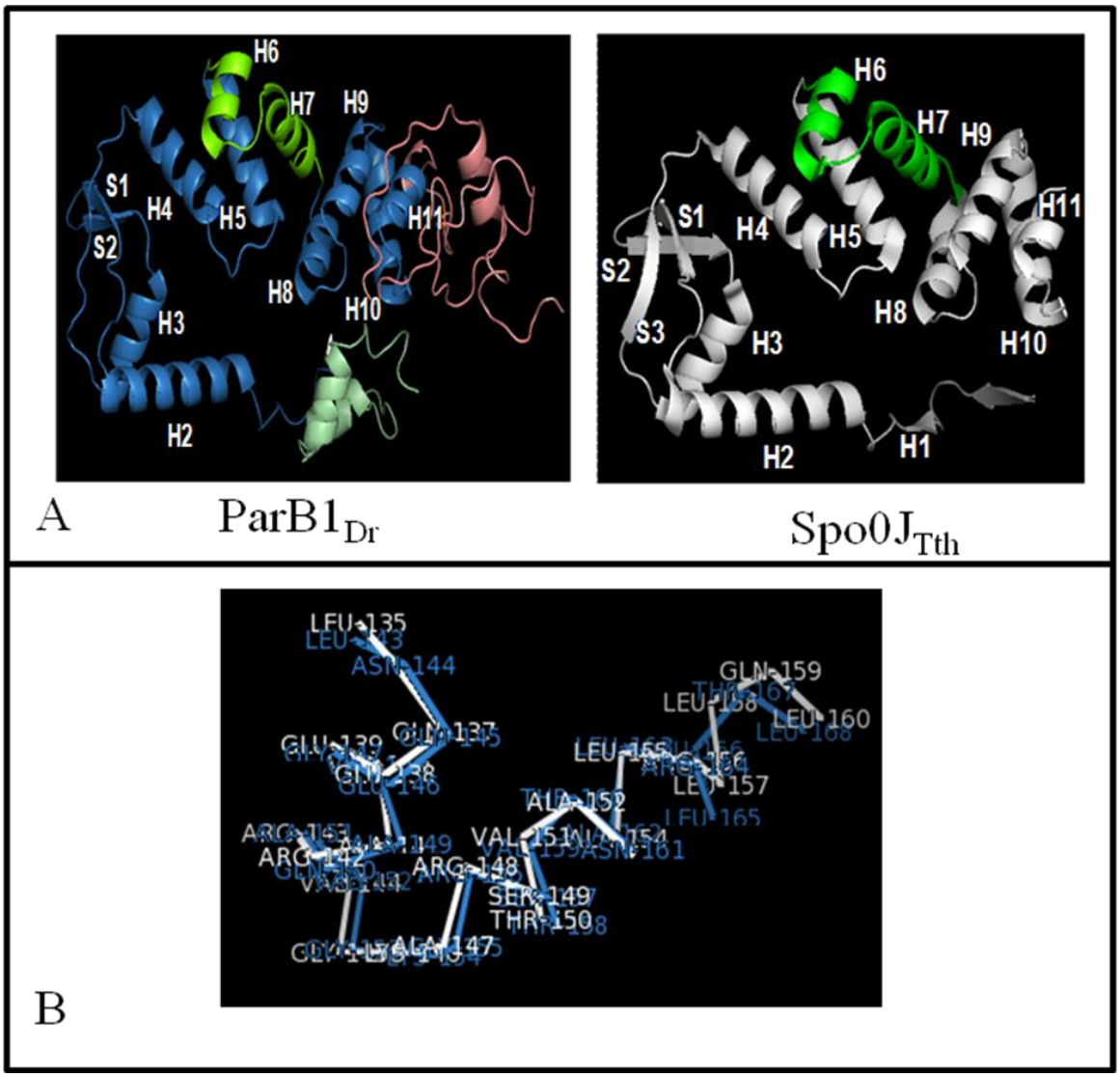

Fig3.1.4: 3-D model of ParB1 of *D. radiodurans*: A) the 3-D model of ParB1 with its homologue $Spo0J_{Tth}$. i) The homology model of ParB1, the Helix turn Helix core domain

in green and extra N-terminal (light green) and C-terminal (light pink) with respect to the 1VZ0 model are highlighted. ii) The template $Spo0J_{Tth}$ molecule (1VZO). **B)** Wire diagram of overlapped Helix turn Helix region of ParB1 and Spo0J.

3.1.3.2.3 Comparative analysis of ParA family proteins with ParA's of this bacterium:

ParA belongs to the P-loop NTPase family proteins (Leipe *et al.*, 2002). The 10 – 18% of total gene products of bacteria belonging to this family (Aravind *et al.*, 2000) are sub grouped into seven subfamilies. Both structural and sequences similarities allowed placing ParA / Soj in a group within *nifH* / MipZ family. After genomic DNA sequencing of *D. radiodurans* nearly 120 genes were annotated as P-loop NTPase. Amongst these, the four ParA proteins are located near origin of replication and co-transcribed with *parB* gene. Different ParA proteins sequence is retrieved from NCBI database and similarities between ParA proteins of *D. radiodurans* and other well characterized ParA proteins were checked to find out the closeness of ParA's of *D. radiodurans* with other know similar proteins. Clustal-W analysis revealed that ParA1 has close similarity with the *T. thermophilus* Soj protein. Both ParA1 and ParA4 showed the extended N-terminal region (Fig 3.1.6). ParA2/A3/A4 showed near about 30% similarity with the known chromosomal ParA proteins at amino acid levels while only at motif level with plasmid encoded ParA proteins (Fig 3.1.5).

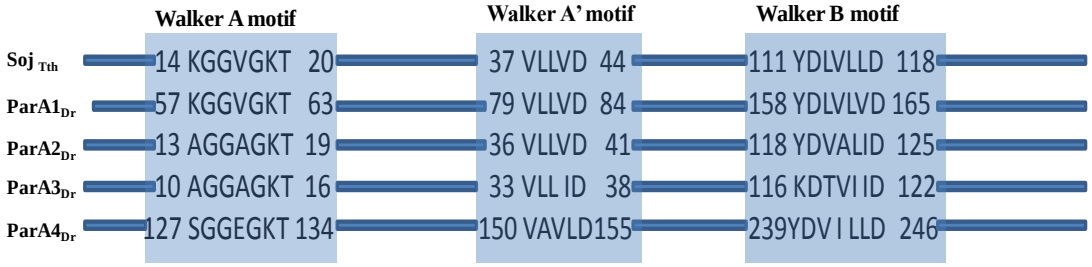

Fig 3.1.5: Graphic representation of deviant walker type motifs in *Deinococcal* ParA proteins.

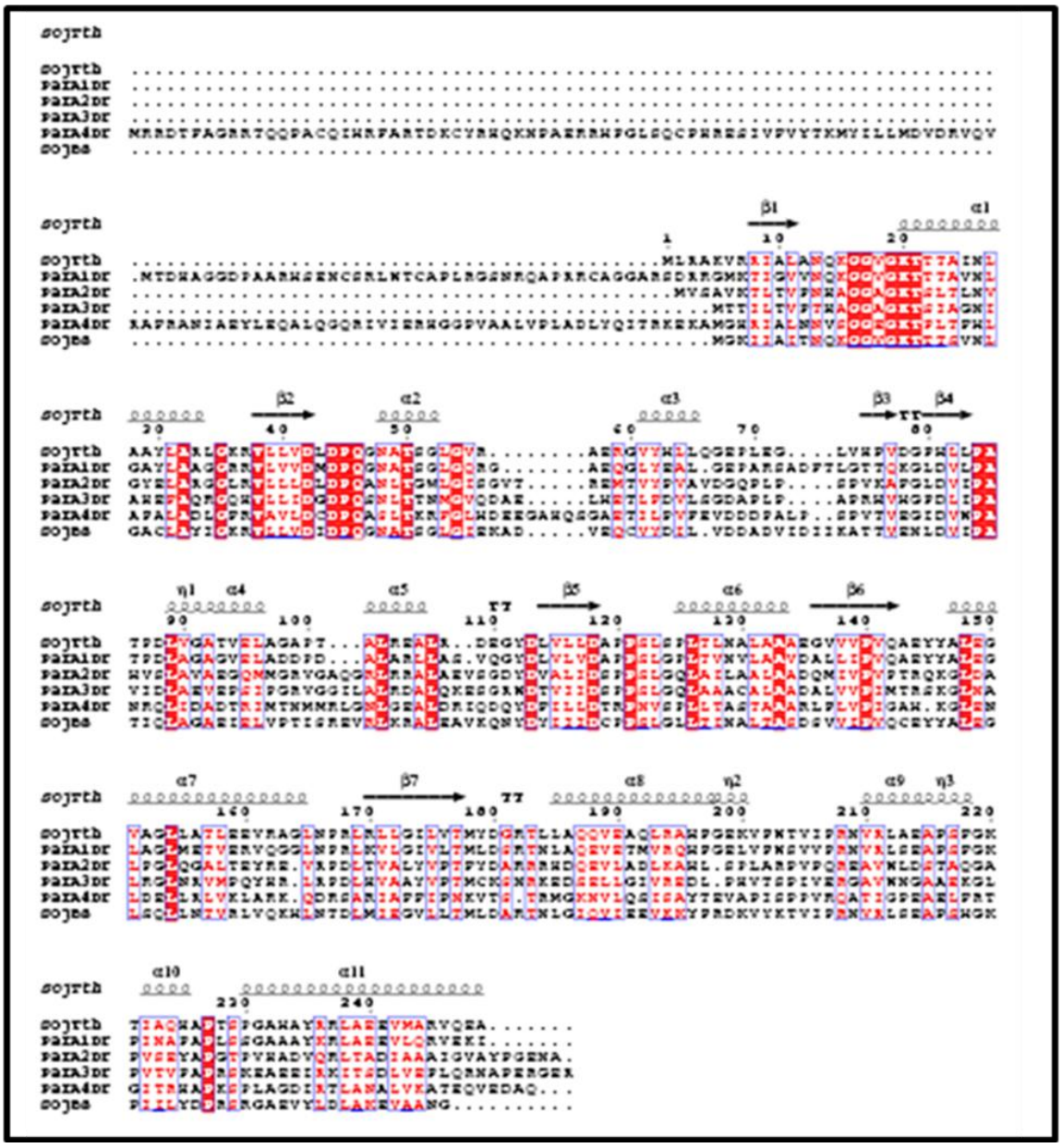

Fig 3.1.6: Multiple alignment of 'ParA' proteins: Sequence alignments of ParA proteins: Sequence of different ParA proteins were retrieved from NCBI, homology between sequences was checked by Clustal-X analysis. Boundaries of the secondary structure were defined using online ESPript program (Easy Sequencing in post script).

The secondary structure shown in this figure corresponds to those of domain of Soj of *T. thermophilus* (PDB .ID: 2BEJ).

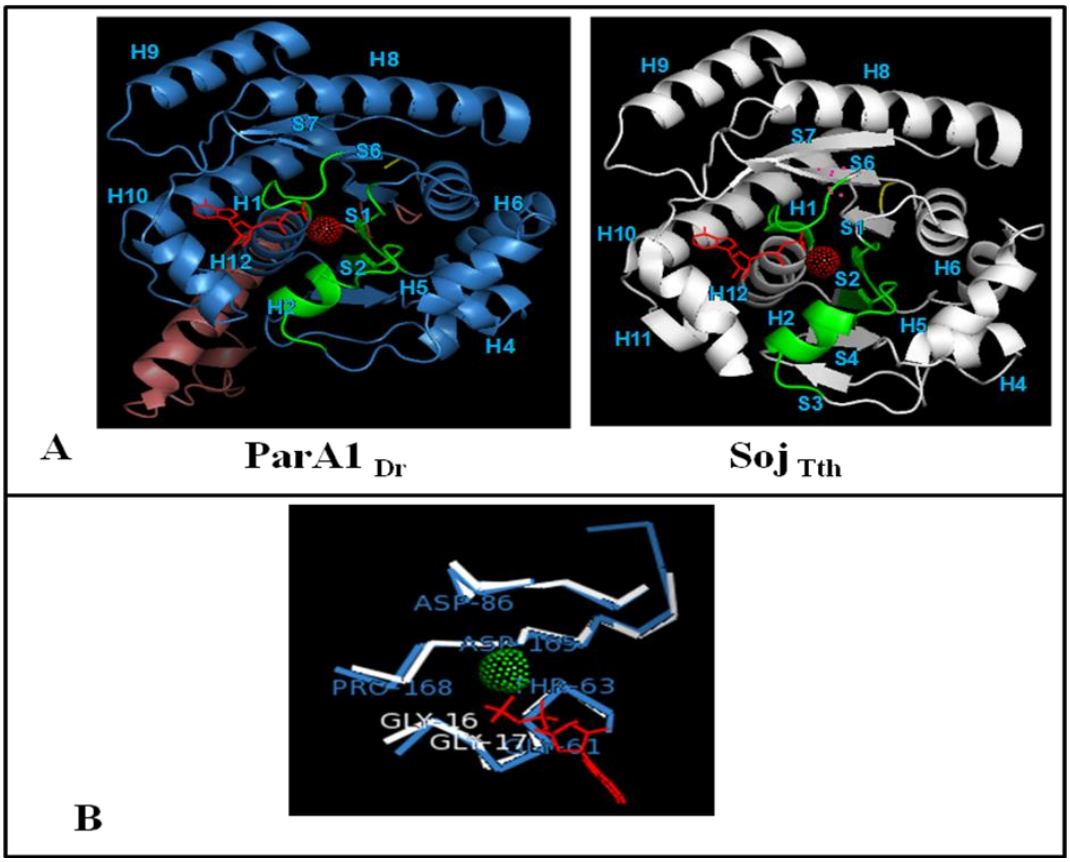

Fig 3.1.7: 3-D model of ParA1 of *D. radiodurans:* A) the 3-D model of ParA1 with it's homolog Soj_{Tth}. i) The homology model of ParB1, the ADP is represented as red sticks and Mg+2 as green/red sphere, active site composed of deviant walker motifs are represented green and extra N-terminal (light pink) with respect to the 2BEJ model are highlighted. ii) The template Soj_{Tth} molecule (2BEJ). **B)** Wire diagram Representation of overlapped Active site with ADP and Mg+2.

To predict the function of protein, we also generated model structure using Soj_{Tth} (PDB ID: 2BEJ) and a model with less than 2^{o}A RMSD was built. ParA1 had shown similarity with the Soj from *T. thermophilus.* It consists of twisted stacked β - strands surrounded by α-helices with some variation (Fig 3.1.7) (Leonard *et al.*, 2005). Interestingly ParA1 and ParA4 had shown extra patch of N-terminal sequence. Although,

the functional significance of this extension is not known, this might help in recognizing its cognate protein (ParB) of this bacterium cannot be ruled out.

3.1.3.2.4 Phylogenetic analysis of 'Par' proteins:

Genome sequence analysis showed the presence of '*par'* operon on each of the three genome replicating units in *D. radiodurans*, except small plasmid. Therefore, the possibility of these proteins performing identical or nearly identical functions and offering functional redundancy would be worth investigating. One of the approaches was to check the similarities and evolutionary relationships. For this, we retrieved the well-characterized 'Par' proteins using NCBI database. MSA of these was done with ParA's of this bacterium, using Clustal X2.1 software and further Bootstrap tree was generated. Results indicated 'Par' proteins on the accessory chromosome (Chromosome II and megaplasmid) are diverged from both chromosomal 'Par' proteins as well from plasmid 'Par' proteins (Fig 3.1.8 a, Fig 3.1.8 b). Interestingly, they have evolved separately from all other 'Par' proteins, including 'Par' proteins from other closely related species too.

Bacterial genome segregation requires at least three factor (i) a cis element (centromere like sequence), (ii) ParB (adaptor protein) and (iii) ParA a motor protein. Bacteria harboring single chromosome had typically shown centromere sequence near the origin of replication, containing 16bp consensus sequence, which was initially identified in *B. subtilis.* Later this consensus sequence was identified in almost all bacteria including that harbor multiple genome replicating units at least on primary chromosome.

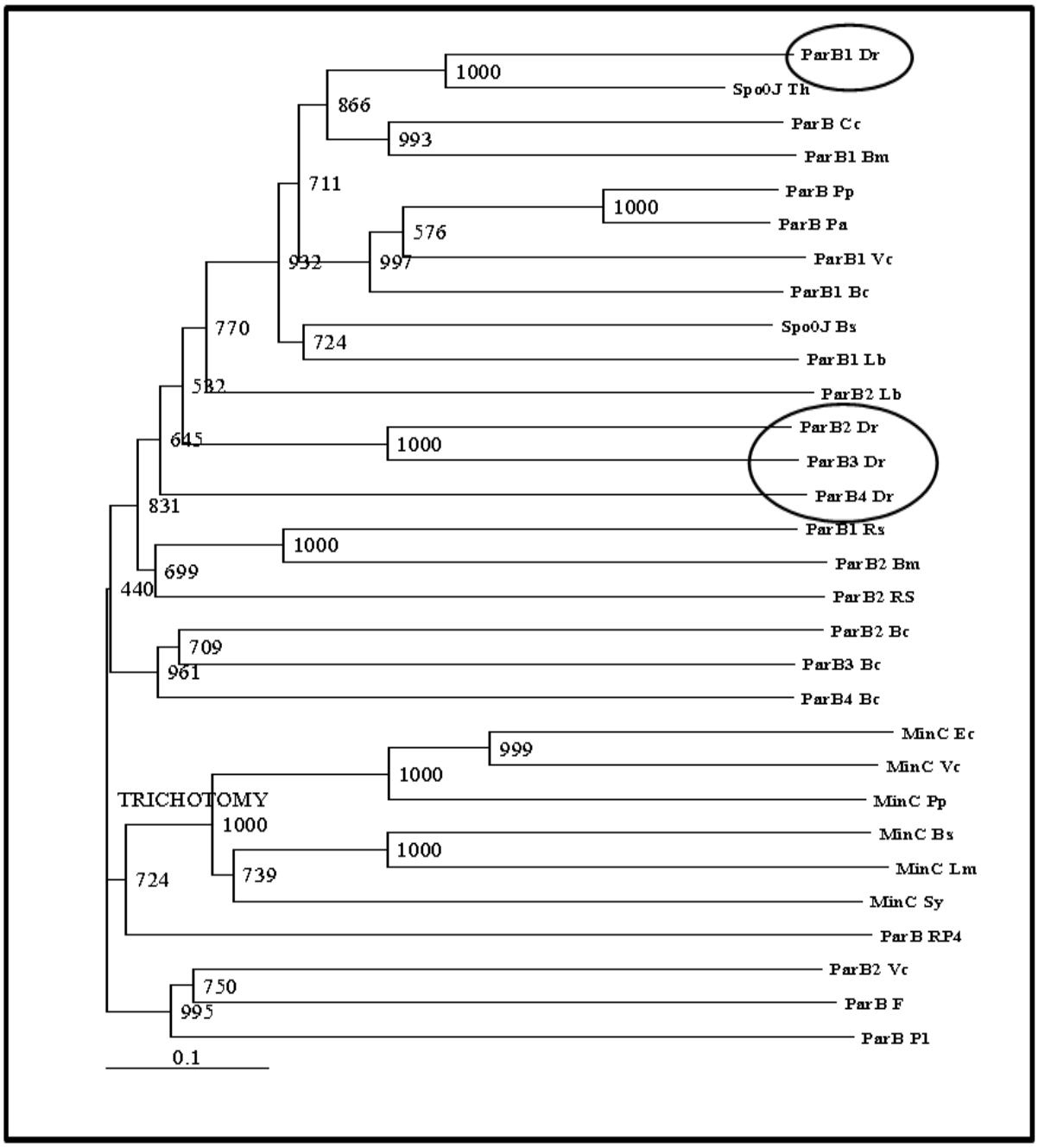

Fig 3.1.8 a: Phylogenetic tree of ParB proteins: Phylogenetic relationship of Deinococcal 'ParB' protein with other 'ParB' homologues was generated by using Clustal –X based on amino acid similarity sequence information was derived from NCBI. Phylogenetic analysis showed ParB1 showed close homology to chromosomal type ParB protein. Other Deinococcal ParB's are diverged from ParB1. Strains are abbreviations : Dr, *Deinococcus radiodurans*; Bs, *Bacillus subtilis*; Cc, *Caulobacter crescentus*; Bm,

Brucella melitensis; Bc, *Burkholderia cenocepacia*; Th, *Thermus thermophilus;* Ec,*Escherichia coli;* Pa, *Pseudomonas aeruginosa;* Pp, *Pseudomonas putida;* Vc, *Vibrio cholerae;* La/Lb, *Leptospira interrogans;* Rs, *Rhodobacter sphaeroides ;* Sy, *Synechocystis.*

D. radiodurans also showed three such kind of sequence which are observed only on primary chromosome i.e. chromosome I, P1 type *parS* homology search showed some conserved boxes on chromosome I, chromosome II and mega plasmid but these sequences lack perfect and a conserved ordered organization of the boxes and IHF binding sites between A1 and A2 boxes. These limitations left a little chance for these elements acting as centromeres in this bacterium but left a greater uncertainties and an open question on how secondary genomes are segregated in this bacterium. The possibility of some other types of cis elements that are involved in segregation of these genomes cannot be ruled out. Chromosome II and mega plasmid of *D. radiodurans* showed a few repetitive sequences upstream to the *parA2B2* and *parA3B3* operon would be worth investigating if these are having some roles in genome maintenance. Similarly, the genome of *D. radiodurans* encodes putative ParA's and four ParB proteins. These were looked for the functional motifs and structural similarities with known 'Par' proteins. Interestingly, we observed that 'Par' proteins are greatly diversified. ParA1 and ParB1 are closer to chromosomal type 'Par' proteins while 'ParA' proteins encoded on secondary genome like chromosome II and mega plasmid diverge from known P-loop ATPases and form a separate group.

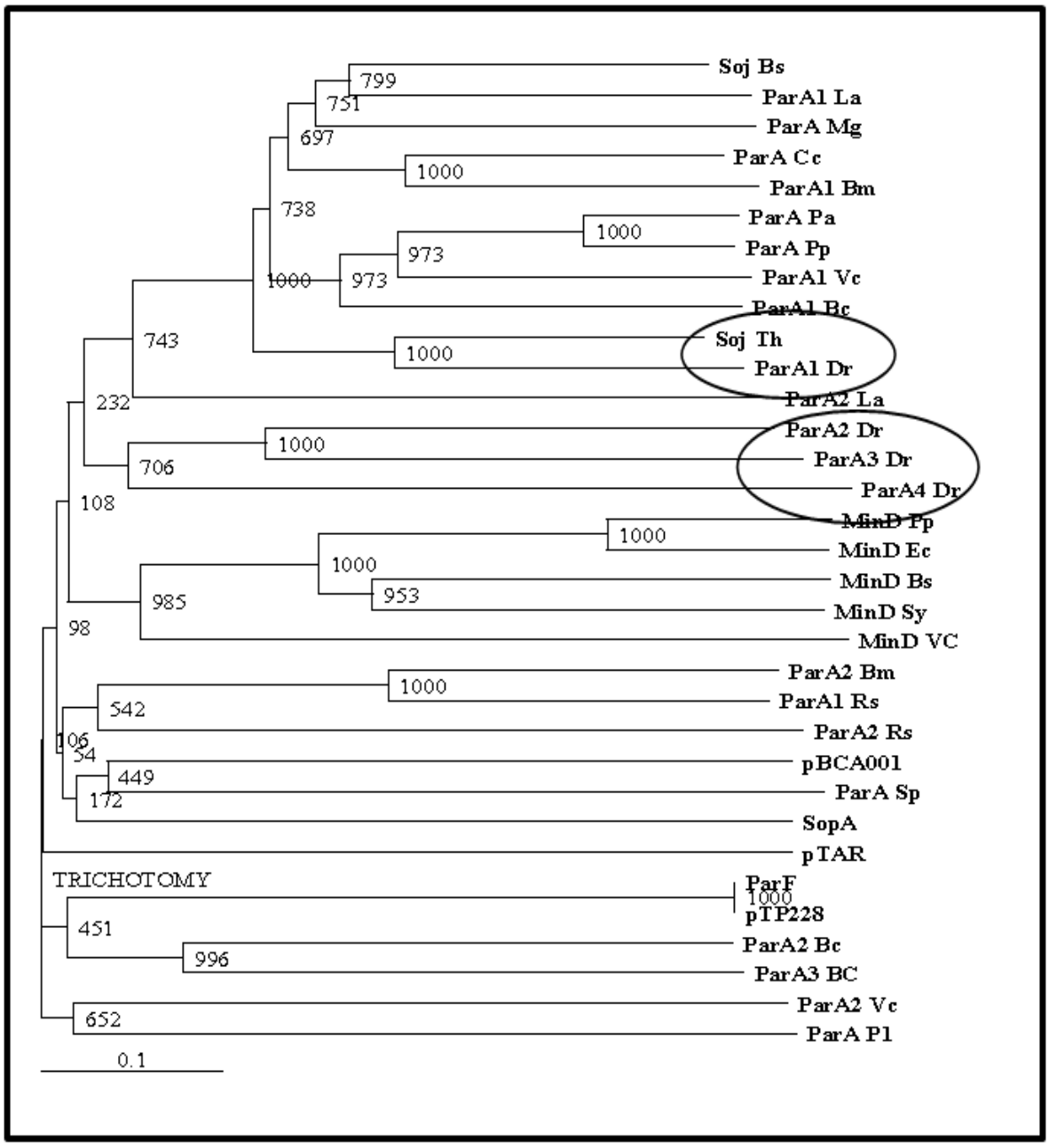

Fig 3.1.8b: Phylogenetic tree of ParA proteins: Phylogenitic relationship of Deinococcal 'ParA' protein with other 'ParA' homologues was generated by using clustal – X based on amino acid similarity sequence information was derived from NCBI. Phylogenetic analysis showed ParA1 showed close homology to chromosomal type ParA's. Other Deinococcal ParA's are diverged from ParA1. Dr, *Deinococcus radiodurans*; Bs, *Bacillus subtilis*; Cc, *Caulobacter crescentus*; Bm, *Brucella melitensis*; Bc, *Burkholderia cenocepacia*; Th, *Thermus thermophilus;* Ec,*Escherichia coli;* Pa, *Pseudomonas aeruginosa;* Pp, *Pseudomonas putida;* Vc, *Vibrio cholerae;* La/Lb, *Leptospira interrogans;* Rs, *Rhodobacter sphaeroides ;* Sy, *Synechocystis*

.

We observed that ParB proteins from all the genome replicating elements cluster in same group and are nearly similar except HTH motifs. However, ParA's differ significantly and ParA of chromosome I cluster with most of the chromosomal type ParAs. ParA's of secondary genomes clustered with other ParA's and separately from chromosome I ParA of this bacterium. These analyses allow us to predict that different 'Par' proteins in *D. radiodurans* might have specific roles in growth and maintenance of this bacterium and needs to be validated further.

CHAPTER 3.2

Functional characterization of chromosome I partitioning system.

Recent advances in optical techniques have helped in better understanding of chromosome segregation in bacteria. Based on real time interaction studies of centromere's and 'Par' proteins, two major mechanisms of bacterial genome segregation have been suggested. These are pushing or pulling mechanisms, which paradigmatically involve three factors like cis element or centromere like sequence and two trans acting factors like ParB and ParA. Due to polymerization/depolymerization of motor protein force is generated to move duplicated DNA towards opposite poles within cell. For example in R1 plasmid, first step is ParR (ParB of R1 plasmid) binds to *parC* (centromeric region of R1 plasmid) to form nucleoprotein complex, second step ParM (ParA of R1 plasmid) filament interacts with the ParR bound plasmid DNA get stabilized followed by the insertion of ParM (motor protein). The force generated due to ParM polymerization is utilized for pushing plasmid molecules towards opposite poles. In addition, genome partitioning systems have been reported in majority of bacterial chromosomes, partition system in bacteria with single chromosome or multiple chromosomes comprised of *parAB* operon and its cognate centromeric sequence (Blasius *et al.*, 2008;Hazan and Ben-Yehuda, 2006;Surtees and Funnell, 2003)**.** There are few exceptions where partitioning proteins are not identified in bacteria like *E. coli*, etc. The chromosomal segregation shares similarity with the type I plasmid segregation system. In cases like chromosome I of *V. cholerae* and *C. crescentus* it is demonstrated that chromosome segregation occurs by pulling mechanism (Fogel and Waldor, 2006;Shebelut *et al.*, 2010). It is shown that the levels of its intrinsic ATPase activity regulate the polymerization/ depolymerization dynamics of ParA. PFGE and genomic DNA sequence analysis showed that the bacteria from the diverse phylogenetic groups

e.g. *Agrobacterium tumefaciens, Sinorhizobium meliloti, D. radiodurans, V. cholerae. etc.* have multiple chromosomes.

Bioinformatic analyses of genome partitioning system in *D. radiodurans* have predicted (i) the presence of putative centromeres in chromosome I and (ii) that ParB proteins are different in DNA binding motifs while ParA's are greatly diversified. Thus it appears that chromosome I contains complete set of '*par'* elements i.e. ParA1B1 (*trans* factors), *segS* elements (centromere like sequence) and 'Par' proteins showing close homology with 'Par' proteins of *T. thermophilus.* Therefore, the prediction on presence of centromeres and functional 'Par' proteins require functional validation both *in vitro* and *in vivo* and has been carried out in this chapter.

3.2.1 .Materials and methods:

3.2.1.1 Expression of recombinant ParB1 and ParA1 proteins:

The DR0012 (ParB1) and DR0013 (ParA1) ORF's were PCR amplified from genomic DNA using dr0012F and dr0012R primers for *dr0012* (*parB1*) gene and dr0013F and dr0013R primers for *dr0013* (*parA1*) gene as mentioned in Table 2.4. PCR products were ligated at *Nde*I and *Xho*I sites in pET28a+ to yield pET0012 and pET0013, respectively. Confirmed by restriction analysis and sequencing, recombinant plasmids were transformed into *E.coli* BL21 DE3 *pLysS* for expression of recombinant ParA1/ParB1 proteins.

3.2.1.2 Purification of recombinant ParA1 /ParB1proteins:

His tagged recombinant ParA1 and ParB1 proteins were purified using nickel-affinity chromatography as described earlier in the materials and methods chapter. In brief, 'Par' protein expressing cells were lysed in cell lytic express (Sigma Chemical Company, USA) and inclusion bodies were separated from cytosolic fraction by centrifugation. Recombinant ParB1 protein was purified under native conditions as described in material and methods section(Kota *et al.*, 2010). However, majority of ParA1 is present in the inclusion pellet, these inclusion bodies were dissolved in buffer B (100 mM NaH2P04, 10mM Tris-HCl, pH 8.0 and 8M urea) and purified using Ni-NTA sepharose as described in manufacturers protocol (QIAgen, Germany). Purified protein to near homogeneity was refolded by serial dilution of urea with concurrent increase in DTT concentration and again repurified under native conditions using nickel affinity column buffer supplemented with 10% glycerol. Finally the fractions showing more than 99% purity were pooled and dialyzed in a buffer (20mM Tris-HCl, 50 mM NaCl, 1mM DTT, 1mM EDTA, 1 mM PMSF and 50% glycerol) and stored in small aliquots at -20ºC till further use. Recombinant proteins were confirmed by mass spectrometric analysis (The Centre for Genomic Applications, New Delhi).

3.2.1.3 DNA protein interaction studies:

For DNA binding assay of ParB1 protein, the 300bp putative *segS*1, *segS*2 *and segS*3 sequences located on chromosome I, were PCR amplified from genomic DNA of *D. radiodurans* using *segS*1F , *segS*1R for *segS*1, *segS2*F, *segS2*R for *segS*2 and *segS3*F, *segS3*R for *segS*3 (Table 2.4). The amplified PCR products were gel purified and labeled at 5' end using polynucleotide kinase. DNA binding activity was assayed taking different concentration of purified recombinant ParB1 and ParA1 in 20µl reaction buffer

containing 50mM Tris-HCl pH 8.0, 5mM $MnCl_2$, 75mM NaCl, 0.1mM DTT with labeled substrate at 37^{o}C for 10 min and products were analyzed. For competition assay, ParB1 was incubated with increasing concentration of competitor DNA (250 bp) up to 100 fold (Das and Misra, 2011).

3.2.1.4 Measurements of ATPase activity:

ATPase activity of recombinant ParA1 was measured with increasing concentration of purified ParA1 (0.18 μM to 0.92 μM) in a buffer containing 50mM HEPES pH7.6, 50mM KCl, 5mM $MgCl_2$, 30mM Sodium acetate, 100μg/ml BSA & 2mM ATP at 37ºC for 1h. Release of inorganic phosphate was measured using modified malachite green protocol (Kota *et al.*, 2010). Effect of DNA (*segS* elements) on ParA1 ATPase activity was also measured by incubating 1μm concentration of ParA1 with different nucleoprotein complexes formed due to pre-incubation of ParB1 (0.3μM) with DNA (10nM). The reaction was carried in above mentioned buffer at 37^{o}C for 1h. Reaction was terminated by addition of 1/4th volume of malachite green reagent followed by a further incubation for 20 min. The release of Pi was measured at 630nm and quantified using standard procedure essentially described in (Yakunin *et al.*, 2004). The ATPase activity was calculated as nano moles Pi formed min^{-1} μg^{-1} protein.

3.2.1.5 Cloning of *seg*S elements on mini-F plasmid and plasmid stability studies:

The 300 bp of three *segS* elements were PCR amplified from genomic DNA of *D. radiodurans* using *segS*1F, *segS*1R for *segS*1, *segS2*F, *segS2*R for *segS*2 and *segS3*F, *segS3*R for *segS*3 (Table 2.4). The mini-F plasmid pDAG203 was digested with *SexA*I restriction enzyme, digested plasmid is blunted by end filling with Klenow fragment. The

*segS*1, *segS*2 and *segS*3 PCR products were ampilied by using *pwo* Polymerase, cloned in pDAG203 plasmid and recombinants were confirmed by restriction analysis and nucleotide sequencing (Lemonnier *et al.*, 2000). The recombinant plasmids were designated as pDAGS1, pDAGS2, pDAGS3 respectively. Both recombinant plasmids and pDAG203 vector were separately transformed into *E. coli* MG1655. In parallel, pDSWparA1B1 was generated by PCR amplification of the putative *parA1-parB1* operon using *parA1*GF and *parB1*GR primers, cloned at *BamH*I and *Hind*III sites in pDSW209 vector (Weiss *et al.*, 1999). Clones were confirmed by restriction digestion as well as by western blotting. Expression of proteins is monitored by measuring amount of proteins expressed after IPTG induction using GFP specific antibodies. Recombinant proteins were expressed into *E. coli* harboring pDAGS3 / pDAG203 plasmids. The stable inheritance of pDAGS1, pDAGS2, pDAGS3 plasmids were compared with pDAG203 as control by scoring chloramphenicol resistance in daughter cells as described in (Godfrin-Estevenon *et al.*, 2002). In brief, these cells were grown in absence of chloramphenicol (Cm) an antibiotic marker on pDAG203 plasmid, and then cells were selected in presence of Cm^R (15µg ml^{-1}).

3.2.1.6 Determination of plasmid to chromosome ratio:

E. coli cells harboring recombinant plasmids containing *segS*1/*segS*2/*segS*3 (pDAG derivatives) and pDAG203 vector were grown in LB medium supplemented with chloramphenicol (15µg ml^{-1}). Total DNA of 5 clones for each recombinant plasmid was prepared using protocol as described in material and method section (Sambrook J and Russell DW, 2001)**.** Ratio of plasmid to total DNA was determined using PCR analysis, for plasmid specific *cat* gene and chromosome specific *xer*C genes were PCR amplified

by taking 20ng and 150ng template respectively. Products were analyzed on agarose gel and the band intensity was estimated densitometrically. Ratio of *cat* to *xer*C yield was estimated and analyzed.

3.2.1.7 Construction of *parB1* deletion mutant in *D. radiodurans:*

The pNOK0012 was constructed to generate *parB1* deletion mutant in *D. radiodurans.* In brief, the 1kb upstream to DR_0012 ORF was PCR amplified using dr_0012UF and dr_0012UR primers, similarly 1kb downstream to DR_0012 was PCR amplified using dr_0012DF and dr_0012DF primers (Table 2.4) and cloned at *Kpn*I-*EcoR* I and *BamH*I-*Sac*I sites in pNOKOUT vector respectively. The recombinant plasmid pNOK0012 was linearized with *Xmn*I and transformed into *D. radiodurans a*s mentioned in material method section(Khairnar *et al.,* 2008). Transformants were maintained through several generations to obtain homozygous replacement of *parB1* with *npt*II cassette, generation of homozygous mutant was confirmed by PCR amplification of *parB1* using internal primers, *parB1*iF and *parB1*iR.

3.2.1.8 Generation of GFP - ParB1 / GFP- ParA1 translation fusion protein:

The *parB1, parA1* gene was PCR amplified using *parB1G*F, *parB1G*R, *parA1G*F, *parA1G*R primers (Table 2.4) and cloned at compatible sites in pDSW209 to generate N-terminal translation fusion GFP protein (Weiss *et al.,* 1999) to yield pHJ0012. Subsequently *gfp-parB1* chimera was PCR amplified from pHJ0012 using GfpF and dr0012R primers (Table 2.4). In parallel the p11559 was modified by sub cloning a 42bp linker (5’ CATATGAGATCTAGTAC TGAGCTCGTCGACCTTAAGCTCGAG 3’) at its *Nde*I and *Xho*I sites generating *Nde*I, *Sca*I, *Sac*I, *Sal*I, *Afl*II and *Xho*I cloning sites

downstream to existing promoter and the resultant plasmid was named as pVHS559. PCR amplified *gfp-parB1* chimera was sub-cloned at *Sac*I and *Xho*I sites of pVHS559 to yield pD12GFP.

D. radiodurans cells harboring vector and recombinant pD12GFP plasmids were grown in TYG broth containing spectinomycin (75µg ml^{-1}) and culture was induced by using IPTG, for *E. coli* (500 µM) and for *D. radiodurans* (10mM). Inducible expression of GFP-ParB1 chimera on pHJ0012 and pD12GFP plasmids was confirmed in both *E. coli* and *D. radiodurans* respectively, by immunoblotting using antibodies against GFP (Clontech, Takara, Japan) using protocols as described earlier (Rajpurohit and Misra, 2010).

3.2.1.9 Microscopic studies:

Culture harboring plasmids which were used for localization studies were induced with different IPTG concentration as mentioned in the text. Induced culture was stained with DAPI and fluorescence microscopy of *D. radiodurans*, its derivatives and *E. coli* cells was carried out using Zeiss Axio Imager (Model- LSMS10 META, Carl Zeiss) equipped with Zeiss AxioCam HRm camera. Both GFP and DAPI fluorescence's were imaged. Micrographs were superimposed for localization of GFP-ParB1 spot on DAPI stained nucleoid (Donovan *et al.*, 2010;Fiebig *et al.*, 2006;Gordon *et al.*, 2004;Lau *et al.*, 2003;Li and Austin, 2002).

Similarly, Effect of *parB1* deletion on anucleation of the cells was demonstrated by florescence microscopy. Wild types as well as *parB1* mutant cells were grown for overnight, cells were stained with DAPI and subsequently imaged using fluorescence

microscope (Model- AXIOCAM, MRC5, and Carl Zeiss). A large number of cells were examined from both wild type and *parB1* mutant populations for the comparison of anucleation frequency at different time intervals of growth.

3.2.1.10 Oligomerization studies using sedimentation assay and light scattering:

Sedimentation assay was carried by taking 750ng ParA1 (1µM), 100ng *segS* elements (0.25nM), 200ng ParB1 (~0.25µM) in a buffer containing 50mM HEPES pH7.6, 50mM KCl, 5mM $MgCl_2$, 30mM sodium acetate, 100µg/ml BSA and 1mM ATP, the reaction was done in different combination as mentioned in the text (Bouet *et al.*, 2007). For analysis different reaction mixtures incubated at 37^{o}C for 30 mins were centrifuged at 22,000 x g for 30 min at 4^{o}C and the proteins were analyzed on 16% -18% gradient SDS-PAGE. Protein bands were visualized with silver nitrate and ParA1 band intensity was quantified by densitometric scanning using Gene Genius Image Quant software (SynGene, Inc.).

Light scattering was carried out using ~1 µM ParA1 incubated with ~25nM ParB1 and ~5nM of different *segS* centromeric sequences in 400 µl reaction buffer (50mM HEPES pH 7.6, 50mM KCl, 5mM $MgCl_2$ 100µg/ml BSA and 30mM sodium acetate), in presence and absence of 1mM ATP as described in text (Bouet *et al.*, 2007). The scattered light intensity was measured at 90^{o} from 150nm pinhole at 37^{o}C for 10s with 10 shots at 10 minutes intervals using 25 mW He-Ne laser light source at 630 nm. The data obtained as kilo counts per second were analyzed using inbuilt software with the machine and data was represented as fold change in intensity of scattering of light (Hassan *et al.*, 2004).

3.2.2.0 Results:

3.2.2.1 ParA1 and ParB1 were expressed in *E. coli* and purified to homogeneity

Genomic DNA of *Deinococcus radiodurans* was prepared using standard protocol (Battista *et al.*, 2001)and the *DR0012 (parB1), DR0013(parA1)* genes were PCR amplified and cloned as mentioned in materials and methods section. The cloning of all the genes was confirmed by restriction digestion analysis and respective recombinant plasmids were named as pET0012, pET0013 (Fig 3.2.1). Recombinant plasmid was prepared and digested with restriction enzymes used for cloning and the release of DNA fragment by double digestion confirmed the cloning of these genes. These clones were sequenced to confirm the correctness of the insert and the absence of any mutation that could have incorporated during PCR amplification. Confirmed recombinant plasmids were transformed into *E. coli* BL21 DE3 *pLysS* cells and induced with IPTG. The expression of ParB1 of 34.0 kDa and ParA1 of 35.0 kDa was observed on SDS – PAGE. Using Ni-NTA chelating sepharose, these proteins were purified to near homogeneity (Fig 3.2.1). ParB1 protein was purified under native condition where as ParA1 was purified under denaturation condition, further refolded by serial dilution of urea. Peptide mass fingerprints of both these proteins confirmed their identity as ParA1 and ParB1 of *D. radiodurans*.

3.2.2.2 ParB1 showed specific interaction with predicted centromere:

Different plasmid or chromosomal segregation mechanisms suggests ParB specifically interact with the centromere sequences to form nucleoprotein complex and plays an important role in DNA segregation. Purified recombinant ParB1 protein was checked for

known characteristics of other ParB type proteins. ParB1 interactions with different *segS* elements (centromere like sequences) were checked as mentioned in methods section.

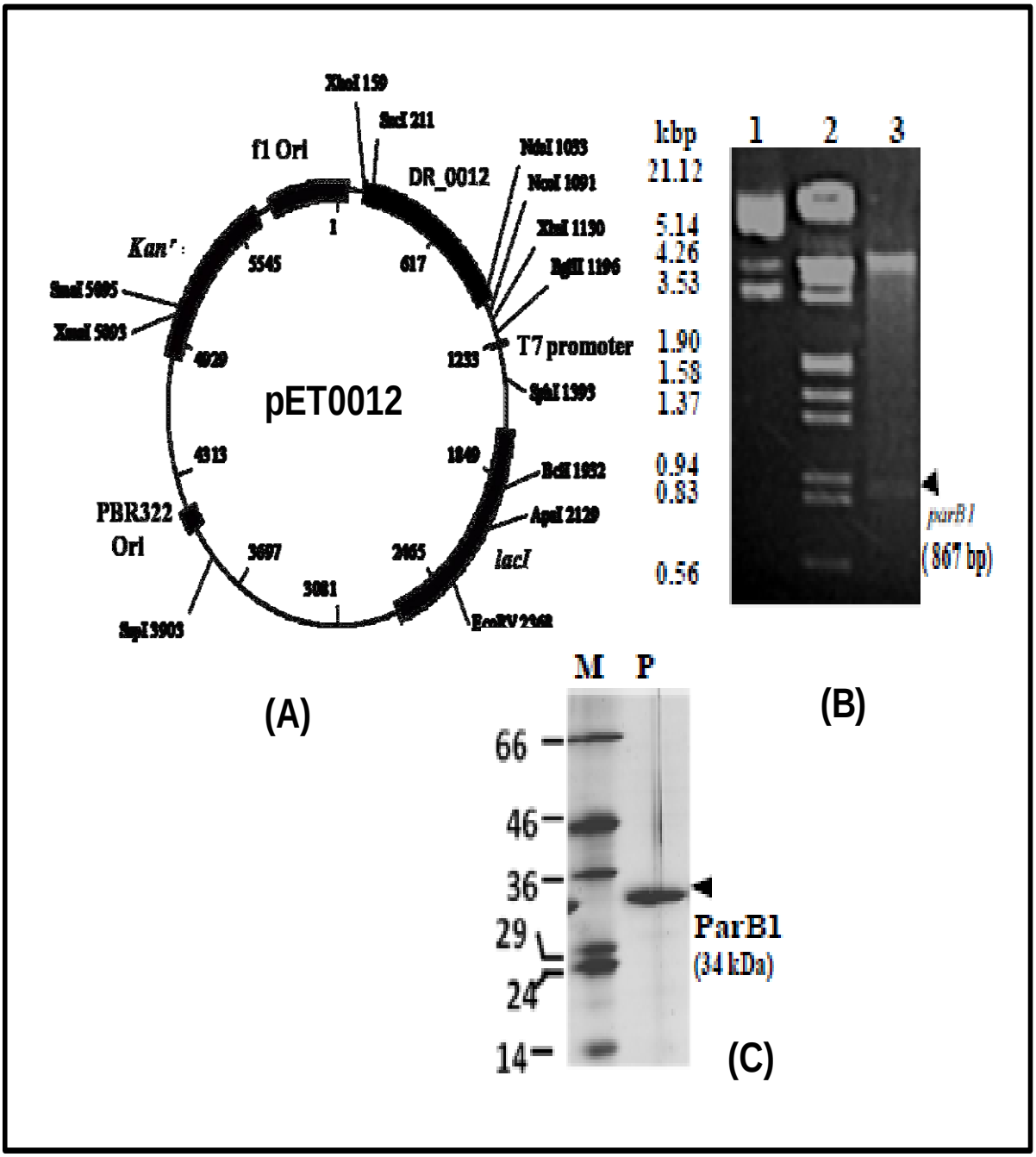

Fig 3.2.1.(**a) Cloning, expression and purification of 'ParB1' protein**. **A)** Partial restriction map of the pET0012. **B)** Analysis of restriction digestion products of recombinant pET0012, undigested plasmid (lane1), marker (lambda DNA *Hind*III

&*EcoR*I) (lane 2) and double digested pET0012 plasmid (*Nde*I /*Xho*I).**C)** Purified ParB1 protein (lane P) along with protein size markers (lane M).

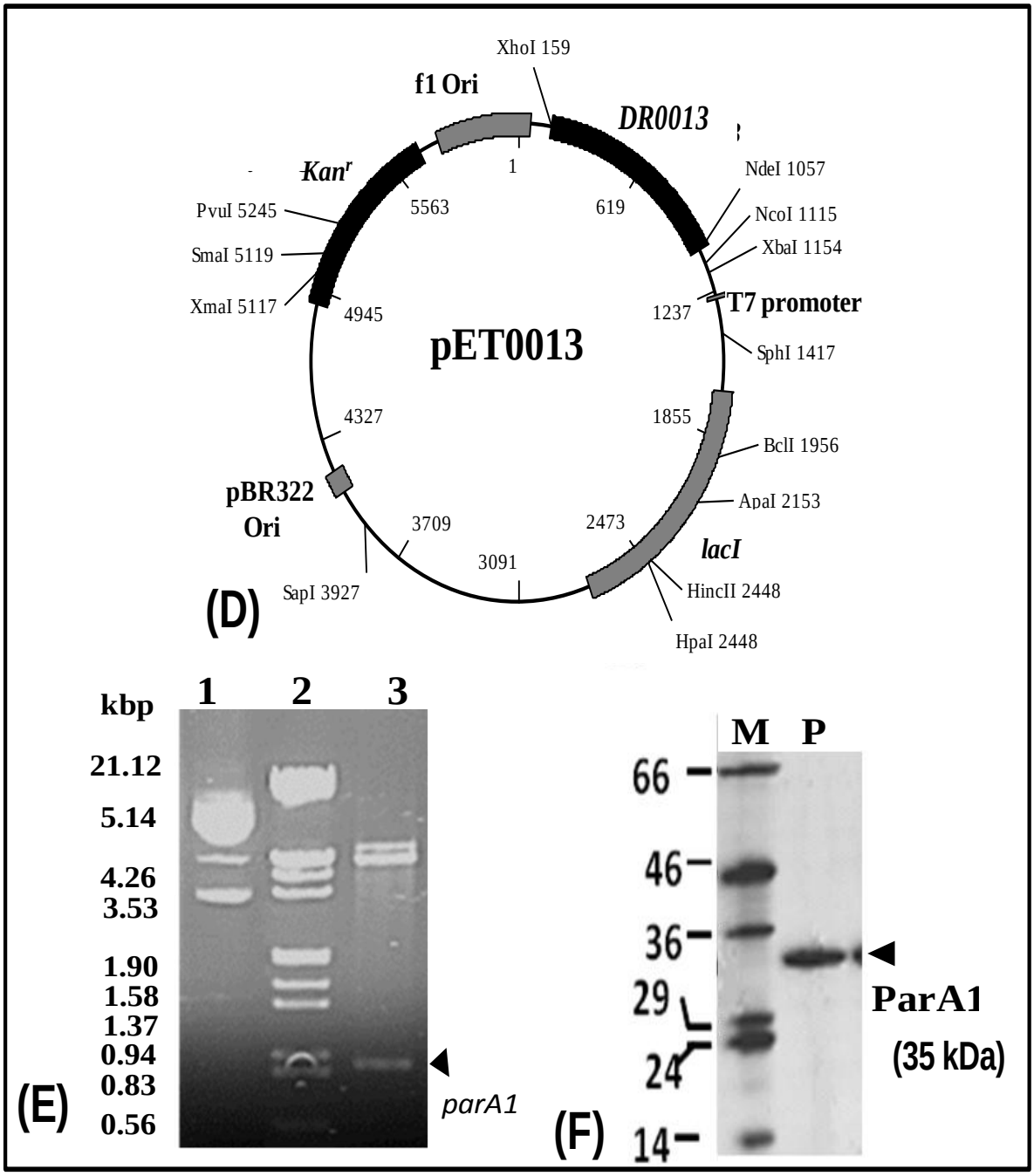

Fig 3.2.1.(b) Cloning, expression and purification of 'ParA1' protein. **D)** Partial restriction map of the pET0013 plasmid. **E)** Analysis of restriction digestion products of recombinant pET0013 plasmid, undigested plasmid (lane1), marker (lambda DNA *Hind*III &*EcoR*I) (lane 2) and double digested pET0012 plasmid (*Nde*I /*Xho*I).**F)** Purified ParB1 and ParA1 protein (lane P) along with protein size markers (lane M).

ParB1 showed binding with all three *seg*S (*segS*1, *segS*2 and *segS*3) elements with equal affinity (Fig. 3.2.2). The ParB1 interaction with all three *segS* elements was specific, which remained unaffected even in presence of 100 fold higher molar ratio of nonspecific DNA (Fig. 3.2.2) suggesting that ParB1 interacts specifically with the *segS* elements (centromere like sequences) like other known ParB proteins.

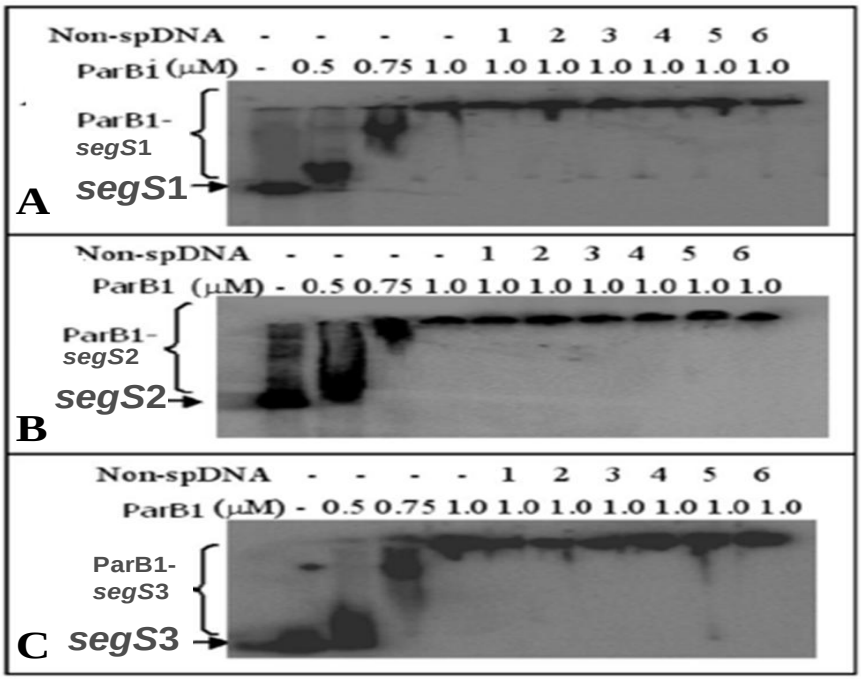

Fig. 3.2.2: ParB1 interaction with *segS* type centromere's of chromosome I.

300bp PCR product of all three chromosomal type centromere *segS*1 (A), *segS*2 (B) and *segS*3 (C) were PCR amplified and approximately products of each element was labeled with [^{32}P] γ ATP and incubated with different concentrations of recombinant ParB1. For competition with non-specific DNA, the *segS* elements were incubated with ParB1 and chased with 1:1 (1), 1:5 (2), 1:10 (3), 1:20 (4), 1:50 (5) and 1:100 (6) higher molar ratio of 250bp nonspecific dsDNA (Non-sp DNA). Products were separated on 5% native PAGE, dried and auto radiograms were developed by using Typhoon phosphorimager.

3.2.2.3 ParA1 is a DNA binding ATPase *in vitro*:

Recent studies revealed ParA proteins interact nonspecifically with DNA and undergo polymerization. Interaction of ParA polymer with the ParB helps in separation of newly duplicated DNA to opposite side of the cell. We have also hypothesized that ParA1 might behave like Soj of *B. subtilis or T. thermophilus*. The functional domain search analysis showed that ParA1 contain deviant Walker type ATPase domains and a characteristic arginine pair implicated in the DNA protein interaction and functioning as a DNA binding ATPase. The purified recombinant ParA1 was checked for its interaction with DNA. It showed dsDNA binding activity *in vitro* (Fig 3.2.3). Gel mobility shift assay of ParA1 with a 400bp dsDNA yielded multiple mobility retarded DNA bands suggesting concentration dependent binding of ParA1 on DNA.

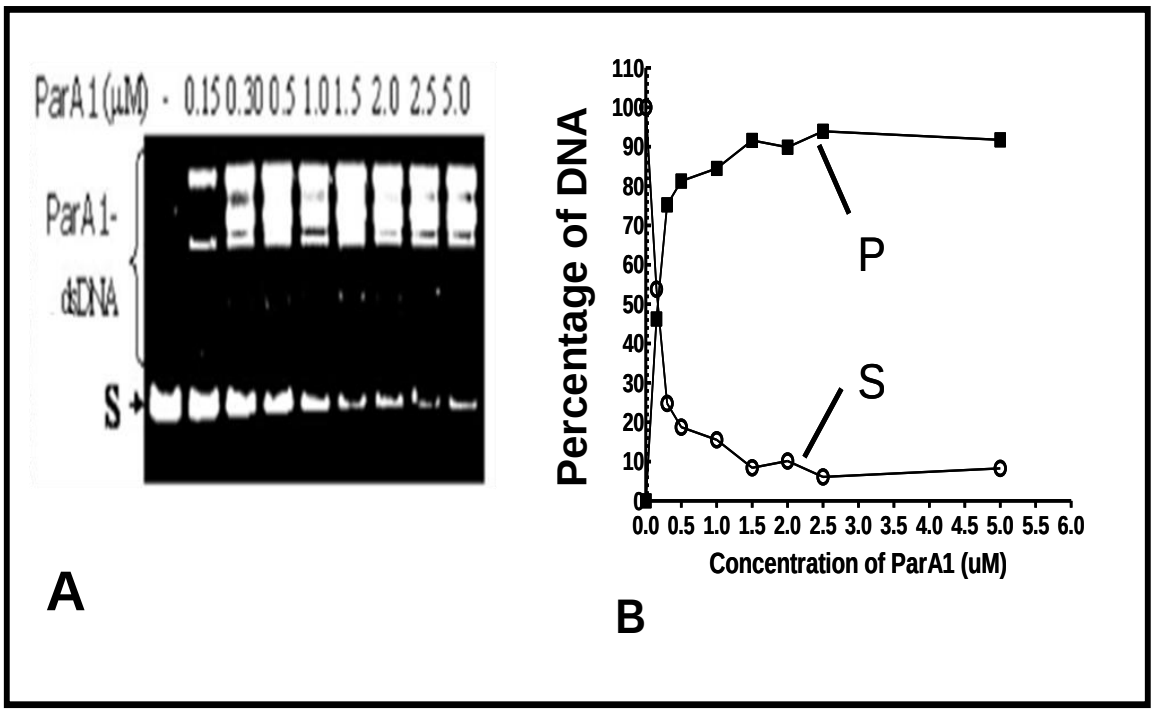

Fig 3.2.3: DNA binding activity of ParA1: A) DNA binding activity of purified ParA1 was checked with 400bp PCR amplified nonspecific DNA substrate (denoted as S) and increasing concentration of protein and products were analyzed on 1.2 % Agarose gel. B)

Amount of the bound and unbound DNA was quantitated and plotted as percentage of substrate. Abbreviation used in this figure is percentage of bound DNA to total DNA as (P) and unbound DNA to total DNA as (S)

Similarly, the ATPase activity of ParA1 was checked with cold ATP as a substrate and the release of Pi was measured. ATPase activity was monitored with increasing concentration of ParA1 as mentioned in methods section. ParA1 alone showed weak ATPase activity (Fig3.2.4). As ParA1 showed nonspecific interaction with DNA, the possibility of ATPase activity stimulated by DNA as checked. ParA1 showed ATPase activity and its activity was stimulated in presence of double stranded DNA.

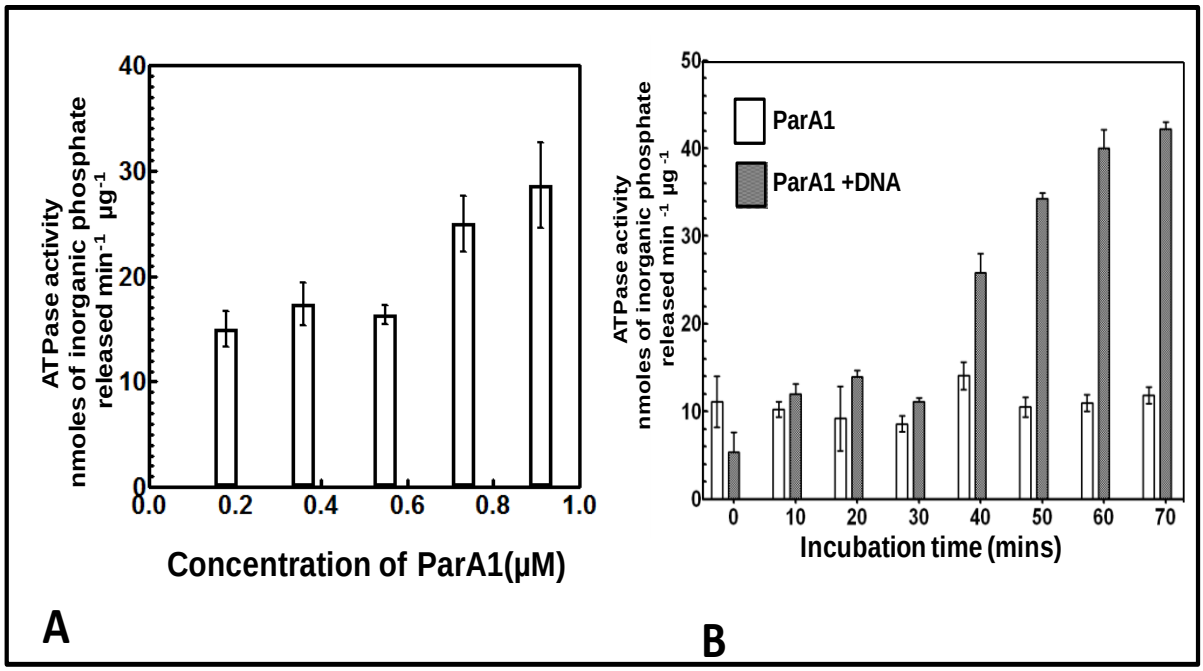

Fig 3.2.4: ATPase activity of ParA1: A) ATPase activity of ParA1 was checked with increasing concentration of ParA1 from 0.18 µM to 0.91 µM was incubated with 1mM ATP for 60 min and release of inorganic phosphate was measured at O.D 630nm. **B)** Stimulation of ATPase activity was monitored by taking activity 1µM concentration of ParA1 with 1mMATP, release of inorganic phosphate was estimated in presence and absence of ~ 5nM concentration of 300 bp dsDNA.

3.2.2.4 Interaction of ParA1 filament with DNA:

Functional analyses of ParA1 in different organisms showed that ParA interacts non-specifically with the dsDNA and also contain weak ATPase activity. ParA1 interaction with DNA can be possible either through wrapping around the DNA like ParA of P1 plasmid etc or sequestration on DNA and forming higher order oligomeric structure like SopA of F plasmid. To ascertain how ParA1 is interacting with the DNA, the sedimentation and light scattering analysis was done.

Sedimentation analysis:

Sedimentation analysis was carried out as mentioned for ATPase assay i.e. 1µM concentration of ParA1 was incubated in ATPase buffer in presence and absence of DNA (*segS1*) and reaction was incubated at 37^{o}C for 30 min.

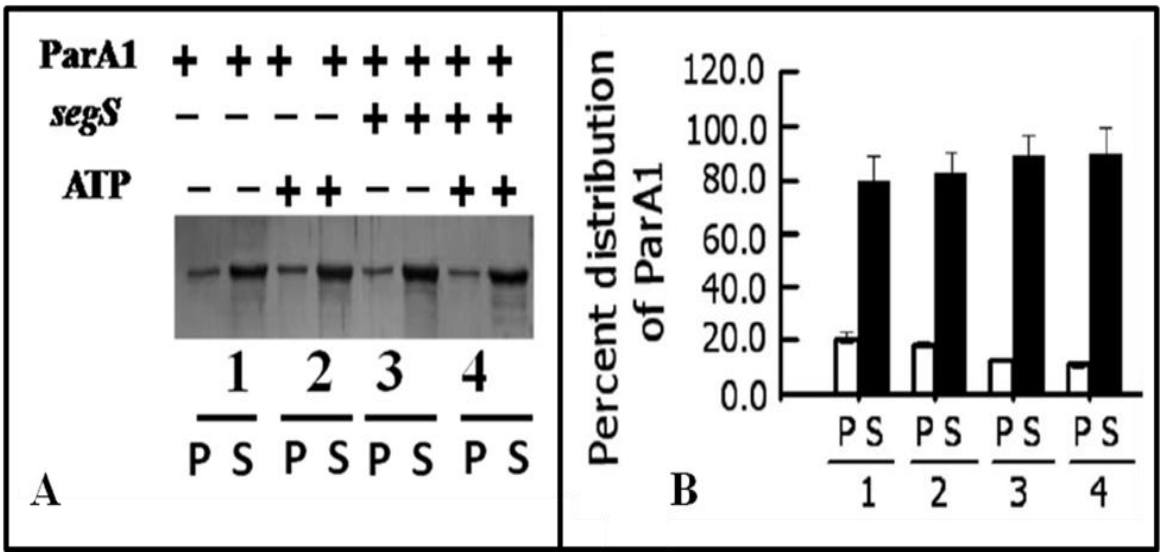

Fig 3.2.5 Interaction of ParA1 with DNA by using sedimentation analysis: Recombinant ParA1 was incubated with DNA, ATP and in presence of both. Mixtures were incubated at 37^{o}C for 30 min, these mixtures were centrifuged at 22,000 x g for 30 min and both supernatant (S) and pellets (P) fractions were analyzed on SDS-PAGE (**A**).

Gel was stained with silver nitrate and the intensity of protein band corresponding to ParA1 was estimated by densitometric scanning from the respective gel (**B**). Amount of ParA1 in pellet was measured by densitometric analysis as shown in this graph.

The distribution of ParA1 between pellet and supernatant was monitored on SDS-PAGE gel (Bouet *et al.*, 2007). Nearly 20% of protein in case of ParA1 incubated alone goes to pellet, which did not change with DNA in presence and absence of ATP (Fig3.2.5). It has been shown that SopA sequesters on DNA to produce the larger size pellet of these proteins upon centrifugation. However ParA1 in presence or absence of DNA does not form higher oligomeric structures, indicating ParA1 can interact with DNA without forming higher oligomeric structures.

Light scattering analysis:

The light scattering approach has been used earlier for determining the dynamic variations in size of macromolecular complexes.

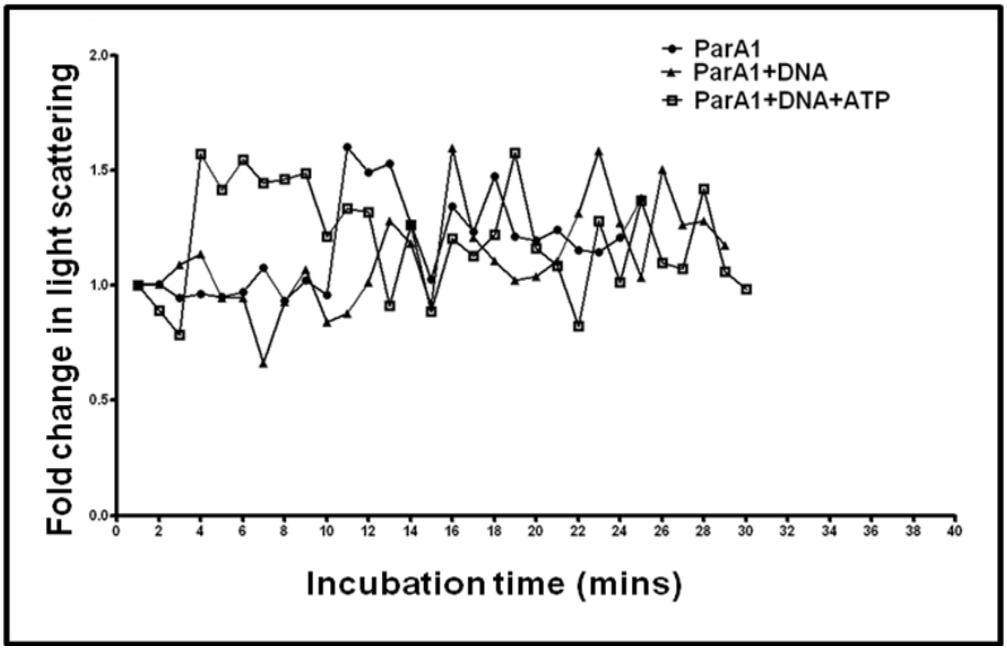

Fig 3.2.6: Light scattering analysis: Light scattering studies of ParA1 incubated with DNA in presence and absence of ATP. Light scattering spectra was recorded as a function of time. Data presented here is the mean of values obtained with 10 shots at every single time point from a representative experiment.

The effect of ATP, DNA on oligomerization of ParA1 was also checked through light scattering. Results showed that there was no significant change in amount of light scattering (counts/sec) when ParA1 was incubated with DNA in presence or absence of ATP (Fig 3.2.6). Sedimentation results as well as light scattering results specified that the ParA1 interacts with dsDNA and doesn't sequester on it to form super order structures (Hassan *et al.*, 2004).

3.2.2.5 ParA1 interaction with ParB1 bound with DNA:

The ATPase activity of some members of the ParA and MinD one of the proteins regulating mini cell formation in bacteria, family proteins has been shown to get stimulated *in vitro* by the cognate ParB bound to cognate centromere. The MinE (mini cell regulatory protein) stimulation of ATPase of MinD is required for the proper functioning of MinD *in vivo*.

Stimulation of ATPase activity of ParA1

Bioinformatic analysis indicated that ParA1 is close to ParA homologues belonging to the deviant Walker type ATPase family. Since, the ATPase activity of ParA family protein is stimulated by its cognate ParB, the possibility of ParA1 activity also stimulated by ParB1 could be envisaged and monitored *in vitro*. Purified ParB1 was incubated with different *segS* elements (hereafter referred as *segS*-ParB1 complex) and then ParA1 was added to it. The release of inorganic phosphate was measured using malachite green reagent as mentioned in methods. ATPase activity stimulation was observed when ParB1 was

incubated in presence of centromeric sequences. The extent of ATPase activity stimulation was different with different centromeric sequences ranging from 2.16 fold with DP1 to 21.9 fold with *segS*3. ATPase activity stimulation was several folds higher with *segS*3 as compared to *segS*1 (3.25 fold) and *segS*2 (9.33 fold), which is interesting (Fig 3.2.7). Nevertheless, these results suggested that ParA1 was a dsDNA binding Walker type ATPase protein *in vitro* and its activity was stimulated in presence of *segS*-ParB1 complex. Since, ParB1 alone and / or with *segS* elements did not show ATPase activity, the characteristic increase in ATPase activity of ParA1 in presence of both of these elements was interesting to note. Stimulation of ParA's ATPase activity upon interaction with ParB/ homologues bound on centromeric sequences, have been reported as one of the factors contributing to the dynamic change in the polymerization/depolymerization kinetics of such proteins (Ringgaard *et al.*, 2009). Therefore, the functional significance of *segS*-ParB1 stimulated ATPase activity on the polymerization / depolymerization dynamics of ParA1 was hypothesized and checked.

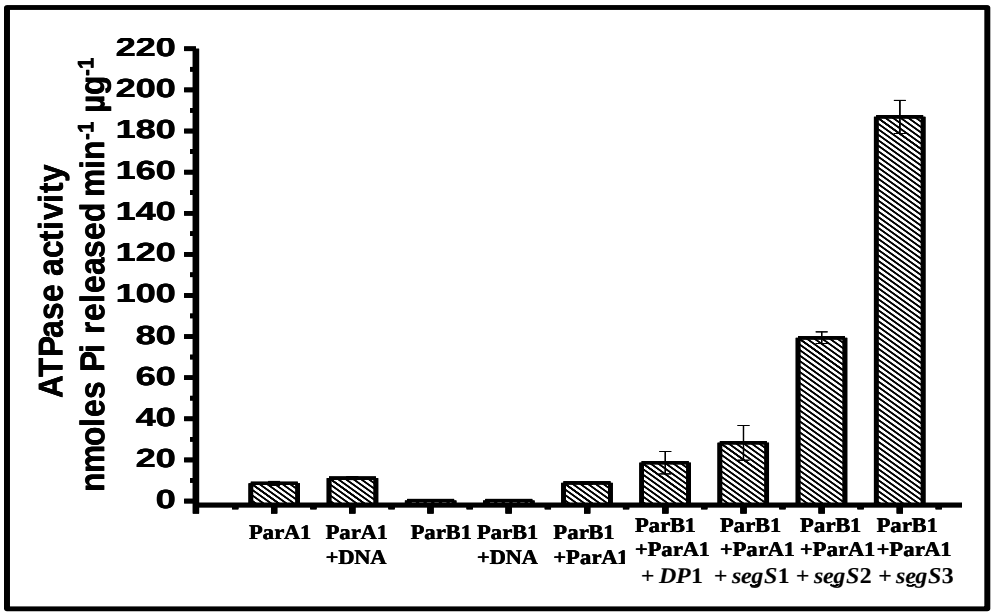

Fig 3.2.7: Stimulation of ParA1 ATPase activity: ATPase activity of ParA1, ParB1 with and without DNA, similarly ParA1+ParB1 was incubated with aberrant *parS* (DP1+A1B1), *segS*1 (S1+A1B1), *segS*2 (S2+A1B1) and *segS*3 (S3+A1B1) of chromosome I, release of inorganic phosphate was measured as described in methods.

Polymerization or depolymerization of ParA1 with ParB1

ParA1 has shown differential stimulation of ATPase activity with different *segS* complexes. In order to check ParB1 effect on ParA1 oligomerization in presence and absence of different *segS* elements, the sedimentation assay was done. Purified recombinant ParA1 protein was incubated with different *segS* complexes in presence and absence of ATP and the distribution of ParA1 between pellet and supernatant were monitored. ParA1 alone showed certain levels of sedimentation, which did not change in presence of ATP (Fig 3.2.8).

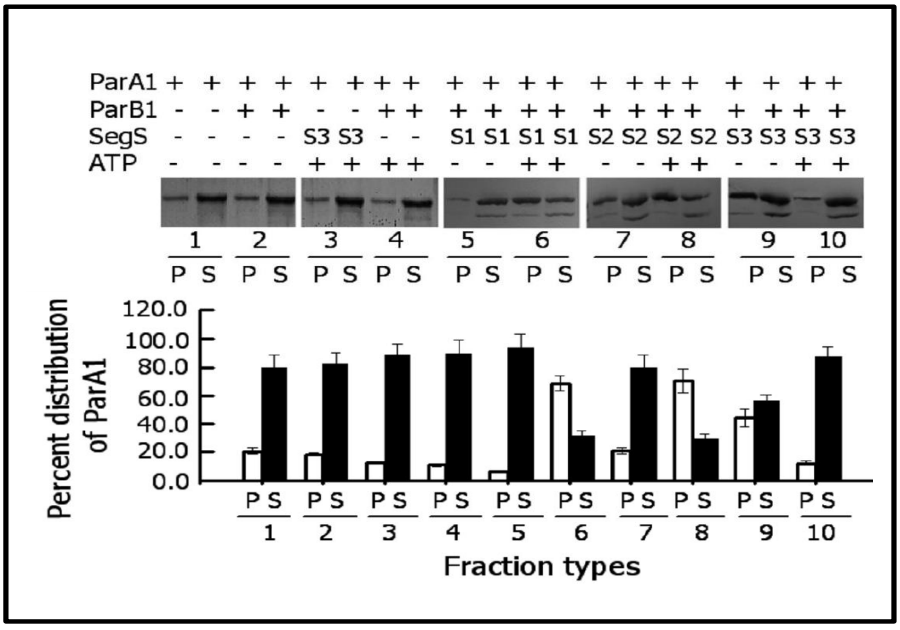

Fig 3.2.8: Interaction of ParA1 with ParB1 nucleoprotein complex: Sedimentation analysis of ParA1 in presence of its cognate putative chromosome I partitioning components. Recombinant ParA1 was incubated with *segS*1 (S1), *segS*2 (S2), and *segS*3 (S3), ParB1 and ATP in different combinations. Mixtures were centrifuged at 22,000 g

for 30 min and both supernatant (S) and pellets (P) fractions were analyzed on SDS-PAGE. Gel was stained with silver nitrate and the intensity of protein band corresponding to ParA1 was estimated by densitometric scanning from the respective gel.

However in presence of ParB1- *segS*1/*segS*2 complexes without ATP, the amount of ParA1 had increased significantly in pellet (Fig 3.2.8). This increase of ParA1 in pellet was relatively more with *segS*3 as compared to *segS*2. However in presence of ATP, the levels of ParA1 in pellet increased in case of *segS*1 and *segS*2, where as it decreased significantly in case of *segS*3. This showed that although ParB1 forms complex with all *segS* elements, the interactions of ParA1 with *segS*3-ParB1 complex was different in presence of ATP. Presumably, it dissociates faster from a hypothetical {*segS*3- ParA1B1} complex in presence of ATP as compared to similar types of complexes with *segS*1and *segS*2 (Fig 3.2.8). This result also agrees with an independent observation where the faster mobility of *segS*3-ParA1B1 nucleoprotein complex was observed in presence of ATP. The ATP effect on faster mobility of *segS*3 nucleoprotein complex, the higher sedimentation of ParA1 in mixture containing ParA1 incubated with *segS*3-ParB1 complex, and the greater stimulation of ATPase activity in presence of *segS*3, together suggested a correlation between ATPase activity stimulation and depolymerization of ParA1 polymer. ATPase activity stimulation mediated depolymerization of ParA, which provides the force for the movement of replicated genome in the direction of higher concentration of ParA as has been suggested earlier (Gerdes *et al.*, 2010).

Light scattering analysis:

ParA1 behaved differently in presence of different *segS* complexes indicating a change in the degree of polymersation of ParA1 protein. Sedimentation analysis and supershift assays have shown that ParA1 depolymerised from *segS*3 complex in presence of ATP.

The effect of ATP, *segS* elements and ParB1 on oligomerization of ParA1 was also checked through light scattering. ParB1 and ParA1 individually did not change the amount of light scattering significantly.

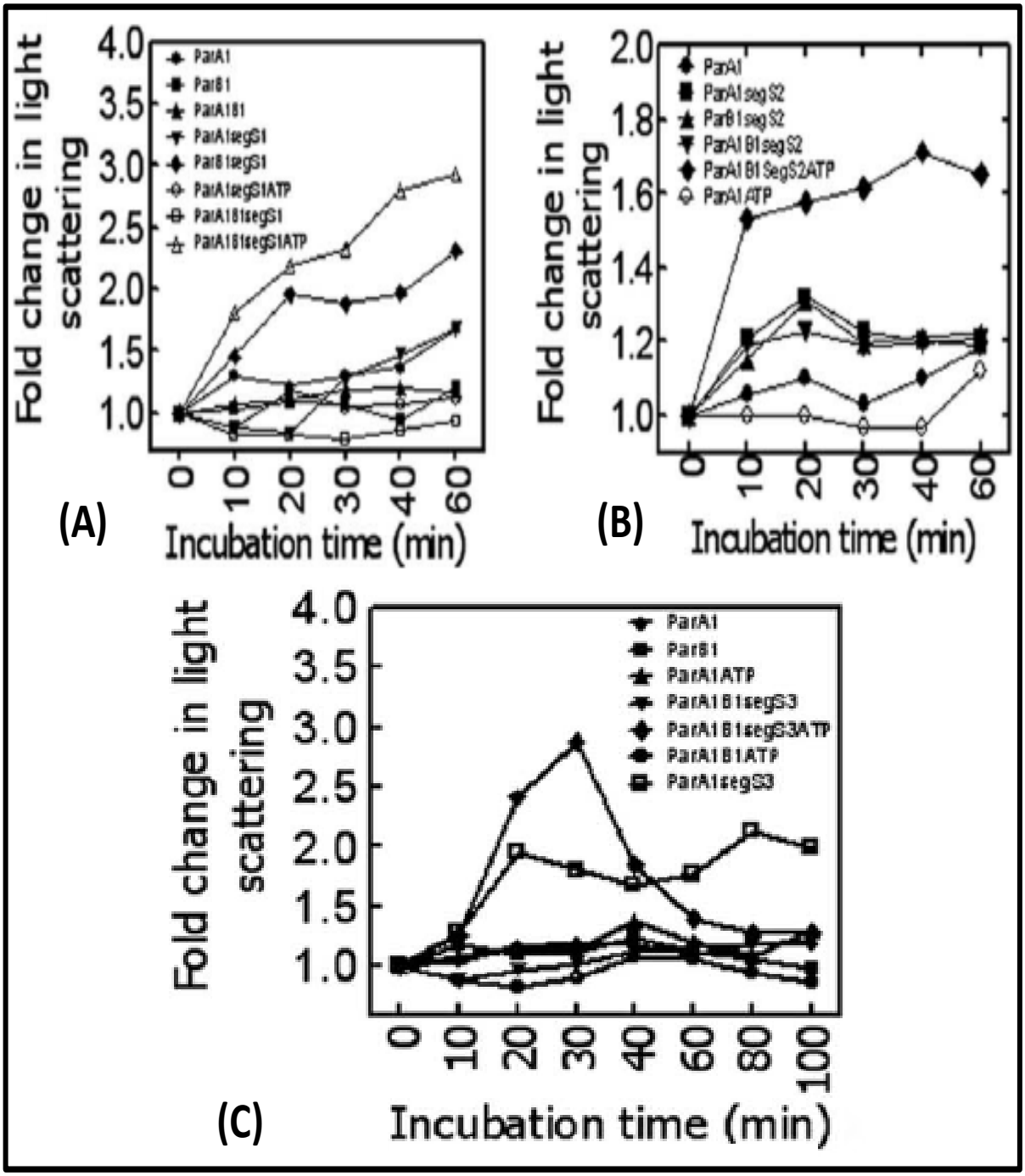

Fig 3.2.9 Interaction of ParA1 with ParB1 nucleoprotein complex studied using Light scattering analysis: Light scattering studies of ParA1 incubated with ParB1 and *segS* elements in presence and absence of ATP. The recombinant purified ParA1 (ParA1) and ParB1 (ParB1) were taken alone and together in different combinations with *segS*1 (**A**) / *segS*2 (**B**)/ *segS*3 (**C**) and ATP and light scattering spectra was recorded as a function of time. For experiments where both ParA1 and ParB1 were incubated with *segS* elements, the ParB1 was pre incubated with *segS* before ParA1 was added. For ATP effect, the ATP was added last in any given combination.

However, the incubation of ParA1 with *segS*-ParB1 complexes of all three *segS* elements showed a steady increase in light scattering, albeit in absence of ATP (Fig 3.2.9). In presence of ATP, the increase in light scattering was continued for 60 min in case of *segS*1 and *segS*2. With *segS*3 however, the initial increase in light scattering for 30 min followed to a sharp decrease, indicating the possibility of a rapid change in macromolecular interaction between ParA1 and *segS*3-ParB1 complex. The light scattering approach has been used earlier for determining the dynamic variations in size of macromolecular complexes. An increase in light scattering with time has been attributed to an increase in size of ParA protein polymers (Bouet *et al.*, 2007) while the decrease in light scattering has been suggested due to disassembly of ParA filament (Ringgaard *et al.*, 2009;Soberon *et al.*, 2011). It may be noted that ParA belonging to type I categerory of ParA proteins polymerizes in presence of ATP and DNA. Such an interaction of this complex with Spo0J (ParB) stimulates the intrinsic ATPase activity of Soj (ParA) leading to its depolymerization (Pratto *et al.*, 2008;Pratto *et al.*, 2009;Ptacin *et al.*, 2010). Thus, a rapid decrease in light scattering, faster gel mobility and relatively lesser amount of ParA1 in pellet in presence of *segS*3 and ATP, may possibly suggest that the higher ATPase activity of ParA1 upon interaction with ParB1-*segS*3 complex, could lead to its rapid depolymerization. *In vitro* results obtained so far suggested that the ParB1 is a sequence specific centromere binding protein and ParA1 is a DNA binding

ATPase. Sequence specific interaction of ParB1 to all three *segS* elements with nearly similar Kd values indicated a strong possibility of multiple centromere like sequences functioning in chromosome I partitioning in *D. radiodurans*

3.2.2.6 *In vivo* characterization of chromosome I partition proteins:

In vivo characterization of chromosome I partition system was carried out by the analyzing the functions of both *cis* elements and partitioning proteins in genome segregation. *In vitro* results produced some interesting observations like *segS*1 and *segS*2 elements bound to ParB1 produced stable complex with ParA1 even in presence of ATP while these interaction behaved differently with *segS*3. We hypothesized that the differential stimulation of ParA1 activities could be due to the minor changes in the centromere sequences. In order to test the hypothesis and to check the *in vivo* functions of these *segS* elements as centromere like sequences and thus in genome segregation, we employed different methods like stabilization of unstable plasmid, looking for genomic instability and *in vivo* monitoring of the dynamics of ParA1 protein.

Plasmid stabilization

Earlier, the plasmid stability assay using unstable vectors like mini-F plasmid pDAG203 (Hirano *et al.*, 1998), has been employed for the characterization of genome partitioning systems in other bacteria (Dubarry *et al.*, 2006;Godfrin-Estevenon *et al.*, 2002). Functional complementation of complete '*par*' system is a direct method to show that these 'Par' proteins are involved in the chromosome segregation. Plasmid stabilization assays was done using unstable mini-F plasmid pDAG203. All three *segS* elements (*segS*1, *segS*2 and *segS*3) were PCR amplified and cloned in pDAG203, yielding pDAG

derivatives i.e. pDAGS1, pDAGS2, pDAGS3, respectively (Fig 3.2.10a). Cloning was confirmed by restriction analysis as described in methods (*Fig* 3.2.10b) and transformed into *E. coli*. Cells harboring these derivatives were grown to different generations in minimal CSA medium (M9 salts, 0.2% glucose , 2% casamino acids) and the numbers of cells conferring chloramphenicol resistance (a phenotype encoded on pDAG203) were scored as mentioned in material and methods. Interestingly, the cells carrying pDAGS1, pDAGS2 showed nearly 100% stable inheritance of respective plasmids independent of ParA1B1 (Fig 3.210c) while stability of plasmid pDAGS3, in terms of cells expressing chloramphenicol resistance, was although significantly high even in absence of ParA1B1 as compared to control, it improved further to nearly 100 % when both ParA1B1 (Fig 3.210d) were co-expressed using pDSWparA1B1 vector (Fig 3.2.11)**.** However, the possibility of any changes in copy number in terms of amount of plasmid DNA per unit chromosomal DNA and mutations in *segS* elements have been ruled out (Fig 3.2.10e). These results indicated that (i) all three *segS* elements could function like bacterial centromere, (ii) we hypothesized unknown proteins in *E. coli* are functional complementing 'Par' proteins. These proteins recognize *segS*1 and *segS*2 which increased plasmid stability in host cells while *segS*3 recognition by *E. coli* complements were partial and required cognate ParA1B1 for its complete inheritance in dividing population. Differential functions of different segS elements in stabilizing instable plasmid in *E. coli* could be due to slight difference in their nucleotide sequence. These results suggested that *segS*3 functions differently from *segS*1 and *segS*2 and the function of *segS*3 required ParA1B1 for its complete segregation in *E. coli*. The molecular basis of

*segS*1 and *segS*2 stabilizing the unstable mini-F plasmid independent of its cognate partitioning proteins in *E. coli* is not clear.

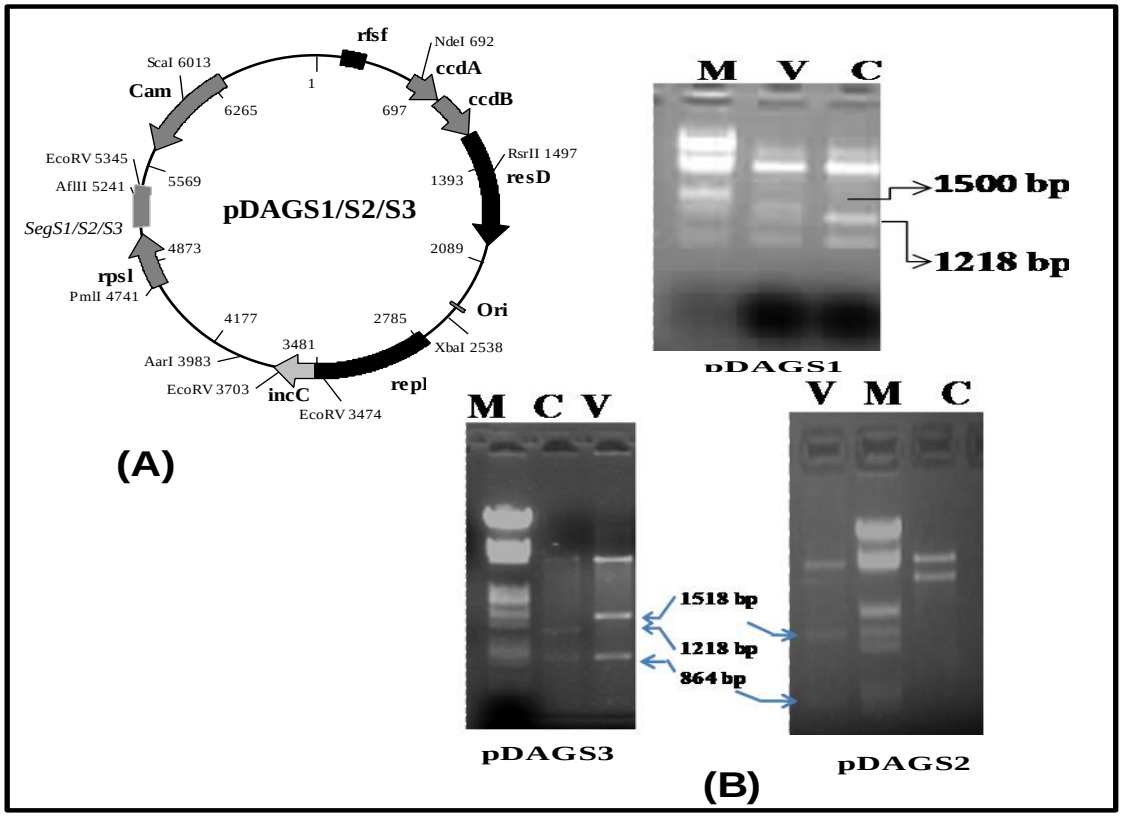

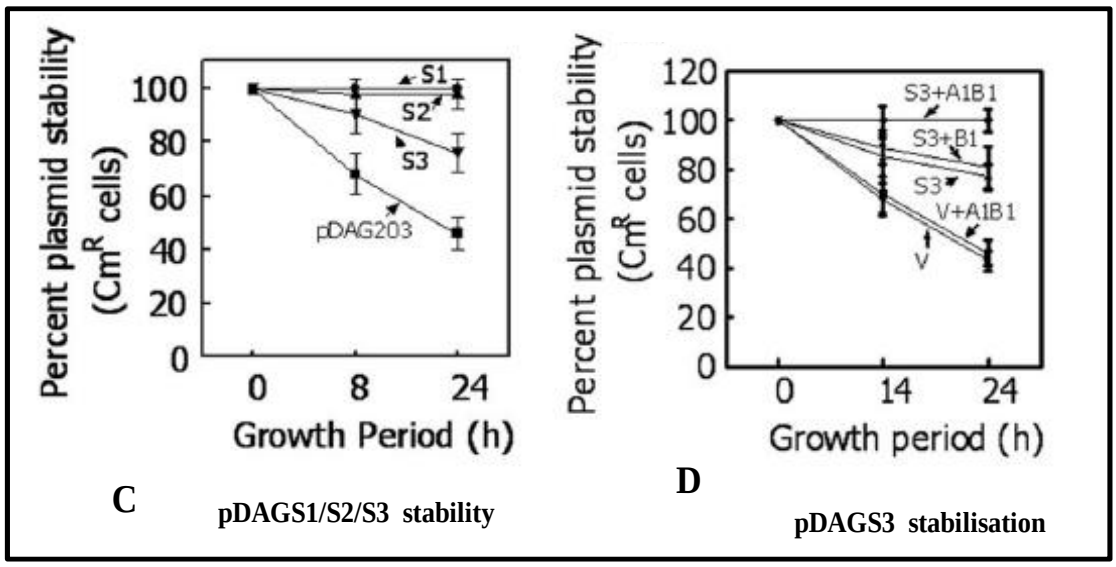

Fig 3.2.10: **Centromere activity assay of *segS* elements using plasmid stability test in *E. coli*. A)** The *segS*1 (S1), *segS*2 (S2) and *segS*3 (S3) elements were cloned in unstable mini-F plasmid (pDAG's derivatives) partial restriction map of plasmid is represented **B**) Restriction analysis: Lane C: pDAG203 digested with *EcoR*I, Lane M: lambda *Hind*III/*EcoR*I double digested Lane **V**: pDAG S derivatives digested with *EcoR* I. **C)** Cells carrying recombinant plasmids pDAGS1 (S1), pDAGS2 (S2) and pDAGS3 (S3) and pDAG were checked for plasmid stability as a function of chloramphenicol resistance. **D)** The pDAGS3 harboring cells co-expressing either ParB1 (S3+B1) or ParB1 and ParA1 together (S3+A1B1) were checked for plasmid stability as a function of chloramphenicol resistance. Data were compared with cells carrying vector pDAG203 alone (V) and also co-expressing both ParA1 and ParB1 in vector background (V+A1B1).

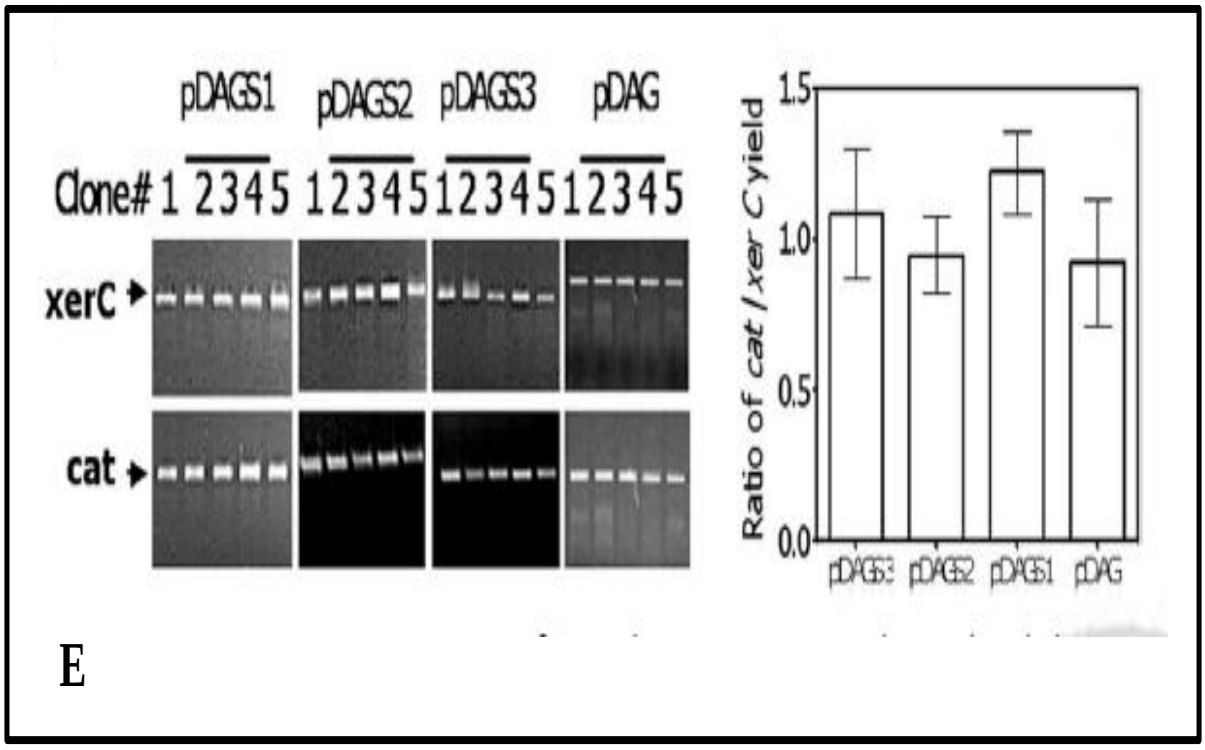

Fig 3.2.10e: Determination of plasmid to chromosome ratio: Genomic DNA prepared from 5 independent clones (1-5) of *E .coli* harboring each pDAGS1, pDAGS2, pDAGS3 and pDAG203 (pDAG) and relative proportions of plasmid (*cat*) and genomic DNA (*xerC*) were checked in each clone (C) and the ratios of *cat*/*xerC* were calculated (D).

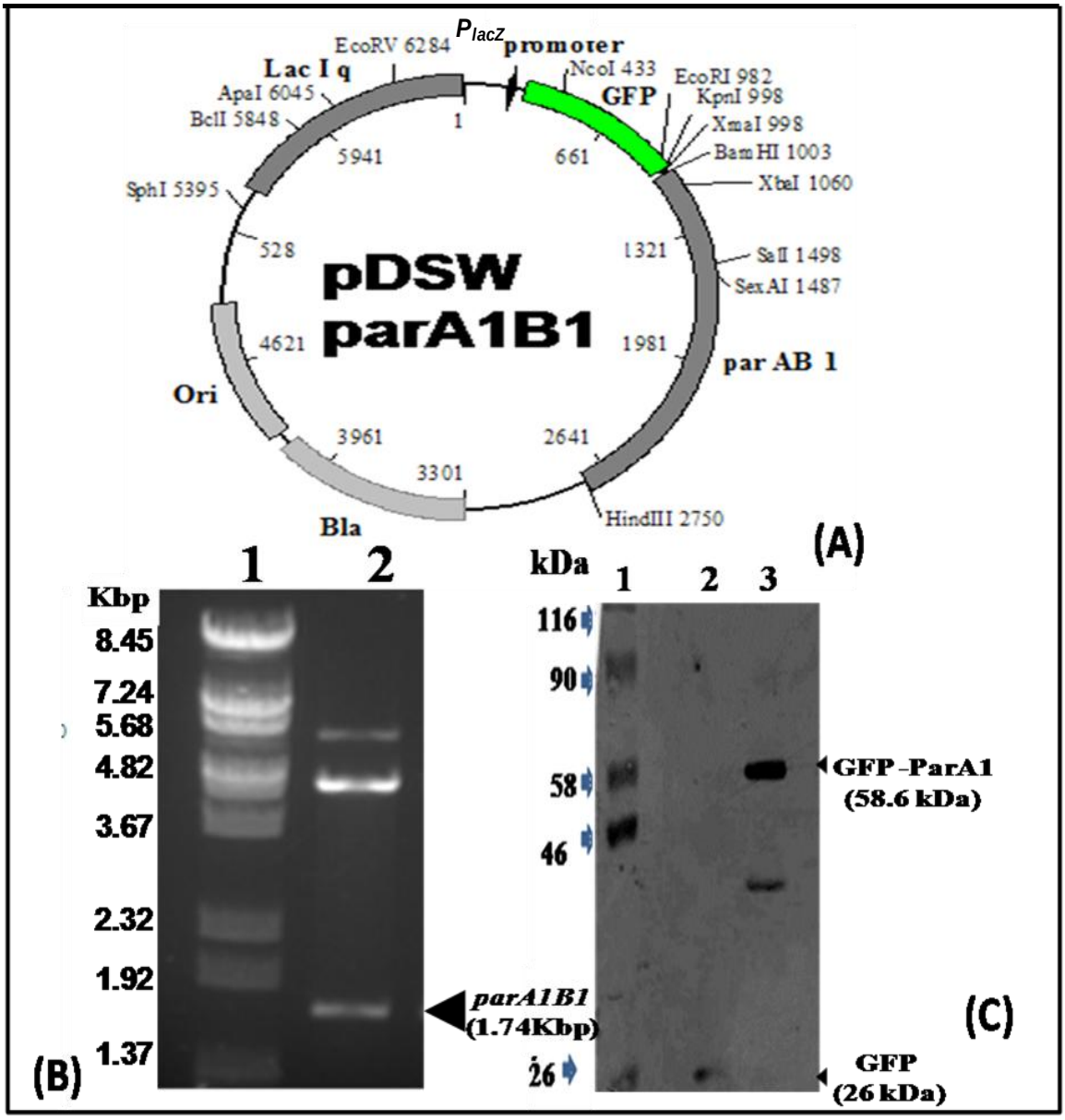

Fig 3.2.11: Construction and expression of pDSW parA1parB1 plasmid: A) Partial restriction map of pDSW parA1ParB1 plasmid. **B)** Confirmation of pDSW parA1ParB1 plasmid by restriction analysis: Lane 1: lambda *Hind*III/*EcoR*I double digested Lane 2: pDSW parA1ParB1 plasmid double digested with *BamH*I and *Hind*III. **C)** Confirmation of GFP-ParA1 translational fusion by Immuno blotting: Lane 1: SDS7B2 prestained marker. Lane 2: GFP induced *E. coli cell* lysate. Lane 3: GFP-ParA1 induced *E. coli* cell lysate.

Role of ParB1 in genome stability

Plasmid stabilization studies showed the essentiality of ParA1B1 proteins in stabilization of pDAGS3 plasmid. To find out the role of ParB1 in maintenance of *D. radiodurans* genome, we have generated pNOK0012 vector as described in methodology. In brief the ~1 kbp upstream and downstream regions to the DR0012 encoding genomic fragment were PCR amplified and cloned at pNOKOUT (Fig 3.2.12a) and confirmed by restriction analysis. The release of correct size fragment was evident (Fig 3.212b). The pNOK0012 recombinant plasmid was linearized using *Xmn*I restriction enzyme and transformed into *D. radiodurans* wild type cells to generate homozygous deletion of ParB1. The complete replacement of the chromosomal copy of *parB1* from the *Deinococcus* genome with selection marker gene *npt*II was confirmed by PCR amplification of *npt*II cassette, which was absent in wild type (Fig 3.212c). The Δ*parB1* mutant was also confirmed by the absence of PCR amplification of *parB1* encoding sequences in genome of the mutants **(**Fig 3.2.12c). Homozygous *parB1* deletion mutant used in subsequent work is named as Δ*parB1*.

Effect of *parB1* deletion on growth characteristics and genomic instability in *D. radiodurans* was checked. Mutant cells showed significant decrease in turbidity measured at 600nm as compared to wild type cells (Fig 3.2.13a). Deletion of *parB1* showed similar effect as *parB* deletion in other bacteria e.g. *Pseudomonas putida* (Godfrin-Estevenon et al., 2002). Fluorescent micrographs of mutant cells stained with DAPI showed notable effects of *parB1* deletion on genome maintenance under normal growth conditions. During exponential growth phase, these cells showed an increased frequency of anucleated cells and there was no change in the cell morphology (Fig

3.2.14). The anucleation frequency in mutant cells was in range of 8-13 % against less than 1% observed in wild type cells (Table 3.2).

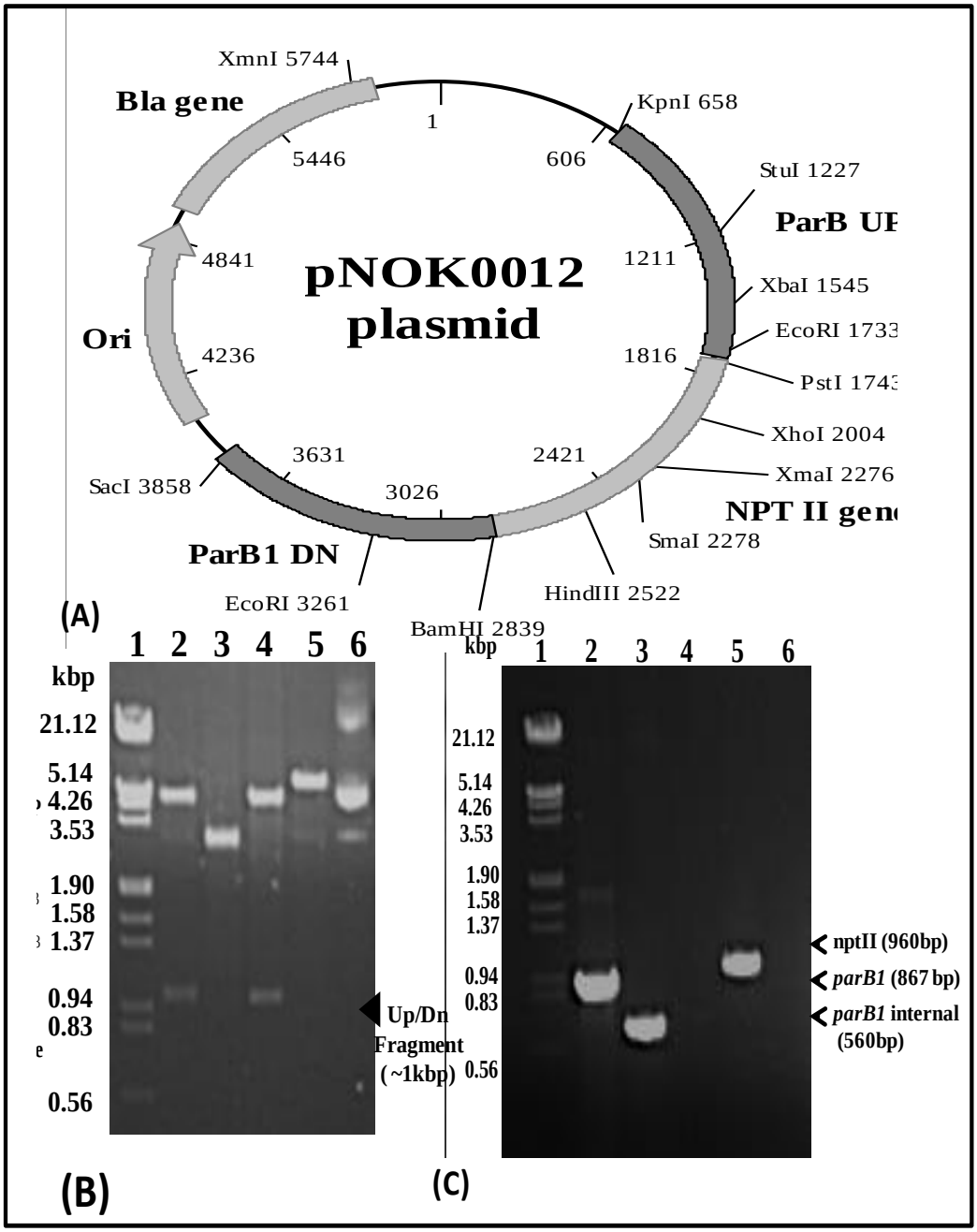

Fig 3.2.12: Generation of Δ*parB1* mutant

A) Partial restriction map of pNOK0012. **B)** Confirmation of pNOK0012 by restriction analysis: Lane1: lambda *Hind*III / *Eco*RI marker. Lane2: pNOK0012

double digested with *Kpn*I / *Pst*I. Lane 3: pNOK0012 double digested with *Kpn*I and *Sac*I. Lane 4: pNOK0012 double digested with *BamH*I and *Sac*I. Lane 5: pNOK0012 digested with *BamH*I. Lane 6: pNOK0012undigested plasmid. **C)** Confirmation of Mutant by PCR analysis: Lane 1: λ *Hind*III / *EcoR* I marker. Lane 2: Amplification of *parB1* gene full length from wild type *D.radiodurans.* Lane 3: The *parB1* gene amplification using internal primers from wild type *D.radiodurans*. Lane 4: Amplification of *parB1* gene using internal primers from Δ*ParB1* mutant. Lane 5: Amplification of *npt*II cassette from Δ*ParB1* mutant Lane 6. Amplification of *parB1* gene using internal reverse external forward primers in Δ*ParB1* mutant.

Micrographs of DAPI stained several tetrad cells were seen as triads possibly because one of the four cells is anucleated and did not survive (Fig 3.2.14 B &C). Also a large number of tetrad populations showed relatively a low density of DNA in one of the four compartments of tetrads. These results suggested that ParB1 interacts with nucleoid i.e. specifically with centromere sequence and helps in genome segregation in *D. radiodurans*.

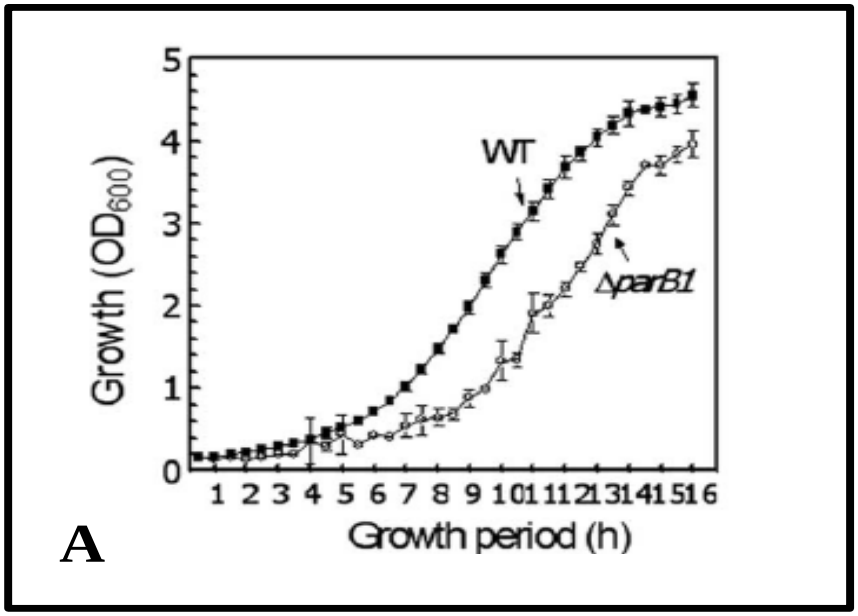

Fig 3.2.13: Effect of ParB1 deletion on genome maintenance in *Deinococcus radiodurans*. A) The *parB1* deletion mutant (Δ*parB1)* of *D. radiodurans* was generated and its growth pattern at OD.600 nm was compared with *D. radiodurans* R1 (WT). **B)**

The effect of *parB1* deletion on anucleation was examined microscopically and the cells grown at different time interval were micro graphed under bright field (BF) and cells stained with DAPI (DAPI). Percentage of anucleation was calculated from the number of cells missing genome from the total number of cells counted. **C)** Percentage of anucleation was measured in wild type (WT) and Δ*parB1* mutant cells in a time dependent, under normal growth conditions.

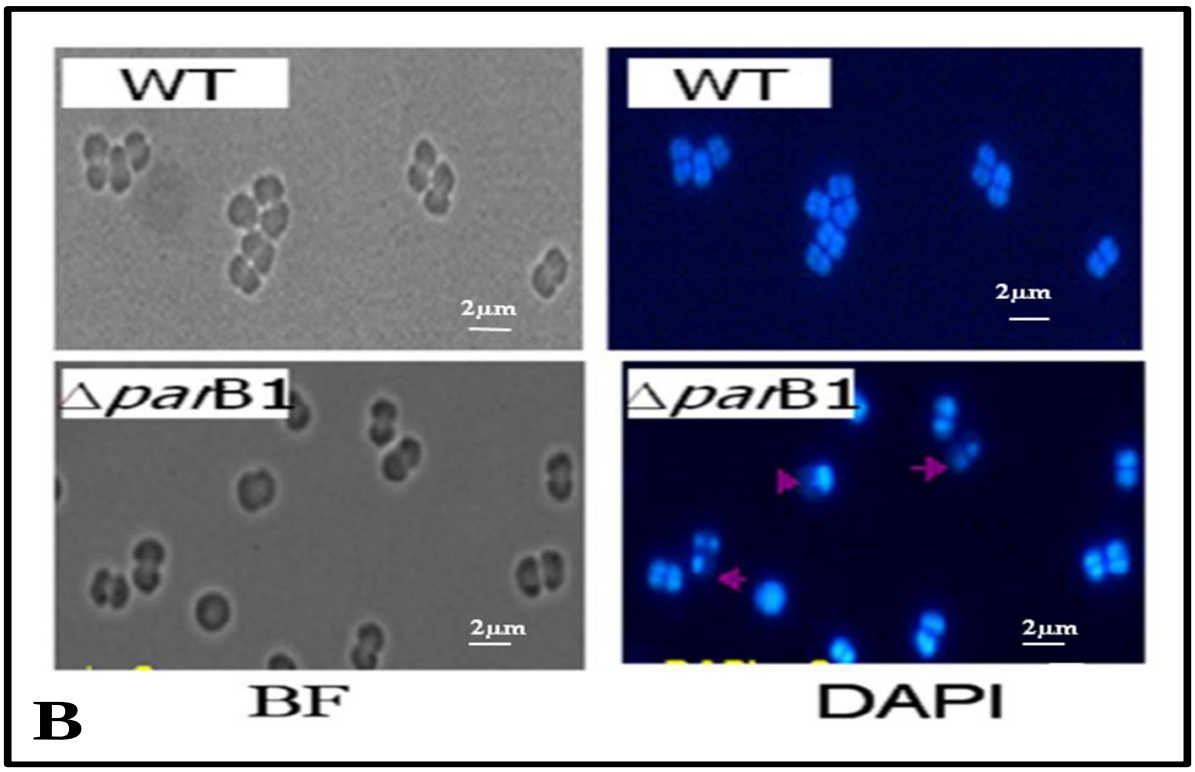

Table3.2: Effect of ParB1 Deletion on anucleation of *D. radiodurans.*

Growth period (h)	Wild type		Δ *parB1* mutant	
	No. of cells counted	Mean anucleation Frequency(%) ± SE	No. of cells counted	Mean anucleation Frequency(%) ± SE
2	189	0.60 ± 0.12	280	8.57 ± 1.34
4	203	0	297	9.42 ± 0.98
6	202	0.049 ± 0.021	258	10.07 ± 1.45
8	249	0	255	10.19 ± 1.58
10	295	0	206	13.39 ± 0.87

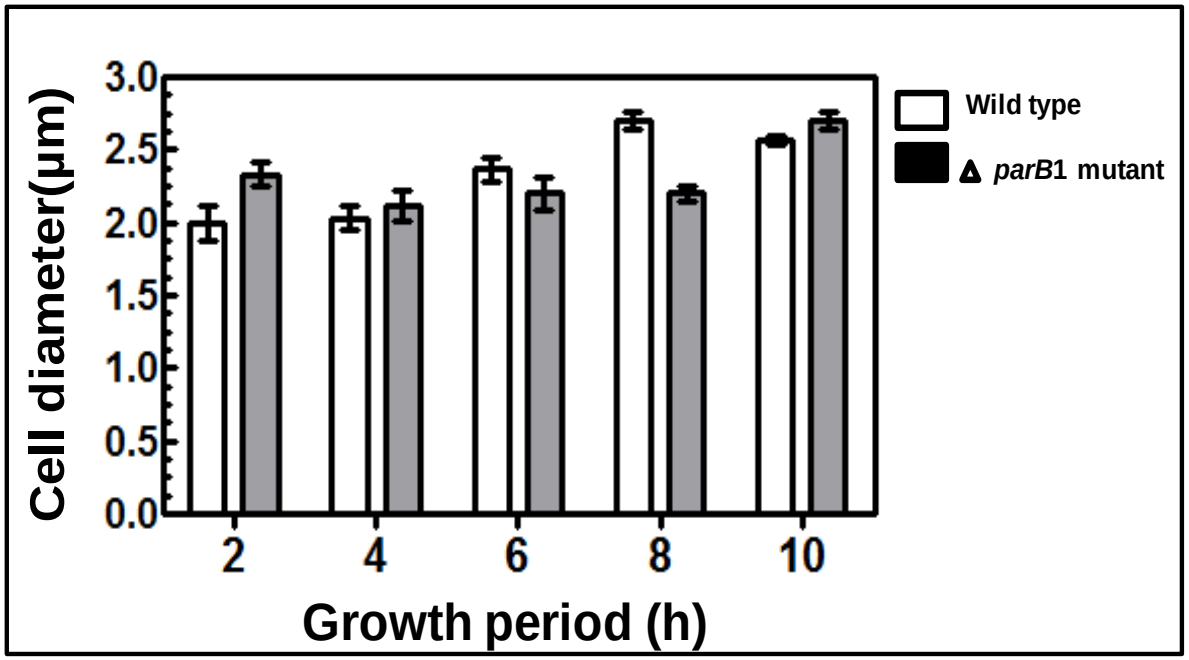

Fig 3.2.14: Effect of ParB1 deletion on *D. radiodurans* cell morphology: The effect of *parB1* deletion on anucleation was examined microscopically and the cells grown at different time intervals were micro graphed under bright field. Cell diameter is calculated by using Image J software and change in cell diameter of *parB1* deletion mutant data is compared with the wild type cells at different time intervals.

Heterogeneity in cell population showing anucleation could be attributed to toroidal packaging of all genome replication units and also to the functional redundancy if contributed by other ParB type proteins encoded on other replication units in this bacterium.

In vivo localization of ParB1 in *D. radiodurans*

Different assays like plasmid stabilization and *parB1* deletion mutant analysis gave a strong indication about ParB1 specificity with centromere sequence and its role in chromosome segregation. In order to study the localization of ParB1 in cells, the pD12GFP was constructed and GFP-ParB1 fusion was expressed in the cells. The cells

harboring pD12GFP plasmid was induced with IPTG and the synthesis of GFP-ParB1 fusion protein was confirmed by immunoblotting using GFP antibodies (Fig 3.2.15).

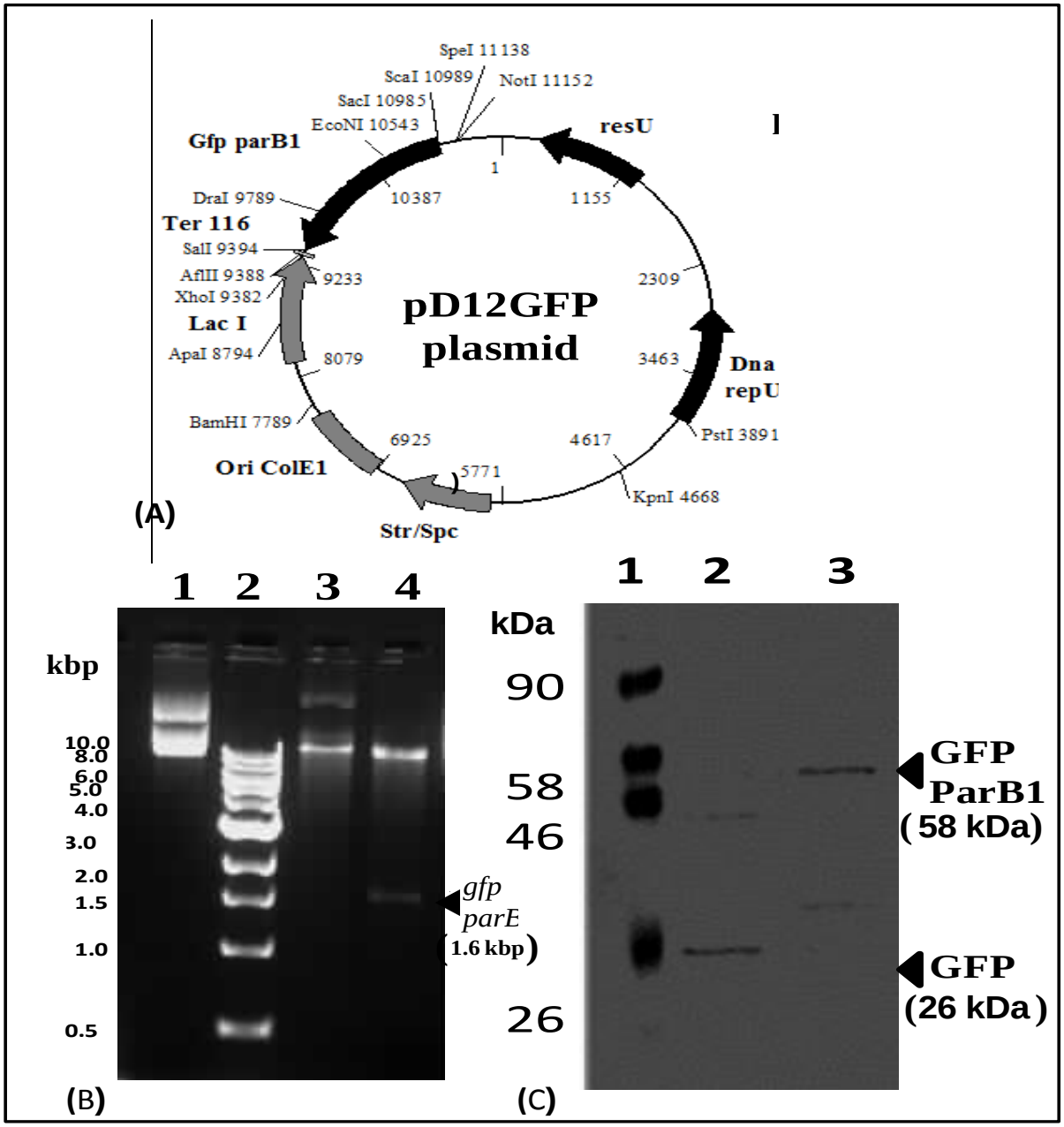

Fig 3.2.15: Generation of GFP-ParB1 translational fusion protein: A) Partial restriction map of pD12GFP plasmid. **B)** Confirmation of pD12GFP plasmid by restriction analysis: Lane1: Undigested pD12GFP plasmid. Lane 2: 1Kb NEB marker. Lane 3: pD12GFP digested with *Xho*I. Lane 4: pD12GFP double digested with *Sac*I and. *Xho*I. **C)** Confirmation of ParB1-GFP translational fusion by Immunoblotting: Lane 1:

SDS7B2 prestained marker. Lane 2: GFP Induced *D. radiodurans* cell lyaste. Lane 3: GFP Induced *D. radiodurans* cell lysate.

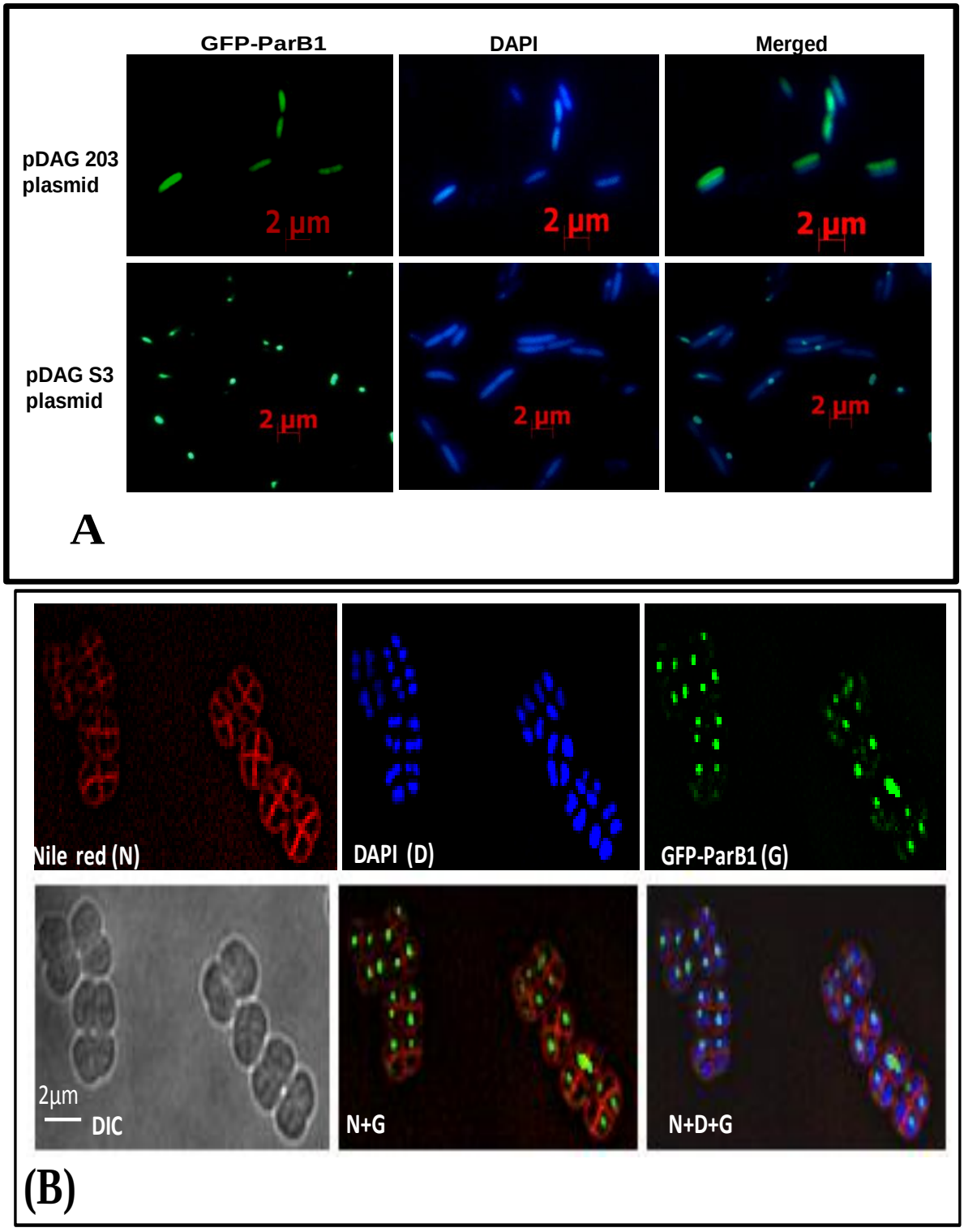

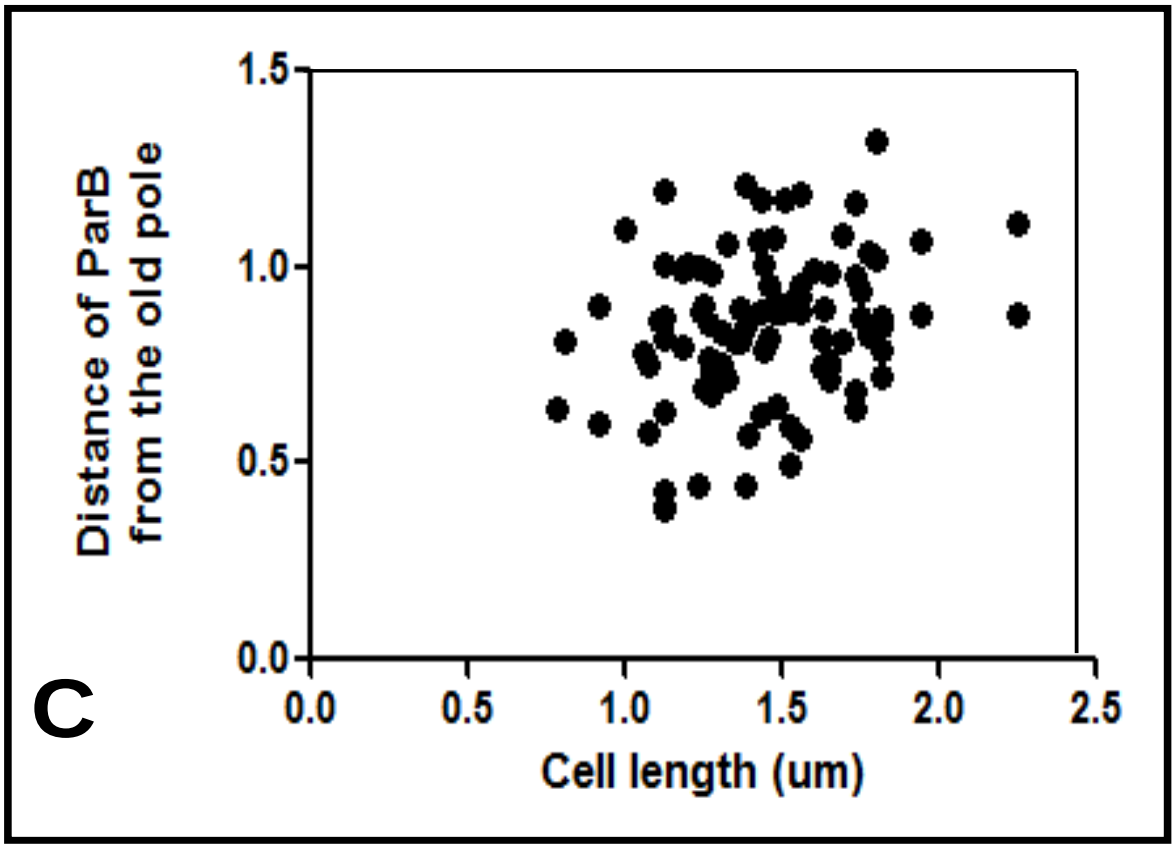

Fig 3.2.16. Interaction of GFP-ParB1 with nucleoid. GFP-ParB1 were expressed by inducing with IPTG Culture was photographed for GFP fluorescence (GFP- ParB1) as (G) and cells stained with DAPI (D) and Nile red (N). These images were merged (Merged) to localize the position of GFP spot on nucleoid. (**A**) *E. coli* cells harboring pDAG203 vector (pDAG) and pDAGS3 (pDAGS3), with IPTG. (B) *D. radiodurans.* (C) Statistical analysis of GFP- ParB1 localization with in *D. radiodurans*.

Microscopic examination of *D. radiodurans* cells expressing GFP-ParB1 fusion showed the presence of at least one fluorescent focus per cell, which was not observed in wild type cells harboring p11559- GFP vector control. Staining cells with DAPI checked localization of GFP-ParB1. Overlapping the micrographs of GFP and DAPI fluorescence showed that GFP-ParB1 formed foci directly on nucleoid of *Deinococcus* cells (Fig 3.2.16 b). On the other hand when GFP-ParB1 fusion was expressed in *E. coli*, GFP-ParB1 was found distributed throughout the cells and no foci formation was observed in

wild type cells. Functional complementation of *segS*3 element using pDAGS3, GFP-ParB1 showed the discrete foci formation on DNA, which was not observed in cells harboring pDAG203 as a vector control (Fig 3.2.16a).

These results suggest that ParB1 nucleates on *segS*3 sequence present on plasmid in *E. coli* and on genome in *D. radiodurans*. Statistical analysis of GFP – ParB1 localization was done by using Image J software. Results indicated GFP-ParB1 localized at two distinct positions with in the cell i.e. mid cell position or ¾ position (Fig 3.2.16b).

Role of ParA1 in chromosome segregation

Different bacterial segregation models (plasmid or chromosome) represent movement of paired or duplicated plasmid or chromosome because of the functional interaction between ParB and ParA protein. Our *in vitro* data indicated that ParA1 interacts with ParB nucleoprotein complexes while *in vivo* results provided evidence on plasmid stabilization by the ParA1, ParB1 and *parS* in Δ*sopABC* mini-F plasmid derivative pDAGS3 in *E. coli*. However, the mechanisms by which ParA1 and ParB1 stabilize unstable plasmid were not clear. Previous models showed that plasmids are stabilized due to involvement of ParA protein and hence we further looked for functioning of ParA1 protein. In order to investigate the role of ParA1 in segregation, we checked the localization as well as dynamics of ParA1 protein in cells harboring cognate partitioning system.

Localization of ParA1 protein:

For GFP-ParA1 localization studies, the pHJ0013 plasmid (P_{lac}-*gfp-parA1*) or pDSWparA1B1 plasmid (P_{lac}gfp-parA1parB1) were generated and transformed in *E. coli*

JM109. These cells were grown till exponential phase and induced with 100 µM IPTG. The synthesis of GFP-ParA1 fusion protein was confirmed by immunoblotting using GFP antibodies.

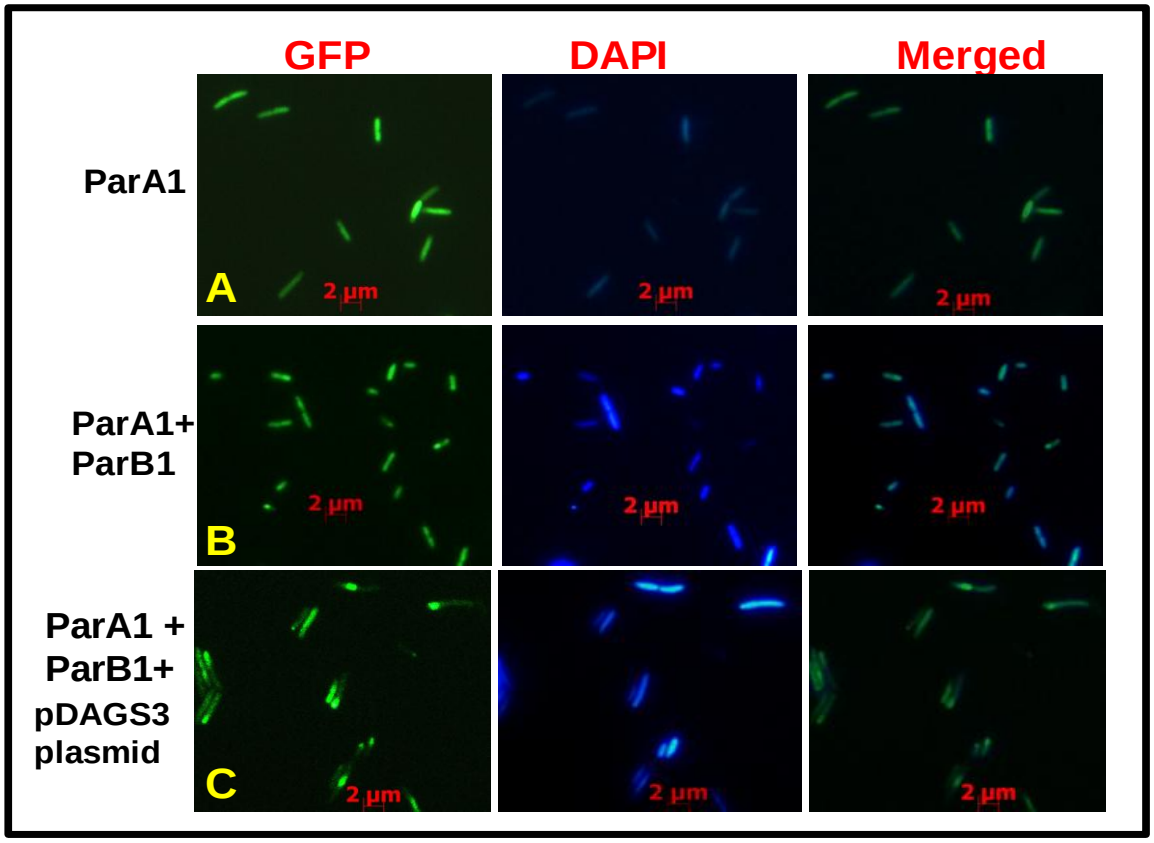

Fig 3.2.17: Localization of GFP-ParA1 in *E. coli* cells: *E. coli* cells expressing GFP-ParA1 (A) and GFP-ParA1 along with ParB1 were transformed with pDAG203 vector (B) and pDAGS3 plasmid (C) and micro graphed for GFP, DAPI fluorescence. Both images were merged.

Cells were stained with 4'-6-diamidino-2-Phenylindole (DAPI) and mounted on 1% Agarose slant and microscopy was performed as described in methods. Results showed that the GFP-ParA1 fusion protein is co-localized with the *E. coli* nucleoid (Fig 3.2.17a) and also the localization of GFP-ParA1 has not changed in presence of ParB1 (Fig 3.2.17 b). Distribution of GFP- ParA1 was measured by Image J software (Fig 3.2.17.d).

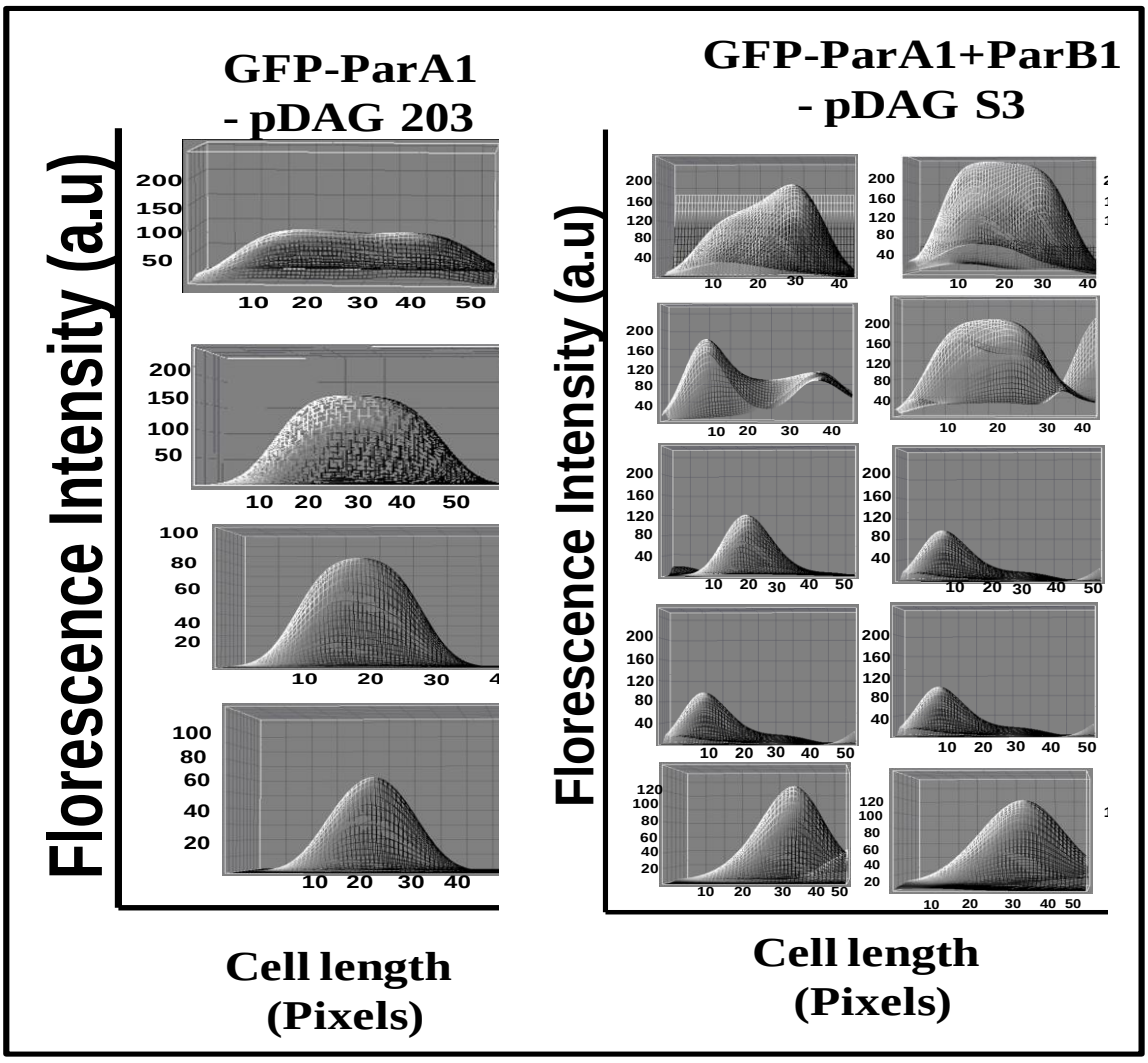

Fig 3.2.17(d). Statistical analysis of GFP-ParA1 localization throughout the length of *E. coli* cells. The GFP fluorescent images taken in Figure 3.2.17 were scanned, Florescence intensity was measured by using Image – J software.

Dynamics of ParA1

GFP-ParA1 was expressed in *E.coli* JM109 strains containing pDAG *segS*1 (pDAG S1), pDAG *segS*2 (pDAG S2), and pDAG *segS*3 (pDAG S3) plasmids individually and the dynamics of the ParA1 was studied using Time lapse microscopy (Fig 3.2.19) GFP-

ParA1 has shown oscillation from one end to another but degree of movement is varied for different *segS* elements.

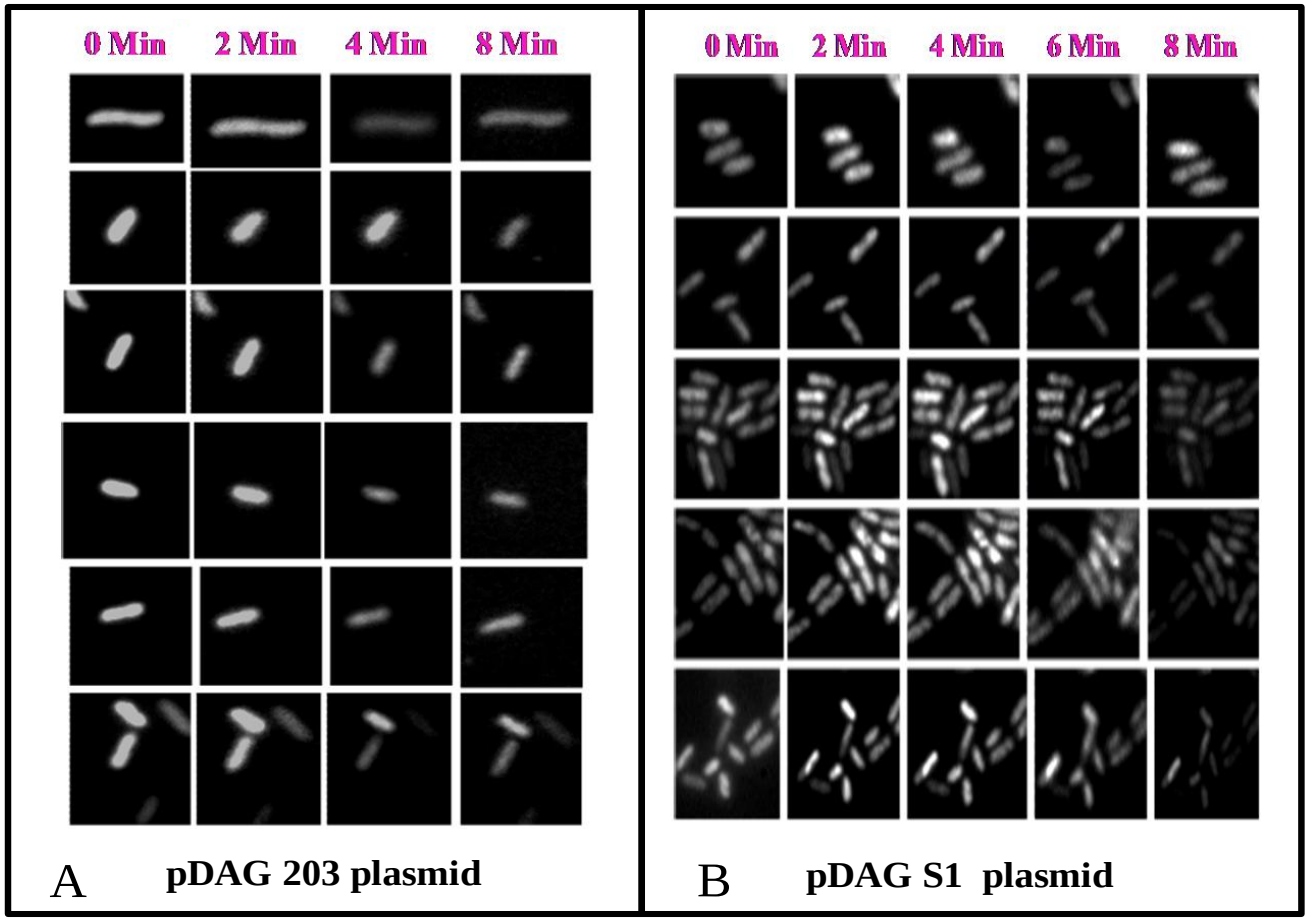

GFP-ParA1 had shown slow movement or no movement with pDAGS1 (Fig 3.2.18b), and faster dynamics with pDAG S2 plasmid and pDAG S3 (Fig 3.2.18c, d) compared to pDAG or pDAG S1 plasmid. Thus the dynamics of GFP ParA1inside the cells in presence of with *segS* elements, revealed that these elements indeed as centromere sequences for *Deinococcus* and ParB-*segS*3 nucleoprotein complex is essential for dynamics of ParA1.

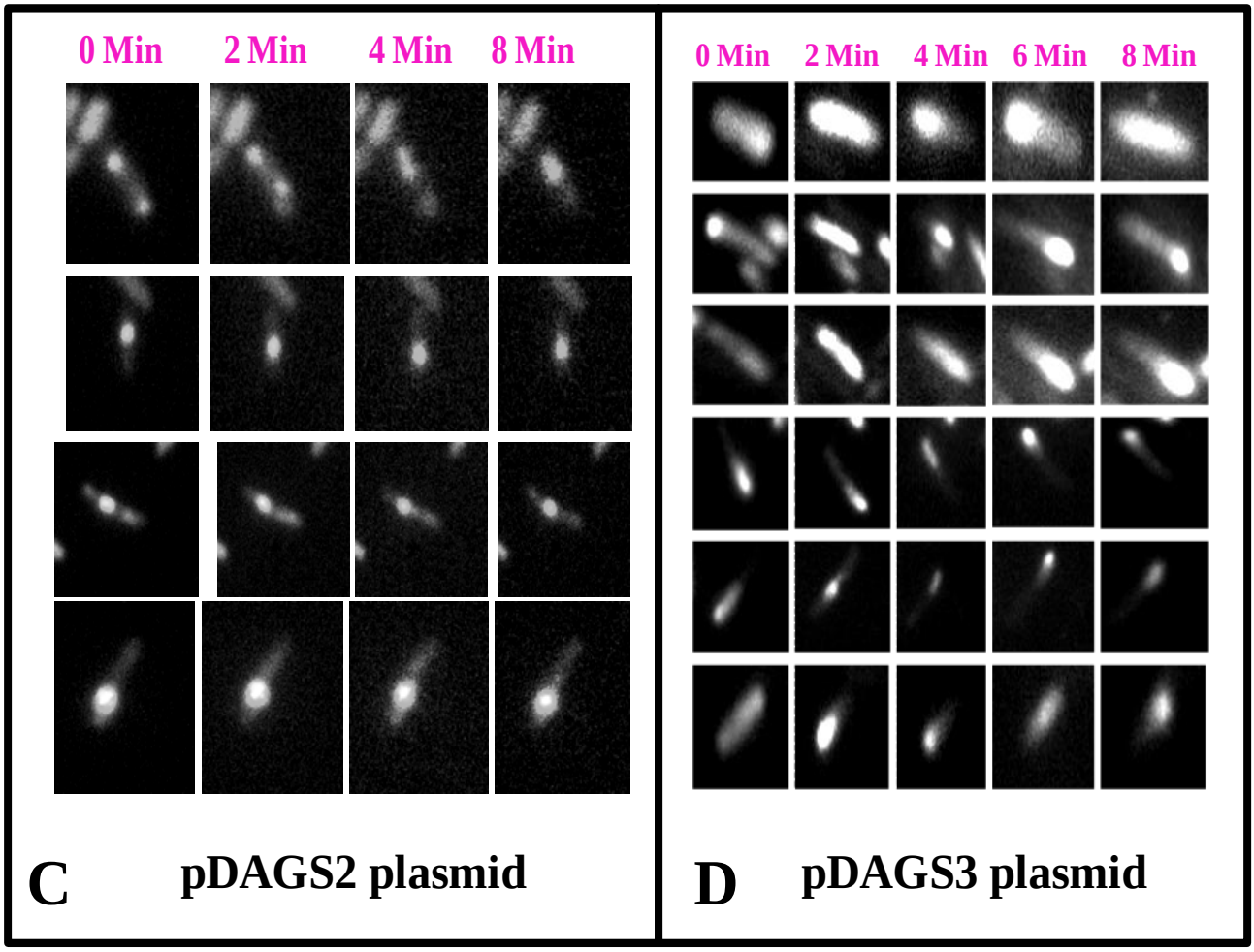

Fig 3.2.18: Dynamics of GFP – ParA1 in *E. coli* cells: GFP-ParA1 along with ParB1 was induced with 100 µM IPTG for four hours in presence of different *segS* elements i.e. pDAG203 plasmid alone **(A)**, pDAGS1 plasmid **(B)**, pDAGS2 plasmid **(C)**, pDAGS3 plasmid **(D)** of *D. radiodurans*. Images were taken at two minute intervals as indicated.

Dynamics of GFP-ParA1 also supported our *in vitro* data as described in this chapter.

Bacteria harboring multiple genome replicating units have been identified. *D. radiodurans* is found to be one such bacterium harboring multiple genome replicating units (Slade and Radman, 2011).

Genome sequence of this bacterium revealed several interesting facets (White *et al.*, 1999). The maintenance of multipartite genome structure and the ploidy in dividing cells of bacteria have been the interesting questions and equally fascinating.

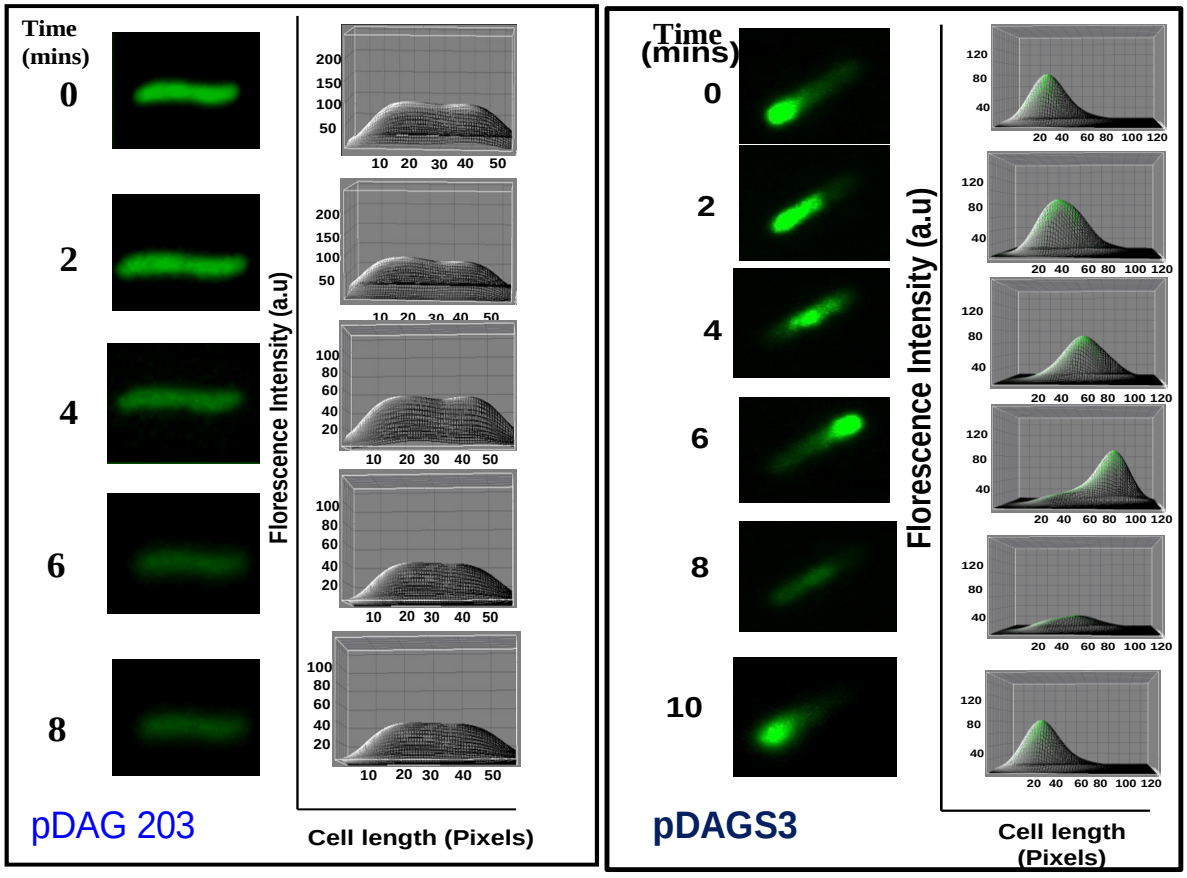

Fig 3.2.19: GFP –ParA1 florescence distribution in *E. coli* : The Florescence intensity of GFP – ParA1 was measured in *E. coli* cells harboring pDAG203 and pDAGS3. Localization of GFP-ParA1 was measured in time dependent manner and florescence intensity distribution with in single E.coli cell are represented over here.

Recent studies in other multichromosome containing bacteria like *V. cholerae* also demonstrated both chromosome I and II encode independent genome segregation systems. This study has brought forth some interesting findings to suggest the role of 'Par' proteins in segregation of DNA in multichromosome bacteria. Chromosome I of *D. radiodurans* contains one functional partitioning system that includes the three chromosomal type centromeric sequences named as '*segS*1-*segS*3*'* and the partitioning proteins ParA1/ParB1. We demonstrated the roles of these elements in segregation of

unstable mini-F plasmid as well as monitoring the ParA1 dynamics and functional significance of ParB1 in *D. radiodurans*.

Chromosome I 'Par' proteins probably obey general principles of known 'Par' proteins e.g. ParA interacts with the DNA and when it encounters to ParB nucleoprotein complex, it stimulates its ATPase activity. As a result the duplicated DNA is pulled to opposite poles. However, the possibility of other types of mechanisms helping in segregation of secondary genomes cannot be ruled out. Nearly 8-13 % loss of nucleoid in Δ*parB1* mutant of *D. radiodurans* in comparison of 1% in normal cells (Table 3.2) further supported the role of ParB1 in genome maintenance. Molecular interaction studies between the ParA1/ParB1 and *segS* elements showed that ParA1 could interact with dsDNA and there is no formation of higher order structures as evidenced from sedimentation analysis and light scattering studies. However ParA1 behaved differently in presence of *segS* nucleoprotein complex i.e. ATPase activity of ParA1 in presence of *segS*3-ParB1 as compared to other centromeric complexes is higher, and the amount of protein in {*segS*3-ParB1P} nucleoprotein complex, but not {*segS*1- ParB1P} / {*segS*2-ParB1P} complex especially in presence of ATP. ParA1 polymerization / depolymerization may be regulated by the levels of its ATPase activity. Both DNA binding of ParA1 and its polymerization/ depolymerization as a function of its ATPase activity are the typical characteristics of other Walker type ATPases associated with genome segregation (Leonard *et al.*, 2004;Leonard *et al.*, 2005;Pratto *et al.*, 2008;Soberon *et al.*, 2011).

D. radiodurans cells expressing GFP-ParB1 produced foci on nucleoid, and the Δ*parB1* mutant similar to other ParB deletion mutant showed effect on the growth and increased

percentage of anucleation as compared to *D. radiodurans* wild type cells. These findings collectively suggested that both *segS* elements and 'Par' proteins encoded on chromosome I of *D. radiodurans* are functionally active and play a role in genome segregation and maintenance of chromosome in this bacterium. GFP-ParA1 in presence of ParB1 and centromere sequence showed dynamicity, similar to the ParA of pB171 plasmid as well as Soj of *B. subtilis.* Overall studies indicate (i) the ParA1 as a DNA binding ATPase, (ii) the ParB1 as a sequence specific centromere binding protein, (iii) the ATPase activity of ParA1 was stimulated in presence of both ParB1 and dsDNA that seems to be regulating the dynamics of ParA1 polymerization, (iv) *segS* elements function like bacterial centromere's for unstable plasmid segregation and ParB1 has a role in genome maintenance in *D. radiodurans*. ParA1 dynamics was very fast in presence of *segS3* elements. An attempt was made to generate homozygous deletion mutant, as cells approaching to homozygous replacement of *segS*3 with selection marker loose viability. This might indicate for a strong possibility of *segS*3 acting as a preferred centromere during ParAB1 mediated partitioning of chromosome I in *D. radiodurans* and segregation of DNA mostly likely by pulling type mechanism.

CHAPTER 3.3

Molecular studies on chromosome II partitioning proteins

The roles of 'Par' proteins in chromosome segregation have been understood better in bacteria containing single set of 'Par' proteins. The pleiotropic roles of 'ParA' proteins have also been demonstrated in functions like, origin localization, cell division and gene regulation in *B. subtilis* (Ireton *et al.*, 1994; Lee *et al.*, 2006;Lee *et al.*, 2003;Ogura *et al.*, 2003; Sharpe and Errington, 1995; Wu and Errington, 2004), cell division and cell cycle progression in *C. crescentus* (Mohl *et al.*, 2001), chromosome organization, cell growth, and motility in *P. aeruginosa* (Bartosik *et al.*, 2004;Lasocki *et al.*, 2007), cell morphology in *P. putida* (Godfrin-Estevenon *et al.*, 2002;Lewis *et al.*, 2002) and cell division in *S. coelicolor* (Jakimowicz *et al.*, 2007;Kim *et al.*, 2000). Pleiotropic effects of 'ParA' proteins may depend upon the adaptation of bacteria to particular environmental condition. The involvement of 'Par' proteins in cell division regulation has been mostly observed in some bacteria containing single chromosome. Recently, the deletion mutant of 'ParA' proteins showed defect in cell division in different bacteria like *B. subtilis*, *C. crescentus*, *P. aeruginosa* and *S. coelicolor*. Molecular basis of cell division inhibition by ParA is not understood.

D. radiodurans harbors four ParA like proteins, which are encoded in an operon and these proteins belong to weak walker type of ATPase family. Clustal W analysis of *D. radiodurans* 'Par' proteins showed nearly 40 % sequence similarity within these proteins. Phylogenetic analysis revealed 'Par' proteins on the accessory chromosome are diverged from the 'Par' proteins of primary chromosome (chromosome I of *D. radiodurans*) as well as from 'Par' proteins of other bacteria. Since, ParA2 encoded on chromosome II in

D. radiodurans is distinctly different from chromosomal ParA's, the functional characterization of ParA2 has been carried out and reported in this chapter.

3.3. 1 Materials and Methods:

3.3. 1.1 Cloning of recombinant ParA2 protein:

The 780 bp DNA fragment encoding putative ParA (DRA0001) type protein on chromosome II (ParA2) of *D. radiodurans* was PCR amplified from genomic DNA using dr_A0001F and dr_A0001R primers. The PCR product was digested, cloned at *Nde*I-*Xho*I sites in pET28a+ to yield pETA2 and confirmed by restriction digestion as well as by sequencing. For making CFP translation fusion, the *drA0001* was PCR amplified using forward primer *parA2*CF and reverse primer *parA2C*R (Table) having *Hind*III and *BamH*I sites incorporated at the 5' of the primers. PCR product was cloned at *Hind*III and *BamH*I sites in pAMCYAN (Clonetech Inc) to yield pA2CFP. The pETA2 WAS transformed into *E. coli* BL21 DE3 *pLysS* for the expression of recombinant protein while PA2CFP WAS transformed into *E. coli* MG1655 strain. The inducible expression of his tag recombinant ParA2 was confirmed by SDS -PAGE and ParA2-CFP by immunoblotting using GFP antibodies.

3.3.1.2 Expression and purification of recombinant proteins:

The recombinant pETA2 plasmid is transformed into *E. coli* BL21 (DE3) *pLysS*, induced with 250 µM IPTG, 6x histidine tagged protein was purified by nickel -affinity chromatography under denaturation condition as mentioned in material and method section. In brief, the IPTG induced cell pellet was directly suspended in Cell Lytic

Express (Sigma Chemical Company, USA) and incubated at 37^{o}C for 1h with mild agitation. Lysate was centrifuged at 15,000x g for 30 min and the pellet containing majority of the recombinant protein in inclusion bodies got separated from clear supernatant. This inclusion pellet was resuspended in buffer B containing 100 mM NaH_2P0_4, 10mM Tris-HCl, pH 8.0 and 8M urea. Mixture was incubated at room temperature for 30 min and clear supernatant obtained from centrifugation at 12,000 x g for 20min, and purified using Ni- NTA. Different eluted fractions were checked on 10% SDS-PAGE and nearly pure fraction were pooled and refolded by serial dilution of urea with concurrent increase in DTT concentration. The fractions showing near to homogeneity in ParA2 preparation were pooled and dialyzed in buffer containing 20mM Tris-HCl, 50mM NaCl, 1mM DTT, 1mM EDTA, 1mM PMSF and 50% glycerol. The protein was stored in small aliquots at -20ºC for subsequent uses. The mass spectrometric analysis of ParA2 proteins was carried out commercially (The Centre for Genomic Applications, New Delhi). The peptide mass fingerprints of recombinant polypeptide matched with ParA2 encoding from chromosome II of *D. radiodurans* and ensured homogeneous preparation.

3.3.1.3 DNA protein interaction studies:

DNA binding activity assay of ParA2 protein was done using 300bp DIG labeled dsDNA, 300 bp of DNA was amplified from *D. radiodurans* using forward primer DP2F and reverse primer DP2R. DNA was purified from gel (QIAgen Inc., Germany) and labeled at 3'end with dig-dUTP (Roche Biochemicals, Germany) following manufacturers protocols. Reaction was carried out by increasing concentration of ParA2 protein (100-1000ng) in buffer containing 50mM HEPES pH8.0, 100mM NaCl, 5mM

$MgCl_2$, 30mM Na-Acetate and nearly 10 picomoles of labeled dsDNA substrate. Reaction was incubated at 37^oC for 20 min in a 20µl reaction. Mixtures were separated on 5 % native PAGE and digoxigenin labeled DNA probe was immuno blotted with anti-Digoxigenin-AP antibodies (Roche biochemical's Germany) and signals were detected using NBT / BCIP (Roche Biochemical) color reagent using manufacturer's protocol.

3.3.1.4 Measurements of ATPase and GTPase activities:

ATPase activity of recombinant ParA2 was checked using a modified protocol as described in (Kota *et al.,* 2010). In brief, reaction was carried out with increasing concentrations of ParA2 (0.1 to 1µg) in 50mM HEPES pH 8.0, 100mM NaCl, 5mM $MgCl_2$ and 30mM Sodium acetate, incubated at 37^oC for 20 min with and without DNA**.** Reaction was stopped using malachite green reagent and ATP hydrolysis was indirectly measured by checking release of inorganic phosphate at O.D 630nm and levels of Pi quantified using standard procedure essentially described in (Yakunin *et al.,* 2004). ATPase activity was calculated as nmoles Pi formed per min/ µg protein. For studying the effect of dsDNA on ATPase activity of ParA2, the dsDNA was pre-incubated with ParA2 and then incubated with ATP for different time period and assayed as described above. Similarly GTPase activity of $FtsZ_{Dr}$ (*D. radiodurans*) was measured as the release of Pi from GTP and estimated as described above. In brief, ~4 µg purified recombinant FtsZ was incubated with 1mM GTP for 1h at 37^oC in reaction mixture containing 25mM PIPES, pH 7.6, 50mM KCl, 5mM $MgCl_2$ and 1mM GTP. The reaction was stopped with malachite green reagent and release of inorganic Pi was measured as described above. For studying the effect of ParA2 on GTPase activity of FtsZ, the above reaction mixture

was incubated with FtsZ with and without 3µg ParA2, 200ng DNA and 1mMATP as required. The DNA, ATP, ParA2 and FtsZ controls were processed in parallel under identical conditions.

3.3.1.5 Sedimentation Analysis:

For studying the effect of ParA2 on FtsZ polymerization, ~2µg FtsZ protein was incubated in 25mM PIPES, pH 7.6, 50mM KCl, 5mM $MgCl_2$ and then ~1.5µg ParA2 was added along with 200ng dsDNA and 1mMATP. These mixtures were incubated at 37^{o}C for 30 min and centrifuged at 20,000g for 20 min. Both pellets and supernatants were separated and analyzed on 12% SDS-PAGE. Protein bands were visualized with Commasie staining and quantified by densitometric scanning.

3.3.1.6 Construction of *parB2* deletion mutant in *D. radiodurans*:

pNOKA0002 was made to generate *parB2* deletion mutant in *D. radiodurans*, pNOKA0002 was constructed by amplifying 1kb upstream to DRA0002 ORF was PCR amplified using drA0002UF and drA0002UR primers, similarly of 1kb downstream to DRA0002 using drA0002DF and drA0002 DR primers for downstream fragment (Table 2.4) and PCR amplified products were digested and cloned at *Apa*I-*EcoR*I and *BamH*I-*Sac*I sites respectively. The recombinant plasmid pNOKA0002 was linearized using *Xmn*I restriction enzyme and linearized plasmid was transformed into *D. radiodurans a*s mentioned in material method section. Transformants were selected through several generations to obtain homozygous replacement of *parB2* with *npt*II cassette, generation of homozygous mutant was confirmed by PCR amplification of *parB2 using* internal primers *parB2iF* and *parB2iR*.

3.3.1.7 Microscopic studies:

ParA2-CFP is expressed from pA2CFP plasmid in *E. coli* MG1655 strain, culture was grown to 0.3 O.D and induced with 100 µm IPTG, cell were grown up to 0.6 O.D, 1ml of cells were taken and DAPI (2µg μl^{-1}) was added and incubated for 30 min. To confirm ParA2 co-localization with the nucleoid, the chloramphenicol (100µg μl^{-1}) was added 1hr before 0.6 O.D culture, stained cells with DAPI as mentioned above. Fluorescence microscopy of *E. coli* cells was carried using Zeiss Axio Imager (Model- LSMS10 META, Carl Zeiss) equipped with Zeiss AxioCam HRm camera. Both CFP and DAPI fluorescence's were imaged. Micrographs were superimposed for localization of ParA2-CFP on DAPI stained nucleoid.

Effect of *parB2* deletion on anucleation in *D. radiodurans* was carried out using, both Δ*parB2* mutant and wild type cells, 1ml of exponential growing cells of wild type as well as mutant were taken and stained with 0.2µg μl^{-1} of DAPI was added and incubated for 30 min and cells were analyzed under florescence microscope. In brief, the 5µl cells expressing these proteins in different combinations were mounted onto 1% agarose coated slide and pictures were taken on Axio Imager M1 Florescence Microscope (Carl Zeiss) in different combinations and the images were analyzed using Axiovision 4.8 Rel software. Final image preparation was done using Adobe Photoshop CS3 software. Cell length measurements were done using Axiovision 4.8 software graph was analyzed and plotted by using Graph pad prism (Donovan *et al*., 2010).

3.3.1.8 Co-localization of ParA2-CFP and FtsZ-YFP and Fluorescence microscopic studies:

Co-expression of ParA2 and $FtsZ_{Ec}$ YFP was achieved by co-transforming pETA2 and pLAU85 in *E. coli* cells. These transformed cells were grown in LB supplemented with kanamycin (25µg /ml) and ampicillin (100µg /ml) overnight, expression of ParA2 proteins was achieved with 200µM IPTG while $FtsZ_{Ec}$ YFP with 0.005% arabinose using standard protocols (Sambrook J and Russell DW, 2001). Expression of recombinant proteins were confirmed by immunoblotting using respective antibodies as described earlier (Khairnar *et al.*, 2007). 1ml of exponential growing cells were taken and Fluorescence microscopy of *E. coli* cells were carried out as described earlier (Weiss *et al.*, 1999) using Axio Imager M1 Florescence Microscope. In brief, the 0.3 O.D *E. coli* cells were induced for 4hr with 200µM IPTG, these IPTG induced cells were further treated with 0.005% arabinose half an hour before fluorescence microscopic experiments was carried out.

3.3.2.0 Results:

3.3.2.1 The *parB2* mutant of *D. radiodurans* showed pleiotropic phenotypes:

In silico analysis indicated that ParA2 and ParB2 are diverged from the common pools of chromosomal, plasmid and other cell division regulatory 'Par' proteins. To understand the role of ParB2 in growth and genome maintenance of this bacterium, we generated *parB2* deletion mutant. For that, the ~1K bp upstream and downstream regions to the DRA0002 (*parB2* gene) encoding genomic fragment were PCR amplified and cloned at pNOK vector to generate the recombinant plasmid pNOKA0002 (Fig3.3.1a**)**, which was analyzed on 1% agarose gel after restriction digestion. The release of right size fragments was evident (Fig3.3.1b). The pNOKA0002 recombinant plasmid was linearized and

transformed to *D. radiodurans*. The complete replacement of the chromosomal copy of *parB2* from *Deinococcus* genome with *npt*II selection marker was confirmed by PCR amplification (Fig3.3.1c). The mutant that showed complete replacement of *parB2* with *npt*II was named Δ*parB2* and used in subsequent studies.

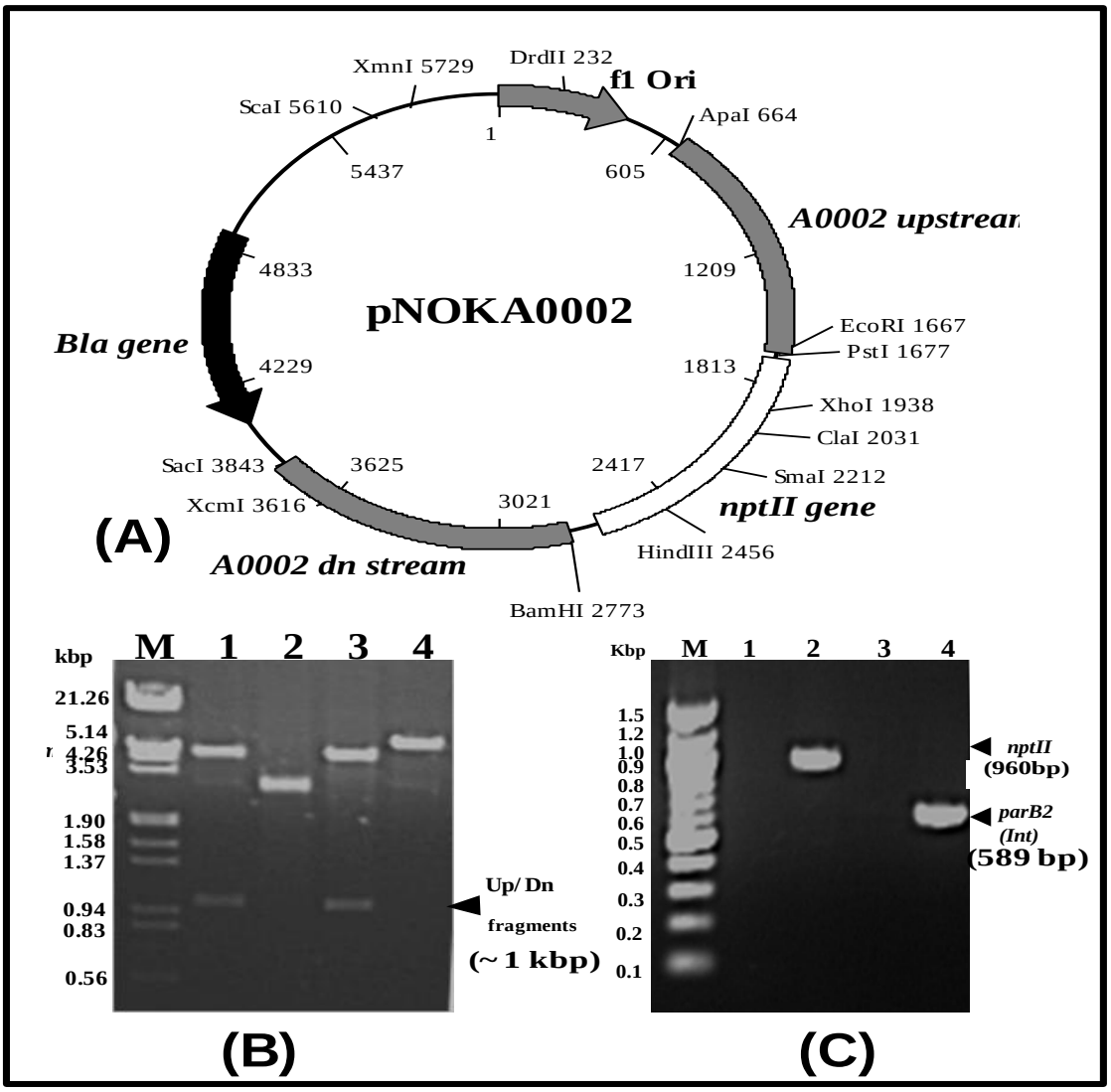

Fig3.3.1 Generation of pNOK A0002 plasmid:

(A) Partial restriction map of pNOKA0002. **(B)** Restriction analysis of pNOKA0002: Lane1: plasmid pNOKA0002 double digested with *Apa*I and *Eco*RI. Lane2: plasmid

pNOKA0002 digested with *Kpn*I *and sca*I. Lane3: pNOKA0002 plasmid digested with *BamH*I. Lane4: pNOKA0002 plasmid is digested with *Xmn*I. Lane M: DNA size marker λ DNA *Hind* III & *EcoR*I *digested*.

(C) Confirmation of *parB2* deletion in bacterial genome: The genomic DNA from prospective mutant and wild type (R1) used as template for PCR amplification of *npt*II cassette and *parB2* gene. Lane M: 100 bp ladder. Lane1: Amplification of *npt*II cassette in wild type. Lane 2: *npt*II cassette amplification in *parB2* mutant. Lane3: PCR amplification of *parB2* gene by using *parB2iF* and *parB2iR* primers in *parB2* mutant cells. Lane4: PCR amplification of *parB2* gene using *parB2iF* and *parB2iR* primers in *D. radiodurans* wild type cells.

Effect of *parB2* deletion on various phenotypes of *D. radiodurans*

The *parB2* deletion mutant was generated and the effect of *parB2* deletion on growth as well as genome stability was checked. The functional role of ParB2 on the growth *was* monitored by measuring O.D 600 nm. Mutant cells showed a significant reduction in the turbidity (Fig.3.3.2) as compared with wild type *D. radiodurans*.

Reduction in growth can be correlated with loss of chromosome. Therefore, the anucleation phenotype of the mutant was checked. The 1ml of exponential growing culture of *D. radiodurans* wild type and Δ*parB2* was stained by DAPI as mentioned in methods, micrographs of nearly 1000 cells were observed. From analysis of the results we concluded that ~6% cells have shown anucleation phenotype i.e. loss of nucleoid within the mutant cells (Fig 3.3.3)

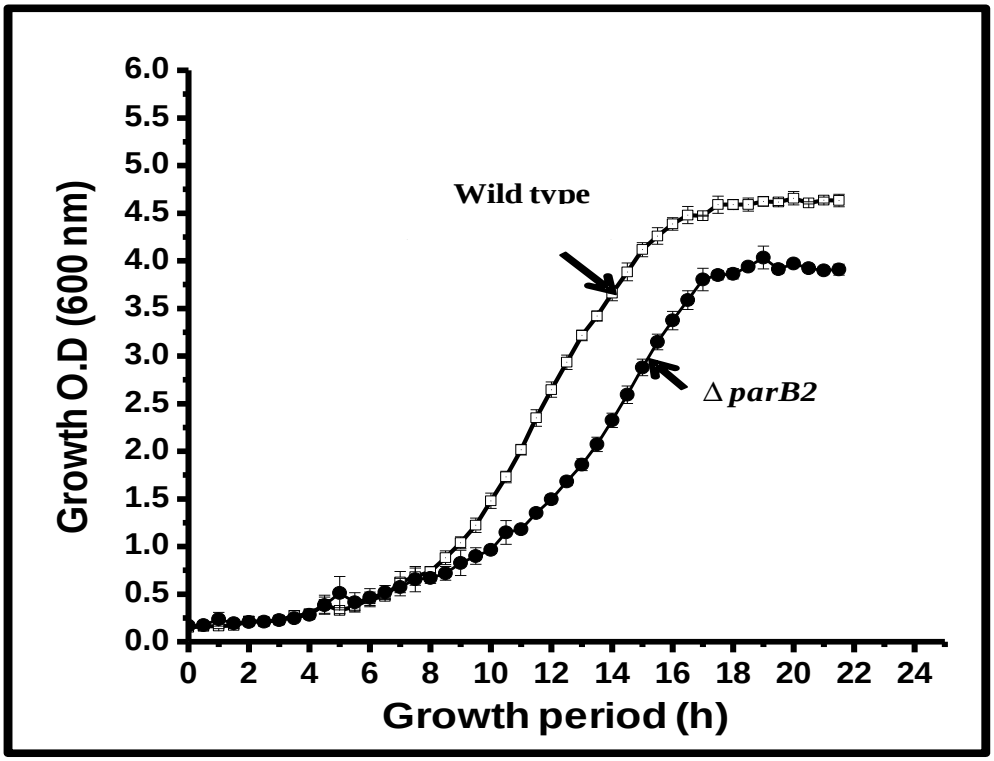

Fig 3.3.2: Growth curve analysis: wild type (-O-), *parB2* mutant (- Δ-) and *parB2* mutant in presence of Kanamycin 15µg ml^{-1} of *D. radiodurans* culture grown was monitored by measuring O.D at 600 nm.

Interestingly, the deletion of ParB2 also caused the change in the cell morphology, where as such a phenotype was not observed with ParB1 deletion mutants. Nearly 1500 cells were micro graphed, out of these 350 cells showed greater than 3.6 µm cell diameter as compared to wild type *D. radiodurans* R1 strain. The t-test analysis indicates significant change in the cell diameter as compared to wild type cells (Fig 3.3.4b). Increase in cell diameter in mutant cells indirectly indicated either the inhibition of cell division or hyper activation of origin of replication producing large number of replication initiation in these cells.

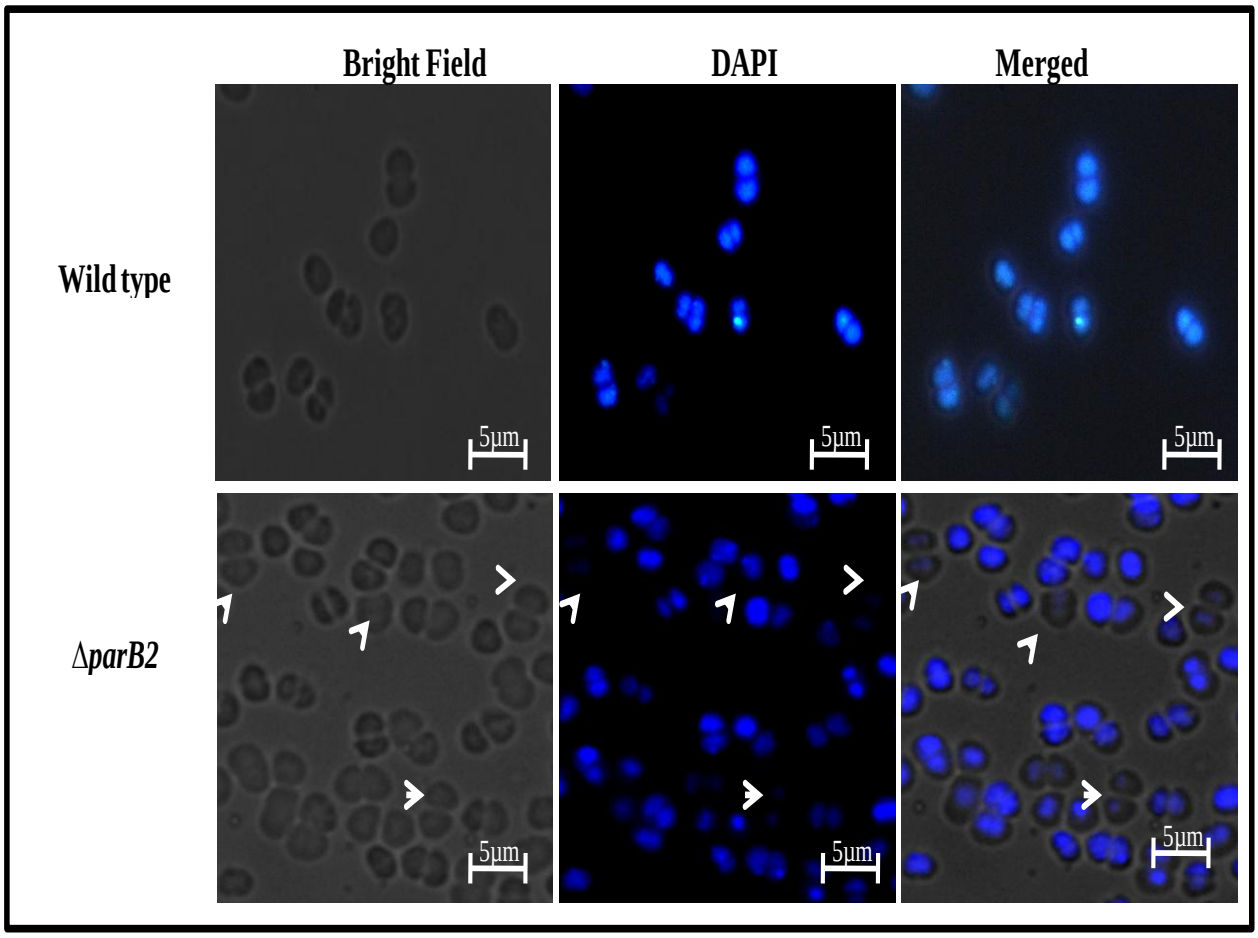

Fig 3.3.3: Effect on chromosome segregation: Wild type (*D. radiodurans*) and Δ*parB2* cells grown for 4 hrs and stained with DAPI (0.2µg μl^{-1}), Micrographs corresponding to bright field, DAPI and merged florescent pictures are shown over here, and arrows indicate anucleated cells.

Deletion of *parB* in few bacteria like *B. subtilis*, *C. crescentus* had changed stoichiometry of ParA to ParB, In the absence of ParB relative concentration of ParA increases, which further inhibited cell division process by unknown mechanism. Since, the deletion of *parB2* in *D. radiodurans* also made change in cell morphology, so we hypothesized the possible effect of *parB2* deletion in the inhibition of cell division process.

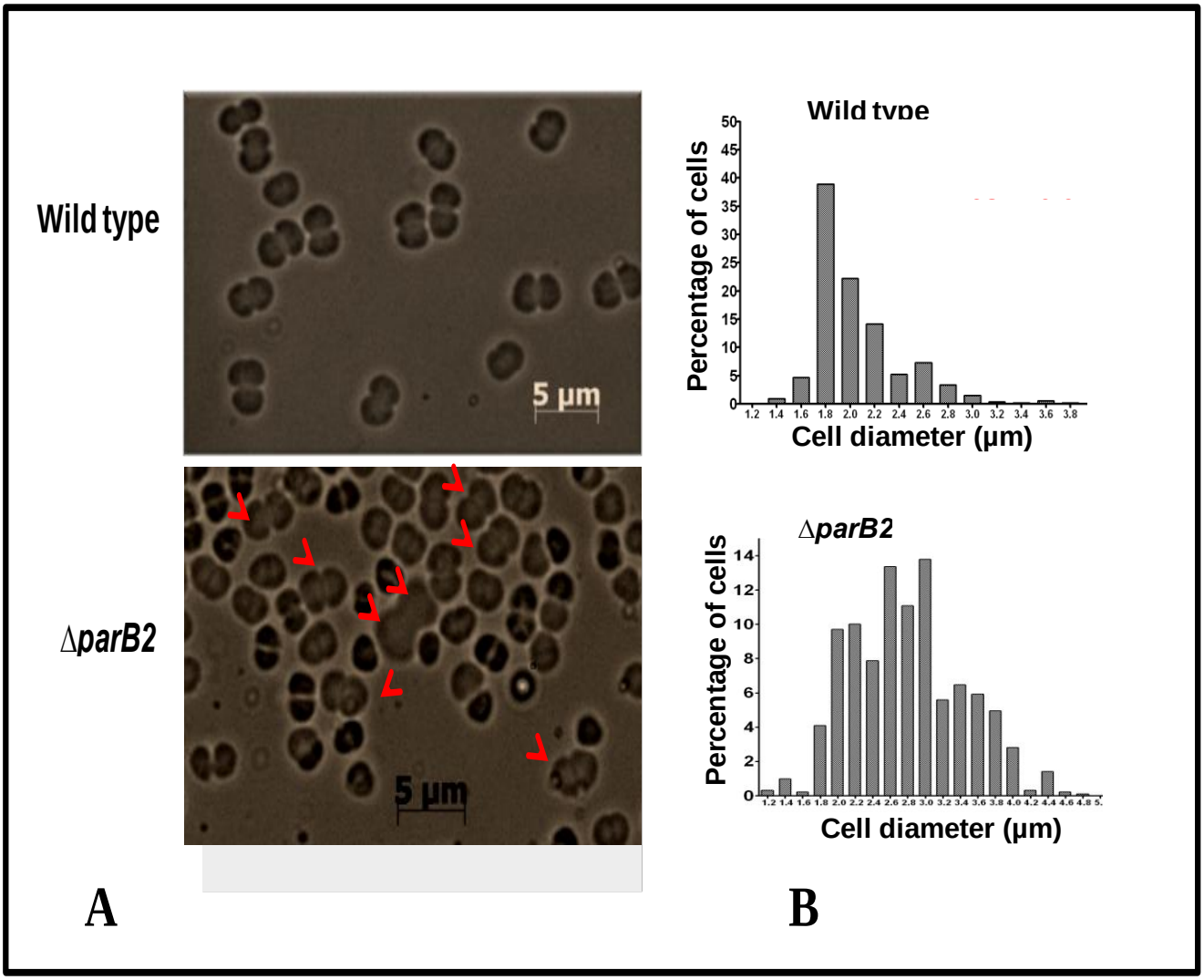

Fig3.3.4: Effect of ParB2 on cell morphology: A) Micrographs of 1ml of exponential growing cells of *D. radiodurans* wild type and Δ*parB2* cells are observed using Axio Imager M1 Florescence Microscope**. B)** Cell diameter of individual cell was measured using Image J software and plotted by using Graph pad prism 4.8 software. Mutant cells appeared as increased in cell diameter.

In order to study the cell division process and the mechanism(s) underlying *parB*2 deletion on cell division, the exponentially growing *parB2* mutant and wild type cells were stained with the Nile red and DAPI separately and cells were micro graphed (Fig3.3.5). Intriguingly, nearly 60% of *parB2* mutant cells were found with septum trapped chromosome when as compared with wild type *D. radiodurans* (Fig3.3.5). In

addition, some cells had shown increase in the nucleoid content as well. Since, *parB*2 deletion would not have affected ParA2 expression in *parA*2*B*2 operon, we argued if this effect of *parB*2 deletion was due to defect if duplicated genome separation and /or was the cause of change in the ratio of ParA2 to ParB2. We tested the later hypothesis by over expressing ParA2 on recombinant plasmid p11559A2 in the wild type *D. radiodurans* cells. *D. radiodurans* cells over expressing ParA2 showed an increased percentage of cells with septum trapped DNA as compared to wild type (Fig3.3.5). Nearly similar phenotype of higher frequency of septum trapped chromosome was observed in both *parB2* deletion mutant and ParA2 over expressing cells. These results collectively suggest that the ratio of ParA2 to ParB2 is critical for regulation of genome segregation or in cell division regulation process. Similar observation has been reported earlier in case of *C. cresentus* (Mohl *et al.,* 2001). This hypothesis was further tested by studying the effect of recombinant ParA2 expressing to different levels in *E. coli*, which does not have ParB2 and cell division is better understood. Initially ParA2 protein was expressed using pA2CFP plasmid constructed by cloning his tagged *parA2* gene under the control of *lac* promoter of pAMCYAN vector in *E. coli*. ParA2 was over expressed and it effect was checked on growth of this bacterium and compared with *E. coli* vector control. Transgenic *E. coli* expressing ParA2 showed nearly no change in O.D at 600nm as compared to vector control grown under similar conditions (Fig 3.3.6a). However, the ParA2 expressing cells

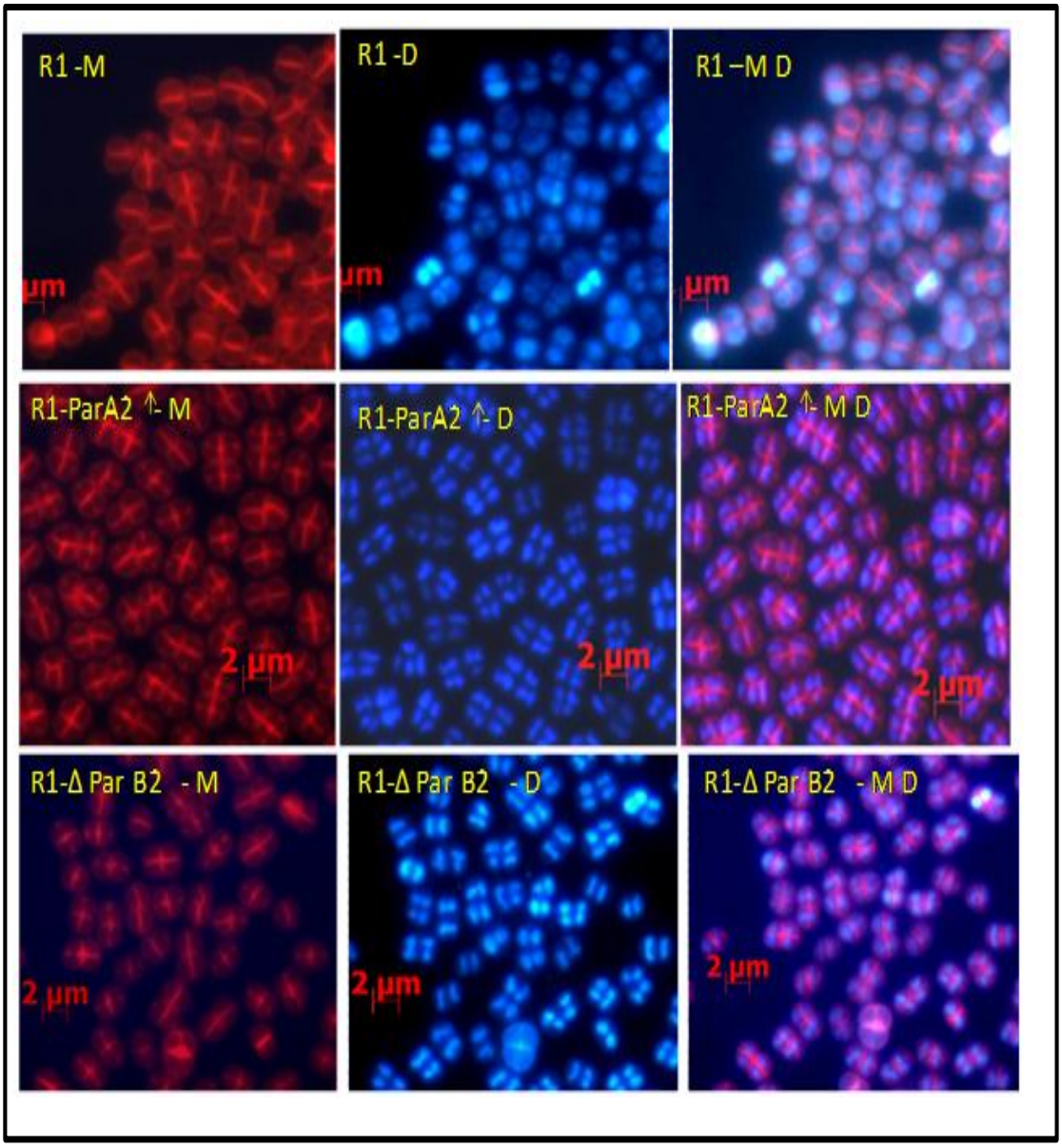

Fig3.3.5 (a): ParB2 effect on cell division process: Micrographs of wild type *D. radiodurans* cells (R1) *parB2* deleted (Δ*parB*2) and ParA2 over expressed cells (ParA2 ↑), exponential growing cell were stained with Nile red are represented as R1M (wild type), Δ*parB2* M (*parB2* deletion mutant), ParA2 ↑ M (ParA2 over expressed strain). Similarly cells stained with DAPI are represented as R1D (wild type), Δ*parB2* D (*parB2* deletion mutant), ParA2 ↑ D (ParA2 over expressed strain), both the micro graphs are overlapped on each other to generate merged represented as R1MD (wild type), Δ*parB*2 MD (*parB2* deletion mutant), ParA2 ↑ MD (ParA2 over expressed strain).

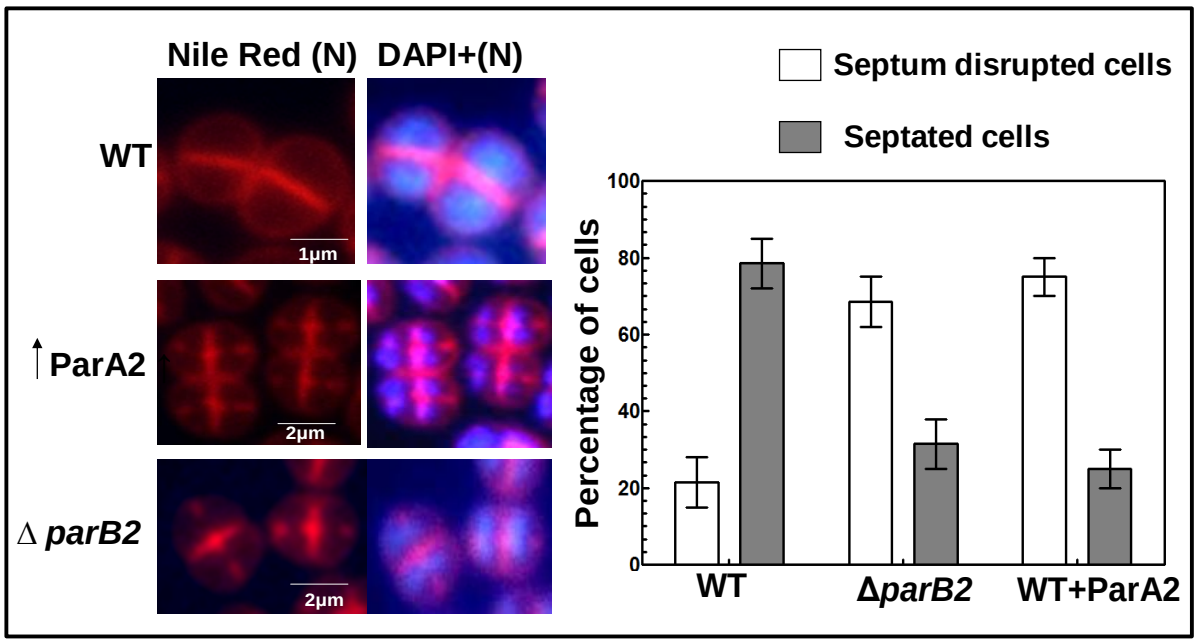

Figure 3.3.5b: Statistical analysis of cell division inhibition: Enlarged view of figure 3.3.5 a (A) showing septum disruption is represented and number of abnormal septa formed due to change in ratio of ParA2 to ParB2 was measured (B)

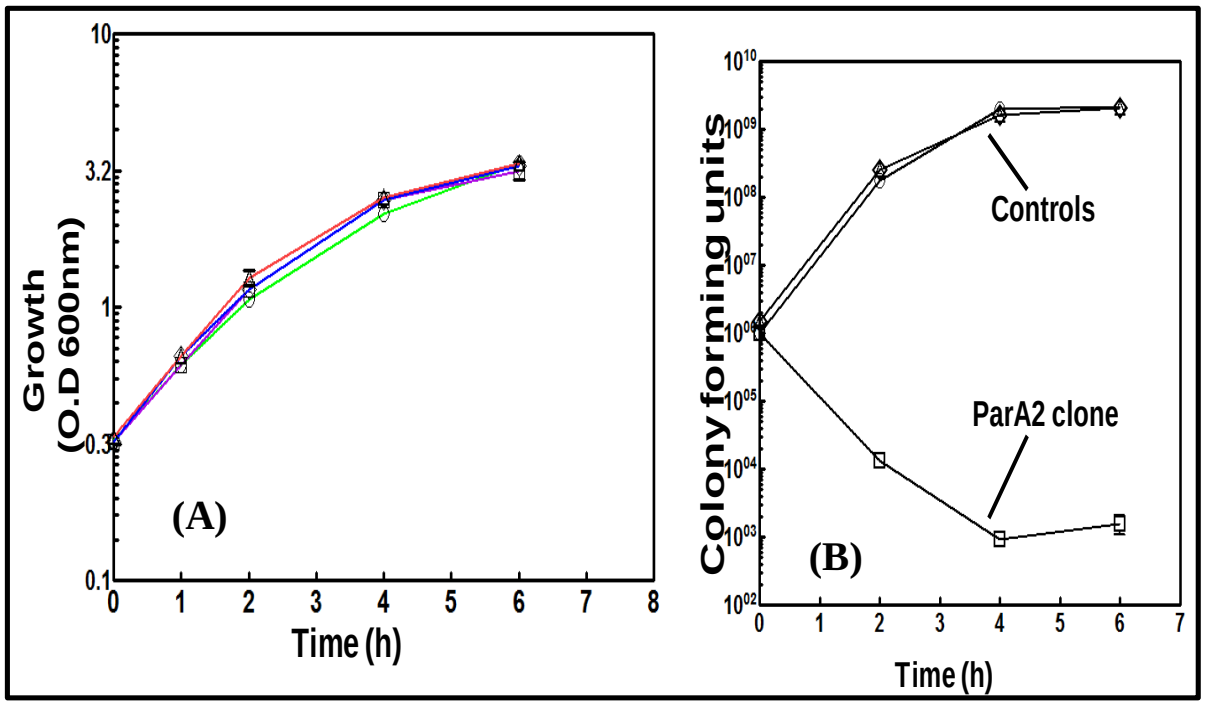

Fig 3.3.6: Effect of ParA2 expression on growth characteristics of *E. coli*: *E. coli* cells harboring expression vector pAMCYAN (green color line) represented as (- Δ-)

and plasmid expressing ParA2 (red color line) represented as (- O -) were induced with IPTG and compared with uninduced cells harboring pAMCYAN (blue color line) and ParA2 (black color line) (- ◊ - / and -□-) .The effect of ParA2 expression on **(A)** optical density and **(B)**.cell forming units was monitored.

showed a dramatic reduction in number of colony forming units (CFU) upon induction with IPTG (Fig 3.3.6b)**.** The reduction in colony forming units (CFU) was directly correlated with the amount of ParA2 made with time during post IPTG induction which was confirmed by immunoblotting of ParA2 protein using anti (His) 6 antibodies. Interestingly, ParA2 over expression showed cell elongated phenotype in *E. coli*, which showed nearly similar O.D 600 but different CFU (Fig 3.3.7).

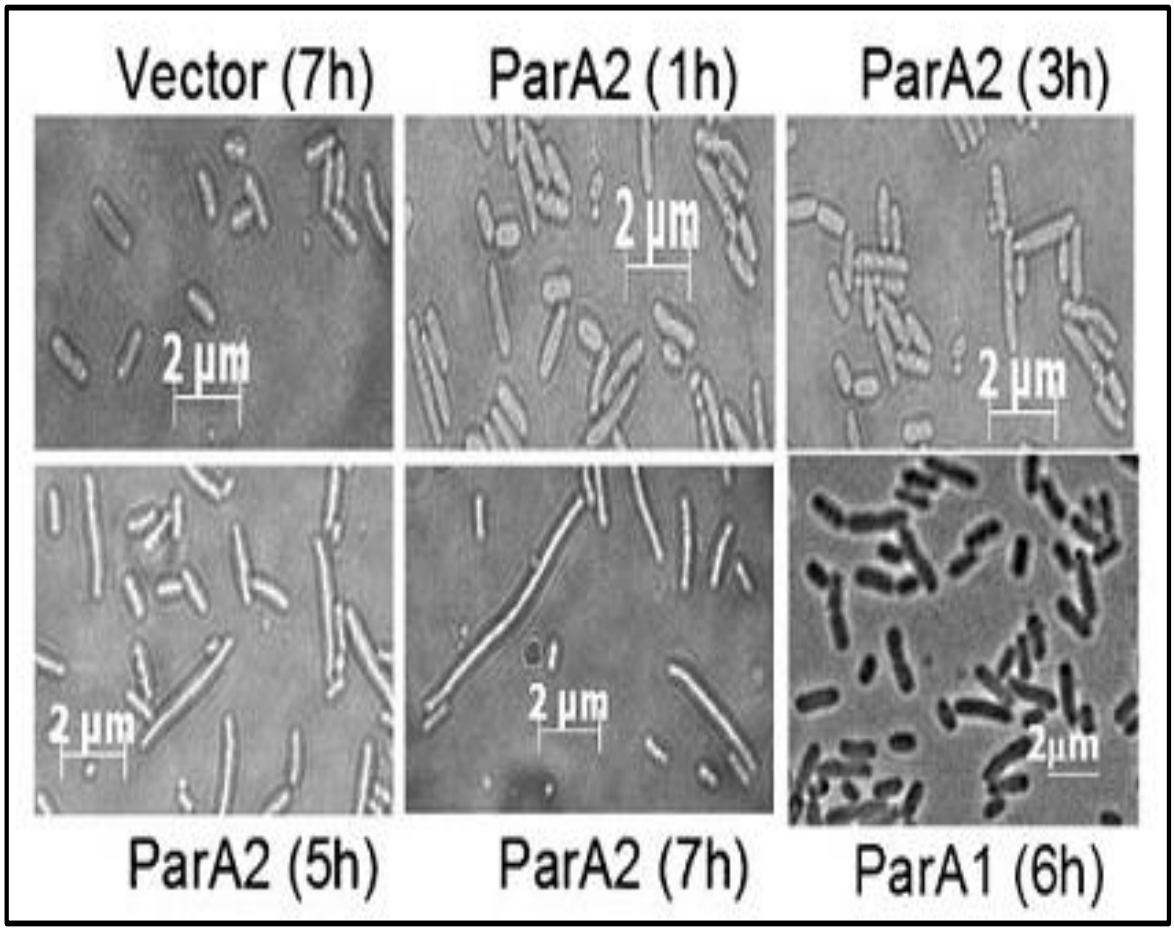

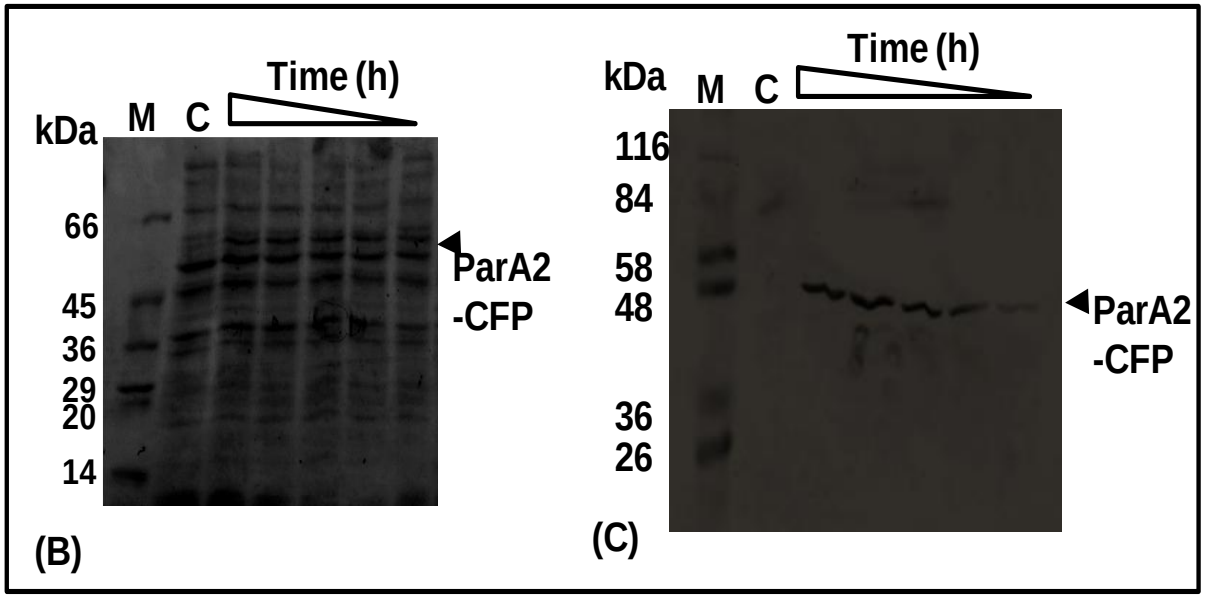

Fig 3.3.7.Effect of ParA2 expression on increase in cell size of *E. coli*: A) *E. coli* cells harboring pAMCYAN, pDSParA1 and pA2CFP plasmid were grown in absence and presence of IPTG (pAMCYAN +IPTG and pA2CFP +IPTG) for 5h and cells were imaged. B) Expression of ParA2 CFP was checked in cells incubated for increasing time with IPTG, by SDS-PAGE (B) and immunoblot analysis (C).

Cell length was measured by using Axiovision REL 4.8 software and plotted by using Graph Pad prism software. The t-test results of change in cell length of ParA2 over expressing cells is significant as compared to un induced or vector control, which further supported the ParA2 functions in dose dependent manner and that is causing *E. coli* cell size increase. Unlike vector (Fig3.3.8a) and uninduced ParA2 (Fig3.3.8b) controls, the ParA2 cells induced with IPTG (Fig3.3.8c) showed a gradual increase in number of *E. coli* cells with larger cell size. Cells induced for 4h and more showed a very large population of cells with more than 2µm length as compared to controls that had nearly all the population of less than 2µm size. These results suggested that the increase in cell length and decrease in CFU of cells expressing ParA2 was possibly due to negative effect of this protein on cell division.

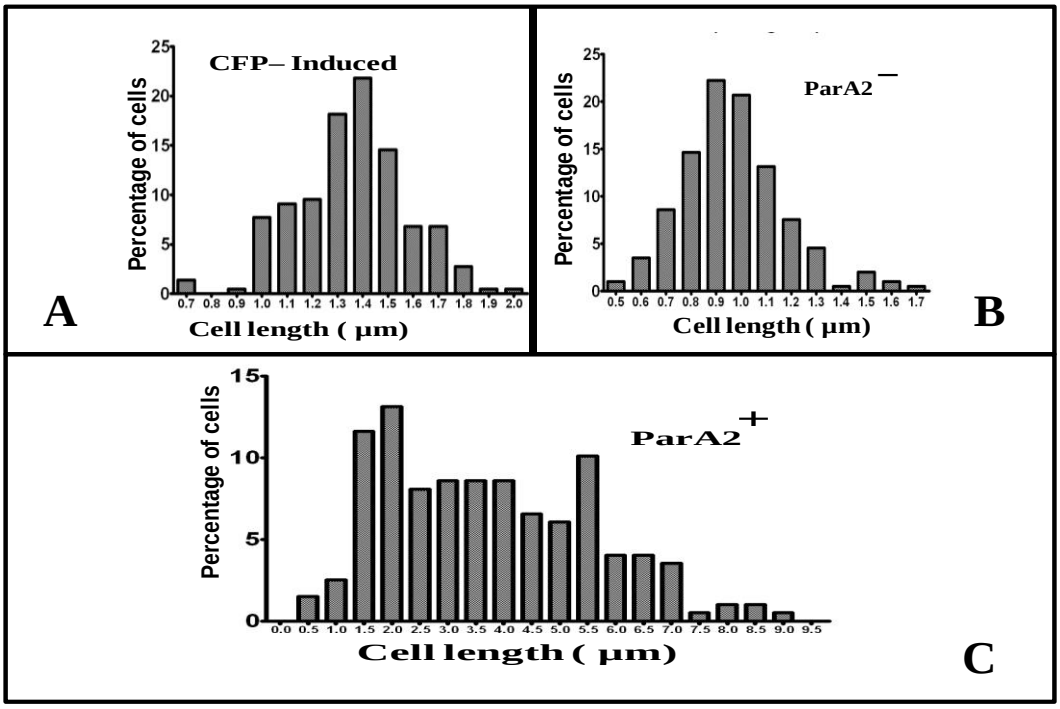

Fig3.3.8: Analysis of ParA2 expression on increase in cell size of *E. coli:* Cell length of CFP induced **(A)**, ParA2 uninduced **(B)** , ParA2 induced **(C)** *E. coli* was measured after 4hr of post IPTG induction by Axio vision rel. 4.8 software and the percentage of relative frequency of cells showing different sizes was calculated using Graph pad Prism 5 software.

3.3.2.2 Mechanism(s) of ParA2 inhibition of cell division:

Formation of FtsZ ring structure is an important step in initiation of cell division. Cell division studies in *E. coli* and *B. subtilis* indicated that normally the Z ring is formed at the mid cell position in symmetrically dividing bacteria. Selection of division site at the mid of the cell is regulated by at least two well established mechanisms 1) MinCDE system which prevents septum formation at the poles, 2) Nucleoid occlusion mechanism which determines the concentration of nucleoid at the vicinity of Z ring (Bramkamp and van, 2009;Errington *et al.*, 2003). While spatial regulation through MinCDE system is better understood in *E. coli*, the nucleoid occlusion mechanism is not well known.

Genome of *E. coli* and *B. subtilis* encodes two proteins named SlmA and Noc, which could bring about nucleoid occlusion by tightly binding to nucleoid and showed inhibition of FtsZ ring assembly over the DNA (Bernhardt and de Boer, 2005;Cho *et al.*, 2011). Therefore, effect of ParA2 over expression on FtsZ dynamics would be worth investigating.

Effect of ParA2 on FtsZ ring formation.

In order to understand the molecular mechanisms underlying ParA2 effect on *E. coli* cell division, the transgenic *E. coli* BL21 expressing ParA2 was transformed with pLAU85 plasmid expressing *E. coli* FtsZ-YFP fusion under *araBAD* promoter (Lau *et al.*, 2003) and effect of ParA2 on FtsZ ring formation was monitored. FtsZ-YFP expression was induced with arabinose and effect of ParA2 expression on FtsZ assembly was monitored in *E. coli* cells expressing FtsZ-YFP fusion with and without ParA2. The YFP fluorescence was imaged in the pLAU85 plasmids harboring pET28a+ and pETA2 with and without IPTG (Fig3.3.9). The control cells expressing FtsZ-YFP without ParA2 (pET28a+ and pLAU85) and induced with IPTG + arabinose, and arabinose alone, showed FtsZ-YFP ring formation at the mid of the cell and on average single fluorescent spot was observed per *E. coli* cells (Fig3.3.9a). The cells harboring pETA2 and pLAU85 and induced with arabinose showed majority of the cells forming intense FtsZ-YFP ring. However, there are cells also showing relatively longer cell filaments as compared to controls, and formed multiple FtsZ-YFP rings (Fig3.3.9b). This could be accounted to the leaky expression of ParA2 under T7 promoter on pETA2, even in absence of IPTG. *E. coli* BL21 expressing ParA2 and FtsZ-YFP together showed highly elongated cells forming numerous foci in juxtaposed pairs at various places on the inner surface of cell

membrane. These juxtaposed foci did not meet further and also the scattering of FtsZ-YFP foci across the filaments and at the cell poles were observed, where as complete ring formation was witnessed in control cells (Fig3.3.9c). As a consequence, the cells expressing ParA2 possibly failed to form septum constriction and were defective in cytokinesis. These results suggested that ParA2 could inhibit FtsZ ring formation in *E. coli.*

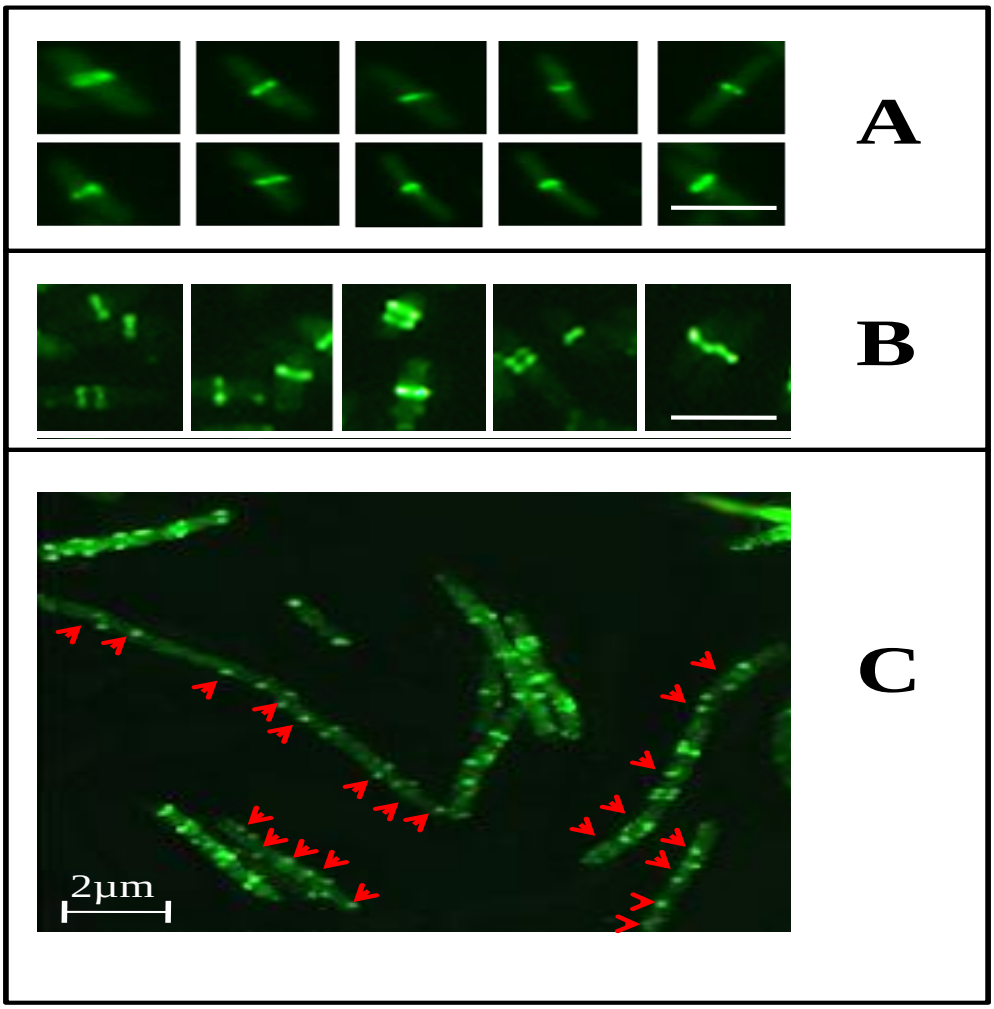

Fig3.3.9: Effect of ParA2 expression on FtsZ ring formation in *E. coli*. The cells expressing FtsZ-YFP under *araBAD* promoter on pLAU85, were further transformed with pET28a (+) (**A**) and pETA2 (**B, C**) plasmids. These cells were induced with 0.005% arabinose and further grown in absence (**B**) and presence (**A, C**) of IPTG. Cells were imaged using Axioimager microscope

Over expression or deletion of Min proteins cause mislocalization of FtsZ of *E. coli* resulted in asymmetric cell division (Lee and Price, 1993; Levin *et al*., 2000; Leutkenhaus, 1997). Although, the ParA2 also shares similarity with MinD family proteins, the co-expression studies of FtsZ-YFP indicated there are few foci formed on inner membrane at the poles in *E. coli* cell expressing ParA2 might rule out the mechanistic similarities of ParA2 with MinD type proteins. It further indicated that ParA2 over expression did not affect the localization of FtsZ, but expression of ParA2 perturbed complete FtsZ ring formation. Co-expression of ParA2 with $FtsZ_{Ec}$ revealed FtsZ complete ring formation is inhibited in presence of ParA2 protein. Inhibition of complete FtsZ ring formation can occur by either direct interaction of FtsZ with the ParA2 protein and inhibit lateral interaction between FtsZ polymers as similar to the MinD protein of *E. coli* or ParA2 might be binding to DNA and inhibiting FtsZ ring formation like SlmA, Noc protein which are involved in nucleoid occlusion.

3.3.2.3 ParA2 effect on characteristics features of recombinant $FtsZ_{Ec}$:

The DRA0001 gene (790 bp) was PCR amplified from genomic DNA of *D. radiodurans* cloned at *Nde*I & *Xho*I sites in pET28a+ vector (Fig3.3.10a). Cloning was confirmed by restriction digestion where recombinant plasmid released a 790 bp fragment and vector alone was not (Fig3.3.10b). The protein was expressed in BL 21 *pLys*S *E. coli strain* and a 30 kDa protein band was induced in SDS-PAGE gel, which corresponds to the estimated molecular weight of His tagged ParA2 protein and which was absent in the controlled cells that were transformed only with pET28a+ plasmid. Recombinant ParA2 was purified to near homogeneity under denaturing conditions, refolded by serial dilution of urea (Fig3.3.10c) and its identity was confirmed by peptide mass fingerprinting.

Simililary Recombinant FtsZ $_{Dr}$ purified to near homogeneity under native conditions (Kruti Mehta and H.S.Misra, unpublished work)

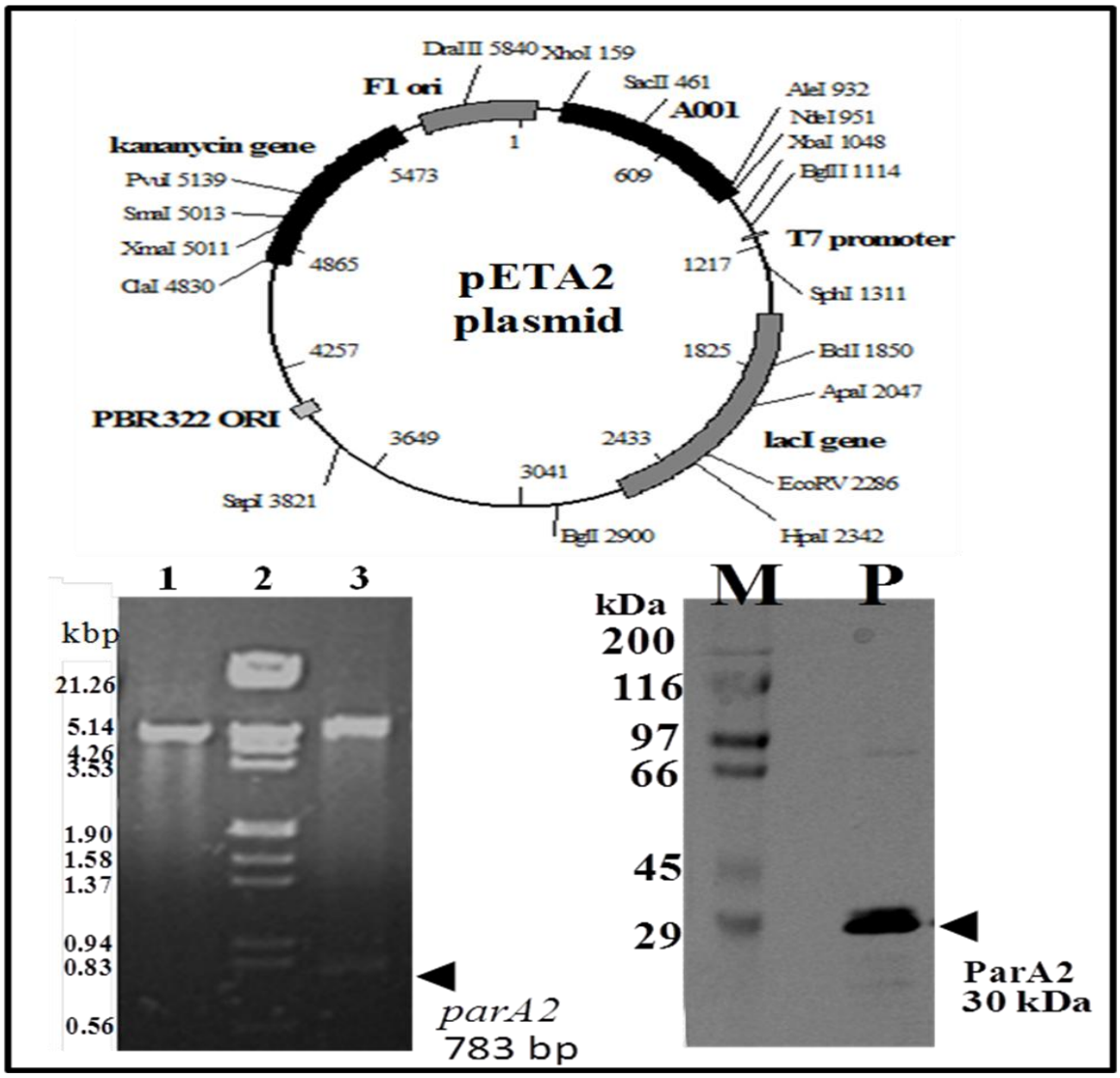

Fig 3.3.10. Expression and purification of ParA2 protein: A) Partial restriction map of the pETA2 plasmid. **B)** Restriction analysis of pETA2 plasmid. Lane1: undigested plasmid. Lane2: lambda DNA *Hind*III & *Eco*RI marker. Lane3: Double digested pETA2 plasmid (*Nde*I /*Xho*I). **C)** Purified ParA2 protein along with SDS 6H2 marker.

The possibility of ParA2 directly inhibiting the FtsZ functions was investigated by looking functional characteristic of FtsZ protein. Since, FtsZ is a GTPase (de *et al.*, 1992)

and undergoes polymerization in presence of GTP, both GTPase activity and sedimentation (polymerization) characteristic of FtsZ were monitored under standard *in vitro* condition as mentioned in methods. Sedimentation pattern of recombinant FtsZ was unaffected in presence of ParA2 incubated with and without ATP and DNA (Fig3.3.12b)**.** Interestingly, it was found that ParA2 in presence of GTP showed higher GTPase activity as compare to FtsZ control (Fig3.3.11). ParA2 hydrolysis of GTP did not change significantly in presence of DNA, ATP and FtsZ (Fig3.3.11compare A2+G with Z+A2+P+G/D). Subtraction of GTP hydrolysis of ParA2 from FtsZ incubated with ParA2 indicated no change in net GTPase activity of FtsZ (Fig3.3.11). These results suggest that ParA2 possibly inhibits FtsZ ring formation by a mechanism that is independent of its direct inhibition of FtsZ functions.

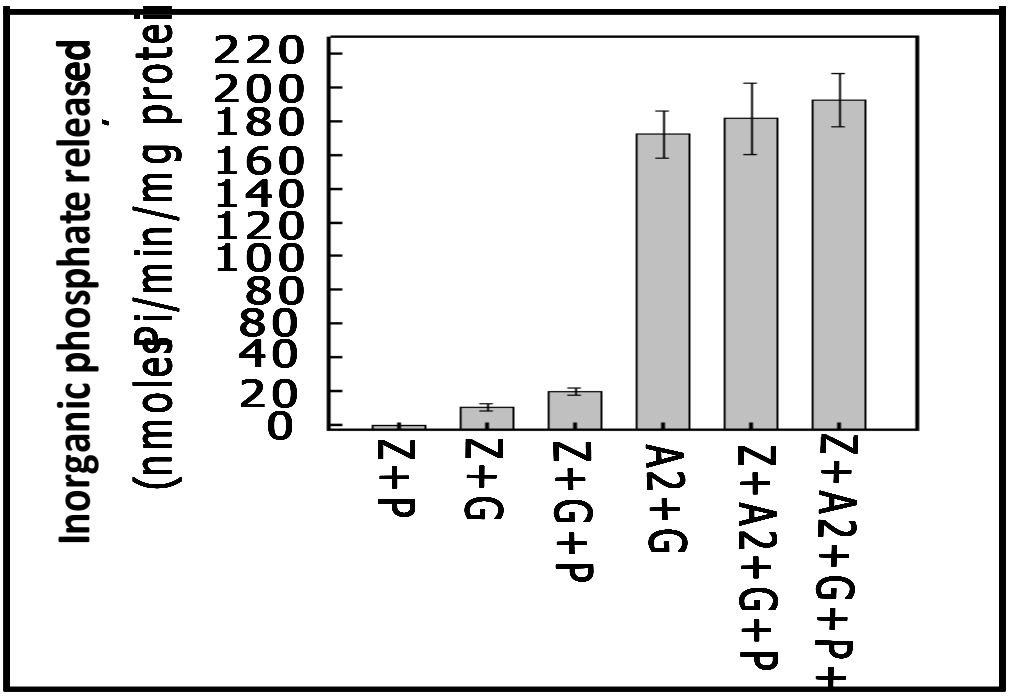

Fig 3.3.11. Interaction of ParA2 with FtsZ by using GTPase assay: The GTPase activity of FtsZ was checked in presence of ParA2, ParA2 with and without GTP, ATP, DNA, reaction was carried out in different combinations and incubated at 37^{o}C for 1h, release of inorganic phosphate is measured by using malachite green method. Abbreviations used in this figure are as Fts Z (Z), ParA2 (A2), ATP (P), GTP (G), and DNA (D).

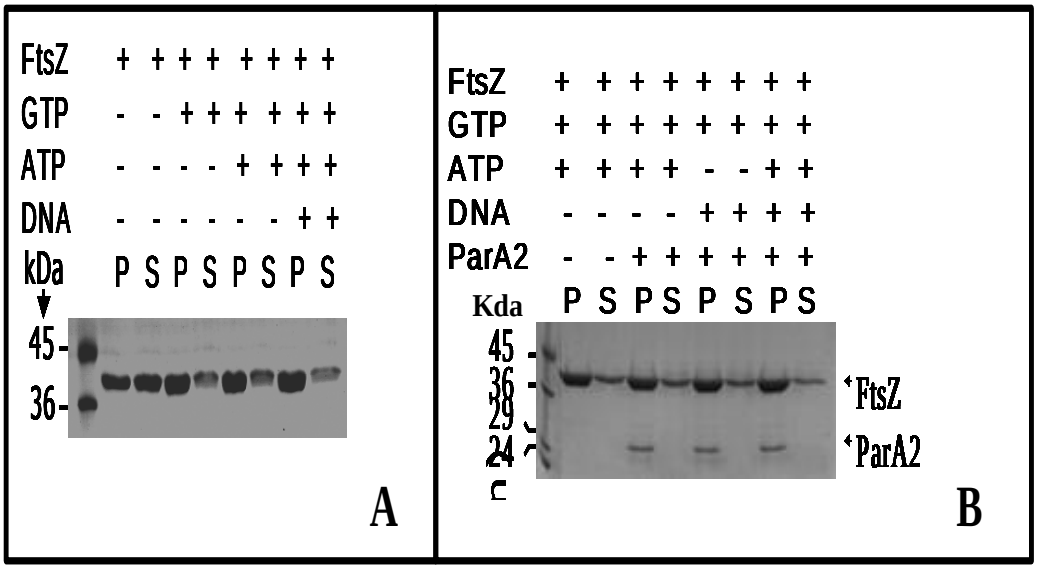

Fig3.3.12 Interaction of ParA2 with FtsZ by using sedimentation analysis: A) Recombinant FtsZ protein was incubated with GTP, ATP, DNA reaction was carried out 37^{o}C for 30 min, these mixtures were centrifuged at 22,000 x g for 30 min and both supernatant (S) and pellets (P) fractions were analyzed on SDS-PAGE. Gel was stained with Coomassie blue and the intensity of protein band corresponding to ParA2 was estimated by densitometric scanning from the respective gel. Amount of FtsZ in pellet and supernatant was measured by densitometric analysis. **B)** Similarly Recombinant ParA2 was incubated with FtsZ and in presence and absence of DNA, ATP and both. Mixtures were incubated at 37^{o}C for 30 min, reaction mixtures were analyzed as mentioned above.

3.3.2.4 Cell division inhibition through Nucleoid occlusion mechanism in ParA2 expressing cells

Purified protein was checked for DNA binding activity, ATPase activity and oligomerization characteristics. ParA2 showed DNA binding activity, which increased

further in presence ATP (Fig3.3.13a), indicating that ParA2 was a DNA binding protein and ATP did not compete with DNA for its binding, rather supported to DNA binding ability of ParA2. Recombinant ParA2 showed a concentration dependent increase in specific ATPase activity, which was further stimulated in presence of dsDNA (Fig3.3.13b). Increase in dsDNA binding activity of ParA2 in presence of ATP and dsDNA stimulation to its ATPase activity indicated the energy dependent cooperative binding of this protein, a characteristic feature observed when the DNA binding motor proteins undergo polymerization (Davis *et al.*, 1992 ; Gerdes *et al.*, 2010 ; Leonard *et al.*, 2005).

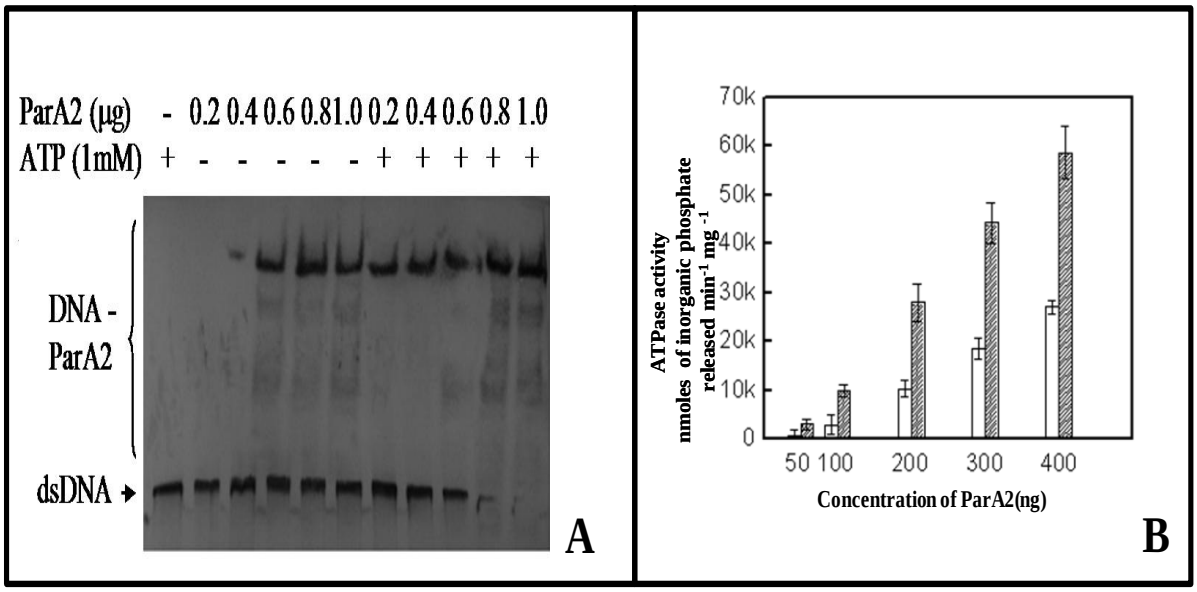

Fig3.3.13. *In vitro* activity characterization of recombinant ParA2 protein: A) The 284bp long dsDNA was purified and labeled at 3 'end by using DIG labeling kit. The ~10 picomoles of Dig labeled DNA was incubated with purified ParA2 in binding buffer (50mM HEPES, 100mM NaCl pH 8.0, 5mM MgCl2, 30mM Na-acetate) for 20 min at 37^{o}C and then separated by 5 % native PAGE. DNA is transferred to nylon membrane and DIG labeled DNA detected by using anti-DIG antibody conjugated with alkaline phosphatase. **B**).ATPase activity of ParA2 was determined with increasing concentration of protein in absence (open bar) and presence (filled bar) of dsDNA.

ParA2–CFP accumulates on nucleoid in *E. coli.*

Since, ParA2 showed DNA binding activity *in vitro*, the possibility of this protein binding to *E. coli* nucleoid was checked by generating C-terminal translation fusion protein. Translation fusion was generated by cloning *parA2* gene in pAMCYAN plasmid to generate pA2CFP plasmid and culture was induced by IPTG.

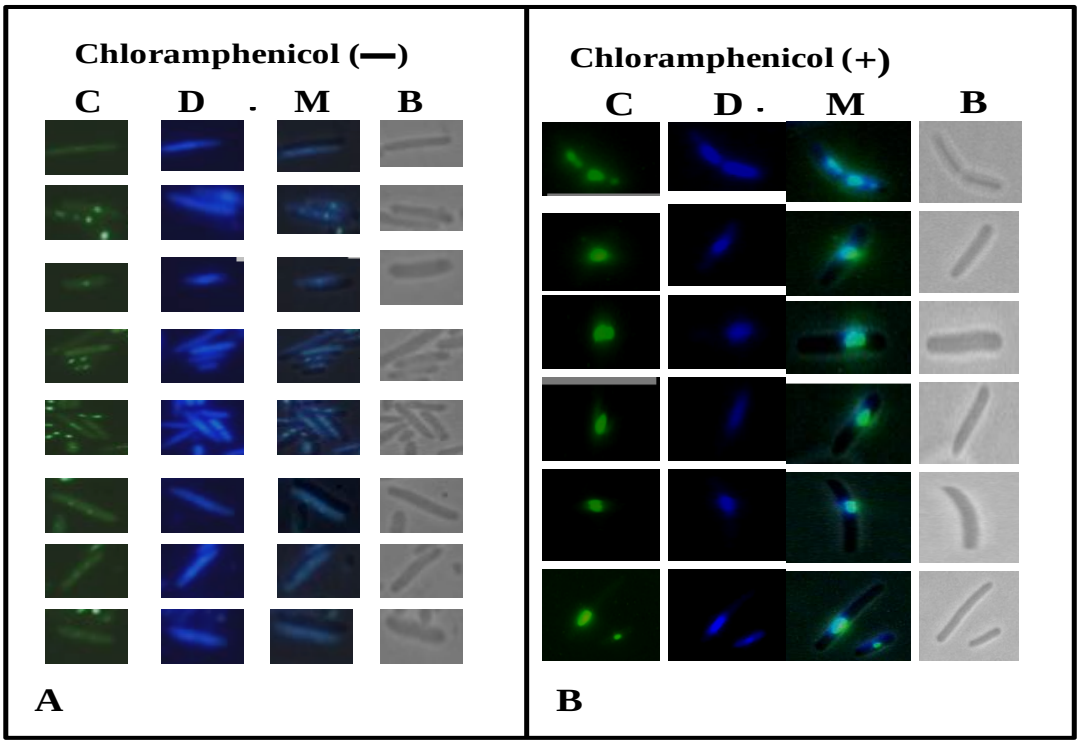

Fig 3.3.14. Localization of ParA2 in *E. coli* cells : (A) *E. coli* JM109 harboring pA2CFP were induced with 100 µM IPTG for 4h. Cells were collected and treated with 2µl DAPI (2µg/ml) and imaged under bright field (B) and under DAPI fluorescence (D) and CFP fluorescence (C). **(B)** These cells were also treated with chloramphenicol (100µg/ml) for 1h and imaged as mentioned above These images were superimposed (M) for locating the ParA2-CFP foci position in *E. coli* cells.

Expression of ParA2 changed the cell morphology i.e. the length of *E. coli* cells expressing ParA2-CFP increased several folds (Fig3.3.7& Fig3.3.8) as compared to pAMCYAN vector control grown under identical conditions, as well as uninduced

transgenic *E. coli* (Fig3.3.7& Fig3.3.8). This further confirmed that both ParA2-CFP and ParA2 alone are making similar phenotypic change in *E. coli*. Exponential growing cells were stained with DAPI micrographs showed in most of the cells nucleoid spreading across the cell filaments as normally observed in typical *E. coli* cells (Fig3.3.14a) except few cells have shown DNA condensation. Overlapping micrographs of bright field, DAPI stained and CFP fluorescent cells confirmed the localization of ParA2-CFP all along the nucleoid of *E. coli* cells (Fig3.3.14). To further confirm ParA2 binds to dsDNA exponential growing ParA2-CFP expressing cells was treated with Chloramphenicol (translation inhibitor) of 100 μgml^{-1}, chloramphenicol treated cells showed condensation of the DNA along with it ParA2-CFP florescent signal also condensed (Fig3.3.14b), suggesting ParA2 could bind to *E. coli* nucleoid, which could be a possible mechanism of cell division inhibition and a cause of cell size increase.

ParA2 complements for SlmA phenotype in *E. coli.*

Deletion of ParB2 in *D. radiodurans* or over expression of ParA2 in *E. coli* as well as in *D. radiodurans* inhibited cell division process mostly by preventing FtsZ ring formation. *In- vitro*, *in-vivo* experiments suggested ParA2 randomly binds to DNA. Here we hypothesized binding of ParA2 with nucleoid could possibly inhibit the cell division a known functions of the Nucleoid occlusion proteins , SlmA in *E. coli* (Bernhardt and de Boer, 2005;Cho *et al.*, 2011) and the 'Noc' protein in *Bacillus subtilis* (Wu *et al.*, 2009). These proteins are known to inhibit cell division by bringing nucleoid occlusion at the vicinity of FtsZ ring formation. Thus, the possibilities of ParA2 inhibiting cell division by either nucleoid occlusion or on other hand it may be through the affecting DNA replication and genome segregation. The functional complementation of ParA2 in *slmA*

single and *slmA minCDE* double mutant phenotypes of *E. coli* was examined. *E. coli* strain TB85 (Δ*slmA*) and *E. coli* strain TB86 (Δ*minCDE* Δ*slmA*) were transformed with pA2CFP plasmid and expression of ParA2-CFP was confirmed by immunoblotting. The *slmA* mutant expressing ParA2 grew similar to *slmA* single mutant control. The *slmAminCDE* double mutant expressing ParA2 helped these cells to recover the growth defect of double mutant in rich medium (Fig3.3.15a). Since, ParA2 expression did not posed lethality in *slmA* single mutant, which could be anticipated if this protein had affected DNA replication or genome segregation in *E. coli*, suggesting that ParA2 does not seem to be affecting these DNA metabolic processes at least in this background.

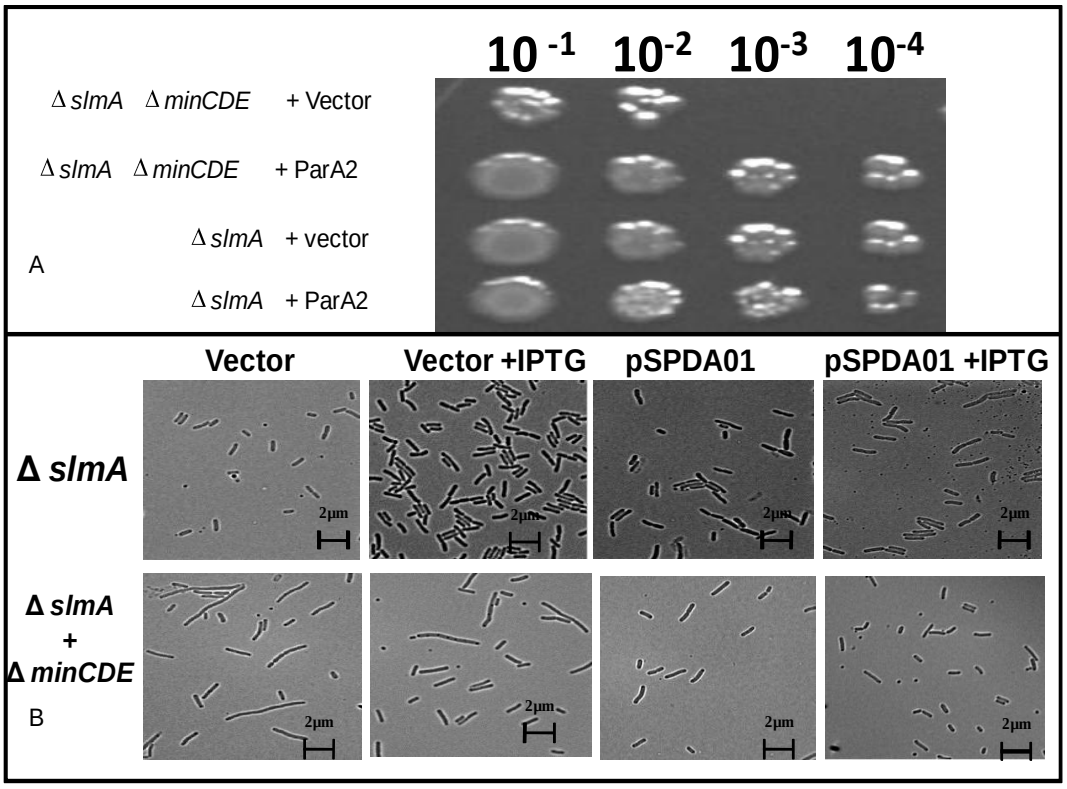

Fig 3.3.15: Functional complementation studies: The *slmA*, *slmA*Δ*min*CDE double mutants of *E. coli* were transformed with pAMCYAN (vector) and pA2CFP (ParA2). **A)** Induced cells were spotted in different dilutions and growth of different culture was recorded after overnight **B)** Similarly micrographs of ParA2 trans-complemented culture was checked by inducing cultures with 100 μm IPTG.

On the other hand, the over expression of ParA2 in *slm*A*min*CDE double mutant showed functional complementation and these cells showed asymmetric cell division producing a very high frequency of polar cell bodies (Fig3.3.15b). Asymmetric cell division has been observed in *E. coli* cells lacking MinCDE system. This indicated that ParA2 expression could make *slm*A*min*CDE double mutant to behave like *min*CDE single mutant. These results therefore, suggested that ParA2 effect on cell division was possibly not by affecting DNA replication or other related DNA metabolism but most likely by functioning similar to SlmA protein in *E. coli*, which is known for bringing nucleoid occlusion to the vicinity of septum formation.

Bacteria's having multiple chromosomes like *V. cholerae, B. coencephacia* etc. encodes partitioning system on both primary and secondary chromosomes. Indespensibility of cognate '*par*' system for their segregation (Egan and Waldor, 2003;Hui *et al.*, 2010;Passot *et al.*, 2012) and also in controlling and coordinating segregation process (Mohl *et al.*, 2001) have been demonstrated. Here the deletion of *parB2* showed pleiotropic effects such as growth defect, anucleation and cell morphology as studied in this thesis. The effect of ParB deletion in regulation of cell division has been shown in *C. crescentus* (Mohl et al., 2001). In case of *C. crescentus*, it is shown that the deletion of *parB* resulted in change in the ratio of ParA to ParB in the cell, which could result in the blockage of cell division. ParB2 mutant of *D. radiodurans* and over expression of ParA2 showed septum breakage and nucleoid occlusion was observed at the vicinity of FtsZ ring growth.

Studies on FtsZ regulation in *B. subtilis and E. coli* showed spatiotemporal regulation of FtsZ could be either by direct interaction with FtsZ and modulating its activities almost

similar to MinD inhibit lateral interaction of FtsZ and formation of FtsZ ring at the poles. SlmA in *E. coli* (Bernhardt and de Boer, 2005) and Noc in *B. subtilis* (Wu *et al.*, 2009) strongly interact with the nucleoid and prevents FtsZ ring formation on nucleoid. *In vitro* studies of ParA2 along with FtsZ revealed nearly no change in the functional characteristics of FtsZ. However ParA2 is found to be a strong DNA binding ATPase and co localizes along the nucleoid. This overall mechanism is analogues to the nucleoid occlusion mechanism reported in other bacteria.

To further confirm ParA2 inhibiting cell division process through nucleoid occlusion mechanism, we checked the functional complementation of ParA2 protein in *slmA* mutant as well as in *slm*A*min*CD mutant. We found that the expression of ParA2 in *slm*A mutant of *E. coli* showed functional complementation to SlmA loss and rescued the cells from lethality (Bernhardt and de Boer, 2005). The results presented in this thesis together suggested that ParA2 in absence of ParB2 or in higher ratio regulates cell division by inhibiting FtsZ ring progression in *E. coli* by nucleoid occlusion mechanism and to septum breakage in *D. radiodurans.*

CHAPTER 4

Discussion

Segregation of duplicated genome is a pre-requisite for cell division. Regulation of these two mutually inclusive processes has been better understood in eukaryotes possibly because of the large cell size with a better characterized cytoskeleton and an ease to image the real time protein-protein and DNA protein interactions in the cells. However, in prokaryotes these two processes have been studied with limited details. Like in eukaryotes, the faithful transmission of genetic information from one cell to other cells by accurate genome partitioning is also coordinated with cell division in bacteria (Gerdes *et al.*, 2010). Here, the genome partitioning mainly occurs by either pushing or pulling of duplicated genome toward the cell poles. This involves three core components (i) an origin-proximal centromere or similar *cis*-element (ii) a centromere binding and (iii) P-loop Walker ATPases, which through polymerization/ depolymerization dynamics provide force leading to the movement of centromere (Gerdes *et al.*, 2010;Hayes and Barilla, 2006). Understanding on the mechanisms of genome segregation has come mainly from bacteria segregating low copy plasmids and or single circular chromosome. Recently, the genome sequence of several bacteria from the diverse phylogenetic groups, have been published. *Deinococcus radiodurans* (White *et al.*, 1999) along with some other notable ones like *Agrobacterium tumefaciens, Sinorhizobium meliloti* (Kahng and Shapiro, 2003), and human pathogen *Vibrio cholerae* (Heidelberg *et al.*, 2000) harbors multipartite genome and both primary as well as secondary chromosomes in many of these bacteria contain multiple centromeres (Livny *et al.*, 2007). However, the molecular basis of multipartite genome segregation and the nature of chromosome partitioning systems in these organisms are not studied, except *Vibrio cholerae and Burkholderia cenocepacia* (Dubarry *et al.*, 2006; Fogel and Waldor, 2005 & 2006; Yamaichi *et al.*, 2007). *D. radiodurans* is a polyextremophile with an extraordinary resistance to gamma radiation (Slade and Radman, 2011). Genome sequence of this bacterium revealed several interesting facets (White *et al.*, 1999). Amongst these, the presence of multipartite genome system, ploidy and multicopy genes were speculated to hold key for its extreme phenotypes. This bacterium contains four genetic elements designated as chromosome I (2.65 Mb), chromosome II (412 kb), megaplasmid (177 kb) and small plasmid (46kb). The maintenance of multipartite genome and ploidy in dividing cells of bacteria has been the interesting questions and equally intriguing.

In order to understand the mechanisms of genome segregation in this bacterium, its genome sequences was searched for the presence of typical partitioning proteins and centromere like elements. Results showed that chromosome I and chromosome II have some of the conserved boxes of P1 *parS* element. But these were lacking the complete structure of P1 *parS* and did not have the binding site for integration host factor (IHF) between the 'B' boxes responsible for ParB binding. Because of these limitations, the possibility of chromosome I and chromosome II have plasmid type centromeres were conceptually ruled out. However, chromosome I contained three chromosomal type (*B. subtilis* type) centromeric sequences named as *segS*1, *segS*2 and *segS*3 while chromosome II does not have typical *B. subtilis* type chromosomal centromeres. Genome sequence of this bacterium was found containing multiple sets of genes for both ParA and ParB partitioning proteins. These are organized in form of *parAB* operon on chromosome I, chromosome II and megaplasmid. Small plasmid did not have these proteins encoded upon. Functional motif analysis in these proteins showed that ParA of chromosome I (ParA1) is very close to its homologues reported from chromosomes of different bacteria. While ParA encoded on chromosome II (ParA2) and mega plasmid's (ParA3 and ParA4) are clustered much away from chromosomal type ParA's in phylogenetic tree and these clustered with aberrant ParA proteins closer to cell division regulatory proteins in bacteria. ParB's encoded from all four '*par*' operons (ParB1 on chromosome I, ParB2 on chromosome II and ParB3 and ParB4 on mega plasmid) were nearly similar except some crucial differences in helix turn helix motifs of these proteins. ParB proteins of accessory chromosome showed change in the helix7 known to function in recognition of the centromere like sequence (Leonard *et al.*, 2004), where as ParA1 and ParA4 of *D.*

radiodurans had extra N-terminal region (Leonard *et al.*, 2005). The *ParB2* deletion mutant showed a higher frequency of anucleation as compared to wild type cells. Although, the functional significance of these structural changes in ParB variants of *D. radiodurans* is not understood, the possibility of these ParB's recognizing different types of centromeric sequences or having pleiotropic effects cannot be ruled out. These results indicated that chromosome I most probably contains both *cis* elements and trans acting factors of genome partitioning similar to chromosomal type. Absence of typical centromeric sequences either *parS* type or *B. subtilis* type, in chromosome II and megaplasmid and clustering of their ParA proteins with a different class of regulatory proteins might argue that partitioning of chromosome II and megaplasmid might follow different mechanisms. The possibility of either aberrant P1 *parS* type element without IHF binding region and or a completely unknown centromere functioning in these secondary genomes partitioning using the different sets of correspondingly encoded 'Par' proteins cannot be ruled out and would be worth investigating.

The functional significance of both centromeric sequences and putative partitioning proteins were evaluated experimentally. It is observed that an unstable mini-F plasmid pDAG203 (Dubarry *et al.*, 2006;Lemonnier *et al.*, 2000), bearing putative centromere's of chromosome I could stabilize in dividing population of *E. coli* at much higher frequency than pDAG203 plasmid vector. Interestingly, *segS*1 and *segS*2 elements could help nearly 100% segregation of pDAG203 irrespective of cognate ParA and ParB proteins expression *in trans*. In case of *segS*3, though cells containing pDAG203 bearing *segS*3 could segregate this plasmid at much higher frequency than vector alone but this frequency increased further when the cognate ParAB operon was expressed in these cells.

This suggested that *segS* elements have property of centromere and *segS*1 and *segS*2 could be recognized by perhaps uncharacterized trans acting factors in *E. coli*, which would be worth studying independently. Molecular interaction studies between the ParA1/ParB1 and *segS* elements suggested that ParA1 could form polymers in presence of dsDNA as evidenced from sedimentation analysis and light scattering studies. Higher ATPase activity of ParA1 in presence of *segS*3-ParB1 as compared to other centromeric complexes, and the faster gel mobility of a hypothetical {*segS*3-ParB1P} nucleoprotein complex, but not {*segS*1- ParB1P} / {*segS*2-ParB1P} complex specially in presence of ATP, suggested that ParA1 is a DNA binding protein and the ParA1 polymerization / depolymerization may be regulated by the levels of its intrinsic ATPase activity. Both DNA binding of ParA1 and its polymerization / depolymerization as a function of its ATPase activity, are the typical characteristics of ATPases associated with genome segregation. Further studies will be required to understand the real-time functioning of *segS* and ParA1B1, and the oscillation of ParA1 proteins on genome of *D. radiodurans*. Results obtained on the ParA1B1 dependent role of *segS*3 elements in mini-F plasmid stability and nearly 8-13 % loss of nucleoid in Δ*parB1* mutant of *D. radiodurans* in comparison of 1% in normal cells strongly supported the roles of both *segS* and 'Par' proteins of this bacterium in its genome segregation.

Results presented here report for the first time, that (i) the ParA1 was a DNA binding ATPase, (ii) the ParB1 was sequence specific centromere binding protein, (iii) the ATPase activity of ParA1 was stimulated in presence of both ParB1 and dsDNA that seems to be regulating the dynamics of ParA1 polymerization, (iv) *segS* elements function like bacterial centromere's for unstable plasmid segregation and ParB1 has a

role in genome maintenance in *D. radiodurans*. These findings collectively suggested that both *segS* elements and 'Par' proteins encoded on chromosome I of *D. radiodurans* are functionally active and play a role in genome segregation and maintenance of chromosome in this bacterium. Time lapse fluorescence microscopy showing the formation of GFP-ParA1 gradient in *E. coli* cells having unstable plasmid cloned with *segS* elements further suggesting a characteristic feature associated with pulling mechanisms of genome segregation in bacteria.

Chromosome II is not found to contain the typical bacterial centromeres of either P1 plasmid type (*parS*) and / or chromosomal type. Multiple sequence alignment and homology search analysis have grouped ParA2, a ParA type protein encoded on chromosome II of *D. radiodurans* R1, with small ParA's between the chromosome partitioning protein ParA, and cell division regulatory proteins like MinD and MipZ. These proteins were functionally characterized both *in vitro* and *in vivo*. ParA2 was found to be a DNA binding ATPase *in vitro*. ParA2 expressing in *E. coli* inhibited cell division and produced ParA2-CFP foci on nucleoid. These cells showed localization of FtsZ-YFP on membrane but the formation of complete FtsZ ring was not observed. The formation of FtsZ ring a component of divisome is temporally and spatially regulated by the coordination of a large number of cell division proteins forming a functional divisome complex (Adams and Errington, 2009). Further the DNA replication, genome segregation and position of the nucleoid in the cells play regulatory roles in cell division (Lutkenhaus, 2007). In certain bacteria, the spatial regulation of FtsZ is brought about by the mechanism of nucleoid occlusion, which involves proteins like 'Noc' in *Bacillus* (Wu and Errington, 2004) and 'SlmA' in *E. coli* (Tonthat et al., 2011).

These proteins bind to nucleoid and bring occlusion at the vicinity of septum formation. 'SulA' a SOS response protein in *E. coli* (Bridges, 1995;Lowe *et al.*, 2004) functions directly by interacting with FtsZ and by inhibiting its GTPase activity. Further, the cell wall and cell membrane of *D. radiodurans, Bacillus subtilis* and *E. coli* are entirely different in composition and architecture but the divisome components in these bacteria are largely conserved. Except that, the *B. subtilis* and *E. coli* have Div IVA, MinE, respectively, while *D. radiodurans* contains both of these cell division regulatory proteins. *E. coli* cells defective in MinCDE proteins undergo asymmetric cell division at the poles leading to formation of mini cells. The FtsZ from these bacteria have considerable sequence homology with FtsZ from *D. radiodurans* and mechanistically they perform identical functions. Molecular mechanisms underlying ParA2 inhibition of cell division was further investigated around these known facts. It was observed that mixing of ParA2 with FtsZ of *D. radiodurans* and *E. coli* separately, neither affected GTPase activity or polymerization characteristics of FtsZ. Suggesting no direct effect of ParA2 on FtsZ activity and polymerization at least, *in vitro*. Also, the data obtained on ParA2 inhibition of FtsZ ring formation *in vivo* and almost no effect of ParA2 on FtsZ localization to the membrane in both *E. coli* and *D. radiodurans*, further ruled out any possibility of ParA2 inhibiting the binding of FtsZ at the site of Z ring initiation. Although, the possibility of ParA2 inhibiting lateral interaction of FtsZ protofilaments has not been ruled out *in vivo*, it is very clear that the over expression of ParA2 brings nucleoid in the path of FtsZ ring growth, further suggesting the possible role of ParA2 in nucleoid occlusion. ParA2 expressing in *slmAminCDE* mutant of *E. coli* complemented *slmA* mutant phenotype and these cells now produced polar cell division a characteristic

phenotype of *minCDE* mutation in *E. coli*. The *D. radiodurans* expressing ParA2 showed the initiation of septum formation but its further growth was inhibited at nucleoid. Functional complementation of ParA2 for SlmA defect in *E. coli* and the arrest of septal growth at the vicinity of nucleoid in ParA2 over expressing *D. radiodurans* suggested that ParA2 play a role in regulation of cell division most likely by nucleoid occlusion mechanism.

Thus, in this study we have first time identified the centromeric sequences from *D. radiodurans* and functionally characterized centromere as well as putative partitioning proteins encoded on chromosome I *in vivo* and *in vitro*. Enhanced stability of unstable mini-F plasmid in presence centromere and its cognate partitioning proteins, oscillation of GFP-ParA1 in *E. coli* harboring plasmid with centromere, and loss of nucleoid in *parB1* deletion mutant of *D. radiodurans* strongly supported the *in vitro* activity characterization of these elements and their roles in genome segregation by pulling mechanisms. ParA2 in absence or lower ratio of ParB2 perform a different function other than genome segregation i.e. in the regulation of cell division has been another new and novel finding from this study. Increase in cell size and anucleation in *parB*2 deletion mutant further suggested the role of ParA2B2 system beyond genome segregation, which would be worth investigating.

CHAPTER 5

Summary, conclusion and future perspectives

This work was carried out to address some of the questions related to chromosome segregation in a radiation resistant bacterium *Deinococcus radiodurans* harboring multipartite genome system. Using databases and on-line software, the primary sequences of ParA's and ParB's encoded on chromosome I, chromosome II and megaplasmid were compared with ParA and ParB homologues from other bacteria. Analyses showed that ParA and ParB encoded on chromosome I are closer to chromosomal type ParA and ParB. Nevertheless, the ParB1 and ParB4 of *D. radiodurans* have slight differences in HTH motifs as compared to chromosomal ParB's of other bacteria indicating the possibility of these proteins might be recognizing centromeric sequences structurally different from conserved cis elements. Similarly, ParA's of this bacterium were compared with ParA type proteins in database and noticed that ParA1 in chromosome I is similar to chromosomal type ParA's while ParA of secondary genome (ParA2, ParA3 and ParA4) were distinctly different from ParA's reported in the literature. Interestingly, ParA of secondary genomes are phylogenetically closer to bacterial cell division regulatory proteins. These analyses therefore, could allow us to speculate that there may not be functional redundancy amongst these proteins.

Using bioinformatic analysis, the centromeric sequences were searched for both P1 type plasmid as well as *Bacillus subtilis* type chromosomal centromeres. Chromosome I showed the presence of centromeric sequences similar to that reported from *Bacillus subtilis*. Thus through this study, we have been able to predict three centromeric sequences in chromosome I named as *segS*1.*segS*2 and *segS*3, and functional prediction of ParA's and ParB's encoded on all the genome replicating units of *D.radiodurans*. Further study was carried out for validation of bioinformatic predictions. *In vitro* studies

with purified recombinant proteins confirmed ParA1 as a DNA binding ATPase and ParB1 as a sequences specific centromere *segS*, binding protein. Co-incubation of ParA1 with *segS* bound ParB1 showed formation of higher order structure as detected by increased light scattering and sedimentation of ParA1 in pellet fraction. This structure was selectively destabilized within 30 min, once ATP was added at least in case of *segS*3 elements. ParA1 incubation with ParB1 bound to *segS*3 showed highest ATPase activity stimulation as compared to *segS*1/*segS*2/*DP*1 elements. These results indicated that ParA1 interaction with *segS*3-ParB1complex was different than similar complex with other putative centromeric sequences. Using plasmid stability assay of mini-F instable plasmid, *parB*1 deletion mutant analysis under fluorescence microscope, it was demonstrated that putative centromeric sequences *segS*1/ *segS*2/ *segS*3 are true bacterial centromeres in *D. radiodurans*. Unlike *segS*3, the *segS*1 and *segS*2 bearing instable plasmid could distribute evenly in dividing population by almost 100% frequency. However, *segS*3 required its cognate ParA1 and ParB1 for its efficient function in plasmid segregation in *E. coli*. Interestingly, the *E. coli* cells bearing *segS*2 and *segS*3 elements cloned plasmid showed dynamic oscillation of ParA1 in presence of ParB1. GFP-ParA1 fusion formed a dynamic fluorescent gradient of ParA from one pole to other within the cell. These results collectively characterized the complete partitioning system of chromosome I in *D. radiodurans*. Characteristic features of these elements indicated a strong possibility of chromosome I segregation might be occurring by pulling mechanism.

In silico analysis also indicated that 'ParA' proteins of secondary chromosome are catgeriosed into separate group between chromosomal and plasmid type of 'ParA'

proteins. Therefore, the 'Par' proteins of its chromosome II were functionally characterized. The *parB2* gene was deleted from the genome of *D. radiodurans* and effect of *parB*2 deletion was monitored on growth and anucleation phenotypes. The *parB2* deletion resulted in growth inhibition and higher frequency of anucleation as well as change in cell morphology. Microscopic examination of mutant and wild type cells (*D. radiodurans*) stained with Nile red and DAPI showed increased percentage of cell division blockage. Molecular basis of *parB2* deletion making impact on cell division was not known. Since, ParA2 and ParB2 are expressing in an operon and in a stoichiometric ratio are important in genome segregation, absence of ParB2 would make change in the ratio of ParA2 within the cell and regulation of cell division due to change in ParA2 stiochiometry cannot be ruled out and was therefore, hypothesized. To test this hypothesis, the ParA2 was over expressed in wild type *D. radiodurans* cells and cell morphology was examined. Interestingly, ParA2 over expressing and *parB2* deletion mutant cells of *D. radiodurans* showed similar phenotype of cell morphology change and cell septum breakage. This supported the hypothesis that change in stiochiometry of ParA2 to ParB2 could have inhibited cell division. Similar observation was also made in the *E. coli* cell expressing ParA2. These cells showed a very high degree of cell elongation by inhibition of FtsZ ring maturation. FtsZ localization in mid cell was not inhibited but the progression of Z ring was inhibited and that would have possibly led to cell elongation. Molecular mechanisms underlying the inhibition of FtsZ ring formation was investigated and found that ParA2 does not interfere directly with the activity and polymerization characteristics of FtsZ *in vitro*. The possibility of ParA2 having roles in resolution of duplicated genome from the vicinity of FtsZ ring growth cannot be ruled

out. ParA2 is characterized as a DNA binding ATPase and expression of ParA2-CFP showed its binding on nucleoid of both *D. radiodurans* and *E. coli* cells, which raised a strong possibility of ParA2 bringing out nucleoid occlusion in these cells. For testing this hypothesis, the ParA2 was expressed on a plasmid, in *slmAminCDE* double mutant background of *E. coli* and the functional loss of SlmA a nucleoid occlusion protein, in *E. coli* was monitored. The cells expressing ParA2 *in trans* showed complete complementation of growth defect in rich medium. Although, ParA2 and SlmA do not have structural similarities and unlike SlmA, ParA2 does not affect FtsZ functions in vitro, these can still be functionally similar in terms of their DNA binding functions may be speculated. This speculation might get strong support from the facts that Noc of *Bacillus subtilis* and SlmA of *E. coli* are two quite different proteins in terms of structure and also Noc does not affect FtsZ activities in vitro, they still play roles in cell division regulation in respective hosts by bringing nucleoid occlusion at the vicinity of FtsZ ring growth. These results suggested that ParA2 over expression inhibited bacterial cell division by interfering with septal ring growth possibly through the nucleoid occlusion mechanism as known for SlmA protein in *E. coli*.

This thesis for the first time reports the characterization of complete genome partitioning system of chromosome I in *D. radiodurans*. The work includes the identification and characterization of centromeric sequences and partitioning proteins. Chromosome II does not have classical bacterial centromere's neither *Bacillus* type nor P1 plasmid type. The role of partitioning protein ParB2 is demonstrated in genome maintenance while ParA2 over expression incidentally showed growth defect in both *E. coli* and *D. radiodurans*. Further studies revealed that this growth defect was largely at the levels of cell division

inhibition, most probably by inhibiting the separation of duplicated genome due to its tight binding on nucleoid in the absence of ParB2. As described above, this study has provided some answer to the question of 'Par' proteins functional redundancy but clearly demonstrated that the mechanism for primary chromosome segregation is mostly like by pulling mechanism as known in both multi chromosome and single chromosome containing bacteria characterized till date. ParB deletion studies have provided significant clues that ParB's are strongly regulating the segregation of cognate genome, it had not completely ruled out however, whether other 'ParB' proteins would work in the absence of one because genome of this bacterium exists in toroidal form and the mere anucleation may not be sufficient to conclude that ParB's are non-redundant.

Work carried out under this thesis has answered some of the questions on mechanisms of genome segregation and functional redundancy of "Par" proteins, and tested the proposed hypotheses both experimentally as well as bioinformatically. It has however, raised and left several questions unanswered. The immediate ones that may require attention include (i) Real-time monitoring of ParB1 protein interaction with centromere's and demonstration of ParA1 dynamic movement on genome leading to duplicated genome segregation in *D. radiodurans*. (ii) How do three *segS* function in chromosome I partitioning *in vivo*, (iii) Functional redundancy of various ParA and ParB proteins during genome segregation, (iv) ParA2 characterization has provided strong clues that this protein is linked between cell division and genome segregation, the factors necessary for ParA2 performing one of these two functions at a given time, at the molecular levels, and (v) whether putative centromeric sequences marginally different from typical *parS* have any role in genome maintenance Further it would be interesting to see if aberrant *parS*

present on chromosome II and mega plasmid, are also centromeric region on these replication units and that would be a novel finding leading to a logical shift in highly focused paradigm on the nature of bacterial centromere's.

Reference List

Adams,D.W., and Errington,J. (2009) Bacterial cell division: assembly, maintenance and disassembly of the Z ring. *Nat Rev Microbiol* **7**: 642-653.

Aravind,L., Wolf,Y.I., and Koonin,E.V. (2000) The ATP-cone: an evolutionarily mobile, ATP-binding regulatory domain. *J Mol Microbiol Biotechnol* **2**: 191-194.

Austin,S., and Abeles,A. (1983) Partition of unit-copy miniplasmids to daughter cells. II. The partition region of miniplasmid P1 encodes an essential protein and a centromere-like site at which it acts. *J Mol Biol* **169**: 373-387.

Bartosik,A.A., Lasocki,K., Mierzejewska,J., Thomas,C.M., and Jagura-Burdzy,G. (2004) ParB of *Pseudomonas aeruginosa*: interactions with its partner ParA and its target parS and specific effects on bacterial growth. *J Bacteriol* **186**: 6983-6998.

Battista,J.R., Park,M.J., and McLemore,A.E. (2001) Inactivation of two homologues of proteins presumed to be involved in the desiccation tolerance of plants sensitizes *Deinococcus radiodurans* R1 to desiccation. *Cryobiology* **43**: 133-139.

Bentchikou,E., Servant,P., Coste,G., and Sommer,S. (2007) Additive effects of SbcCD and PolX deficiencies in the in vivo repair of DNA double-strand breaks in *Deinococcus radiodurans*. *J Bacteriol* **189**: 4784-4790.

Bernhardt,T.G., and de Boer,P.A. (2005) SlmA, a nucleoid-associated, FtsZ binding protein required for blocking septal ring assembly over Chromosomes in *E. coli. Mol Cell* **18**: 555-564.

Blasius,M., Sommer,S., and Hubscher,U. (2008) *Deinococcus radiodurans*: what belongs to the survival kit? *Crit Rev Biochem Mol Biol* **43**: 221-238.

Bloom,K., and Joglekar,A. (2010) Towards building a chromosome segregation machine. *Nature* **463**: 446-456.

Bouet,J.Y., Ah-Seng,Y., Benmeradi,N., and Lane,D. (2007) Polymerization of SopA partition ATPase: regulation by DNA binding and SopB. *Mol Microbiol* **63**: 468-481.

Bouet,J.Y., and Funnell,B.E. (1999) P1 ParA interacts with the P1 partition complex at parS and an ATP-ADP switch controls ParA activities. *EMBO J* **18**: 1415-1424.

Bradford,M.M. (1976) A rapid and sensitive method for the quantitation of microgram quantities of protein utilizing the principle of protein-dye binding. *Anal Biochem* **72**: 248-254.

Bramkamp,M., and van,B.S. (2009) Division site selection in rod-shaped bacteria. *Curr Opin Microbiol* **12**: 683-688.

Bridges,B.A. (1995) Are there DNA damage checkpoints in *E. coli*? *Bioessays* **17**: 63-70.

Cho,H., McManus,H.R., Dove,S.L., and Bernhardt,T.G. (2011) Nucleoid occlusion factor SlmA is a DNA-activated FtsZ polymerization antagonist. *Proc Natl Acad Sci U S A* **108**: 3773-3778.

Clark,A.J. (1971) Toward a metabolic interpretation of genetic recombination of *E. coli* and its phages. *Annu Rev Microbiol* **25**: 437-464.

Cox,M.M., Keck,J.L., and Battista,J.R. (2010) Rising from the Ashes: DNA Repair in *Deinococcus radiodurans. PLoS Genet* **6**: e1000815.

Dabrazhynetskaya,A., Brendler,T., Ji,X., and Austin,S. (2009) Switching protein-DNA recognition specificity by single-amino-acid substitutions in the P1 par family of plasmid partition elements. *J Bacteriol* **191**: 1126-1131.

Daly,M.J., and Minton,K.W. (1995) Interchromosomal recombination in the extremely radioresistant bacterium *Deinococcus radiodurans*. *J Bacteriol* **177**: 5495-5505.

Daly,M.J., Gaidamakova,E.K., Matrosova,V.Y., Kiang,J.G., Fukumoto,R., Lee,D.Y. *et al.* (2010) Small-molecule antioxidant proteome-shields in *Deinococcus radiodurans. PLoS One* **5**: e12570.

Das,A.D., and Misra,H.S. (2011) Characterization of DRA0282 from *Deinococcus radiodurans* for its role in bacterial resistance to DNA damage. *Microbiology* **157**: 2196-2205.

Das,A.D., and Misra,H.S. (2012) DR2417, a hypothetical protein characterized as a novel beta-CASP family nuclease in radiation resistant bacterium, *Deinococcus radiodurans. Biochim Biophys Acta* **1820**: 1052-1061.

Davis.M.A., Martin. K.A., and Austin. S.J.(1992) Biochemical activities of the parA partition protein of the P1 plasmid. *Mol Microbiol*. **6**:1141–1147.

De,B.P., Crossley,R., and Rothfield,L. (1992) The essential bacterial cell-division protein FtsZ is a GTPase. *Nature* **359**: 254-256.

Dedrick,R.M., Wildschutte,H., and McCormick,J.R. (2009) Genetic interactions of smc, ftsK, and parB genes in *Streptomyces coelicolor* and their developmental genome segregation phenotypes. *J Bacteriol* **191**: 320-332.

Desai,S.S., Rajpurohit,Y.S., Misra,H.S., and Deobagkar,D.N. (2011) Characterization of the role of the RadS/RadR two-component system in the radiation resistance of *Deinococcus radiodurans. Microbiology* **157**: 2974-2982.

Donovan,C., Schwaiger,A., Kramer,R., and Bramkamp,M. (2010) Subcellular localization and characterization of the ParAB system from *Corynebacterium glutamicum. J Bacteriol* **192**: 3441-3451.

Draper,G.C., and Gober,J.W. (2002) Bacterial chromosome segregation. *Annu Rev Microbiol* **56**: 567-597.

Dubarry,N., Pasta,F., and Lane,D. (2006) ParABS systems of the four replicons of B*urkholderia cenocepacia:* new chromosome centromeres confer partition specificity. *J Bacteriol* **188**: 1489-1496.

Duggan,D.E.,Anderson,A.W.,and Elliker,P.R.(1963) Inactivation of the radiation resistant spoilage bacterium *Micrococcus radiodurans*. I.Radiation inactivation rates in three substrates and in buffers.*Appl Microbiol* **11**:398-403.

Dunham,T.D., Xu,W., Funnell,B.E., and Schumacher,M.A. (2009) Structural basis for ADP-mediated transcriptional regulation by P1 and P7 ParA. *EMBO J* **28**: 1792-1802.

Dworkin,J., and Losick,R. (2002) Does RNA polymerase help drive chromosome segregation in bacteria? *Proc Natl Acad Sci U S A* **99**: 14089-14094.

Earl,A.M., Rankin,S.K., Kim,K.P., Lamendola,O.N., and Battista,J.R. (2002) Genetic evidence that the uvsE gene product of *Deinococcus radiodurans* R1 is a UV damage endonuclease. *J Bacteriol* **184**: 1003-1009.

Easter,J., Jr., and Gober,J.W. (2002) ParB-stimulated nucleotide exchange regulates a switch in functionally distinct ParA activities. *Mol Cell* **10**: 427-434.

Ebersbach,G., and Gerdes,K. (2001) The double par locus of virulence factor pB171: DNA segregation is correlated with oscillation of ParA. *Proc Natl Acad Sci U S A* **98**: 15078-15083.

Ebersbach,G., and Gerdes,K. (2005) Plasmid segregation mechanisms. *Annu Rev Genet* **39**: 453-479.

Ebersbach,G., Sherratt,D.J., and Gerdes,K. (2005) Partition-associated incompatibility caused by random assortment of pure plasmid clusters. *Mol Microbiol* **56**: 1430-1440.

Egan,E.S., and Waldor,M.K. (2003) Distinct replication requirements for the two *Vibrio cholerae* chromosomes. *Cell* **114**: 521-530.

Egan,E.S., Fogel,M.A., and Waldor,M.K. (2005) Divided genomes: negotiating the cell cycle in prokaryotes with multiple chromosomes. *Mol Microbiol* **56**: 1129-1138.

Erdmann,N., Petroff,T., and Funnell,B.E. (1999) Intracellular localization of P1 ParB protein depends on ParA and parS. *Proc Natl Acad Sci U S A* **96**: 14905-14910.

Errington,J. (2003) Regulation of endospore formation in *Bacillus subtilis*. *Nat Rev Microbiol* **1**: 117-126.

Errington,J., Daniel,R.A., and Scheffers,D.J. (2003) Cytokinesis in bacteria. *Microbiol Mol Biol Rev* **67**: 52-65, table.

Fiebig,A., Keren,K., and Theriot,J.A. (2006) Fine-scale time-lapse analysis of the biphasic, dynamic behaviour of the two *Vibrio cholerae* chromosomes. *Mol Microbiol* **60**: 1164-1178.

Fogel,M.A., and Waldor,M.K. (2005) Distinct segregation dynamics of the two *Vibrio cholerae* chromosomes. *Mol Microbiol* **55**: 125-136.

Fogel,M.A., and Waldor,M.K. (2006) A dynamic, mitotic-like mechanism for bacterial chromosome segregation. *Genes Dev* **20**: 3269-3282.

Funayama,T., Narumi,I., Kikuchi,M., Kitayama,S., Watanabe,H., and Yamamoto,K. (1999) Identification and disruption analysis of the recN gene in the extremely radioresistant bacterium *Deinococcus radiodurans. Mutat Res* **435**: 151-161.

Funnell,B.E. (1988) Mini-P1 plasmid partitioning: excess ParB protein destabilizes plasmids containing the centromere parS. *J Bacteriol* **170**: 954-960.

Galkin,V.E., Orlova,A., Rivera,C., Mullins,R.D., and Egelman,E.H. (2009) Structural polymorphism of the ParM filament and dynamic instability. *Structure* **17**: 1253-1264.

Gerdes,K., and Molin,S. (1986) Partitioning of plasmid R1. Structural and functional analysis of the parA locus. *J Mol Biol* **190**: 269-279.

Gerdes,K., Howard,M., and Szardenings,F. (2010) Pushing and pulling in prokaryotic DNA segregation. *Cell* **141**: 927-942.

Ghosh,S.K., Hajra,S., Paek,A., and Jayaram,M. (2006) Mechanisms for chromosome and plasmid segregation. *Annu Rev Biochem* **75**: 211-241.

Gitai,Z. (2006) Plasmid segregation: a new class of cytoskeletal proteins emerges. *Curr Biol* **16**: R133-R136.

Godfrin-Estevenon,A.M., Pasta,F., and Lane,D. (2002) The parAB gene products of P*seudomonas putida* exhibit partition activity in both P. putida and Escherichia coli. *Mol Microbiol* **43**: 39-49.

Gordon,G.S., and Wright,A. (2000) DNA segregation in bacteria. *Annu Rev Microbiol* **54**: 681-708.

Gordon,S., Rech,J., Lane,D., and Wright,A. (2004) Kinetics of plasmid segregation in *Escherichia coli*. *Mol Microbiol* **51**: 461-469.

Guynet,C., and de la,C.F. (2011) Plasmid segregation without partition. *Mob Genet Elements* **1**: 236-241.

Guynet,C., Cuevas,A., Moncalian,G., and de la,C.F. (2011) The stb operon balances the requirements for vegetative stability and conjugative transfer of plasmid R388. *PLoS Genet* **7**: e1002073.

Hales,L.M., Gumport,R.I., and Gardner,J.F. (1994) Determining the DNA sequence elements required for binding integration host factor to two different target sites. *J Bacteriol* **176**: 2999-3006.

Hassan,P.A., Sawant,S.N., Bagkar,N.C., and Yakhmi,J.V. (2004) Polyaniline nanoparticles prepared in rodlike micelles. *Langmuir* **20**: 4874-4880.

Hatano,T., and Niki,H. (2010) Partitioning of P1 plasmids by gradual distribution of the ATPase ParA. *Mol Microbiol* **78**: 1182-1198.

Hatano,T., Yamaichi,Y., and Niki,H. (2007) Oscillating focus of SopA associated with filamentous structure guides partitioning of F plasmid. *Mol Microbiol* **64**: 1198-1213.

Hayes,F., and Barilla,D. (2006) Assembling the bacterial segrosome. *Trends Biochem Sci* **31**: 247-250.

Hazan,R., and Ben-Yehuda,S. (2006) Resolving chromosome segregation in bacteria. *J Mol Microbiol Biotechnol* **11**: 126-139.

Heidelberg,J.F., Eisen,J.A., Nelson,W.C., Clayton,R.A., Gwinn,M.L., Dodson,R.J. *et al.* (2000) DNA sequence of both chromosomes of the cholera pathogen *Vibrio cholerae*. *Nature* **406**: 477-483.

Helsberg,M., and Eichenlaub,R. (1986) Twelve 43-base-pair repeats map in a cis-acting region essential for partition of plasmid mini-F. *J Bacteriol* **165**: 1043-1045.

Hester,C.M., and Lutkenhaus,J. (2007) Soj (ParA) DNA binding is mediated by conserved arginines and is essential for plasmid segregation. *Proc Natl Acad Sci U S A* **104**: 20326-20331.

Hiemstra,H., Nanninga,N., Woldringh,C.L., Inouye,M., and Witholt,B. (1987) Distribution of newly synthesized lipoprotein over the outer membrane and the peptidoglycan sacculus of an *Escherichia coli* lac-lpp strain. *J Bacteriol* **169**: 5434-5444.

Higgins,D.G., and Sharp,P.M. (1988) CLUSTAL: a package for performing multiple sequence alignment on a microcomputer. *Gene* **73**: 237-244.

Hirano,M., Mori,H., Onogi,T., Yamazoe,M., Niki,H., Ogura,T., and Hiraga,S. (1998) Autoregulation of the partition genes of the mini-F plasmid and the intracellular localization of their products in *Escherichia coli*. *Mol Gen Genet* **257**: 392-403.

Hui,M.P., Galkin,V.E., Yu,X., Stasiak,A.Z., Stasiak,A., Waldor,M.K., and Egelman,E.H. (2010) ParA2, a *Vibrio cholerae* chromosome partitioning protein, forms left-handed helical filaments on DNA. *Proc Natl Acad Sci U S A* **107**: 4590-4595.

Ireton,K., Gunther,N.W., and Grossman,A.D. (1994) spo0J is required for normal chromosome segregation as well as the initiation of sporulation in *Bacillus subtilis*. *J Bacteriol* **176**: 5320-5329.

Jakimowicz,D., Brzostek,A., Rumijowska-Galewicz,A., Zydek,P., Dolzblasz,A., Smulczyk-Krawczyszyn,A. *et al.* (2007) Characterization of the mycobacterial chromosome segregation protein ParB and identification of its target in *Mycobacterium smegmatis*. *Microbiology* **153**: 4050-4060.

Jakimowicz,D., Zydek,P., Kois,A., Zakrzewska-Czerwinska,J., and Chater,K.F. (2007) Alignment of multiple chromosomes along helical ParA scaffolding in sporulating *Streptomyces* hyphae. *Mol Microbiol* **65**: 625-641.

Jensen,R.B., Wang,S.C., and Shapiro,L. (2001) A moving DNA replication factory in *Caulobacter crescentus*. *EMBO J* **20**: 4952-4963.

Jha,J.K., Baek,J.H., Venkova-Canova,T., and Chattoraj,D.K. (2012) Chromosome dynamics in multichromosome bacteria. *Biochim Biophys Acta* **1819**: 826-829.

Kahng,L.S., and Shapiro,L. (2003) Polar localization of replicon origins in the multipartite genomes of Agrobacterium tumefaciens and *Sinorhizobium meliloti*. *J Bacteriol* **185**: 3384-3391.

Kamble,V.A., and Misra,H.S. (2010) The SbcCD complex of *Deinococcus radiodurans* contributes to radioresistance and DNA strand break repair in vivo and exhibits Mre11-Rad50 type activity in vitro. *DNA Repair (Amst)* **9**: 488-494.

Khairnar,N.P., and Misra,H.S. (2009) DNA polymerase X from *Deinococcus radiodurans* implicated in bacterial tolerance to DNA damage is characterized as a short patch base excision repair polymerase. *Microbiology* **155**: 3005-3014.

Khairnar,N.P., Kamble,V.A., and Misra,H.S. (2008) RecBC enzyme overproduction affects UV and gamma radiation survival of *Deinococcus radiodurans*. *DNA Repair (Amst)* **7**: 40-47.

Khairnar,N.P., Kamble,V.A., Mangoli,S.H., Apte,S.K., and Misra,H.S. (2007) Involvement of a periplasmic protein kinase in DNA strand break repair and homologous recombination in *Escherichia coli*. *Mol Microbiol* **65**: 294-304.

Khairnar,N.P., Misra,H.S., and Apte,S.K. (2003) Pyrroloquinoline-quinone synthesized in Escherichia coli by pyrroloquinoline-quinone synthase of *Deinococcus radiodurans* plays a role beyond mineral phosphate solubilization. *Biochem Biophys Res Commun* **312**: 303-308.

Kim,H.J., Calcutt,M.J., Schmidt,F.J., and Chater,K.F. (2000) Partitioning of the linear chromosome during sporulation of *Streptomyces coelicolor* A3(2) involves an oriC-linked parAB locus. *J Bacteriol* **182**: 1313-1320.

Kota,S., and Misra,H.S. (2008) Identification of a DNA processing complex from *Deinococcus radiodurans*. *Biochem Cell Biol* **86**: 448-458.

Kota,S., Kamble,V.A., Rajpurohit,Y.S., and Misra,H.S. (2010) ATP-type DNA ligase requires other proteins for its activity in vitro and its operon components for radiation resistance in *Deinococcus radiodurans* in vivo. *Biochem Cell Biol* **88**: 783-790.

Kota,S., Kumar,C.V., and Misra,H.S. (2010) Characterization of an ATP-regulated DNA-processing enzyme and thermotolerant phosphoesterase in the radioresistant bacterium *Deinococcus radiodurans*. *Biochem J* **431**: 149-157.

Larsen,R.A., Cusumano,C., Fujioka,A., Lim-Fong,G., Patterson,P., and Pogliano,J. (2007) Treadmilling of a prokaryotic tubulin-like protein, TubZ, required for plasmid stability in *Bacillus thuringiensis*. *Genes Dev* **21**: 1340-1352.

Lasocki,K., Bartosik,A.A., Mierzejewska,J., Thomas,C.M., and Jagura-Burdzy,G. (2007) Deletion of the parA (soj) homologue in *Pseudomonas aeruginosa* causes ParB instability and affects growth rate, chromosome segregation, and motility. *J Bacteriol* **189**: 5762-5772.

Lau,I.F., Filipe,S.R., Soballe,B., Okstad,O.A., Barre,F.X., and Sherratt,D.J. (2003) Spatial and temporal organization of replicating *Escherichia coli* chromosomes. *Mol Microbiol* **49**: 731-743.

Lecointe,F., Coste,G., Sommer,S., and Bailone,A. (2004) Vectors for regulated gene expression in the radioresistant bacterium *Deinococcus radiodurans*. *Gene* **336**: 25-35.

Lee,M.J., Liu,C.H., Wang,S.Y., Huang,C.T., and Huang,H. (2006) Characterization of the Soj/Spo0J chromosome segregation proteins and identification of putative parS sequences in *Helicobacter pylori*. *Biochem Biophys Res Commun* **342**: 744-750.

Lee, S., Price C. W., (1993)The *minCD* locus of *Bacillus subtilis* lacks the *minE* determinant that provides topological specificity to cell division. *Mol Microbiol*. 7:601–610.

Lee,P.S., Lin,D.C., Moriya,S., and Grossman,A.D. (2003) Effects of the chromosome partitioning protein Spo0J (ParB) on oriC positioning and replication initiation in *Bacillus subtilis*. *J Bacteriol* **185**: 1326-1337.

Leipe,D.D., Wolf,Y.I., Koonin,E.V., and Aravind,L. (2002) Classification and evolution of P-loop GTPases and related ATPases. *J Mol Biol* **317**: 41-72.

Lemon,K.P., and Grossman,A.D. (2001) The extrusion-capture model for chromosome partitioning in bacteria. *Genes Dev* **15**: 2031-2041.

Lemonnier,M., Bouet,J.Y., Libante,V., and Lane,D. (2000) Disruption of the F plasmid partition complex in vivo by partition protein SopA. *Mol Microbiol* **38**: 493-505.

Leonard,T.A., Butler,P.J., and Lowe,J. (2004) Structural analysis of the chromosome segregation protein Spo0J from *Thermus thermophilus*. *Mol Microbiol* **53**: 419-432.

Leonard,T.A., Butler,P.J., and Lowe,J. (2005) Bacterial chromosome segregation: structure and DNA binding of the Soj dimer--a conserved biological switch. *EMBO J* **24**: 270-282.

Leonard,T.A., Moller-Jensen,J., and Lowe,J. (2005) Towards understanding the molecular basis of bacterial DNA segregation. *Philos Trans R Soc Lond B Biol Sci* **360**: 523-535.

Levin-Zaidman,S., Englander,J., Shimoni,E., Sharma,A.K., Minton,K.W., and Minsky,A. (2003) Ringlike structure of the *Deinococcus radiodurans* genome: a key to radioresistance? *Science* **299**: 254-256.

Lewis,R.A., Bignell,C.R., Zeng,W., Jones,A.C., and Thomas,C.M. (2002) Chromosome loss from par mutants of *Pseudomonas putida* depends on growth medium and phase of growth. *Microbiology* **148**: 537-548.

Li,Y., and Austin,S. (2002) The P1 plasmid in action: time-lapse photomicroscopy reveals some unexpected aspects of plasmid partition. *Plasmid* **48**: 174-178.

Lin,D.C., and Grossman,A.D. (1998) Identification and characterization of a bacterial chromosome partitioning site. *Cell* **92**: 675-685.

Livny,J., Yamaichi,Y., and Waldor,M.K. (2007) Distribution of centromere-like parS sites in bacteria: insights from comparative genomics. *J Bacteriol* **189**: 8693-8703.

Livny,J., Yamaichi,Y., and Waldor,M.K. (2007) Distribution of centromere-like parS sites in bacteria: insights from comparative genomics. *J Bacteriol* **189**: 8693-8703.

Lowe,J., van den,E.F., and Amos,L.A. (2004) Molecules of the bacterial cytoskeleton. *Annu Rev Biophys Biomol Struct* **33**: 177-198.

Lutkenhaus .J., and Addinall .S.G., (1997) Bacterial cell division and the Z ring. *Annu Rev Biochem*, 66: 93–116.

Lutkenhaus,J. (2007) Assembly dynamics of the bacterial MinCDE system and spatial regulation of the Z ring. *Annu Rev Biochem* **76**: 539-562.

Martin,K.A., Davis,M.A., and Austin,S. (1991) Fine-structure analysis of the P1 plasmid partition site. *J Bacteriol* **173**: 3630-3634.

Mascarenhas,J., Volkov,A.V., Rinn,C., Schiener,J., Guckenberger,R., and Graumann,P.L. (2005) Dynamic assembly, localization and proteolysis of the *Bacillus subtilis* SMC complex. *BMC Cell Biol* **6**: 28.

Meima,R., and Lidstrom,M.E. (2000) Characterization of the minimal replicon of a cryptic Deinococcus radiodurans SARK plasmid and development of versatile *Escherichia coli-D. radiodurans* shuttle vectors. *Appl Environ Microbiol* **66**: 3856-3867.

Minsky,A., Shimoni,E., and Englander,J. (2006) Ring-like nucleoids and DNA repair through error-free nonhomologous end joining in Deinococcus radiodurans. *J Bacteriol* **188**: 6047-6051.

Minton,K.W. (1994) DNA repair in the extremely radioresistant bacterium *Deinococcus radiodurans. Mol Microbiol* **13**: 9-15.

Misra,H.S., Khairnar,N.P., Barik,A., Indira,P.K., Mohan,H., and Apte,S.K. (2004) Pyrroloquinoline-quinone: a reactive oxygen species scavenger in bacteria. *FEBS Lett* **578**: 26-30.

Misra,H.S., Khairnar,N.P., Kota,S., Shrivastava,S., Joshi,V.P., and Apte,S.K. (2006) An exonuclease I-sensitive DNA repair pathway in Deinococcus radiodurans: a major determinant of radiation resistance. *Mol Microbiol* **59**: 1308-1316.

Moe,E., Hall,D.R., Leiros,I., Monsen,V.T., Timmins,J., and McSweeney,S. (2012) Structure-function studies of an unusual 3-methyladenine DNA glycosylase II (AlkA) from *Deinococcus radiodurans*. *Acta Crystallogr D Biol Crystallogr* **68**: 703-712.

Mohl,D.A., and Gober,J.W. (1997) Cell cycle-dependent polar localization of chromosome partitioning proteins in *Caulobacter crescentus*. *Cell* **88**: 675-684.

Mohl,D.A., Easter,J., Jr., and Gober,J.W. (2001) The chromosome partitioning protein, ParB, is required for cytokinesis in *Caulobacter crescentus*. *Mol Microbiol* **42**: 741-755.

Moseley,B.E., and Evans,D.M. (1983) Isolation and properties of strains of Micrococcus (*Deinococcus) radiodurans* unable to excise ultraviolet light-induced pyrimidine dimers from DNA: evidence for two excision pathways. *J Gen Microbiol* **129**: 2437-2445.

Ni,L., Xu,W., Kumaraswami,M., and Schumacher,M.A. (2010) Plasmid protein TubR uses a distinct mode of HTH-DNA binding and recruits the prokaryotic tubulin homolog TubZ to effect DNA partition. *Proc Natl Acad Sci U S A* **107**: 11763-11768.

Ogura,T., and Hiraga,S. (1983) Mini-F plasmid genes that couple host cell division to plasmid proliferation. *Proc Natl Acad Sci U S A* **80**: 4784-4788.

Ogura,Y., Ogasawara,N., Harry,E.J., and Moriya,S. (2003) Increasing the ratio of Soj to Spo0J promotes replication initiation in *Bacillus subtilis*. *J Bacteriol* **185**: 6316-6324.

Onogi,T., Miki,T., and Hiraga,S. (2002) Behavior of sister copies of mini-F plasmid after synchronized plasmid replication in *Escherichia coli* cells. *J Bacteriol* **184**: 3142-3145.

Passot,F.M., Calderon,V., Fichant,G., Lane,D., and Pasta,F. (2012) Centromere binding and evolution of chromosomal partition systems in the *Burkholderiales. J Bacteriol* **194**: 3426-3436.

Levin.P.A., Shim .J.J., and Grossman.A.D. (1998) Effect of *minCD* on FtsZ Ring Position and Polar Septation in *Bacillus subtilis J Bacteriol*. 180: 6048–6051.

Pratto,F., Cicek,A., Weihofen,W.A., Lurz,R., Saenger,W., and Alonso,J.C. (2008) *Streptococcus pyogenes* pSM19035 requires dynamic assembly of ATP-bound ParA and ParB on parS DNA during plasmid segregation. *Nucleic Acids Res* **36**: 3676-3689.

Pratto,F., Suzuki,Y., Takeyasu,K., and Alonso,J.C. (2009) Single-molecule analysis of proteinxDNA complexes formed during partition of newly replicated plasmid molecules in *Streptococcus pyogenes*. *J Biol Chem* **284**: 30298-30306.

Ptacin,J.L., Lee,S.F., Garner,E.C., Toro,E., Eckart,M., Comolli,L.R. *et al.* (2010) A spindle-like apparatus guides bacterial chromosome segregation. *Nat Cell Biol* **12**: 791-798.

Rainey,F.A., Ray,K., Ferreira,M., Gatz,B.Z., Nobre,M.F., Bagaley,D. *et al.* (2005) Extensive diversity of ionizing-radiation-resistant bacteria recovered from Sonoran Desert soil and description of nine new species of the genus *Deinococcus* obtained from a single soil sample. *Appl Environ Microbiol* **71**: 5225-5235.

Rajpurohit,Y.S., and Misra,H.S. (2010) Characterization of a DNA damage-inducible membrane protein kinase from *Deinococcus radioduran*s and its role in bacterial radioresistance and DNA strand break repair. *Mol Microbiol* **77**: 1470-1482.

Rajpurohit,Y.S., Gopalakrishnan,R., and Misra,H.S. (2008) Involvement of a protein kinase activity inducer in DNA double strand break repair and radioresistance of *Deinococcus radiodurans*. *J Bacteriol* **190**: 3948-3954.

Ravin,N.V., Rech,J., and Lane,D. (2003) Mapping of functional domains in F plasmid partition proteins reveals a bipartite SopB-recognition domain in SopA. *J Mol Biol* **329**: 875-889.

Ringgaard,S., van,Z.J., Howard,M., and Gerdes,K. (2009) Movement and equipositioning of plasmids by ParA filament disassembly. *Proc Natl Acad Sci U S A* **106**: 19369-19374.

Roberts,M.A., Wadhams,G.H., Hadfield,K.A., Tickner,S., and Armitage,J.P. (2012) ParA-like protein uses nonspecific chromosomal DNA binding to partition protein complexes. *Proc Natl Acad Sci U S A* **109**: 6698-6703.

Roy,A., Kucukural,A., and Zhang,Y. (2010) I-TASSER: a unified platform for automated protein structure and function prediction. *Nat Protoc* **5**: 725-738.

Sambrook,J. (2001) Molecular cloning : a laboratory manual / Joseph Sambrook, David W. Russell Cold Spring Harbor, N.Y. : Cold Spring Harbor Laboratory.

Sandigursky,M., Sandigursky,S., Sonati,P., Daly,M.J., and Franklin,W.A. (2004) Multiple uracil-DNA glycosylase activities in *Deinococcus radiodurans*. *DNA Repair (Amst)* **3**: 163-169.

Sawitzke,J.A., and Austin,S. (2000) Suppression of chromosome segregation defects of *Escherichia coli* muk mutants by mutations in topoisomerase I. *Proc Natl Acad Sci U S A* **97**: 1671-1676.

Schumacher,M.A. (2007) Structural biology of plasmid segregation proteins. *Curr Opin Struct Biol* **17**: 103-109.

Schumacher,M.A. (2012) Bacterial plasmid partition machinery: a minimalist approach to survival. *Curr Opin Struct Biol* **22**: 72-79.

Schumacher,M.A., and Funnell,B.E. (2005) Structures of ParB bound to DNA reveal mechanism of partition complex formation. *Nature* **438**: 516-519.

Sengupta,M., Nielsen,H.J., Youngren,B., and Austin,S. (2010) P1 plasmid segregation: accurate redistribution by dynamic plasmid pairing and separation. *J Bacteriol* **192**: 1175-1183.

Sharpe,M.E., and Errington,J. (1995) Postseptational chromosome partitioning in bacteria. *Proc Natl Acad Sci U S A* **92**: 8630-8634.

Shebelut,C.W., Guberman,J.M., van,T.S., Yakhnina,A.A., and Gitai,Z. (2010) *Caulobacter* chromosome segregation is an ordered multistep process. *Proc Natl Acad Sci U S A* **107**: 14194-14198.

Slade,D., and Radman,M. (2011) Oxidative stress resistance in *Deinococcus radiodurans. Microbiol Mol Biol Rev* **75**: 133-191.

Slade,D., Lindner,A.B., Paul,G., and Radman,M. (2009) Recombination and replication in DNA repair of heavily irradiated *Deinococcus radiodurans*. *Cell* **136**: 1044-1055.

Smith,M.D., Abrahamson,R., and Minton,K.W. (1989) Shuttle plasmids constructed by the transformation of an Escherichia coli cloning vector into two *Deinococcus radiodurans* plasmids. *Plasmid* **22**: 132-142.

Soberon,N.E., Lioy,V.S., Pratto,F., Volante,A., and Alonso,J.C. (2011) Molecular anatomy of the S*treptococcus pyogenes* pSM19035 partition and segrosome complexes. *Nucleic Acids Res* **39**: 2624-2637.

Surtees,J.A., and Funnell,B.E. (1999) P1 ParB domain structure includes two independent multimerization domains. *J Bacteriol* **181**: 5898-5908.

Surtees,J.A., and Funnell,B.E. (2003) Plasmid and chromosome traffic control: how ParA and ParB drive partition. *Curr Top Dev Biol* **56**: 145-180.

Sweet,D.M., and Moseley,B.E. (1976) The resistance of *Micrococcus radiodurans* to killing and mutation by agents which damage DNA. *Mutat Res* **34**: 175-186.

Tessema,M., Lehmann,U., and Kreipe,H. (2004) Cell cycle and no end. *Virchows Arch* **444**: 313-323.

Thanbichler,M., and Shapiro,L. (2006) MipZ, a spatial regulator coordinating chromosome segregation with cell division in *Caulobacter*. *Cell* **126**: 147-162.

Tinsley,E., and Khan,S.A. (2006) A novel FtsZ-like protein is involved in replication of the anthrax toxin-encoding pXO1 plasmid in Bacillus anthracis. *J Bacteriol* **188**: 2829-2835.

Tonthat,N.K., Arold,S.T., Pickering,B.F., Van Dyke,M.W., Liang,S., Lu,Y. *et al.* (2011) Molecular mechanism by which the nucleoid occlusion factor, SlmA, keeps cytokinesis in check. *EMBO J* **30**: 154-164.

Vecchiarelli,A.G., Han,Y.W., Tan,X., Mizuuchi,M., Ghirlando,R., Biertumpfel,C. *et al.* (2010) ATP control of dynamic P1 ParA-DNA interactions: a key role for the nucleoid in plasmid partition. *Mol Microbiol* **78**: 78-91.

Weiss,D.S., Chen,J.C., Ghigo,J.M., Boyd,D., and Beckwith,J. (1999) Localization of FtsI (PBP3) to the septal ring requires its membrane anchor, the Z ring, FtsA, FtsQ, and FtsL. *J Bacteriol* **181**: 508-520.

White,O., Eisen,J.A., Heidelberg,J.F., Hickey,E.K., Peterson,J.D., Dodson,R.J. *et al.* (1999) Genome sequence of the radioresistant bacterium *Deinococcus radiodurans* R1. *Science* **286**: 1571-1577.

Wientjes,F.B., and Nanninga,N. (1989) Rate and topography of peptidoglycan synthesis during cell division in *Escherichia coli*: concept of a leading edge. *J Bacteriol* **171**: 3412-3419.

Wu,L.J., and Errington,J. (2004) Coordination of cell division and chromosome segregation by a nucleoid occlusion protein in *Bacillus subtilis. Cell* **117**: 915-925.

Wu,L.J., Ishikawa,S., Kawai,Y., Oshima,T., Ogasawara,N., and Errington,J. (2009) Noc protein binds to specific DNA sequences to coordinate cell division with chromosome segregation. *EMBO J* **28**: 1940-1952.

Yakunin,A.F., Proudfoot,M., Kuznetsova,E., Savchenko,A., Brown,G., Arrowsmith,C.H., and Edwards,A.M. (2004) The HD domain of the *Escherichia coli* tRNA nucleotidyltransferase has 2',3'-cyclic phosphodiesterase, 2'-nucleotidase, and phosphatase activities. *J Biol Chem* **279**: 36819-36827.

Yamaichi,Y., and Niki,H. (2000) Active segregation by the *Bacillus subtilis* partitioning system in Escherichia coli. *Proc Natl Acad Sci U S A* **97**: 14656-14661.

Yamaichi,Y., Fogel,M.A., and Waldor,M.K. (2007) par genes and the pathology of chromosome loss in *Vibrio cholerae*. *Proc Natl Acad Sci U S A* **104**: 630-635.

Yamaichi,Y., Fogel,M.A., McLeod,S.M., Hui,M.P., and Waldor,M.K. (2007) Distinct centromere-like parS sites on the two chromosomes of *Vibrio spp*. *J Bacteriol* **189**: 5314-5324.

Yanagida,M. (2005) Basic mechanism of eukaryotic chromosome segregation. *Philos Trans R Soc Lond B Biol Sci* **360**: 609-621.

Zahradka,K., Slade,D., Bailone,A., Sommer,S., Averbeck,D., Petranovic,M. *et al.* (2006) Reassembly of shattered chromosomes in *Deinococcus radiodurans*. *Nature* **443**: 569-573